The development of *S*-trityl L-cysteine based inhibitors of Eg5 as anticancer chemotherapeutics.

Submitted in fulfilment of the requirements for the degree of

Doctor of Philosophy by

James Arthur Dudley Good MSci.

2012

The Beatson Institute for Cancer Research,

Faculty of Medicine,

University of Glasgow.

Author's Declaration

I declare that except where explicit reference is made to the contribution of others, this thesis is the result of my own work and has not been submitted for any other degree at the University of Glasgow, or any other institution.

Signature:

Printed name: (James A.D. Good)

Copyright Notice

Abstract

The kinesins are a class of microtubule based motor proteins which have extensive involvement in the orchestration of the mechanics of mitosis. The most studied of these is the kinesin spindle protein Eg5, which is crucially involved in the establishment of the bipolar spindle in prometaphase. Inhibition of this protein results in monopolar mitotic spindles and subsequently mitotic arrest, which can lead to apoptosis in cancer cell lines.

S-Trityl L-cysteine (STLC) was identified as a selective small molecule inhibitor of Eg5 which binds to an allosteric pocket formed by the loop L5 of Eg5. In this thesis, I present the structure based design and development and optimisation of the STLC scaffold to produce orally available potential drug candidates. This was accomplished by optimising the lipophilic binding interactions of the trityl group, and investigating a number of hydrophilic optimisation vectors from the same moiety. The L-cysteine tail was optimised to improve the potency and metabolic stability, and fluorination as a means of altering the lead candidates' drug like properties investigated. In order to improve efficacy in multi-drug resistant (MDR) cell lines overexpressing the P-glycoprotein transporter, I also investigated a number of strategies related modifying to the terminal α-carboxylic acid.

The optimised candidates display growth inhibition ≤ 50 nM across multiple tumour cell lines, and possess favourable metabolic, toxicological and physicochemical attributes. Evaluation *in vivo* confirms their anti tumour activity, and finally strategies for the further progression and development of the lead series in targeting haematological malignancies are discussed.

Acknowledgements

"If I have seen further, it is by standing on the shoulders of giants."[1]

My thanks to Professor Frank Kozielski for his excellent support, mentoring and guidance and to Professor Simon Mackay for welcoming me to SIPBS, invaluable support and expert advice. I also thank Prof. Martin Drysdale for his support and advice throughout, Dr. Oliver Sutcliffe for his help at the outset of the project and Prof. Mike Olson for advice.

I am grateful to Cancer Research UK for funding this studentship, and all those at the Beatson Institute for Cancer Research, University of Glasgow and the Strathclyde Institute of Pharmacy and Biomedical Sciences who enabled me to accomplish the work described within.

It takes a team pulling together to make a successful project, and this was no exception. Without the hard work and endeavour, not to mention help and guidance from colleagues and collaborators, very little would have been possible. Thanks to Dr. Fang Wang for her companionship during the first three years, Dr. Oliver Rath for his hard work on the biology for this project, Dr. Kristal Kaan for her great structural work, and all other group members past and present for their help: Sandeep, Marta, Venkat and Alex, and Dawid and Gosia for listening to my mentoring!

Of course my deepest gratitude also extend to my colleagues at SIPBS at the University of Strathclyde, who welcomed me with open arms, provided many fantastic experiences to enrich and enliven the last few years. In no order: Sabin, Jessica, Giacomo, Nahoum, Jude, Nizar, John, Rachel, George, Murad, Bilal and the many others too numerous to name. You know who you are.

For all the friends, lovers and lunatics outside the world of science who have enriched my life immeasurably since I moved to Glasgow some years ago, a hearty cheers, a slap on the back and a kiss on the lips. Cheers Fraser, Scott, Eilidh, Geoff, Mike and Matt in particular. To my wonderful family, thanks for their love and support and in particular Arthur Spencer for his inspiration and encouragement at all times.

Table of Contents

Abbreviations & Definitions

ABC	ATP-binding cassette
Ac	Acetyl
ADME	Absorption, distribution, metabolism and excretion
ADP	Adenosine diphosphate
a.k.a.	Also known as
AML	Advanced myeloid leukaemia
ATP	Adenosine triphosphate
AUC_{last}	Area under the plasma concentration-time curve from time zero to the time of the last measurable concentration
BimC	"Blocked in mitosis"
$C_{(0)}$	Initial back-extrapolated plasma drug concentration at time zero, following intravenous injection
cLog	Calculated Log
C_{max}	Maximum (peak) plasma drug concentration
cat.	Catalytic
CDK1	Cyclin-dependent kinase-1
CENP-E	Centromere associated protein-E
CI	Chemical ionisation
Cl	Apparent total body clearance of drug from plasma
Cl_{int}	Intrinsic hepatic clearance
Cmpd	Compound
Conc.	Concentrated
CYP	Cytochrome
d	Day
DMEM	Dulbecco's modified eagle medium
DMF	Dimethylformamide
DMP	Dess-Martin periodinane
DMPK	Drug metabolism and pharmacokinetics
DMSO	Dimethylsulfoxide
DLT	Dose limiting toxicity
EC_{50}	Half maximal effective concentration
e.g.	*Exempli gratia*
EI	Electron impact

F	Bioavailability
FMOC	Fluorenylmethyloxycarbonyl
fu	Fraction unbound
GC-MS	Gas chromatography mass spectrometry
GI_{50}	Concentration required to achieve 50 % growth inhibition
h	Hour
hERG	Human *ether-a-go-go* related gene
HKLP2	Human kinesin-like protein 2
HPLC	High performance liquid chromatography
HRMS	High resolution mass spectrometry
hs	*Homo sapiens*
HT	High throughput
IC_{50}	Median inhibitory concentration
i.e.	*Id est*
iv	Intravenous
K_i^{app}	Estimated apparent K_i value
KSP	Kinesin spindle protein
LC-MS	Liquid chromatography–mass spectrometry
L.E.	Ligand efficiency
m	*Meta*
m-CPBA	*Meta*-chloroperoxybenzoic acid
MCAK	Mitotic centromere-associated kinesin
MDR	Multidrug resistance
MIA	Maximum observed inhibitory activity
min	Minute
Mont. KSF	Montmorillonite KSF clay
Mpt.	Melting point
MS	Mass spectrometry
MT-stimulated	Microtubule-stimulated
MTD	Maximum tolerated dose
MWt	Molecular weight
n/a	Not available/applicable
n-BuLi	*n*-Butyllithium
Ncd	Nonclaret disjunctional
NCI	National Cancer Institute

n.d.	Not determined
n.i.	No inhibition
NMR	Nuclear magnetic resonance
o-	*Ortho*
p-	*Para*
po	*Per os* (by mouth)
p-TSA	*para*-Toluenesulfonic acid
PAMPA	Parallel artificial membrane permeability assay
PBS	Phosphate buffered saline
PgP	P-glycoprotein
PLK	Polo-like kinases
ppm	Parts per million
rac-	Racemate
RNA	Ribonucleic acid
RNA*i*	Ribonucleic acid interference
rt	Room temperature
RTV	Relative tumour volume
SAR	Structure activity relationship
STDC	*S*-trityl-D-cysteine
STLC	*S*-trityl-L-cysteine
t	Time
$t_{½}$	Half life
t_{max}	Time to reach peak plasma concentration after administration
T3P®	2,4,6-Tripropyl-1,3,5,2,4,6-trioxatriphosphinane 2,4,6-trioxide
TBAF	Tetra-*n*-butylammonium fluoride
t-BOC	*tert*-Butoxycarbonyl
T/C	Treatment group to control group ratio
TFA	Trifluoroacetic acid
THF	Tetrahydrofuran
TPX2	Targeting protein for XKLP2
V_D	Apparent volume of distribution
w/v	Weight/volume
XKLP2	*Xenopus* kinesin-like protein 2
Z	Zosuquidar trihydrochloride

List of Figures

List of Tables

List of Schemes

Chapter 1. Introduction

1.1. An overview of anti-mitotic therapy

1.1.1. Cancer

1.1.1.1. Overview

The war on cancer was formally declared in 1971.[2] In the subsequent years, protracted efforts have yielded many improvements in cancer care and treatment.[3] However, many manifestations of this complex and heterogeneous disease remain intractable to medicine's best efforts.[4] Cancer is a disease characterised by uncontrolled cell proliferation,[5] and the targeting of cellular division represents a key strategy in its treatment. Anti-mitotic chemotherapy formed the cornerstone of initial approaches to treat and suppress malignancies,[6] and now the radical and elegant subsequent demarcation of mitosis into distinct mechanistic stages regulated by a complex symphony of proteins allows for the design of more specific and targeted therapies. Our aim has been to design one such new therapy, through targeting a crucial protein to mitosis.

1.1.1.2. The hallmarks of cancer

Cancer is an exceedingly complex and heterogeneous group of disease states. Decades of endeavour however have yielded great progress in our understanding of cancer biology and tumourigenesis, summarised succinctly by Hanahan and Weinberg in 2000.[5] In this seminal paper, they outlined the hallmarks of cancer: six acquired characteristics which collectively give rise to cancerous disease states (Figure 1).

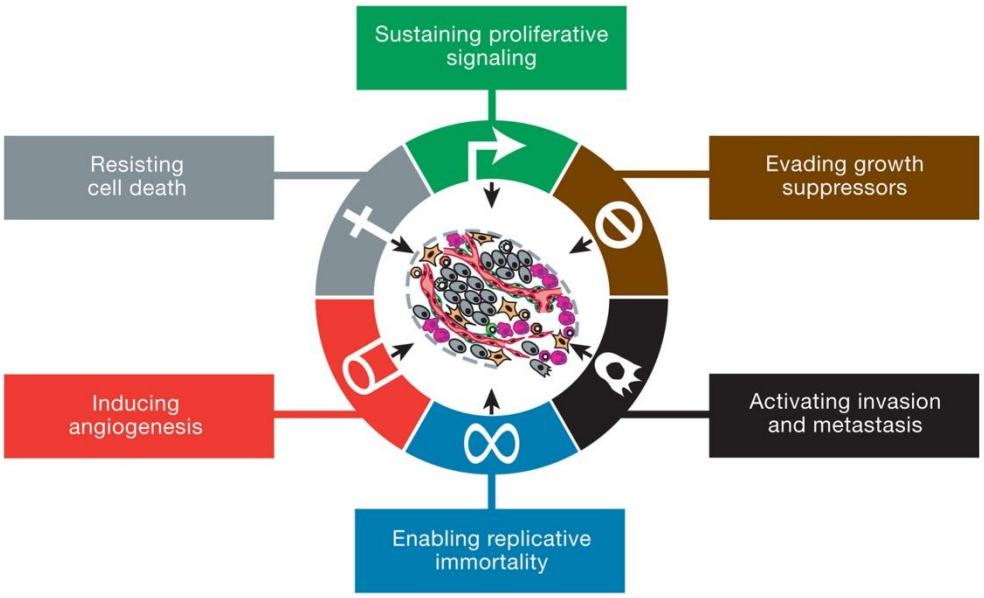

Figure 1 – The hallmarks of cancer.

Six acquired characteristics proposed to form an underlying basis for the majority of cancerous disease states. Reproduced with permission from reference 7. Copyright 2011, Elsevier.

These attributes, which may be acquired in parallel and in various orders, are proposed to provide an underlying basis for tumourigenesis. Self-sufficiency in growth signals and insensitivity to anti-growth signals describes the ability of tumour cells to become independent of and insensitive to the body's natural growth signals that regulate normal tissue proliferation. Apoptosis causes significant attrition to cell populations as tumours develop, and the ability to evade programmed cell death forms a further stage in carcinogenesis. Collectively, these three abilities involving deregulation from routine cellular growth mechanisms are not sufficient for tumour development, as normal cells are still replicatively limited. To enable continued expansion, malignant cells develop unlimited replicative potential through maintenance of telomeres and evading senescence. Tumour cells require nutrition to fuel their growth, and to accomplish this acquire the ability to induce and sustain angiogenesis. The invasion of surrounding tissues is ultimately the cause of lethality in 90% of cancer patients,[8] and the ability to metastasise which is typically the final change in the progression of cancer.[5]

1.1.1.3. Emerging hallmarks

In the subsequent years since the demarcation of the six initial hallmarks of cancer, four additional emerging or enabling characteristics have been recognised.[7] The emerging hallmarks are the ability of cancer cells to adjust cellular energy metabolism to limit it principally to glycolysis, and the implicit ability for nascecent malignancies to evade detection or destruction by the immune system. Of the enabling characteristics, while not a direct function of tumour cells, it is now recognised that the inflammatory response of the body to tumour cells actually can be counterproductive and may favour and accelerate tumour progression. Finally, guard systems which ensure genomic integrity under normal circumstances operate efficiently to ensure mutation rates in cell populations are low. Cancer cells exhibit multiple mutations which suggests malfunction of these guardian pathways, leading to increased rates of mutation, thereby enabling the emergence of other hallmarks. Strategies targeting all these traits are under investigation, with our focus on disrupting the unregulated growth of cells.

1.1.2. Cell division

1.1.2.1. The stages of mitosis

Mitosis is the process by which a single cell divides, through a coordinated and discrete series of mechanical events to produce two genetically identical daughter cells (Figure 2).[9-11] At the onset of mitosis in prophase, chromosome condensation commences and is accompanied with a change in the dynamics of cytoplasmic microtubules and the separation of the duplicated centrosomes. These nucleate two asters of microtubules which will go on to form the poles of the nascent mitotic spindle. At prometaphase, the nuclear envelope breaks down and the chromosomes begin attaching to the microtubules of the developed bipolar spindle. This attachment is mediated by protein complexes termed kinetochores. Metaphase is reached upon complete attachment to the spindle apparatus. The chromosomes then congress and align to the metaphase plate, at a point equidistant between the two centrosome poles, prior to the commencing anaphase. This is achieved by a combination of microtubule dynamics and mitotic proteins. During anaphase the sister chromatids separate. Initially in anaphase A, each translocates to a spindle pole before spindle elongation in anaphase B. The nuclear envelope reforms on each chromatin in telophase, before cytokinetic separation of the two daughter cells.

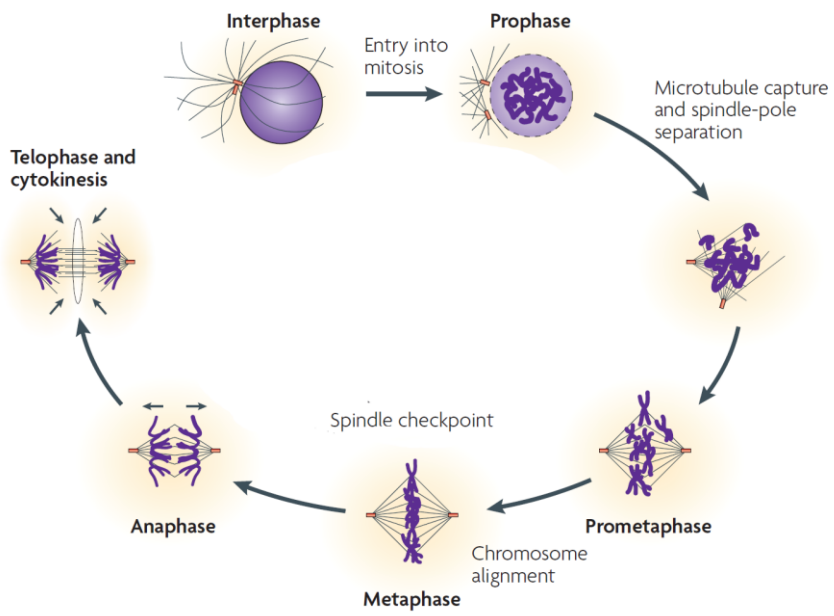

Figure 2 – Schematic illustration of the phases of mitosis.

Modified from reference 12.

1.1.2.2. The mitotic spindle

The mitotic spindle apparatus serves as the fundamental mechanical platform through which many of the processes described above occur. It is a self-organising molecular machine whose primary role is separation of the duplicated set of chromosomes to disparate locations within the cell through transport to either end of its poles (Figure 3).[13] Half of a replicated chromosome must arrive at opposite spindle poles for accurate genetic partition in the formation of two healthy daughter cells. Chromosomal segregation is achieved through two mechanisms, both of which are reliant on the microtubule scaffold of the spindle. Microtubules are rigid and polar polymers formed from α- and β-tubulin heterodimers which exhibit complex polymerisation dynamics during which they rapidly polymerise and depolymerise. The most prevalent expression of this behaviour in cells is termed dynamic instability.[14] Associated with this activity is the hydrolysis of GTP by β-tubulin subunits to produce energy for mechanical work.[13, 14] The second way in which microtubules facilitate separation is by serving as tracks utilised by the mechanochemical proteins involved in mitosis (section 1.2.2.2).[15]

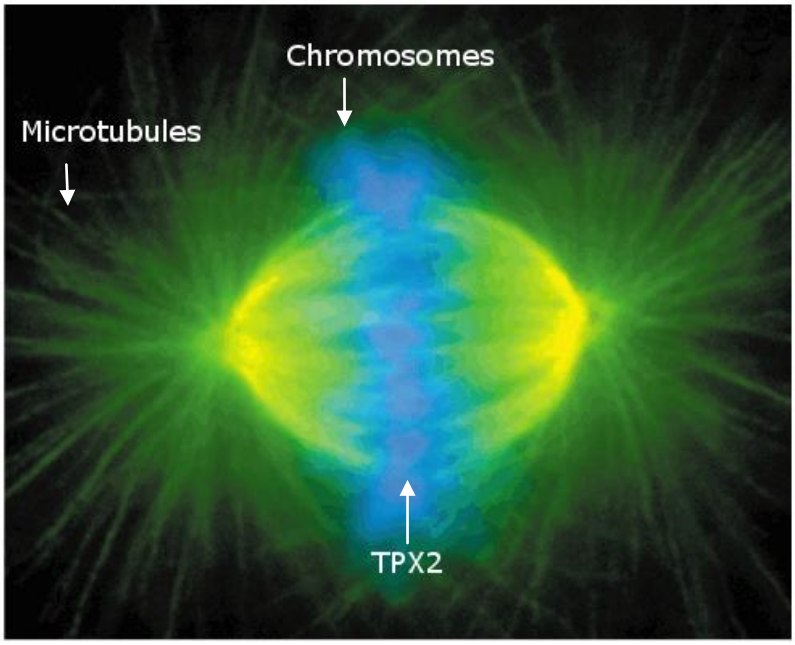

Figure 3 – The organization of the mitotic spindle *in vitro*.

A static immunofluorescence photograph of a mitotic spindle from a cell in tissue culture. Key to immunostaining: microtubules appear in green; chromosomes in blue; TPX2 (a protein involved in spindle pole organization)[16] in red; overlapping TPX2/microtubule regions are yellow. Modified from reference 13.

1.1.3. Anti-mitotic drugs

1.1.3.1. Targeting the mitotic spindle

All present anti-mitotic drugs target the mitotic spindle and interfere with the dynamics of microtubule polymerisation.[14, 17] They may be classed into three families based on chemical structure: vinca alkaloids, taxanes and epothilones (**1-3**, Figure 4). While each binds to an independent site on the β-tubulin microtubule subunit, the principles underlying the mechanism of action are conserved for the three classes. Rapid modulation of the dynamic equilibrium is required throughout all stages of mitosis, and interference from microtubule binding drugs has a profound knock-on effects on the mitotic spindle's ability to accurately segregate chromosomes.[14] Structural aberrations in the spindle are typically detected by the constitutive spindle assembly checkpoint,[18] resulting in mitotic arrest which ultimately leads to programmed cell death.[19] While this covers the overall fundamental behind microtubule binding drugs, the specific attributes and effects of each class are distinct and complex.[14, 17] Vinca alkaloids depolymerise microtubules, whilst the taxanes and epothilones stabilise microtubules, resulting in extensive formation of αβ-tubulin heterodimers.[14] In the case of the taxanes, the nature of the effects on microtubule polymerisation is known to be dependent on drug concentration.[20, 21] Taxanes have also been observed to be cytotoxic against cells in both mitosis and interphase, and are likely to induce cell death through multiple mechanisms.[22] Epothilone A (**3**) has been demonstrated to occupy the same cavity on β-tubulin as paclitaxel (**1**), however while the binding sites overlap, the two molecules bind in distinct conformations through discrete interactions and do not share a pharmacophore.[23] While understanding the complexity exhibited by these cytotoxic drugs in relation to their effects on tumours remains a non-trivial affair, they possess great clinical utility.[19, 24] The taxane family members paclitaxel and docetaxel are used in therapy against two of the most prevalent forms of the disease in the United Kingdom, lung and breast cancer.[12, 25] Clinical applications of vinca alkaloids include the treatment of lymphomas, acute leukaemias and testicular cancer.[12] Another class of natural products known to interfere with microtubule dynamics is the epothilones. Epothilone A (**3**) has recently been approved in the US in combination with capecitabin in treatment of locally advanced or metastatic breast cancer, including those resistant to previous therapies.[17] Serious shortcomings however persist with microtubule binding treatments: namely toxicity and resistance.

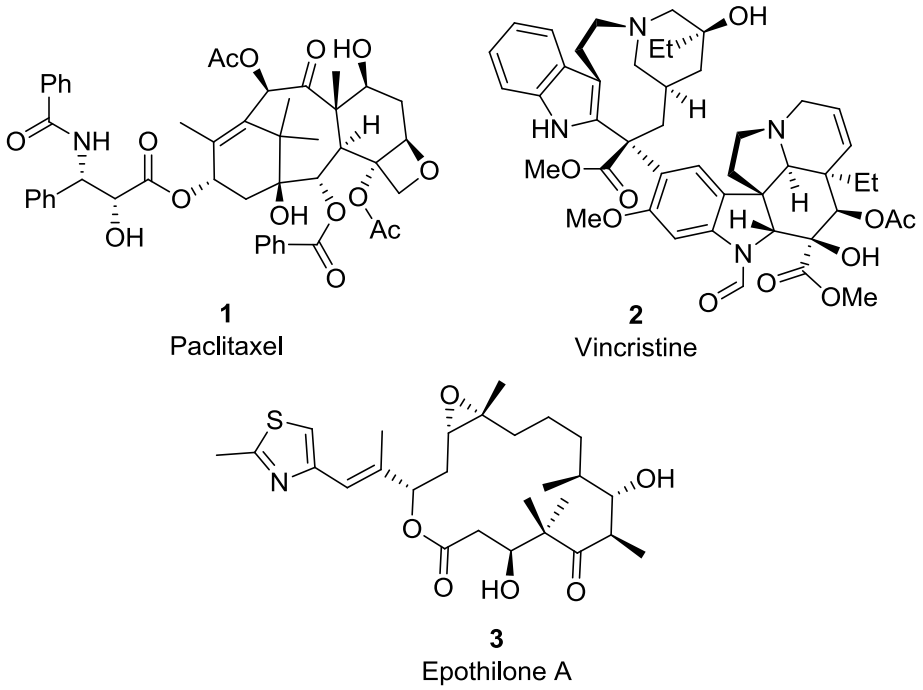

Figure 4 – Structures of selected microtubule based anti-mitotic drugs.

Members of the taxane, vinca alkaloid and epothilone families respectively: paclitaxel (1), vincristine (2) and epothilone A (3).

1.1.3.2. Limitations of microtubule based anti-mitotic agents

Taxanes and vinca alkaloids are highly cytotoxic agents and use in therapy gives rise to serious adverse effects.[12, 26] As a key constituent of the cytoskeleton, microtubules possess a number of functional roles outside of mitosis, including in axonal transport in neurons.[27] Resultantly, peripheral neuropathy is a common and severe toxicity amongst microtubule targeting drugs.[28] Myelosuppresion, resulting from the cytotoxicity of anti-mitotics towards rapidly proliferating bone marrow cells is another regularly encountered dose limiting toxicity (DLT).[12, 26, 29]

The other major concern with these regimens is resistance, which may be either acquired or innate. Certain cancers remain unresponsive to currently available anti-mitotic chemotherapies,[4] and determining the factors that govern tumour chemosensitivity is one of the most profoundly important currently unresolved questions in cancer chemotherapy.[5, 19, 24] Acquired resistance can emerge through mutations affecting drug binding or by differing expression levels of β-tubulin isotypes.[30] High levels of expression of the βIII tubulin isotype are associated with more aggressive tumours and increased resistance to chemotherapy. Efficacy is also known to be reduced through increased expression of microtubule-associated proteins which regulate microtubule polymerisation dynamics, and can stabilise them against depolymerisation. In leukaemia, evidence suggests other

cytoskeletal proteins can also affect chemosensitivity.[30, 31] Another pathway for resistance aside from epigenetic factors involves transmembrane proteins. The ATP-binding cassette (ABC) encoded family of cellular efflux pumps function to remove xenobiotics from the cellular environment, and their presence can reduce drug efficacy and lead to the emergence of multi drug resistance in tumour cells.[32] Although the physiological relevance in human cancers remains to be entirely discerned, the vinca alkaloids and taxanes are both recognized substrates for the ABC-encoded P-glycoprotein (Pgp) pump.

1.1.4. The next generation of therapeutic agents

1.1.4.1. Improvements to treatments and new cellular targets

The broad clinical efficacy and commercial success of current microtubule binding drugs, and conversely their well defined limits have led to extensive investigations aimed at improving them.[12, 17, 33] This has yielded some success with many novel and modified agents: the recently approved epothilone ixabepilone® displays activity against the previously resilient βIII tubulin isotypes and is not subject to efflux by Pgp, whilst a new formulation of paclitaxel with albumin affords reduced toxicity.[17, 34] Focus has also turned to novel routes of intervention in mitosis that overcome the limitations relating to microtubule targeting drugs by acting on more specific targets. The anti-tumour activity of the vinca alkaloids and taxanes were first discovered in the 1950s and 1970s respectively,[35, 36] and since then the complex processes controlling mitosis have been elucidated in extraordinary detail and revealed a myriad of target proteins. Principle amongst the potentially druggable targets are members of the kinase and kinesin families.[12, 33, 37] Our group has been investigating the kinesin motor proteins involved in mitosis as potential targets in cancer chemotherapy (section 1.2.2.2). As instigators of phosphotransfer cascades integral to signalling transduction, protein kinases have emerged as one of the most important classes of oncological drug targets of recent years.[38] Kinases may contribute to cancer biology through occupying key roles in oncogenic signalling cascades, acting to aid tumour growth and development, or mutationally activated kinases which may themselves trigger oncogenic transformations, of which interference with the latter is a proven strategy for therapeutic intervention.[39] Of the kinases involved in mitosis, the most intensively investigated as therapeutic targets are the polo-like kinase and Aurora kinase families. For more detailed information on the involvement of kinases in the cell cycle and as oncology targets, the reader is referred to a number of excellent reviews.[38-40]

1.1.4.2. Aurora kinases

Three members of the Aurora family are known in humans, Aurora A, B and C, and their primary functions relate to the accurate alignment and segregation of chromosomes to ensure genomic integrity is maintained during mitosis.[10, 41] Aurora A has a critical role in regulating the timing of entry into mitosis, centrosome maturation and is also involved in spindle assembly and centrosome separation through phosphorylation of the kinesin motor protein Eg5 (section 1.2.3).[41, 42] Aurora B is critically involved in the early stages of mitosis through regulating proteins affecting spindle microtubule dynamics during spindle

formation, subsequently encouraging correctly aligned chromosomal kinetochore attachment to the developed spindle and regulation of the spindle checkpoint controlling further progression.[41] In the latter stages of mitosis, Aurora B assists in spindle cleavage furrow formation which is required for the successful completion of cytokinesis. The role of Aurora C is much less well delineated, although it may overlap with that of Aurora B. Interestingly, with the exception of in the testis, the expression of Aurora C is comparatively limited.[12] Inhibitors with pan-Aurora specificity or selectivity for either Aurora A or Aurora B have reached clinical trials, with the most advanced in phase 2.[41, 43] However, it is not yet apparent which of the Aurora family members represents the best therapeutic target and the response to the first round of clinical candidates has been limited, with the best responses to date in leukaemic cancers.[44]

1.1.4.3. Polo-like kinases

The other heavily investigated family of mitotic kinases are the polo-like kinases (PLK), of which five members (PLK1, PLK2, PLK3, PLK4 and PLK5) are present in humans.[45] Only PLK1 is highly expressed in mitosis, with the roles of the other family members much less clearly understood.[12, 45] PLK1 is pivotal to the regulation of multiple key events throughout cell division, including controlling entry into mitosis and centrosome maturation, enabling separation of replicated sister chromatids through phosphorylating a binding protein termed cohesion, and also in kinetochore dynamics initiating anaphase.[45] A number of roles for PLK1 are also apparent in cytokinesis and leading to mitotic exit, including regulating the kinesin motor protein MKLP2 in cytokinesis and phosphorylating enzyme complexes involved in cleavage furrow formation. Elevated PLK1 expression is apparent in multiple cancers and corresponds to a poor prognosis, which may be linked to its ability to negatively regulate the important tumour suppressor p53.[45, 46] As such a significant mitotic regulator, PLK1 has emerged as an important prognostic and therapeutic oncology target, with several inhibitors now in phase 2 clinical trials.[47] Modest responses have been recorded for the inhibitors for which data is available, with the most promising indications in non-small cell lung cancers.[44, 47]

1.2. Molecular motors in cell division

1.2.1. The kinesin superfamily

1.2.1.1. Overview

Eukaryotic cells possess a plethora of molecular machines that coordinate intracellular transport, and are fundamental in organising the cellular architecture. They are categorised into three protein superfamilies: myosin, kinesin and dynein.[48-50] All employ hydrolysis of adenosine triphosphate (ATP) to produce a directed force along microtubule (or actin for dynein tracks) in performing their multiple roles. The kinesins comprise of a superfamily of at least 650 distinct microtubule dependent motor proteins, so far found only in eukaryotes.[51] This superfamily is divided into fourteen families (kinesin-1 to kinesin-14) by phylogenetic analysis of their characteristic motor domains of 330-440 residues in size.[52] Outwith their motor domains however, they are structurally divergent with very little sequence conservation. The motor domain is situated at either the N-terminal (N-type kinesins), internally (Kin I/ M-type kinesins), or the C-terminal (C-type kinesins).[49] N-terminal motors move towards the plus-end of microtubules (β-tubulin), whereas C-type kinesins travel to the microtubule minus end (α-tubulin). M-type kinesins (kinesin-13) diffuse rather than move along microtubules until the end where they show microtubule depolymerisation activity.[53]

1.2.1.2. Structure of N-type kinesins

The first member of the kinesin family to be identified was conventional kinesin (Kif5s, Kif5B, KHC, kinesin-1 family),[54, 55] which is ubiquitously present in the human body as a protein dimer consisting of identical heavy chains conjoined through a pair of light chains.[56] A prototypical N-terminal kinesin, it consists structurally of three distinct domains (Figure 5).

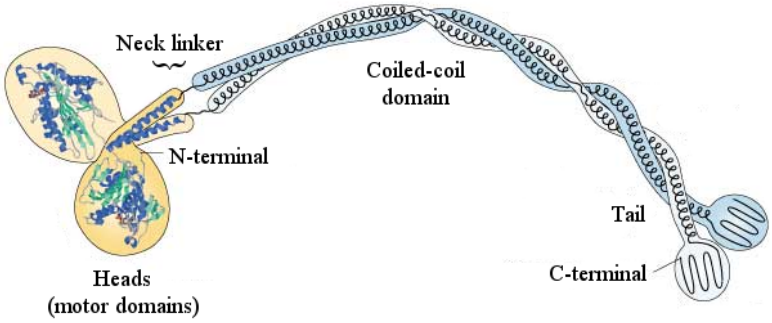

Figure 5 – Domain organisation of conventional kinesin, a typical N-type kinesin. Modified from references 42 and 57.

The conserved motor domain contains the nucleotide binding pocket and microtubule interacting regions, followed by a neck/neck linker region. This connects the motor domain to an internal α-helical region, thereby forming a coiled coil which is responsible for oligomerisation into dimers or higher oligomers. Following the coiled-coil region is the C-terminal tail domain, where interactions with cargo occur either directly or indirectly. This site affords kinesins their diverse functionalities across transport, meiosis and mitosis.[49, 51]

1.2.2. Kinesin functions

1.2.2.1. Intracellular transport

Kinesins are extensively involved in intracellular transport. In axonal transport, they are responsible for movement of mitochondria, synaptic membrane and vesicle precursors, while in dendritic transport their cargoes include vesicles and messenger RNA protein complexes.[51] Outside these processes, their roles include transport from the Golgi apparatus and translocation of lysosomes and endosomes. Microtubule dynamics depend heavily upon kinesins.[58] As well as an indirect influence through transporting microtubule regulators, kinesins directly affect microtubule dynamics, and are extensively involved in mitosis.

1.2.2.2. Kinesins in mitosis

The mitotic spindle apparatus serves as a suitable substrate for kinesin based motility events that lead to the generation of forces necessary for bipolar spindle formation, chromosome congression to the metaphase plate and segregation during anaphase, as well as cytokinesis.[59] The establishment of a bipolar spindle requires the separation of the duplicated centrosomes through the sliding of overlapping antiparallel microtubules, a process which requires the collaboration of different plus-end directed kinesins, such as Eg5 and Kif15/HKLP2, as well as the antagonistic action of minus-end directed motors including KifC1/HSET and dynein.[60] Chromosomal dynamics are also controlled by members of the kinesin-4 and kinesin-10 families termed chromokinesins: these associate to chromosome arms during mitosis, and contribute to the generation of forces, named polar ejection forces, that push the chromosome arms away from the poles and counter forces that drive chromosomes towards the poles.[61] This generates the oscillatory motion of chromosomes observed in vertebrate cells.[62] Kif18A, a member of the kinesin-8 family, is also known to be involved in chromosome congression in prometaphase.[63, 64] Kinesins such as CENP-E contribute to the process of chromosomal congression to the metaphase plate, and to the capture of microtubules by the kinetochores.[65, 66] At the same time, kinetochore associated Kif18A dampens microtubule dynamics,[67] while depolymerising kinesin-13 family members promote destabilisation of the microtubule-kinetochore interactions.[68] Such kinesin driven microtubule depolymerisation contributes to kinetochore microtubule dynamics,[69] and is involved in the mechanism through which kinetochores correct erroneous microtubule attachment states to ensure genomic stability.[70] During post-metaphase events, MKLP-2 is responsible for the relocation of the

chromosome passenger protein complex from the inner centromeres to the central spindle in anaphase.[71] All kinesin-6 family members and Kif4 undertake roles in the translocation of the regulatory proteins to the spindle midbody, and are necessary for completion of cytokinesis.[71-74]

1.2.2.3. Kinesin inhibitors for chemical biology and therapy

Inhibitors of mitotic kinesins may act as biochemical tools through which the processes involved in mitosis may be understood further and to investigate potential pathways for treatment.[59, 75, 76] The synergistic activity of multiple antagonistic and complementary motor proteins, such as the kinesins described, is responsible for controlling the dynamic balance witnessed during spindle morphogenesis and subsequent chromosome movements. Interference with RNA*i* has suggested that at least twelve human kinesins are essential for the successful completion of cell division.[63] It therefore follows that inhibition of these kinesins with specific small molecule inhibitors can elucidate the mechanisms underlying mitosis and their key regulators, and significantly may be used to disrupt mitosis for therapeutic purposes. While understanding the physiological relevance of many of the kinesins described above will take further investigations, kinesin-5 family member Eg5 already represents an attractive target in cancer therapy.

1.2.3. Homo Sapiens Eg5

1.2.3.1. Structure and regulation

Human Eg5 (*hs*Eg5, Kif11, KSP, kinesin spindle protein, KNSL1; kinesin-5 family) is a N-type kinesin involved in assembly of the bipolar spindle in the early prometaphase stage of mitosis.[77, 78] The founding member of the kinesin-5 family, known as "blocked in mitosis" (BimC) kinesin, was identified in *Aspergillus nidulans* in 1990.[79] It is structurally distinct amongst kinesins as it forms a homotetramer consisting of two parallel homodimers arranged in antiparallel association.[80, 81] Eg5 travels towards the plus-end of microtubule tracks,[80] however it moves relatively slowly[63, 65] when compared to conventional kinesin.[82] Targeting of Eg5 to the spindle is proposed to occur through phosphorylation of a threonine in a consensus sequence (BimC box) in the C-terminal tail domain by Cyclin-dependent kinase-1 (Cdk1).[78] TPX2 (targeting protein for XKLP2) has additionally been demonstrated to regulate Eg5 activity and localisation,[83] while in *Xenopus laevis* the kinase Aurora A also regulates Eg5.[42]

1.2.3.2. In mitosis

Across a variety of fungal, insect and vertebrae cells kinesin-5 orthologs are critical in establishing spindle bipolarity through separating the duplicate spindle poles.[84] The homotetrameric structures of kinesin-5 family members are proposed to help them achieve this through the crosslinking of antiparallel arrays of oppositely polarized microtubules, and sliding them apart through their processive movement (Figure 6). This behaviour has been observed directly *in vitro* during assays which examined the motion of *Xenopus* Eg5 along immobilised microtubule tracks while cross-linked to free bundles of microtubules.[85] Eg5 orthologs in non-mammalian species are required once spindle bipolarity has been established for maintaining the spindle.[84] The evidence for this role in mammalian cells remains ambiguous;[84, 86] other kinesins are known to facilitate this activity in humans, such as the depolymerising Kif2a (kinesin-13 family) and another plus-end directed N-type kinesin HKLP2 (kinesin-12 family), suggesting that the involvement of Eg5 is likely to be secondary.[49, 74, 75]

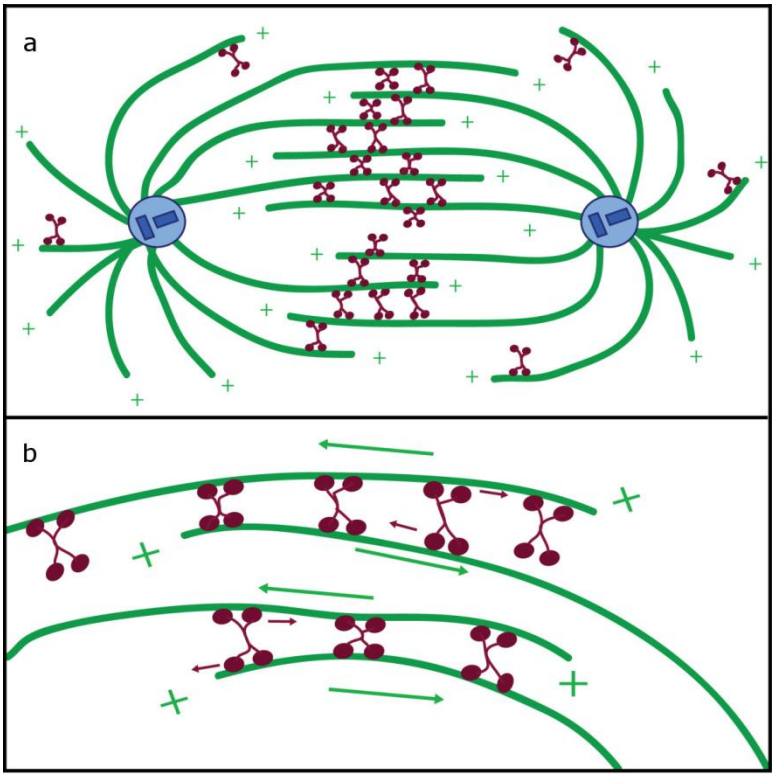

Figure 6 – Schematic depictions of the role of Eg5 in organising spindle bipolarity.

In Figure 6a, the tetrameric Eg5 motors (red) have organised the microtubules (green) nucleated from the centrosomes (blue) to form a stable bipolar spindle. Figure 6b illustrates Eg5 crosslinking the antiparallel microtubule arrays and consequently shifting both polewards. Modified from reference 82.

1.2.3.3. Outwith mitosis

The role of Eg5 outside mitosis remains much less investigated than in cell division, however a number of functions have been identified. Most recently Eg5 was identified to be active during interphase in translation: the efficiency of polypeptide synthesis decreased when Eg5 was depleted by RNA*i* or small molecule inhibition in a mammalian cell line.[87] This study by Bartoli *et al.* was the first to detect Eg5 activity in interphase, so the specific attributes of its involvement remain to be explicitly deciphered. Eg5 is also expressed in terminally post mitotic neurons and may have a role in neuronal development.[88] Neurons form the backbone of the central nervous system, and neuronal growth enables the formation signalling pathways throughout the body.[89] Each neuronal cell in vertebrates contains a single projecting axon and multiple branched dendrites whose cytoskeleton is comprised of microtubules. As with the mitotic spindle, multiple microtubule-based motors are conceived to coordinate and manage their structural organisation and development.[88, 89] Eg5 was initially identified as being present in terminally differentiated neurons in *Mus musculus*, and subsequently was recognised to regulate the microtubule growth of axons and dendrites. Depletion or inhibition of Eg5 in axons results in a temporal rapid growth increase (Figure 7).[90, 91]

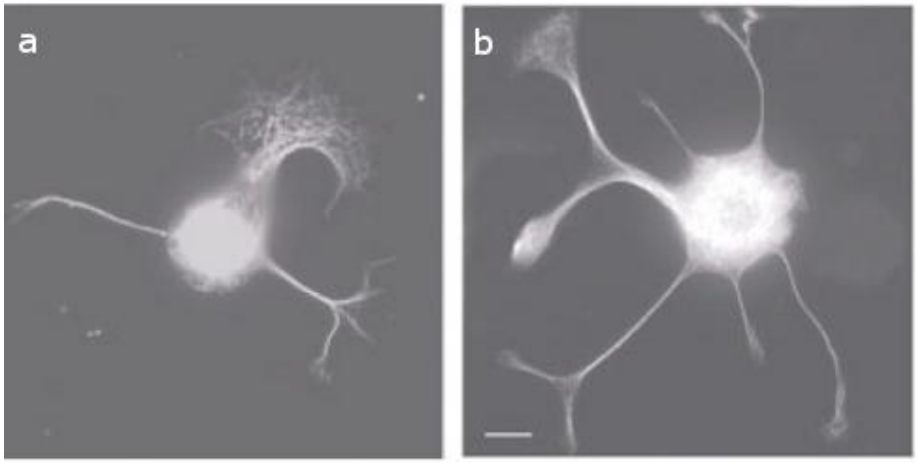

Figure 7 – Eg5 controls the rate of axonal growth in rat sympathetic neurons.

Cultures are immunostained for β-III tubulin. Figure 7a: neurons without Eg5 inhibitor visualised 4 h after plating. Figure 7b: neuronal growth after 4 h in the presence of the small molecule Eg5 inhibitor monastrol (4). Reproduced with permission from reference 90. Copyright 2004 John Wiley & Sons, Inc.

This “growth cone” of projected microtubules however appears uncontrolled and unable to turn appropriately to reach the intended synapse.[92] In dendrites, inhibition of Eg5 with the specific small molecule inhibitor monastrol (section 1.2.4.1) results instead in a prolonged, rather than temporal, increase in observed growth.[91] Collectively, these studies suggest that Eg5 may serve to regulate the growth of these microtubule emanations through cooperation with cytoplasmic dynein.[91, 93, 94] As a much slower motor than dynein,[80] its effect may be to limit the rate at which the faster motor performs its work.[94] The mechanics behind the manipulations of microtubules by the kinesin in these regions are yet to be completely elucidated, although antiparallel arrays of microtubules are known to be present towards the leading process of migratory neurons.[94]

1.2.4. Inhibition of Eg5

1.2.4.1. Monastrol and the loop L5 allosteric site

Interest in the mitotic kinesins as potential targets in cancer treatment began following the discovery of the first selective mitotic kinesin inhibitor, the 1,4-dihydropyrimidine-based compound monastrol (**4**, Figure 8a).[95] This inhibitor weakly and selectively inhibits Eg5 in a reversible manner and was identified in a high throughput (HT) phenotype based screen targeted towards identifying novel anti-mitotic agents. Exposure to cells produced a distinctive monoastral spindle phenotype in cells comparable to that observed with RNA*i* mediated depletion (Figure 8b).[63, 95]

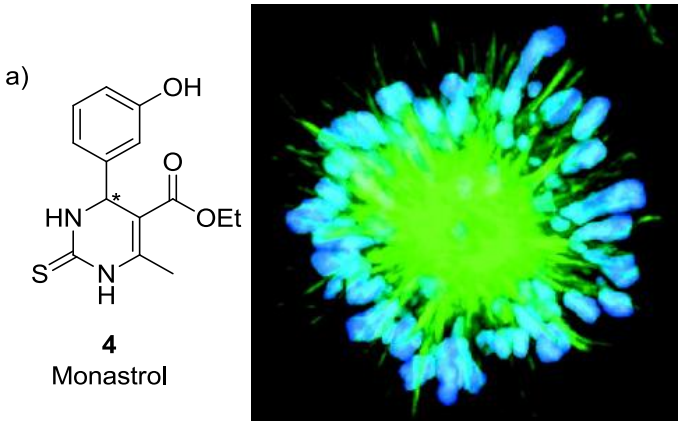

Figure 8 – a) Structure of monastrol (4); b) the "monoastral" monopolar inhibition phenotype. BS-C-1 cells were treated with 68 µM monastrol for 4 h and immunofluorescence stained. α-Tubulin is green, chromatin appears in blue. Modified from reference 95.

This was the first example of a compound which disrupted the mitotic spindle apparatus selectively without affecting tubulin. Biochemical characterisation revealed **4** as ATP uncompetitive and non-competitive towards microtubules, suggesting an allosteric mode of action.[96] The crystal structure of the ternary monastrol·Eg5·ADP complex was solved and confirmed binding at an allosteric site formed by helix α2/loop L5 and helix α3, approximately 12 Å removed from the nucleotide (Figure 9).[97] Amongst the kinesins, monastrol is specific for Eg5,[95, 98] and remarkably is also specific within the kinesin-5 family for only the vertebrae homologs.[99] This specificity has been attributed to the length of the loop L5 which forms the induced fit site;[97] Turner *et al.* found this loop to be longest in kinesin-5 orthologs from a panel of nine kinesins from three different families.[100] That non-mammalian kinesin-5 orthologs such as *A. nidulans* BimC are not inhibited does suggest a deficit in our understanding.

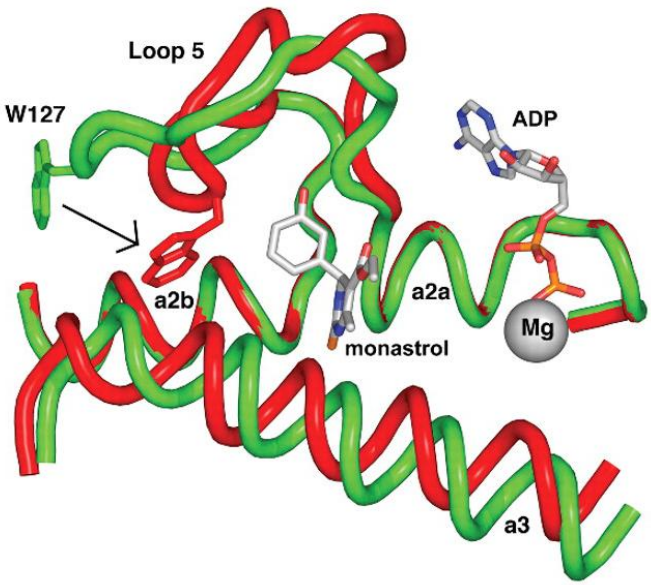

Figure 9 – A comparison of the crystal structure of Eg5·ADP in the absence (green) and presence of monastrol (red).

Note the translocation of the loop L5 with the terminal Trp 127. Modified from reference 101.

1.2.4.2. Eg5 as a cancer target

After the discovery of monastrol and its biochemical elucidation, several more selective allosteric Eg5 inhibitors were identified that also induced mitotic arrest *in vitro*.[102-104] The first to demonstrate anti-tumour activity *in vivo* was CK0106023 (**5**, Figure 10).[105]

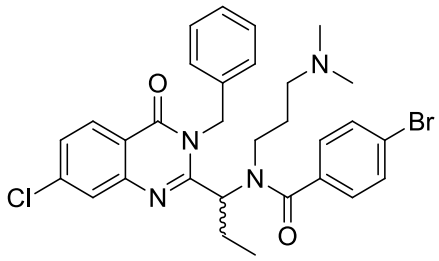

5
CK0106023

Figure 10 – Structure of the quinazoline derivative CK0106023.

Exposure to **5** produced robust mitotic arrest in a number of cancer cell lines, including several subject to multidrug resistance (MDR). During xenograft studies with nude mice bearing human ovarian carcinoma SKOV3 tumours, **5** exhibited comparable anti-tumour activity to paclitaxel. Tumour growth was inhibited by treatment with CK0106023 by on average 71% at 25 mg/kg, with a single partial regression in a cohort of eight mice. Treatment with paclitaxel at its maximum tolerated dose (MTD) of 20 mg/kg afforded 73% average growth inhibition. Characterisation of CK0106023 confirmed selectivity amongst kinesins for Eg5 and correlated with the biochemical mode of action displayed by monastrol. Excised tumours displayed the phenotypical monopolar mitotic spindles seen in cell culture (Figure 8b), implying efficacy through the proposed mechanism of action. This triggered enormous interest in Eg5 as a new oncology target, subsequently leading to the development of numerous potent and selective inhibitors acting at the loop L5 pocket.[76, 106, 107] Inhibition of Eg5 is now validated as a potential route to disrupt mitosis in a broad spectrum of cell culture and tumour xenograft experiments. These include in paclitaxel resistant tumour cells,[108] and in a large scale nude mice xenograft experiments with the clinical candidate ispinesib (section 1.4.1), complete responses were recorded for a number of tumours of varying histological origins.[109] Investigation into the role of Eg5 in cancer has identified overexpression in a number of cancers, although this could simply be as a result of increased proliferation.[110-112] In mice, overexpression has been shown to cause errors in chromosome segregation leading to aneuploidy; the physiological relevance of these findings however remains to be defined.[113]

1.2.4.3. Structural origins of inhibition

The involvement of loop L5 provides the mechanical basis for the allosteric inhibition of Eg5. Kinesin motility is controlled by a series of conformational changes cascading throughout the protein upon ATP binding, hydrolysis and subsequent ADP release, which in turn determines affinity towards microtubules.[114] Amidst these processes, the conserved region known as the "neck linker" switches upon ATP binding from a mobile free state to a rigid docked pose, and in doing so swings from a rearward facing position towards the plus-end of microtubule tracks.[115] This swing of the neck linker drags the cargo attached to the COOH terminus, and also conveys the structural changes necessary for processivity in kinesin oligomers.[114] Key to controlling these processes is the ɣ-phosphate sensing machinery, comprising of switch I and switch II, which through interacting with each other and forming H-bonds to the ɣ-phosphate of the bound nucleotide, conduct the conformational changes from the nucleotide site to the neck linker that realise docking, and consequently kinesin motility. Although the loop L5 allosteric site on Eg5 is distal from the neck linker, local inhibition induces a ~ 6 Å shift in the main chain of switch I, and crucially, widens the gap between switch II helices α-4 and α-5 by ~ 6 Å (Figure 11).[97] This opens a space into which the neck linker docks into a stable rigidified conformation. Kinetic investigations into monastrol binding have found that during inhibition, the Eg5:ADP complex stabilises and the rate of ADP release is dramatically decreased.[116] Thus when the L5 allosteric pocket forms, the neck linker remains locked, and the Eg5 motor is unable to process along microtubules to form the bipolar spindle.

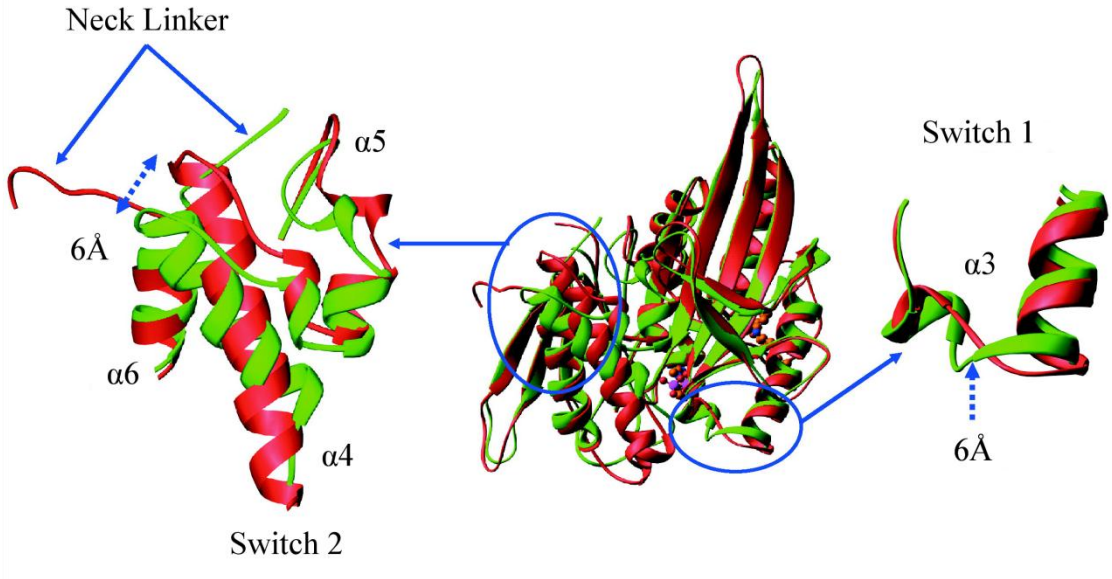

Figure 11 – Comparison of the conformation of switch I, switch II and the neck linker before (red) and after monastrol binding (green).

The depicted region is the switch-2 region, which is located on the opposite side of the motor domain from the monastrol binding site. Modified from reference 97.

1.2.4.4. Cell death mechanism

How Eg5 inhibitors trigger cell death *in vitro* has been revealed in great detail. After mitotic arrest, the spindle checkpoint is activated which eventually results in cell death in certain tumour cell lines. [108, 117] This occurs primarily *via* the intrinsic apoptotic pathway, with mediation by the proapoptotic protein Bax and subsequent caspase activation.[117, 118] A number of other cell fates may also take place (Figure 12).

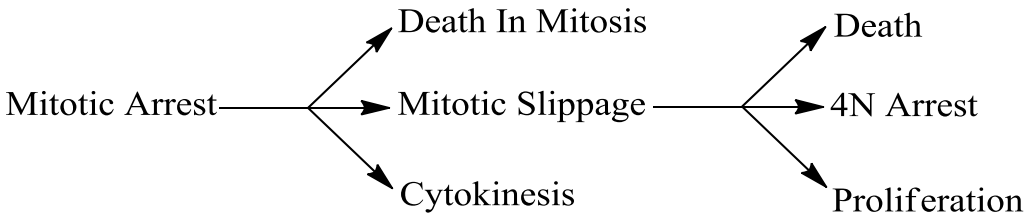

Figure 12 – Possible cell fates following mitotic arrest induced by Eg5 inhibition. Modified from reference 119.

Cells may slip from mitotic arrest and re-enter the cell cycle; those which have not undergone proper chromosome segregation and cytokinesis after exiting arrest will exist as tetraploid cells.[104, 106] These may in turn undergo cell death, remain in a quiescent state or continue proliferating by mechanisms unknown.[119] No effects of Eg5 inhibitors have been observed on cells in interphase (section 1.2.3.3).[108]

Allosteric loop L5 inhibition is reversible, and after transient Eg5 inhibition cells can continue proliferating.[95, 119] This has important ramifications in drug design, since potential drug candidates should have the pharmacodynamics and pharmacokinetics necessary to induce robust mitotic arrest in the first instance. Interestingly, a study by Orth *et al.* illustrated that the breast cancer cell line MCF7 was less robust at recovering after mitotic arrest than cells from normal tissue, thereby suggesting that Eg5 inhibitors could be preferentially cytotoxic against tumours.[119] Rello-Verano *et al.* also demonstrated that tetraploid HCT116 cells are more susceptible to Eg5 inhibitors than their diploid precursors cells, typically undergoing an apoptotic-like cell fate.[120] As with microtubule based anti-mitotic drugs, the cellular responses induced by Eg5 inhibition vary between cell lines and even intracellular differences are apparent.[24 121] A clearer understanding of the biomarkers that differentiate between eventual possible cell fates would provide a great advantage in determining the most appropriate cancer treatment. However, discriminating between these factors remains a complex and sometimes contradictory affair, complicated further by the histological heterogeneity evident in cancer. One emerging factor is that

cells more susceptible to apoptosis are more responsive Eg5 inhibition.[121, 122] In addition, the duration of mitotic arrest appears to have little bearing on the subsequent fate of the cell.[24, 119, 121] While differences between cell lines may be partially attributed to epigenetic factors, this cannot be the case when genetically identical sister cells respond discretely. One theory of how this differentiation arises is that two competing networks of cellular responses are at play when a cell undergoes arrest in mitosis: one operates to generate cell death signals which initiate apoptosis, while opposing this the levels of cyclin B1 begin to degrade, which can allow the cell to slip from mitosis.[24] Alternatively, Shi *et al.* have proposed that sensitivity to inducing apoptosis with anti-mitotic drugs is affected by the anti apoptotic protein XIAP.[121] Clearly while progress is being made, further work needs to be done to further our understanding in this seminal field.

1.3. *S*-trityl L-cysteine

1.3.1. Biological background

1.3.1.1. History of discovery

One of the first Eg5 inhibitors to be identified was *S*-trityl L-cysteine (STLC: **6**, Figure 13a), whose origins as an anticancer agent began over fifty years ago. After the observation was made in 1954 that leukemic white blood cells incorporated radiolabelled cysteine, *S*-alkylated derivatives of cysteine were investigated as potential anticancer agents.[123, 124] STLC was initially synthesized for this purpose in 1959,[125] and demonstrated *in vivo* murine leukaemia anti-tumour activity through mechanisms unknown at the Cancer Chemotherapy National Service Center of the National Cancer Institute (NCI) from the 1960s onwards.[126, 127] It was not until 1992 that Paull *et al.* recognised STLC as a cytotoxic anti-mitotic agent which did not affect microtubules when examining compounds of known anti-tumour activity from the NCI.[128] During a HT screening programme involving NCI libraries, our group finally identified STLC and several other compounds as Eg5 inhibitors in 2003.[104] STLC is therefore a serendipitously discovered rationally designed anticancer agent.[125]

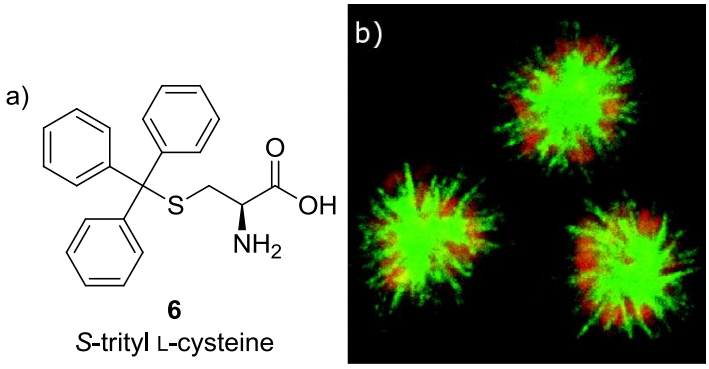

Figure 13 – a) Structure of STLC (6); b) monopolar spindles in HeLa cells treated with STLC. Modified from reference 104.

1.3.1.2. Biological activity

STLC is a tight binding allosteric inhibitor which inhibits the *in vitro* basal ATPase activity of Eg5 with $K_i^{app} \approx 150$ nM.[129, 130] It binds at the same loop L5 allosteric site formed for monastrol,[131, 132] and induces the phenotypic monopolar spindle indicative of mitotic arrest through Eg5 inhibition in cell culture.[104, 129] Across the NCI_{60} panel of cancer cell lines, STLC exhibits a mean $GI_{50} = 1.31$ µM.[104] As with other Eg5 inhibitors, docetaxel resistant prostate cancer cell lines remain sensitive to STLC treatment,[133] and anti-tumour activity *in vivo* has been demonstrated in various xenograft models.[126, 127] Proteomic analysis of the fate of HeLa cells treated with STLC revealed death occurred primarily by activation of the spindle checkpoint and the intrinsic apopototic pathway.[134] STLC is selective for Eg5; the other human mitotic kinesins which have been evaluated (MKLP-1, MKLP-2, CENP-E, Kif22, Kif2A, MCAK and KifC1) are not affected.[129] Additionally, conventional kinesin (*hs*Kif5B), *Drosophila* Ncd and the kinesin-5 ortholog *A. nidulans* BimC are not inhibited by STLC.[104] Outwith the kinesins, constrained derivatives of STLC were recently reported as weak inhibitors of the hepatitis C virus NS5B polymerase.[135]

1.3.2. Eg5–STLC crystal structure

The crystal structure of STLC in complex with Eg5 has been solved, and allows description at the molecular level of the key interactions in the inhibitor-binding pocket (Figure 14).[132, 136] The three phenyl rings of the trityl head group are situated in the predominantly hydrophobic core of the allosteric inhibitor binding-site, in three discrete pockets (P1-P3, Figure 15).[137, 138] Several key interactions are observed contributing to the overall binding of the trityl head group: the phenyl ring in P1 forms an offset stacked π···π interaction with Tyr211, while in P2 the phenyl ring is locked into position by both an edge-face interaction with the phenyl ring of Trp127, and a C–H···π interaction with the pyrrolidine ring of the neighbouring Pro137 on its opposing face.[132] In the P3 pocket, a C-H···π interaction is evident between the isopropyl side chain of Leu 214 and the third phenyl ring's π-electron cloud. Co-workers in the Mackay group recently showed by molecular dynamic (MD) simulations that for the trityl head group the majority of the enthalpic contributions to the free energy of binding for STLC stem from short range hydrophobic interactions, although surprisingly several long range electrostatic interactions were also noted.[139] In contrast to the predominantly hydrophobic binding environment of the trityl group, the cysteine tail extends towards the bulk solvent and the amino acid terminus forms several important hydrogen bonding interactions.[132, 136] The primary amine exhibits H-bonding interactions with the main chain carbonyl of Glu117, a side chain oxygen from Glu116 and a structural water molecule, while the carboxylate forms an H-bonding network with several structural water molecules and an NH group of the proximal Arg221 guanidinium. The interactions of the primary amine are by far the most important contribution to the overall free energy of binding of STLC; MD simulations calculated this moiety contributes -10.3 kcal mol^{-1}.[139] The same study demonstrated that contrary to this the enthalpic contribution of the carboxylate to the free energy of binding appears to be repulsive overall. The predominant factor behind this is a repulsive electrostatic interaction between the carboxylate and the anionic diphosphate of ADP. In the Eg5–STLC structure, the more distal changes relating to conformational changes in the neck linker and the ɣ-phosphate sensing machinery of switch I and II that were seen in other Eg5·inhibitor complexes were also present.[97, 140] Interestingly, in the 2 Å structure solved by our group, while in three of four subunits in the asymmetric unit the final inhibitor bound state incorporating a docked neck linker was observed, in the remaining subunit the switch II cluster was only partially rotated and the neck linker undocked.[132] This appears to be a trapped intermediate state, which provides a structural corroboration for the proposed mechanism of ɣ-phosphate cascade inhibition discussed in section 1.2.4.3.

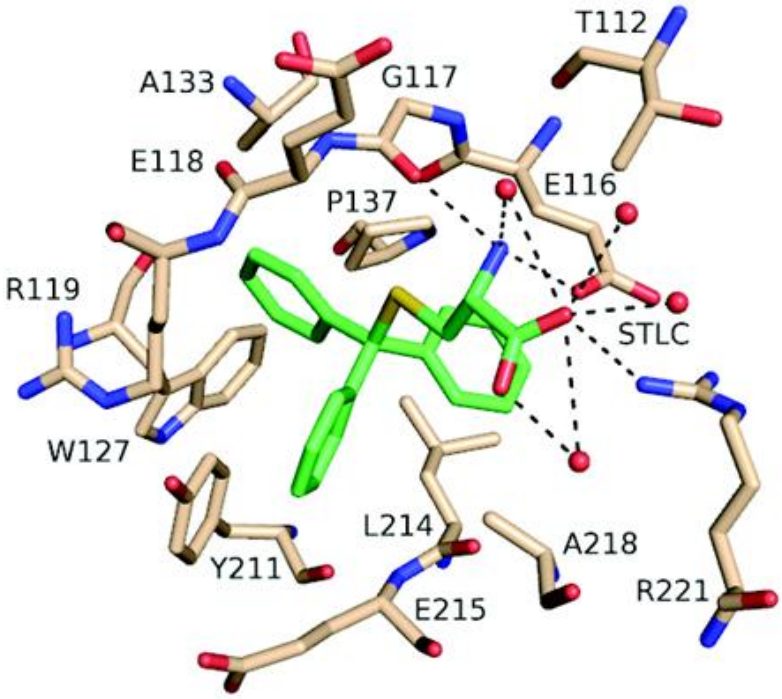

Figure 14 – Molecular interactions of STLC with Eg5.

The protein side chains are coloured by atom type: white (C), blue (N) and red (O). The STLC ligand is coloured by atom type: green (C), yellow (S), blue (N) and red (O). Hydrogen-bonding interactions appear as dashed lines. Modified from reference 132.

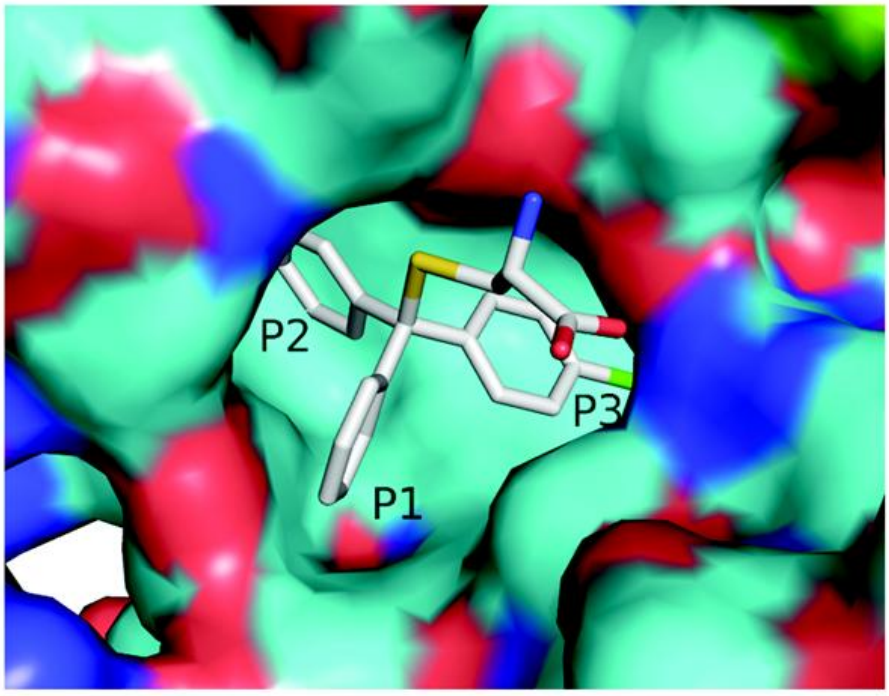

Figure 15 – Surface diagram with an STLC analogue containing a *p*-chlorophenyl ring in the inhibitor binding pocket.

STLC is coloured by atom type: white (C), yellow (S), blue (N) and red (O). Modified from reference 138.

1.3.3. Structure activity relationship of STLC scaffold

1.3.3.1. Trityl head group

Initial structure activity relationship (SAR) studies on STLC were carried out prior to the elucidation of structural data on the Eg5·STLC complex. In the first in depth study by DeBonis *et al.*, a minimum pharmacophore for effective inhibition was established.[130] Incorporation of a small lipophilic *para*-substituent on one phenyl ring of the trityl moiety produced analogues exhibiting improved GI_{50} values of ~ 200 nM in HeLa cells *c/f* GI_{50} = 700 nM for STLC (e.g. **10**, Table 1). The most active compound in a smaller study by Ogo *et al.* had a *p*-trifluoromethylphenyl ring in the trityl group.[141] The crystal structure of the *p*-chlorophenyl analogue **7** has latterly been solved, and demonstrated the halogen substituent to be positioned in the P3 pocket (Figure 15).[137] Bulkier substituents are also tolerated if correctly orientated; docking studies implied the β-napthyl bicycle in **11** was also most likely to bind in the P3 pocket. However fused rings such as fluorene in place of two phenyl rings in the trityl moiety displayed at best weak activity.[130] Replacement of one phenyl ring in the trityl moiety with linear or branched alkyl groups is also tolerated, however when $n < 3$, (where n = the number of carbons in the alkyl group), the activity is greatly diminished (e.g. **13** and **14** *c/f* **12**). This may be due to the entropic penalty incurred with less conformationally restrained lower linear alkyl derivatives. The effect of replacing two phenyl rings with alkyl groups was not reported.

Table 1 – Selected SAR for trityl modifications.

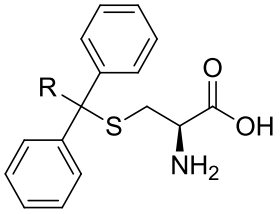

Cmpd	R	Inhibition of basal ATPase activity K_i^{app} (nM)	HeLa cells GI_{50} (nM)
6	Ph	50*	700
7	4-Cl-Ph	200	510
8	4-Br-Ph	250	310
9	4-Me-Ph	100	210
10	4-OMe-Ph	200	200
11	β-napthyl	200	330
12	Et	450	> 5,000
13	n-Pr	175	1,400
14	i-Pr	150	1,080

Notes = * Estimates of the K_i^{app} values vary depending on the buffer and test conditions used, due to STLC and analogues' tight binding nature.[129, 130] Modified from reference 130.

Table 2 – Selected SAR for cysteine modifications.

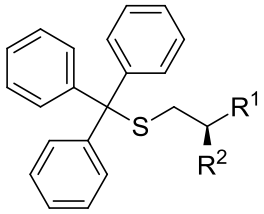

Cmpd	R^1	R^2	Inhibition of basal ATPase activity K_i^{app} (nM)	HeLa cells GI_{50} (nM)
15	CO_2H	H	n.i.	n.d.
16	NH_2	H	150	1008
17	NHAc	CO_2H	n.i.	n.d.
18	NHBoc	CO_2H	n.i.	n.d.
19	OH	H	n.i.	n.d.

Notes: n.d. = not determined; n.i. = no inhibition. Modified from reference 130.

1.3.3.2. Amino acid tail

Although in the crystal structure the terminal carboxylate in the cysteine tail forms several H-bonding interactions with structural water molecules,[132] it is not required for effective inhibition (**15** *c/f* **16**, Table 2).[130] The interactions formed between the primary amine and the peptide backbone are however essential; replacement with bulky secondary or tertiary amines in general completely abolished enzyme inhibition (e.g. **17** and **18**). There is little spatial discrimination between STLC and the D-cysteine analogue STDC, with both exhibiting comparable activities in basal and cellular assays, although STLC is marginally more potent against Eg5.[129] The chain length is also critical: extension of the ethanamine chain in **16** produced compounds which no longer inhibited.[130] Replacement of the primary amine with a hydroxyl resulted in an inactive compounds (**19**), demonstrating that the ability of **16** to form multiple hydrogen bonds with the peptide backbone and also the electrostatic interaction with nearby salt bridge between Glu116 and Arg221 are important. It would appear that the orientations of the H-bonding interactions emanating from the primary amine are crucial, since replacement with a hydroxyl group afforded the inactive compound **19**. In conjunction with the findings from modifying the trityl group, these findings allow a minimum pharmacophore for effective inhibition to be established for the STLC scaffold (Figure 16).[130, 137, 141]

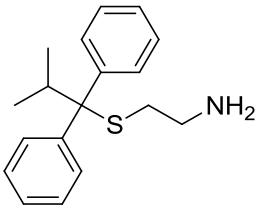

20

Figure 16 – Minimum pharmacophore of STLC for effective inhibition of Eg5.

1.3.4. Molecular recognition by PgP pump

1.3.4.1. Structure and mechanism of efflux

Previous investigations by our group have uncovered that STLC **6** and related analogues were substrates for the multidrug resistance cellular efflux pump Pgp.[137, 139] This is a 170 kDa membrane integrated transporter encoded by the ABCB1 (MDR1) gene. Structurally it comprises of two pseudo-symmetrical halves that each comprise of six transmembrane domains and an ATP binding site.[142] These domains span ~ 70 Å across the surface of the cell membrane, and extend from the extracellular environment through the lipid bilayer by ~ 136 Å. At the core is a ~ 6000 $Å^3$ cavity, lined primarily with hydrophobic residues, which accommodates and binds substrates following capture from the lipid bilayer. Pgp has a number of important endogenous roles in ADME, including intestinal absorption and transport across the blood brain barrier. In addition to these, it serves to protect cells from xenobiotics by effluxing them as they reach the cell membrane.[143] Following the partition of substrates into the lipid bilayer, drugs are taken up into the binding cavity of Pgp through two gateways accessible from the inner membrane leaflet.[142, 144] Upon ATP binding and hydrolysis at the dual nucleotide binding domains, the protein is proposed to undergo a conformational change which results in release of bound substrates from the inner cavity to the extracellular environment, although the exact mechanisms behind this are unclear.

1.3.4.2. Role in resistance in cancer and relationship to STLC

Although resistance in cancer is a multifactorial problem, with more than one mechanism implicated, Pgp is expressed in a number of different cancers, and included amongst its known substrates are anti-mitotic drugs belonging to the taxane and vinca alkaloid families.[32] Unravelling the impact of Pgp related ABC-encoded transporters involvement in mediating resistance and the full extent of their physiological relevance is ongoing. However, *in vitro* these drugs are rapidly effluxed by tumour cell lines that overexpress Pgp, and *in vivo* clear correlations between levels of Pgp expression and the overall efficacy of chemotherapy treatments have been found in breast cancer and certain leukaemias.[145] Investigations into the relationship of STLC with Pgp have shown that the key determinant in affecting the MDR ratio for the STLC analogues is the carboxylate.[137, 139] Whilst STLC had an MDR ratio of ~ 30, the thioethanamine **16** without the carboxylate had an MDR ratio of 1, indicating the growth inhibition activity of **16** was not being affected in the Pgp overexpressing cell line L-MDR1.[137]

1.4. Clinical progress

1.4.1. Clinical candidates

1.4.1.1. Ispinesib and related candidates

In total, nine Eg5 inhibitors have now progressed to clinical trials. The first and to date most intensively investigated is ispinesib, a quinazoline based compound from the same medicinal chemistry programme that generated CK0106023 (**21**, Table 3). Ispinesib has been investigated in monotherapy and in combination against a variety of solid tumours. The best responses have been seen in a group of patients with previously treated metastatic breast cancer, with partial responses observed in three of thirty three.[146] Trials in other advanced cancers have been less successful, with disease stabilisation in a number of other phase 2 monotherapy studies, including head and neck carcinomas, prostate cancer and melanomas.[147-149] Ispinesib has also been tried in combination with various traditional chemotherapies, including carboplatin and docetaxel, however no synergy was recorded with stabilisation again the best recorded response.[150, 151] However, ispinesib is a moderate to significant inhibitor of the cytochrome P450 (CYP) metabolising enzyme CYP3A4, which would contraindicate combination with many chemotherapy agents currently in use.[147, 152] DLTs experienced have typically been haematological related and typical of antiproliferative treatment, with the most prevalent being grade 3/4 neutropaenia.[147, 149] Neurotoxicity has not been observed. Cytokinetics have developed a second generation analogue with GlaxoSmithKline, which incorporates a chromen-4-one heterocycle in place of the quinazoline ring system (SB-743921; **22**).[153] Phase 2 studies are ongoing against Non-Hodgkin's and Hodgkin's lymphomas, with four partial responses recorded so far from a group of thirty.[154] In a phase 1 study against multiple advanced solid tumours, disease stabilisation was again the best response, however one partial response was noted in a patient with cholangiocarcinoma who had been heavily pretreated with exisiting chemotherapy agents.[155] Neutropaenia was again the DLT in both studies.[154, 155] As the first clinical inhibitor disclosed, ispinesib prompted great interest from the pharmaceutical industry, resulting in multiple patent applications on modified quinazoline derivatives.[106, 107] One such fast follow approach from Astra Zeneca led to AZD4877,[156] which has been examined in phase 1 studies against various solid tumours and a combined phase 1/2 study in treatment of refractory acute myeloid leukaemia (**23**, Table 3).[157, 158] Interestingly, AZD4877 was reported to not inhibit five common CYP isoforms, including 3A4.[156] Disease stabilization and neutropaenia were the major findings against solid tumours, while in the leukaemia study the major adverse effects included hypokalemia and

stomatitis.[144, 145] Both branches of study were terminated due to lack of clinical response.[157, 158] A fourth inhibitor based on the ispinesib scaffold has also entered clinical evaluation, the quinazoline ARQ 621 (**24**, Table 3).[159] Phase 1 studies have been completed in patients with solid tumours, and ARQ 621 is much better tolerated than the structurally related candidates **21-23**.[160] The MTD is a weekly dose of 280 mg/m^2 *c/f*, 7 mg/m^2 and 30 mg/m^2 each week for three weeks for ispinesib and AZD4877 respectively, and 4 mg/m^2 every three weeks for SB-743921, in comparable solid tumour study groups.[155, 157, 161] No bone marrow toxicity (i.e. neutropaenia was observed) at this dosage; disease stabilization was the best reported outcome.[160]

1.4.1.2. Candidates based on other scaffolds

Several structurally distinct scaffolds have also been developed (**25-28**, Table 4). Merck KGaA have developed a hexahydro-2*H*-pyrano[3,2-*c*]quinoline based inhibitor which underwent phase 1 trials against various advanced solid tumours (EMD 534085, **25**).[162] However, the best response recorded was disease stabilization in 30% of patients, and no further clinical investigations have been undertaken to date.[163] Following an extensive medicinal chemistry programme incorporating HT screening, crystallography driven SAR optimisation and detailed drug metabolism and pharmacokinetic (DMPK) screening, Merck & Co. produced the dihydropyrrole candidate MK-0731 for clinical studies (**26**).[140] Phase 1 studies in advanced solid tumours produced only prolonged stable disease in some cases, and further investigations for this candidate are not envisaged.[107, 164] Two candidates structurally related to MK-0731 have entered clinical investigations. ARRY-520 (**27**) includes a thiadiazole motif instead of the central dihydropyrrole heterocycle in **26**, and following preclinical *in vivo* studies demonstrating complete tumour regressions against a number of haematological malignancies, entered clinical trials in multiple myleoma and advanced myeloid leukaemia (AML).[165] In the phase 1 AML study, a 2% partial response and 29% disease stabilisation rate was observed from thirty four patients, with continued investigation terminated due to lack of efficacy.[166] However, following promising results in a small scale phase 1 study,[167] an objective response rate of 19% was recorded in patients with relapsed or refractory multiple myeloma after escalation into phase 2 clinical trials, with further studies planned.[168] The primary DLTs with this analogue were neutropaenia and mucositis. [166, 167] Interestingly, in the AML study Grade 1 or 2 QTc prolongation was recorded in ~ 25% of patients,[166] indicating a potential interaction with the human *ether-a-go-go* related gene (hERG) modulated cardiac potassium ion channel, which leads to cardiac arrhythmia.[169] Eli Lilly are evaluating a 2,3-

dihydro-[1,3,4]-thiadiazole based inhibitor, under license from Kyowa Hakko Kirin of Japan in multiple Phase 2 trials (litronesib aka LY2523355; **28**).[170, 171] A phase 1 study in combination with pegfilgrastim in advanced malignancies reported disease stabilization for several patients,[172] however little else has been disclosed about the efficacy of this compound.[171] The first orally bioavailable kinesin inhibitor has been developed by 4SC, which has entered phase 1 trials; however very little is currently known about 4SC-205.[173] One patent from the company implies this compound is based on the indolopyridine inhibitor scaffold discovered by Hotha *et al.* (e.g. **29**, Figure 17).[102, 174]

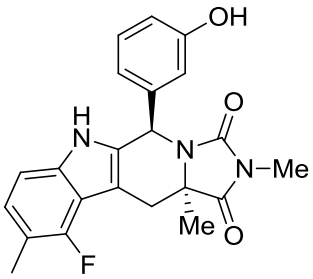

29

Figure 17 – Example of indolopyridine structure from Nycomed patent on Eg5 inhibitors. Nycomed was later acquired by 4SC AG. Structure taken from reference 160.

Table 3 – Clinical Eg5 inhibitors based on the ispinesib scaffold.

Clinical Candidate	Structure	Company	Phase	Investigational Cancers	DLTs
Ispinesib (SB-715992) (**21**)	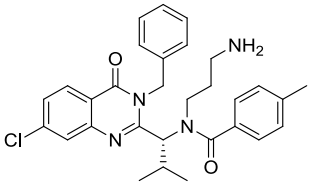	Cytokinetics (licensed to GlaxoSmithKline)	2	Multiple solid tumours, particularly metastatic breast cancer	Neutropaenia and leucopenia
SB-743921 (**22**)	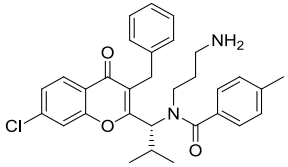	Cytokinetics/ GlaxoSmithKline	2	Advanced solid tumours and lymphomas	Neutropaenia; leucopenia thrombocytopenia
AZD4877 (**23**)	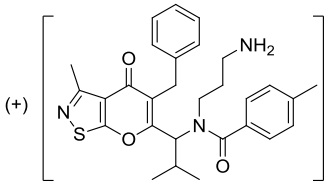	Astra-Zeneca	2 (inactive)	Advanced solid tumours and AML	Neutropaenia; hypokalemia, hypophosphatemia and stomatitis
ARQ 621 (**24**)	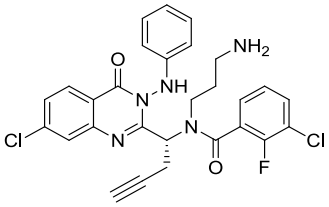	Arqule	1	Advanced solid tumours	Fatigue, intravascular hemolysis and abdominal pain

Table 4 – Eg5 inhibitors in clinical development based on alternative scaffolds.

Clinical Candidate	Structure	Company	Phase	Investigational Cancers	DLTs
EMD 534085 (**25**)	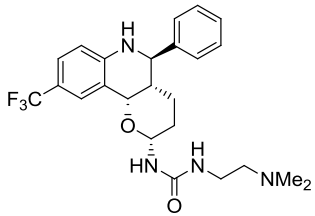	Merck KGaA	1 (inactive)	Solid tumours and haematological malignancies	Neutropaenia and cardiac events
MK-0731 (**26**)	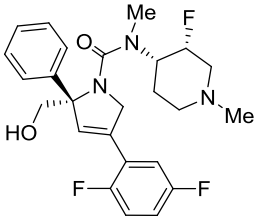	Merck & Co.	1 (inactive)	Advanced solid tumours	Neutropaenia
ARRY-520 (**27**)	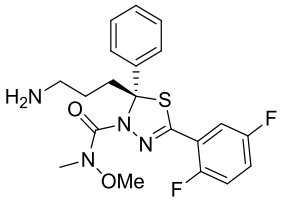	Array Biopharma	2	AML and multiple myeloma	Mucositis, neutropaenia
Litronespib (LY2523355) (**28**)	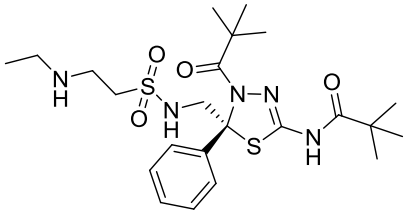	Kyowa Hakko Kirin (under license to Eli Lilly outside Japan)	2	Multiple, including metastatic breast cancer.	Neutropaenia
4SC-205	n/a	4SC AG	1	Solid tumours	n/a

1.4.2. Clinical efficacy

Limited responses have been recorded in the majority of monotherapy trials involving Eg5 inhibitors, which has led some to question the efficacy of targeting Eg5.[44] However most of those conducted have involved groups of heavily pretreated patients, with advanced, refractory cancers. It is perhaps unsurprising given that many had failed to respond to prior treatments that a new anti-mitotic therapy produced only partial responses or disease stabilisation. Pharmacodynamic responses have been recorded for many of the clinical candidates for which data has been reported, indicating that tumour growth inhibition is occurring by the proposed mechanism of action.[157, 161, 166] So what does the future hold for Eg5 based cancer chemotherapy?

One possibility may lie in palliative therapy helping patients manage disease and prolong life, but a more intriguing prospect is the use of Eg5 inhibitors in combination with other treatments. The reasonable responses for ARRY-520 in treating patients with intractable multiple myeloma are to be followed up by clinical trials in combination with existing therapies.[168] Promisingly, this candidate has already exhibited synergy with the proteasome inhibitor bortezomib in *in vivo* xenograft models.[175] Therefore, for effective combination therapies to be developed, it is imperative that Eg5 clinical candidates are well-tolerated, specific and efficacious inhibitors to maximise the potential for achieving useful synergistic effects. Many of the current crop of clinical candidates are molecularly obese (MWt. > 400), and thus are more likely to induce peripheral toxicity and exhibit less desirable DMPK attributes;[176] this effect is compounded by the structural homogeneity amongst known candidates (e.g. **21-24** and **27-28**, Table 3 and Table 4). STLC on the other hand is relatively small and structurally less complex, and with known anti-tumour activity in the unmodified scaffold,[126, 127] represents a promising lead for further optimisation studies. The aim of this project is to make STLC into a viable cancer therapy agent.

Chapter 2. Synthesis

2.1. Synthesis of tertiary alcohols

2.1.1. Grignard reagent and phenyl lithium mediated reductions

Expedient access to a structurally diverse array of STLC derivatives was achieved by thioetherification of tertiary trityl based alcohols, which were prepared using a variety of organometallic mediated reductions. Trityl alcohols **30-38** were synthesised from benzophenone derivatives by reaction with phenyl magnesium bromide (Scheme 1), in typically moderate to excellent yields (Table 5).

Scheme 1 – Synthesis of tertiary alcohols by reduction of substituted benzophenone analogues.

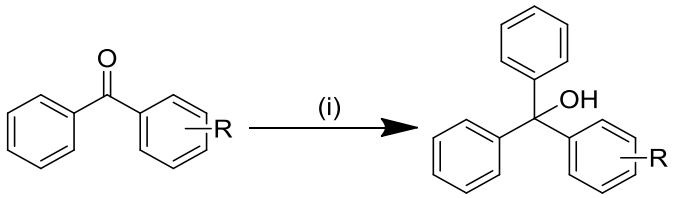

Reagents and conditions: (i) PhMgCl, THF, reflux, 20 h.

Phenyl lithium was utilised to reduce methyl benzoates **39** and **40** to access the phenols **42** and **43**, while the *m*-methoxy analogue **44** was prepared *via* the same route, following a literature procedure to prepare the corresponding methyl ether **41** (Scheme 2a).[177] The tetrahydronapthyl derivative **46** was also prepared by this methodology following esterification of the corresponding acid **45** (Scheme 2b).[178]

Table 5 – Tertiary alcohols prepared by reduction of benzophenone analogues with Grignard reagents.

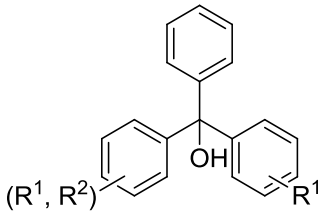

Cmpd	R^1	R^2	R^3	Yield (%)
30[a,b]	2-Cl	H	H	58
31	3-F	H	H	64
32	3-Cl	H	H	69
33	3-Br	H	H	46
34	3-Me	H	H	59
35	3-CF_3	H	H	42
36	4-Et	H	H	87
37[b]	3-Me	4-Me	H	90
38	4-Me	H	4-Me	46

Notes: [a] = synthesised using PhMgX with $ZnCl_2$ by the method of Hatano *et al.*[179]
[b] = prepared using PhMgBr.

Scheme 2 – Reduction of methyl benzoates with phenyl lithium.

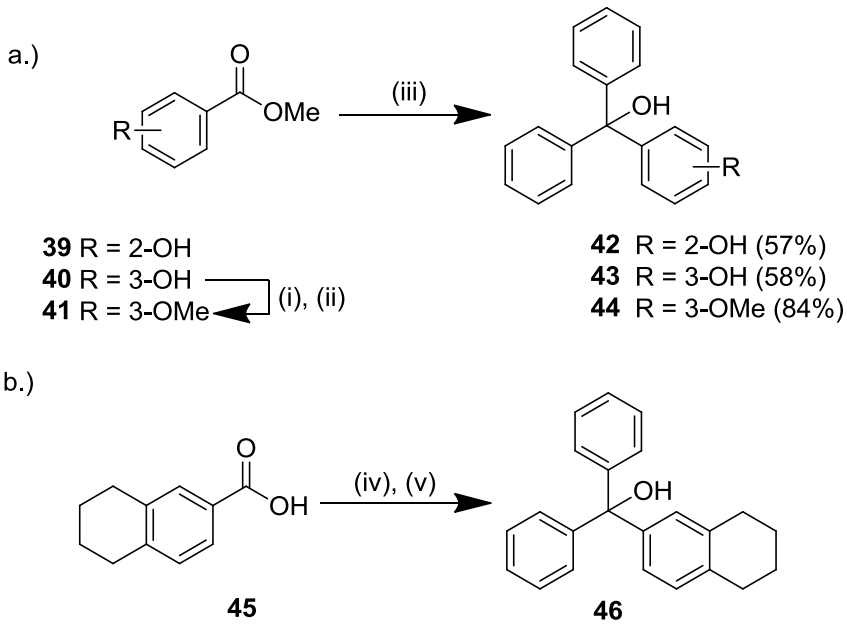

Reagents and conditions: (i) NaH, DMF, 0 °C, 20 min; (ii) MeI, rt, 23 h, 64%; (iii) PhLi, THF, -78 °C, 1 h then -78 °C to rt, 16h; (iv) cat. conc. H_2SO_4, MeOH, reflux, 16 h, 91%; (v) PhLi, Et_2O, -84 °C, 1 h, then -84 °C to rt, 16 h, 56%.

2.1.2. *Lithium mediated organometallic reductions*

2.1.2.1. Lithium halogen exchange with aryl bromides

When suitable ketones or esters were not readily available, the preferred route to synthesise tertiary alcohols structurally related to the trityl group was by reducing benzophenone with lithiated aryl bromides (Scheme 3).

Scheme 3 – General route for the synthesis of trityl alcohols by lithium bromine exchange

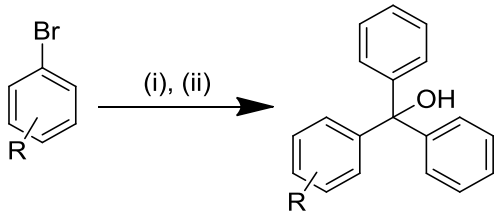

Reagents and conditions: (i) *n*-BuLi, THF, -78 °C, 1 h; (ii) Ph_2CO -78 °C, 6 h, then -78 °C to rt, 16 h.

This provided synthetic access to a wide range of substituents and substitution patterns in the trityl head group, in typically moderate to good yields (**47-68**, Table 6). Lithium halogen exchange was also suitable for synthesising trityl alcohols with substituents on two different phenyl rings, through employing substituted benzophenone derivatives such as 3-hydroxybenzophenone or 4-methylbenzophenone as reagents (**65-68**). For reactions involving bromobenzonitrile substrates, to avoid nitrile reduction and self-condensation or *o*-phenyl deprotonation a different approach was required.[180] Reports in the literature suggested lithiated benzonitriles could be stably formed either by lowering the temperature to -94 °C,[181] or at -78 °C by reversing the order of addition.[180] The cyano-containing trityl alcohols **63-65** were synthesised in reasonable yields by combination of these approaches (Scheme 4).

Scheme 4 – Synthesis of cyano-trityl alcohols 63-65 *via* lithiated benzonitriles.

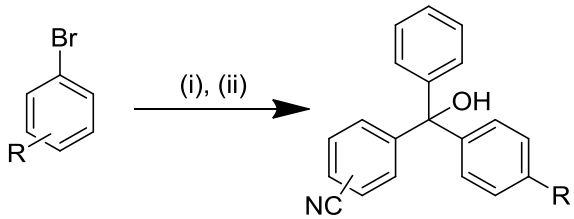

63 3-CN, R = H (81%)
64 4-CN, R = H (68%)
rac-**65** 3-CN, R = Me (67%)

Reagents and conditions: (i) 3-bromobenzonitrile or 4-bromobenzonitrile, THF, -94 °C, 1 h; (ii) Ph_2CO or ≤ -80 °C, 4 h, then -50 °C to rt, 20 h.

Table 6 – Tertiary alcohols prepared by lithiation/lithium halogen exchange.

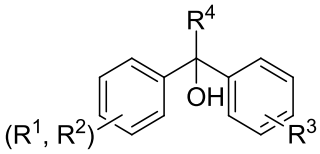

Cmpd	R^1	R^2	R^3	R^4	Yield (%)
47	3-Et	H	H	Ph	44
48	3-*i*-Pr	H	H	Ph	47
49	3-*n*-Pr	H	H	Ph	41
50	3-(2-methyl-1,3-dioxolane)	H	H	Ph	70
51	3-OCF_3	H	H	Ph	23
52	3-SMe	H	H	Ph	54
53	4-Me	H	H	Ph	43
54	4-(2-methyl-1,3-dioxolane)	H	H	Ph	65
55	4-OEt	H	H	Ph	64
56	4-OCF_3	H	H	Ph	38
57	4-SMe	H	H	Ph	76
58	2-F	3-Me	H	Ph	80
59	2-F	4-Me	H	Ph	67
60	2-F	4-OMe	H	Ph	76
61	3-F	4-OMe	H	Ph	60
62	3-Et	4-Me	H	Ph	91
63	3-CN	H	H	Ph	81
64	4-CN	H	H	Ph	68
rac-**65**	3-CN	H	4-Me	Ph	67
rac-**66**	3-OH	H	3-Cl	Ph	39
rac-**67**	3-OH	H	3-Et	Ph	59
rac-**68**	3-OH	H	4-Me	Ph	37
69	H	H	H	3-Pyridyl	29
70	H	H	H	2-(1,3)-Thiazole	41
71	H	H	H	2-(1,3)-Oxazole	27

2.1.2.2. Synthesis of trityl alcohols with phenyl ring replacements

A small selection of analogues replacing one phenyl ring of the trityl group was also prepared (**69-71**, Table 6). Whilst the 3-pyridiyl and thiazole derivatives **69** and **70** were accessible in modest yields under standard lithium halogen exchange conditions as described (Scheme 3), a slightly different approach was needed for the 2-oxazole derivative **71**. Direct lithiation of unsubstituted oxazole at the most acidic 2-position[182] and subsequent reaction with benzophenone furnished the desired tertiary alcohol **71**, albeit in poor yield.[183] The reaction is complicated by the propensity for 2-lithiooxazole **73** to ring open and form valence bond tautomers (e.g. **74**), which could lead to formation of adducts at the 4-position (Scheme 5).[183, 184] The spectral data for **71** however was consistent with successful substitution at the 2-position.[182, 183]

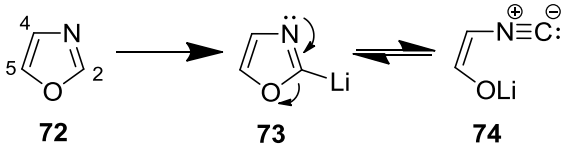

Scheme 5 – Mechanism of 2-lithiooxazole ring opening tautomerism.

2.1.2.3. Preparation of aryl bromides

Whilst the majority of the prerequisite aryl bromides for lithium exchange reactions were available commercially, additional preparation was required for certain trityl substituents. Ketones **75** and **76** required protection as acetals with ethylene glycol prior to lithium halogen exchange, whilst the *m*-substituted *n*-propyl precursor aryl bromide **80** was prepared by a modified version of the Wolff-Kishner reduction with hydrazine hydrate (Scheme 6).[185, 186] A more demanding strategy was required to produce the trityl tertiary alcohol intermediate **62**, substituted with *m*-ethyl and *p*-methyl substituents on a single ring (Scheme 7). Starting from the conveniently substituted 5-bromobenzoic acid **81**, conversion to the Weinreb amide **82** allowed synthesis of ketone **83** to be performed in a controlled manner, thanks to the autoinhibition of further reaction with the Grignard nucleophile by the chelating effect of the *N*-methoxy group.[187, 188] Wolff-Kishner reduction by the Huang Minlon modification furnished aryl bromide **84**, before lithium bromine exchange and subsequent reaction with benzophenone as described afforded the desired tertiary alcohol **62**.[185, 186]

Scheme 6 – Preparation of non-commercially available aryl bromides.

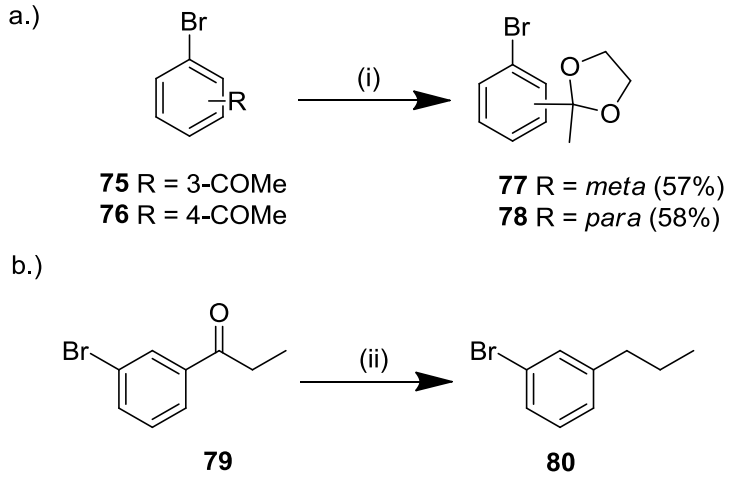

Reagents and conditions: (i) cat. *p*-TSA, ethylene glycol, toluene, reflux, 4 h; (ii) hydrazine hydrate, KOH, ethylene glycol, reflux, 20 h, 68%.

Scheme 7 – Synthesis of the *m*-Et, *p*-Me substituted trityl intermediate 62.

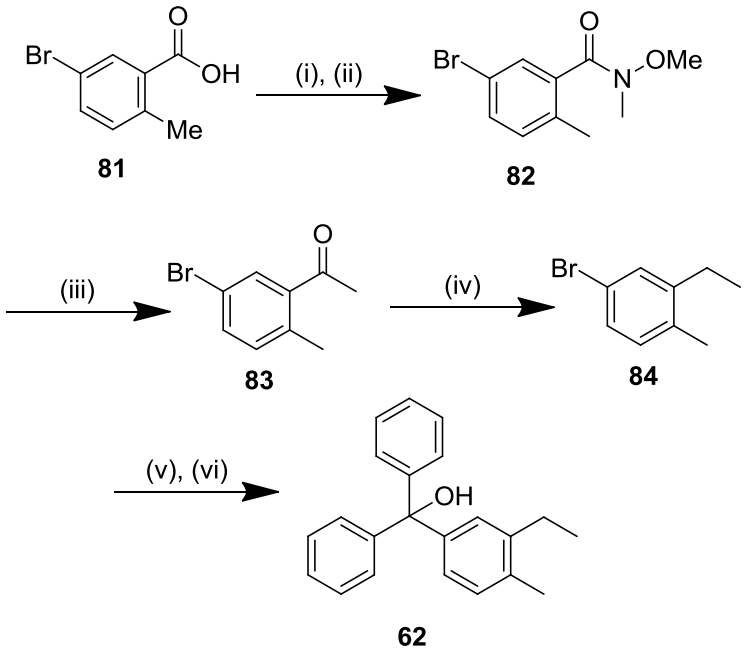

Reagents and conditions: (i) Oxalyl chloride, cat. DMF, CH_2Cl_2, rt, 2 h; (ii) NHMeOMe.HCl, NEt_3, CH_2Cl_2, 0 °C, 1 h, 70%; (iii) MeMgBr, THF, 0 °C, 2 h, 90%; (iv) hydrazine hydrate, KOH, ethylene glycol, reflux, 4 h, 55%; (v) *n*-BuLi, THF, -78 °C, 1 h; (vi) Ph_2CO -78 °C, 6 h, then -78 °C to rt, 16 h, 91%.

2.1.3. Preparation of polar substituted trityl alcohols

In order to investigate the binding interactions of the trityl head group further and modulate physicochemical properties, a range of trityl alcohols with polar, H-bond accepting or donating substituent on one phenyl ring were prepared. The cyano-substituted intermediate trityl alcohols **63-65** provided convenient synthetic starting points for diversification (Scheme 8). Hydrolysis of **63-65** afforded access to the primary amides **85-87**, whereas under harsher and prolonged reaction conditions, the carboxylic acid **88** was obtained. The carboxylic acids **88** and **89** were derivatised to secondary and tertiary amides **91-94** with the amide coupling reagent T3P®, a propylphosphonic anhydride,[189] or reduced with $LiAlH_4$ to produce a CH_2OH motif (**90**).[127] Reduction of the nitriles **63** and **64** afforded amines **95** and **96**, which were acetylated to produce amides **97** and **98**. Oxidation of the thioethers **52** and **57** with *m*-CPBA afforded the sulfones **99** and **100**.

Scheme 8 – Derivatisation of cyano intermediate trityl alcohols 62-64.

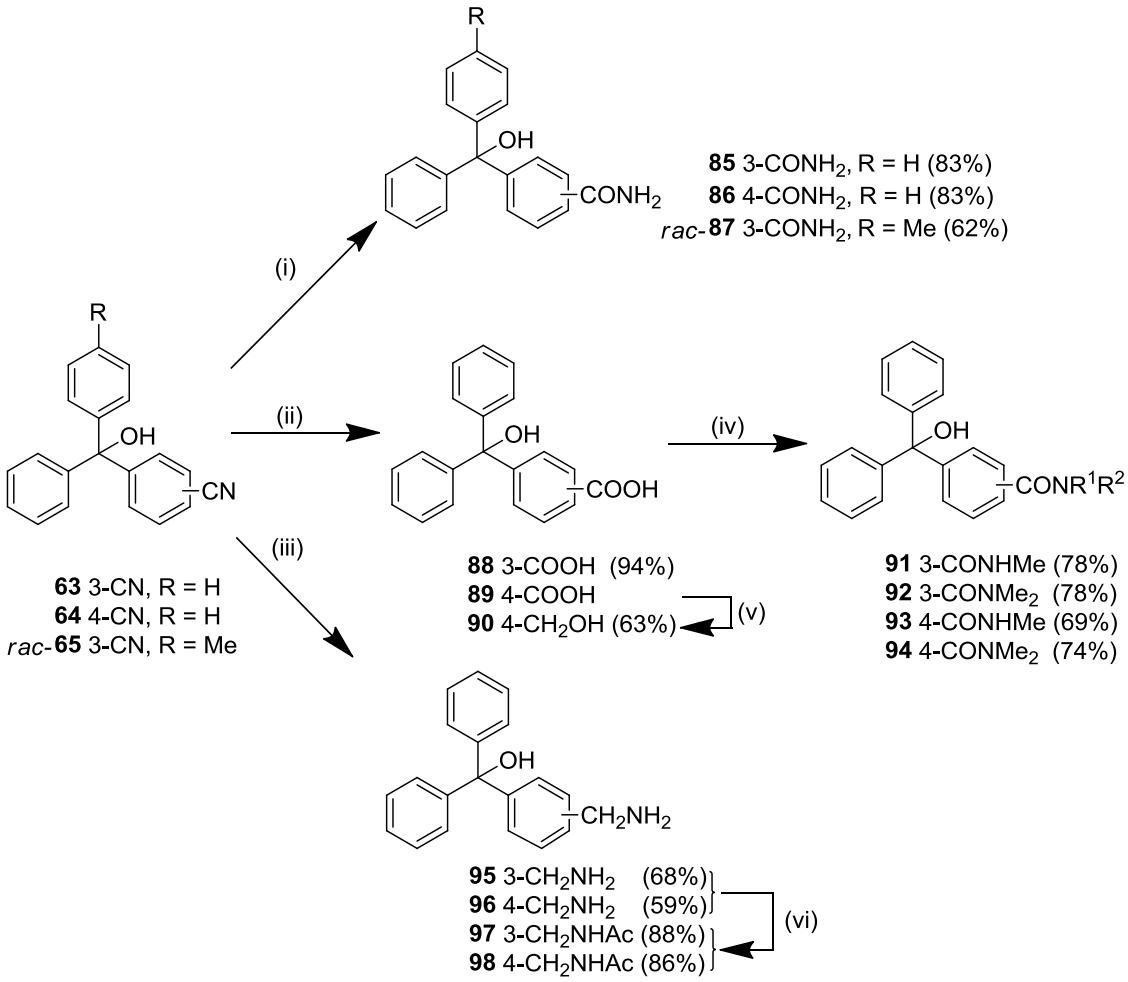

Reagents and conditions: (i) 30% aq. H_2O_2, 6 M aq. NaOH, EtOH, 60 °C, 3 h; (ii) KOH, EtOH/H_2O, reflux, 24 h; (iii) $LiAlH_4$, THF, rt, 22 h; (iv) $NH_2Me.HCl$ or $NHMe_2.HCl$, T3P®, NEt_3, THF, rt, 48 h; (v) $LiAlH_4$, THF, 1 h, 65 °C then 21 h, rt; (vi) Ac_2O, DMF, rt, 4 h.

Scheme 9 – Oxidation of methyl sulfide analogues 51 and 55.

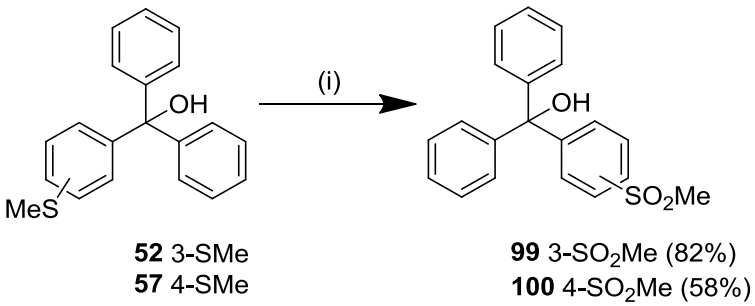

Reagents and conditions: (i) *m*-CPBA, CH_2Cl_2, rt, 3 h.

2.2. Thioetherification

2.2.1. $BF_3{\cdot}Et_2O$ mediated thioetherification of trityl alcohols

The thioetherification of tertiary alcohols was initially carried out by the method previously employed in the synthesis of STLC related analogues in acetic acid with $BF_3{\cdot}Et_2O$.[130]

Scheme 10 – $BF_3{\cdot}Et_2O$ mediated thioetherification

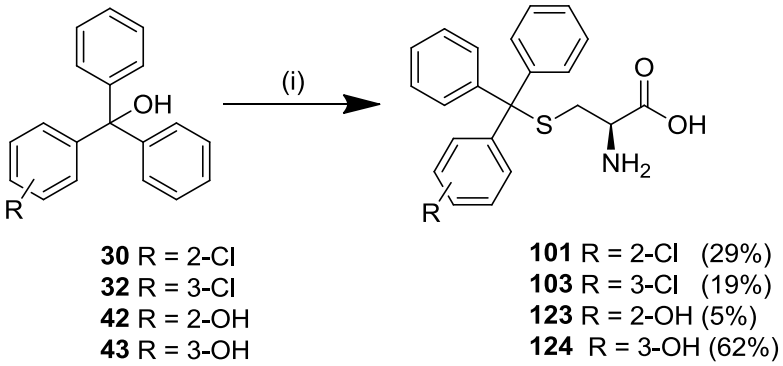

Reagents and conditions: (i) L-cysteine, $BF_3{\cdot}Et_2O$, AcOH, rt, 3 h.

The reaction proceeds through dehydration of the tertiary alcohol facilitated by the Lewis acid to form the trityl carbocation in an S_N1 type mechanism. However, in the hands of the author, the reaction gave unsatisfactory yields, so an alternative method was sought.

2.2.2. Thioetherification in trifluoroacetic acid

Trifluoroacetic acid (TFA) proved suitable as a higher yielding alternative acidic medium for the dehydration of tertiary alcohols and their subsequent thioetherification with thiols (Scheme 11).[190]

Scheme 11 – General route for thioetherification of tertiary alcohols in TFA.

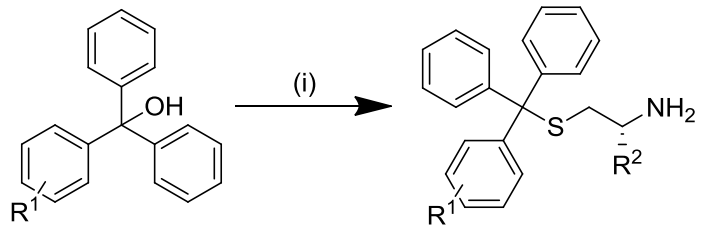

Reagents and conditions: (i) L-cysteine or cysteamine hydrochloride, TFA, rt, 3 h.

Notes: R^1 = refer to Table 7 and Table 8; R^2 = H or *(R)*-CO_2H.

This approach provided a reliable means by which to synthesise a diverse array of STLC analogues in modest to good yields, with a wide range of functional groups tolerated despite the strongly acidic conditions (TFA pK_a = 0.52; Table 7 and Table 8).[191] In common with the thioetherification described previously in acetic acid with $BF_3{\cdot}Et_2O$, this reaction proceeds through protonation of the 3° alcohol, dehydration to form the stable 3° trityl carbocation intermediate **168**, followed by nucleophilic attack by the thiol **169** to generate the thioether product **16** (Scheme 12).

Scheme 12 – Proposed mechanism for TFA mediated thioetherification.

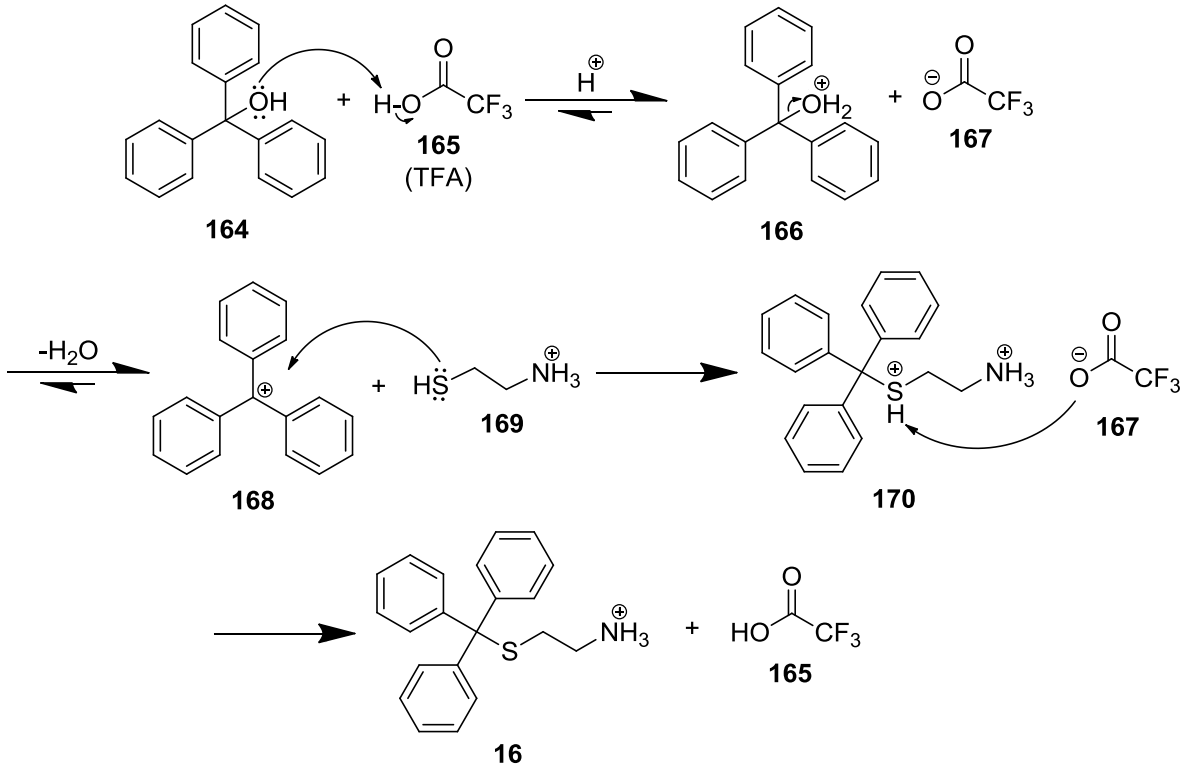

Table 7 – STLC analogues with mono-substituted phenyl rings prepared by thioetherification of trityl alcohols in TFA.

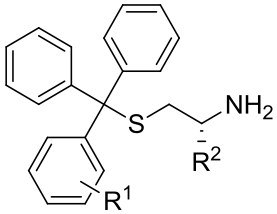

Cmpd	R^1	R^2	Yield (%)
16	H	H	81
102	3-F	H	24
104	3-Cl	H	65
105	3-Br	H	48
106	3-Me	H	55
107	3-Et	H	44
108	3-*i*-Pr	H	69
109	3-*n*-Pr	H	63
110	3-CF_3	H	32
111	3-OMe	H	81
112	3-SMe	H	77
113	3-OCF_3	H	78
114	3-COMe	*(R)*-CO_2H	72
115	3-COMe	H	31
116	4-Me	H	69
117	4-Et	H	85
118	4-OMe	H	18
119	4-OEt	H	58
120	4-OCF_3	H	36
121	4-COMe	*(R)*-CO_2H	55

Cmpd	R^1	R^2	Yield (%)
122	4-COMe	H	95
125	3-OH	H	77
126	3-CN	H	94
127	3-CH_2NH_2	H	72
128	3-$CH_2NHCOMe$	H	82
129	3-CO_2H	H	36
130	3-$CONH_2$	*(R)*-CO_2H	34
131	3-$CONH_2$	H	28
132	3-CONHMe	H	78
133	3-$CONMe_2$	H	86
134	3-SO_2Me	H	82
135	4-CN	H	68
136	4-CH_2OH	H	29
137	4-CH_2NH_2	H	72
138	4-$CH_2NHCOMe$	H	73
139	4-$CONH_2$	H	70
140	4-CONHMe	H	57
141	4-$CONMe_2$	H	88
142	4-SO_2Me	H	62

Table 8 – STLC analogues with more complex substituent patterns prepared by thioetherification of trityl alcohols in TFA.

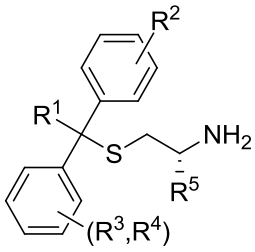

Cmpd	R^1	R^2	R^3	R^4	R^5	Yield (%)
143	3-Pyridyl	H	H	H	H	59
144	2-(1,3)-Thiazole	H	H	H	H	30
145	2-(1,3)-Oxazole	H	H	H	H	27
146	Ph	4-Me	4-Me	H	H	79
rac-**147**	Ph	3-OH	3-Cl	H	H	68
rac-**148**	Ph	3-OH	3-Et	H	H	51
rac-**149**	Ph	3-OH	4-Me	H	H	83
rac-**150**	Ph	3-CN	4-Me	H	H	71
rac-**151**	Ph	3-$CONH_2$	4-Me	H	H	71
152	Ph	H	2-F	3-Me	H	64
153	Ph	H	2-F	4-Me	H	48
154	Ph	H	2-F	4-OMe	*(R)*-CO_2H	50
155	Ph	H	2-F	4-OMe	H	76
156	Ph	H	3-F	4-OMe	H	67
157	Ph	H	Cl	Cl	H	47
158	Ph	H	3-Me	4-Me	*(R)*-CO_2H	68
159	Ph	H	3-Me	4-Me	H	79
160	Ph	H	3-Et	4-Me	*(R)*-CO_2H	71
161	Ph	H	3-Et	4-Me	H	72
162	Ph	H	3,4-$(CH_2)_4$		*(R)*-CO_2H	29
163	Ph	H	3,4-$(CH_2)_4$		H	70

2.3. Synthesis of triphenylbutanamines

*2.3.1. Synthesis of 3,4-dimethyl tritylsubstituted analogue rac-**176***

2.3.1.1. Choice of synthetic route

A more complex synthetic strategy was required for analogues incorporating an isosteric methylene replacement for the thiol linker in STLC (CH_2-trityl analogues). The route devised previously by Wang *et al*. was employed, starting with allylation of the previously prepared trityl alcohol **37** to introduce the carbon scaffold (Scheme 13).[138] Iron trichloride mediates carbon-oxygen bond cleavage in this unusual but efficient methodology developed by Kabalka *et al.*[192] After deprotonation to form the lithium alkoxide **177** this reaction is proposed to proceed through the iron alkoxide complex **178** and then the trityl carbocation intermediate **179**, which forms the new carbon-carbon bond with allyltrimethysilane to furnish alkene **171** (Scheme 14). Hydroboration and consequent oxidation of the alkene **171** yielded the primary alcohol **172**,[193] which was subsequently oxidised to the aldehyde **173** with Dess-Martin periodinane (DMP).[194] The racemic α-aminonitrile **174** was then prepared in a variation of the classical Strecker synthesis, employing Montmorillonite KSF clay as a solid phase acidic catalyst.[195, 196] After hydrolysis of the nitrile *rac*-**174**, hydrogenation of the benzylamine *rac*-**175** in a mild ammonium formate based procedure afforded the target amino acid *rac*-**176** in an overall yield of 6.4%.[197]

Scheme 13 – Synthesis of 3,4-dimethylphenyl triphenylbutanamine *rac*-176.

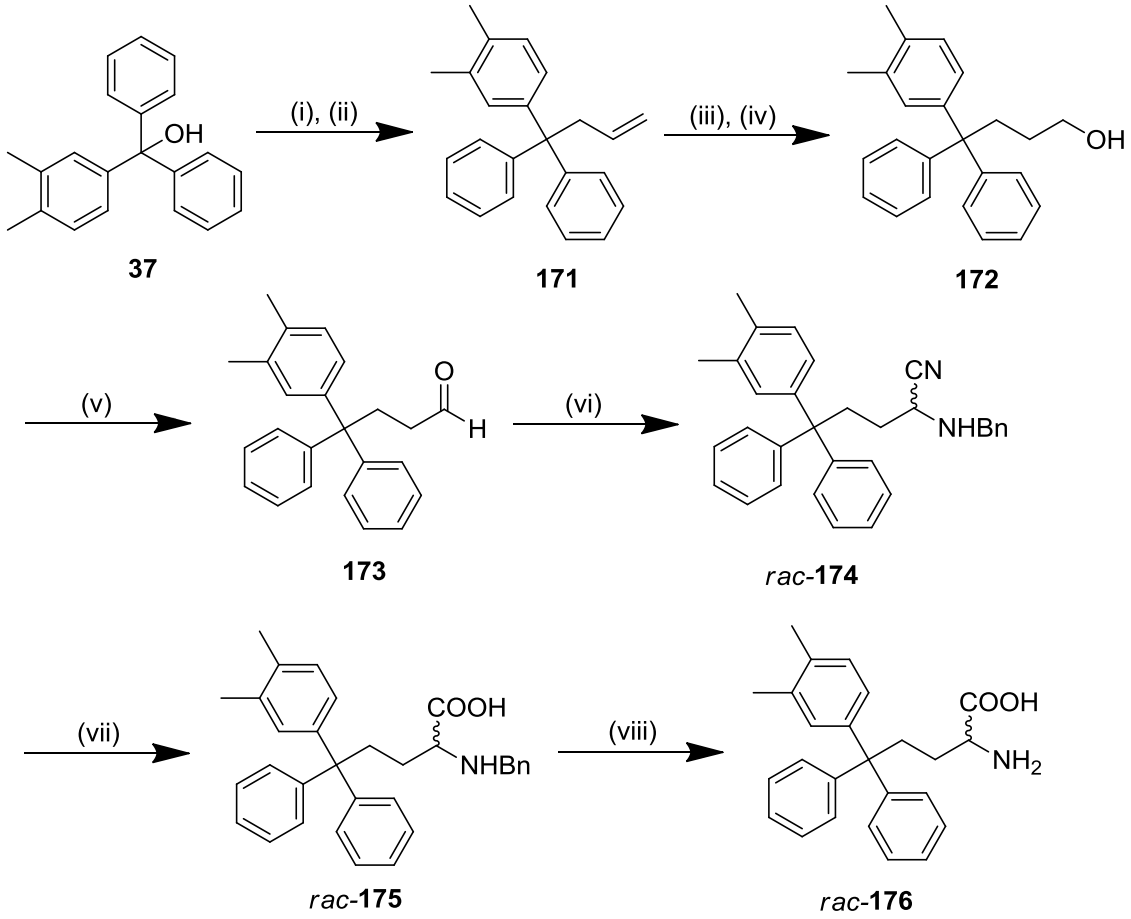

Reagents and conditions: (i) *n*-BuLi, CH_2Cl_2, rt, 30 min; (ii) allyltrimethylsilane, $FeCl_3$, rt, 6 h, 91%; (iii) BH_3·THF, THF, rt, 19 h; (iv) 30% aq. H_2O_2, 3 M aq. NaOH, 58%; (v) DMP, CH_2Cl_2, rt, 4 h, 42%; (vi) Mont. KSF clay, benzylamine, TMSCN, CH_2Cl_2, rt, 2.5 h, 68%; (vii) conc. HCl, dioxane, reflux, 2 d, 57%; (viii) $HCOONH_4$, 10% Pd/C, MeOH, 60 °C, 2 h, 83%.

Scheme 14 – Proposed mechanism for the iron trichloride mediated allylation of triphenylmethanol 37.

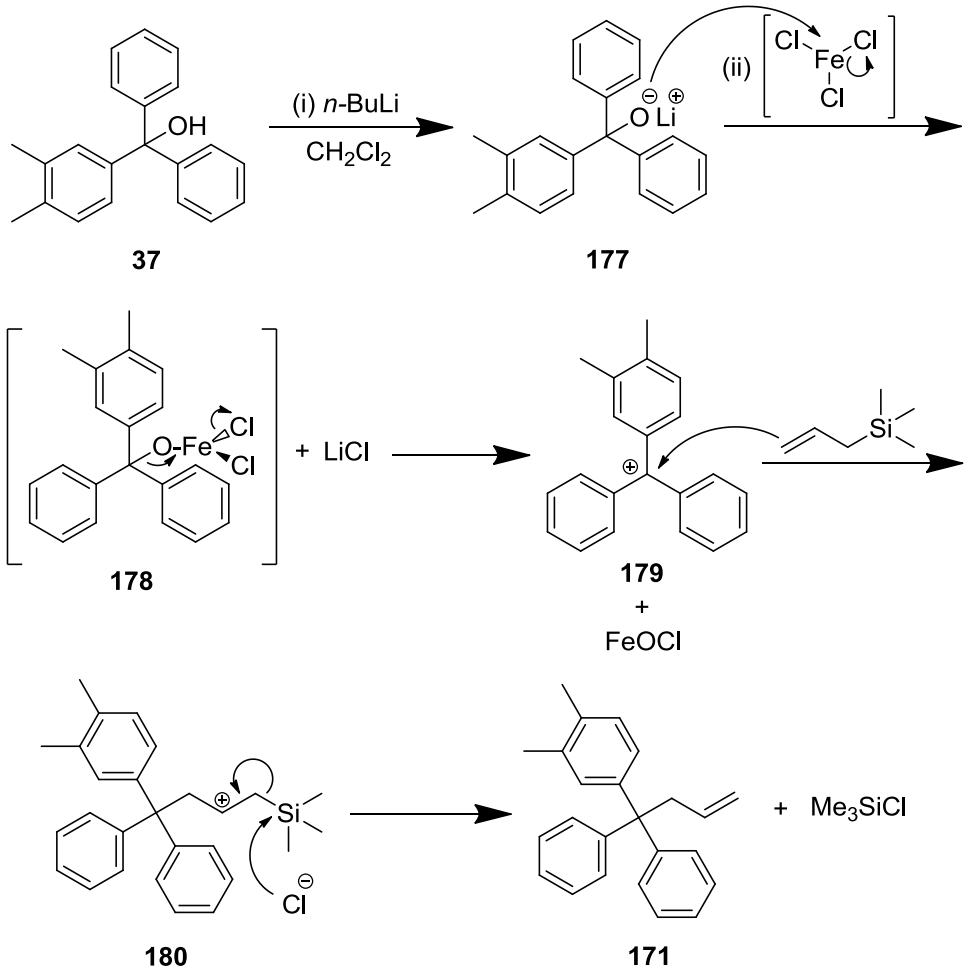

2.3.1.2. Attempted resolution of *rac*-**176**

Attempts to separate the enantiomers of *rac*-**176** by chiral HPLC were not successful. While structurally analogous triphenylbutanamines containing *meta* and *para*-methyl substituents respectively were resolved previously by semi-preparative chiral HPLC with a ChiralPak IC column,[138] upon application of the same method no compound elution was observed for *rac*-**176**. Therefore the method was modified from an isocratic to a varied gradient to increase the proportion of ethanol in the mobile phase. This overcame the elution problems encountered and appeared to afford the resolved enantiomers (Figure 18). However, it was not possible to purify the obtained materials of the TFA/NEt_3 salts required in the mobile phase, even after addition of aqueous ammonia to neutralize the TFA, and flash chromatography to remove the triethylammonium cations. Therefore, it proved impossible to verify whether successful resolution of the enantiomers had been achieved by this method. Unfortunately, both TFA and NEt_3 are required in the mobile phase for successful elution of the zwitterionic *rac*-**176**. Therefore, a more salient strategy would be to resolve the enantiomers of *rac*-**176** at an earlier stage in the synthesis when the zwitterion was not present, such as the α-aminonitrile *rac*-**174**. Limitations on both time and material however prevented further investigation.

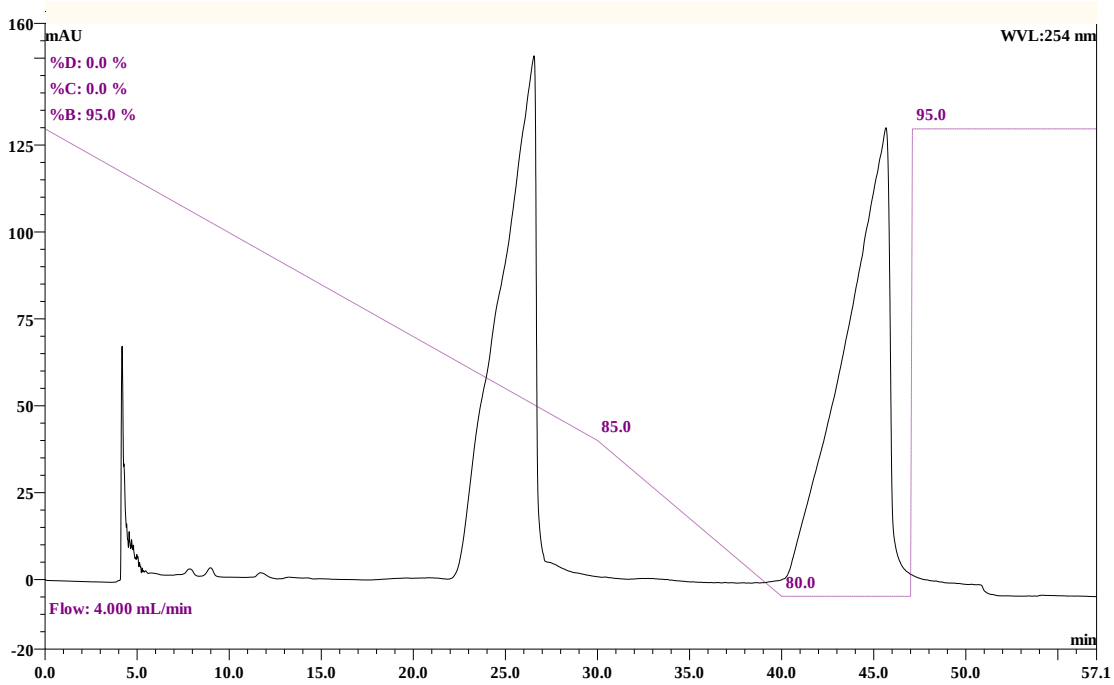

Figure 18 – HPLC trace for attempted resolution of *rac*-176.

2.3.2. *Fluorinated analogues*

2.3.2.1. Overview

To investigate the effect of modulating the pK_a of the primary amine in the lead triphenylbutanamines, we embarked on the synthesis of a series of β-fluorinated analogues of **181** (**182-184**, Figure 19).

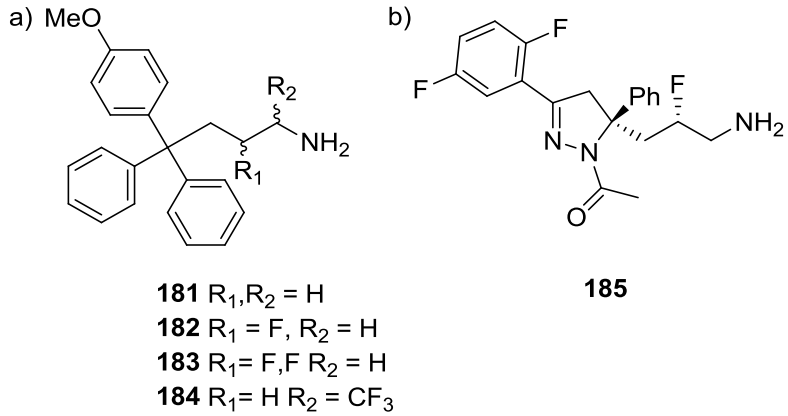

Figure 19 – Proposed and investigated β-fluorinated primary amines.

Figure 19a) Structures of lead 4-methoxy substituted triphenylbutanamine 180 and proposed β-fluorinated analogues 182-184. Figure 19b) Structure of the β-fluorinated dihydropyrazole based Eg5 inhibitor 185.[198]

One potential route to synthesise the mono β-fluorinated analogue **182** was through α-fluorination of an oxazolidinone, followed by removal of the chiral auxiliary and subsequent functional group interconversions to the primary amine.[198, 199] This route was employed by scientists at Merck during the synthesis of the β-fluorinated amine moiety in **185**, an Eg5 inhibitor produced in the lead optimization programme that ultimately produced the clinical candidate MK-0731.[198] More recently, in the literature, several groups concurrently and independently reported varying approaches to accomplish the direct and enantioselective α-fluorination of aldehydes by enamine based organocatalysis.[200-203] We envisaged this as a more direct methodology to procure access to the desired β-fluoro derivative **181**. As overfluorination is a common problem with these types of procedure whenever reaction conditions are not succinctly controlled, this could also provide access to the β,β-difluorinated derivative **183**. (Trifluoro)trimethylsilane (TMS-CF_3) has been well established as a nucleophilic trifluoromethylating agent in the transformation of aldehydes and ketones into α-trifluoromethyl alcohols.[204, 205] Thus, using this reagent would allow synthetic efforts to be directed from a common aldehyde precursor.

2.3.2.2. Synthesis of β-fluorinated primary amine **182**.

The required aldehyde starting material **189** was prepared by the previously described route from commercially available *p*-methoxy trityl alcohol **186** (Scheme 15). Introduction of the α-fluorine to the aldehyde was performed by the method of Beeson *et al.*, with L-proline as the amine organocatalyst and *N*-fluorobenzenesulfonimide (NFSI) providing an electrophilic source of fluorine.[202, 206] The exact mechanism governing fluorine transfer in electrophilic N-F fluorinating agents such as NFSI has not been elucidated, with both nucleophilic and single electron transfer mechanisms proposed as the predominant pathway.[207-209] After workup and quenching of the reaction, ^{19}F NMR of the crude product mixture containing *rac*-**190** and **191** exhibited resonances at δ = -194.2 and δ = -107.6 ppm respectively, in agreement with comparable α-fluorinated aldehydes reported in the literature.[199] However this crude material was not separated, but instead reduced immediately because this type of species is reported to be less stable in comparison to the non-fluorinated aldehyde precursors and unstable on silica gel.[199, 201] Overall, the reaction proceeded smoothly and the alcohols could be readily separated by flash chromatography to furnish the desired mono β-fluorinated *rac*-**192** in 68% yield, and as the minor difluorinated product **193** in 17% yield. Interestingly, although the enhanced acidity of the α-proton in the α-fluorinated aldehyde *rac*-**190** means α,α-fluorination is not unexpected, Beeson *et al.* observed only monofluorinated substrates when utilising bulkier amine chiral auxiliaries under comparable reaction conditions.[202]

Following condensation of L-proline **196** with the aldehyde **189**, the enamine **198** forms and reacts with NFSI to form the fluorinated species **199**: subsequent hydrolysis releases the desired α-fluoro aldehyde **190** (Scheme 16). Marigo *et al*. have proposed that the unexpected stability of the α-fluorinated intermediate **190** towards epimerisation and α,α-difluorination originates from the steric shielding of the remaining α-proton by the chiral substituent on the auxiliary, thus preventing abstraction and ensuing enamine formation for a second time.[201] Thus, through employing the relatively small chiral auxiliary L-proline, this protection was compromised, allowing increased formation of the α,α-fluorinated **191** under the chosen conditions. β-Fluorination was primarily designed to examine the effect on pK_a, lipophilicity and cellular uptake in the lead series, therefore *rac*-**190** was not resolved, although theoretically L-proline imparted modest enantioselectivity for the (*R*)-enantiomer.[202] Bulkier chiral auxiliaries that provide better stereoselectivity and potentially reduced difluorination under these reaction conditions were not investigated. Transformation to the primary amine *rac*-**182** was achieved by functional group

interconversion through tosylation (*rac*-**194**), introduction of the azide (*rac*-**195**) and subsequent reduction to furnish the target compound (Scheme 15b).

Scheme 15 – Synthesis of the β-fluorinated primary amine *rac*-182.

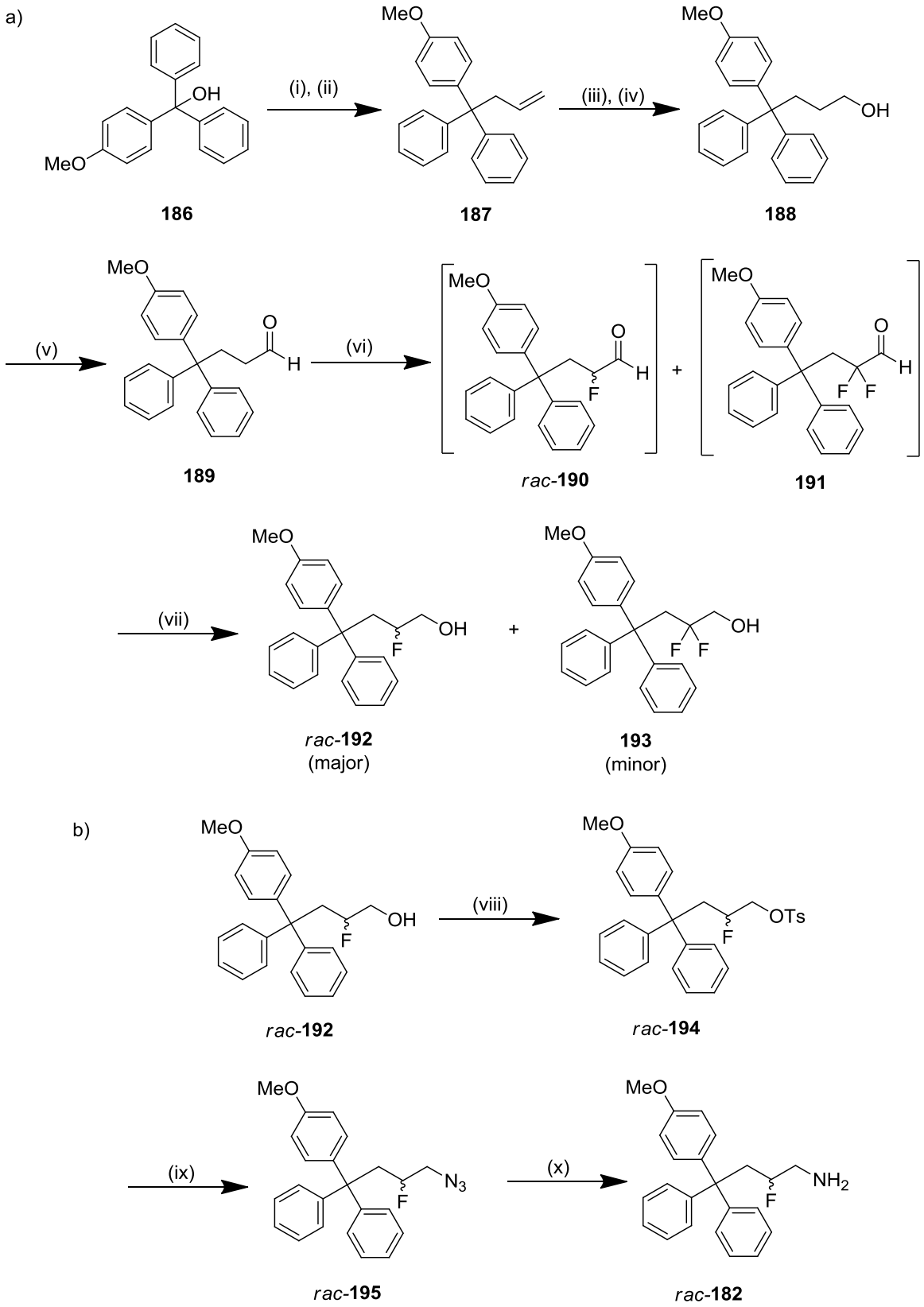

Reagents and conditions: (i) n-BuLi, CH_2Cl_2, rt, 30 min; (ii) allyltrimethylsilane, $FeCl_3$, rt, 6 h, 60%; (iii) $NaBH_4$, conc. H_2SO_4 in Et_2O, diglyme, rt, 18 h then 75 °C, 1 h; (iv) 30% aq. H_2O_2, 3 M aq. NaOH, rt, 5.5 h, 50%; (v) DMP, CH_2Cl_2, rt, 4 h, 83%; (vi) L-proline, NFSI, THF/EtOH, -10 °C, 2 h then rt, 22 h. (vii) $NaBH_4$, CH_2Cl_2/EtOH, rt, 4 h, 68% (191) and 17% (192); (viii) TsCl, pyridine, CH_2Cl_2, rt 3 h, 93%; (ix) NaN_3, DMSO, 40 °C, 18 h, 70%; (x) $HCOONH_4$, 10% Pd/C, MeOH, 60 °C, 2 h, 65%.

Scheme 16 – Mechanism for the enamine catalysed direct asymmetric α-fluorination of aldehydes.

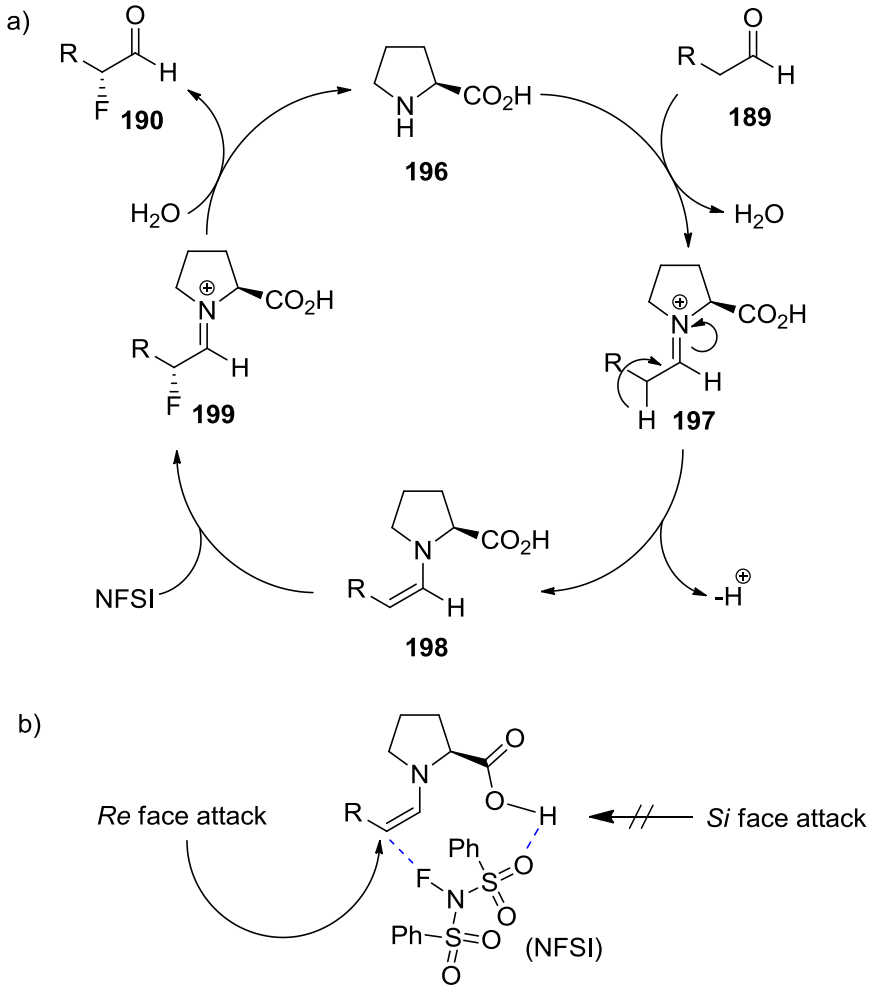

Notes: Scheme 16a) Enamine organocatalytic cycle for α-fluorination of aldehydes; adapted from Marigo *et al.*[210] Scheme 16b) Stereochemical basis for discrimination: adapted from Beeson *et al.*[202] The *Si* face is shielded electronically and sterically by the α-carboxylic acid of L-proline, thus forcing electrophilic fluorination *via* the *Re* face.

2.3.2.3. Synthesis of α-trifluoromethyl amine **184**.

Synthesis of α-trifluoromethyl amine **184** was achieved from the common intermediate aldehyde **189**, with the key step being the trifluoromethylation of **189** with the TMS-CF_3. This organosilicon reagent, known as the Ruppert-Prakash reagent, is a nucleophilic trifluoromethyl synthon with general utility for the trifluoromethylation of various electrophilic species including aldehydes, ketones, esters, acid chlorides and sulphur based electrophiles (reviewed by Prakash *et al.*).[205] Reaction conditions were first optimised using the commercially available **200** (Scheme 17 and Table 9). Modest improvements in yield were realised upon increasing the relative stoichiometry of the TMS-CF_3 and TBAF reagents, and prolonging the duration of the reaction (Entries 1, 3 and 5, Table 9). Upon application of the optimised method with aldehyde **189**, the desired α-trifluoro alcohol *rac*-**202** was obtained in 77% yield (Scheme 18). While the mechanism has not been completely verified, the reaction is proposed to proceed through a catalytic species mediated by a key alkoxide intermediate **206**, with fluorination arbitrated by a putative hypercoordinated silicon species **207** (Scheme 19).[205] At the onset of the reaction, TBAF provides an initiating source of fluoride by which to activate TMS-CF_3, which transfers a CF_3 group to the electrophile aldehyde **189**. This forms the alkoxide species **206**, and as a volatile byproduct Me_3SiF. The high affinity of silicon for the negatively charged alkoxide oxygen in **206** dictates coordination of a second molecule of TMS-CF_3, and thereby the proposed formation of the pentavalent silicon species **207**. This putative key intermediate transfers a CF_3 moiety to another molecule of the aldehyde **189**, which probably precoordinates with the hypercoordinate species **207**, thus ensuring delivery of the CF_3 group is performed in an essentially intramolecular manner. Regeneration of the autocatalytic alkoxide **206** allows continuation until completion, whilst hydrolysing the silylated alcohol **208** affords the desired α-trifluoromethylated alcohol *rac*-**202**. Following formation of *rac*-**202**, synthesis of the α-trifluoroamine *rac*-**184** was accomplished by functional group interconversion through the triflate (*rac*-**203**), introduction of the azide (*rac*-**204**) and subsequent reduction to furnish the target compound (Scheme 18).

Scheme 17 – Trifluoromethylation of phenylpropionaldehyde.

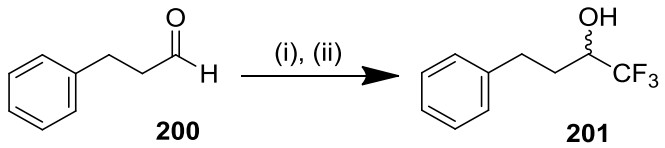

Reagents and conditions: (i) TMS-CF_3, F^- source (5 mol%), rt, 4 h. (ii) Hydrolysis method as indicated in Table 9, rt, 2 h.

Table 9 – Optimisation of Ruppert-Prakash reaction with 3-phenylpropionaldehyde.

Entry	Scale (mmol)	TMS-CF_3 equivalents	F^- source (mol %)	Time (h)	Hydrolysis method	Yield (%)[a]
1	1	1.5	TBAF (5%)	1.5	HCl (excess, 3 M aq.)	40
2	1	1.5	CsF (5%)	1.5	HCl (excess, 3 M aq)	20[b]
3	1	1.5	TBAF (5%)	3.5	TBAF (1 equiv)	42
4	1	2	TBAF (5%)	3.5	TBAF (1 equiv)	49
5	2	2	TBAF (10%)	21	TBAF (1 equiv)	61
6	2	2	CsF (10%)	21	TBAF (1 equiv)	53[b]

Notes: [a] = isolated yield; [b] = impure for starting material and an unidentified impurity.

Scheme 18 – Synthesis of α-CF_3 triphenylbutanamine *rac*-184.

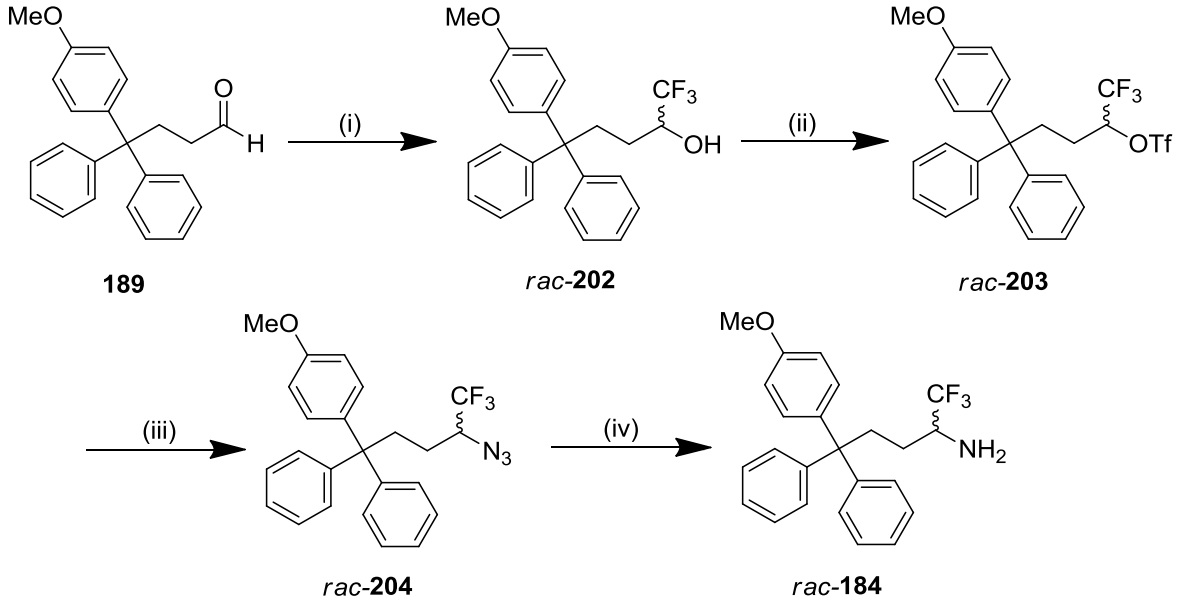

Reagents and conditions: (i) TMS-CF_3, TBAF, THF, rt, 16 h, then TBAF, rt, 3 h, 77%; (ii) Tf_2O, pyridine, CH_2Cl_2, -50 °C, 3 h, 78%; (iii) NaN_3, DMSO, 40 °C, 16 h, 75% (iv) $HCOONH_4$, 10% Pd/C, MeOH, 60 °C, 2 h, 91%.

Scheme 19 – Proposed mechanism for trifluoromethylation of aldehyde 189 with TMS-CF_3.

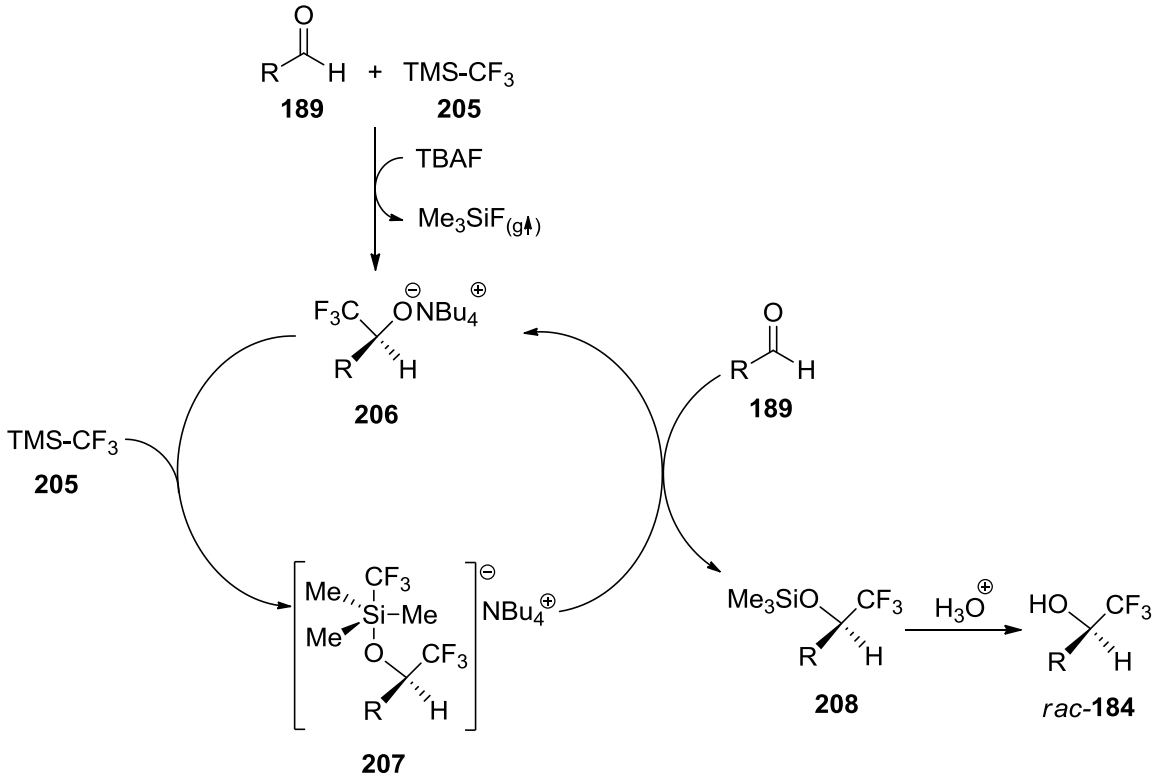

Notes: adapted from Prakash *et al*. and Wiedemann *et al*.[205, 211]

2.4. Carboxylate isosteres

The SAR role of the cysteine was examined in more detail with a small series of analogues incorporating isosteric replacements for the carboxylic acid (Scheme 20). Primary amide **210** was synthesised by treatment of propionic acid derivative **209** with oxalyl chloride to generate the acid chloride, followed by displacement with ammonia. The propionic acid derivative **209** was prepared by thioetherification of trityl alcohol with 3-mercaptopropionic acid under standard conditions (section 2.2.2). Amide isosteres **216-218** were synthesised from *N-tert*-butoxycarbonyl (*t*-BOC) protected STLC **224** with the T3P® coupling reagent, followed by deprotection in TFA.[189] The hydroxamic acid derivative **220** was prepared from the methyl ester of STLC **219** according to a procedure reported by Tegoni *et al.*[212]

Scheme 20 – Synthesis of carboxylate isosteres of STLC.

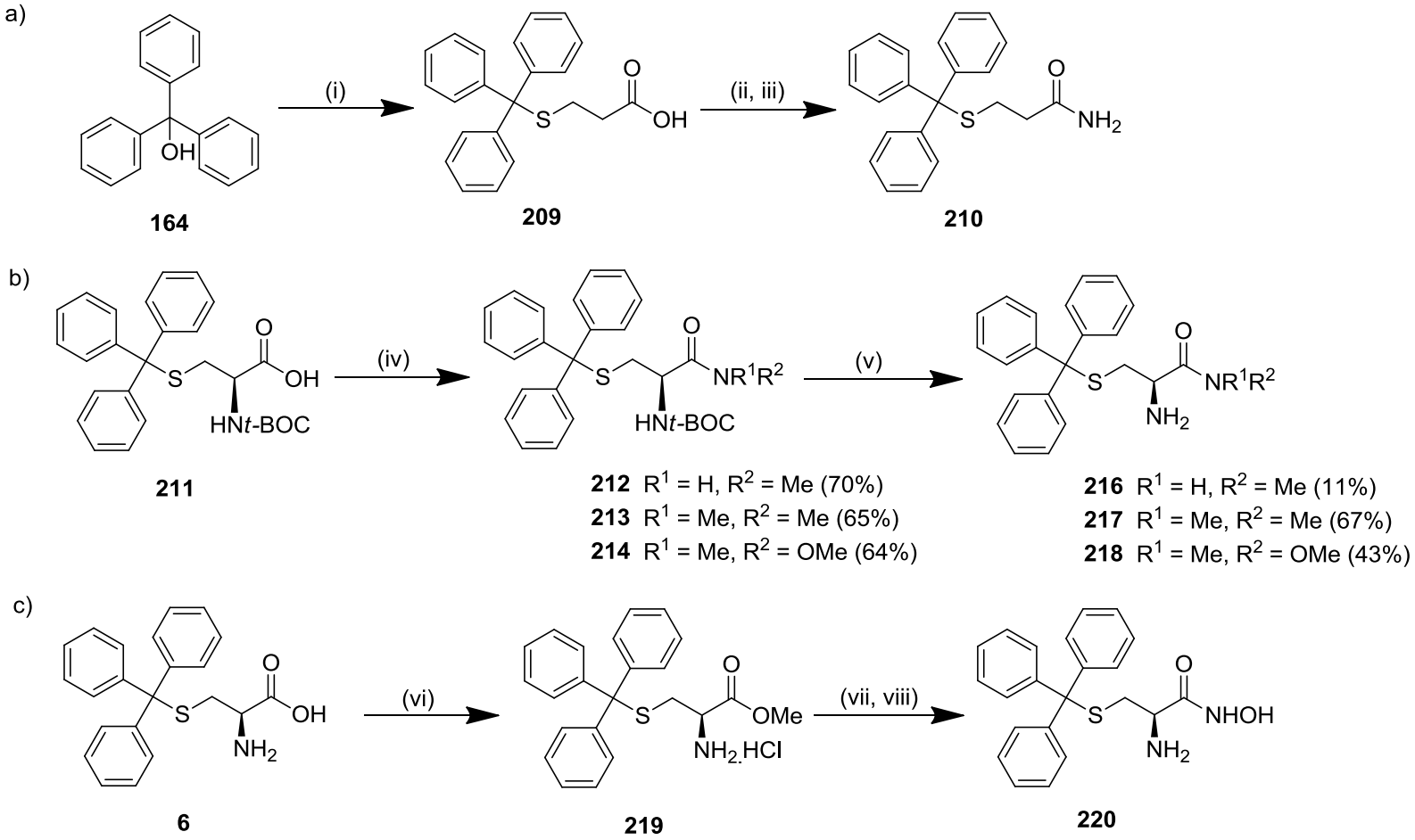

Reagents and conditions: (i) 3-mercaptopropionic acid, TFA, rt, 2 h, 55%; (ii) oxalyl chloride, cat. DMF, CH_2Cl_2, rt, 1.5 h; (iii) NH_3, dioxane, rt, 18 h, 56%; (iv) T3P®, NEt_3, NR^1R^2.HCl, rt, 24 h. (v) TFA, rt, 2 h; (vi) $SOCl_2$, MeOH, rt, 16 h, 98% (vii) conc. aq. NH_4OH, $CHCl_3$, rt, 1 h; (viii) NH_2OH, MeOH, rt, 24 h, then 5 °C, 24 h, 24%.

Chapter 3. Results & Discussion

3.1. Overview

3.1.1. SAR investigation strategies

Examination of the preliminary SAR against the established pharmacophore allowed the potential areas of STLC for further structural modifications to be identified (Figure 20). The most potent STLC derivatives prepared thus far incorporated lipophilic substituents on one phenyl ring of the trityl head group;[130, 137, 141] initial investigations focussed on the expansion of the SAR in this region (section 3.2.1). In the development and optimisation of any lead compound, improvements to the potency must be balanced with ensuring prospective drugs have the necessary physicochemical and pharmacokinetic characteristics to ensure overall efficacy.[213] Therefore while the trityl group occupied a primarily hydrophobic environment,[132, 139] it was necessary to also maximise any potential hydrophilic vectors to achieve optimal drug-like properties. These strategies are discussed in section 3.2.4. In parallel with the optimisation of the hydrophobic and hydrophilic binding interactions of the trityl head group, the SAR of the amino acid tail were investigated.[138] This work was primarily conducted by Dr. Fang Wang, and her key findings are reported in section 3.2.2. Our further joint investigations on the influence of the amino acid tail on DMPK related attributes and its relationship to cellular efflux by the Pgp transporter are discussed in section 3.2.6.

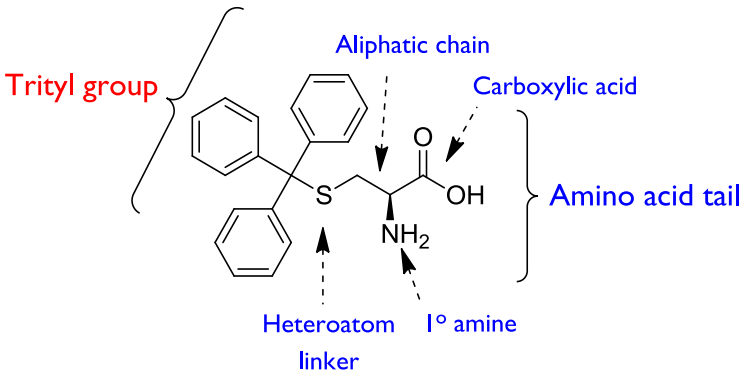

Figure 20 – Structural features of STLC.

3.1.2. Evaluation process for new compounds

Newly synthesised compounds were first evaluated for inhibitory activity by measuring their effect on the basal ATPase activity of Eg5 in the pyruvate kinase/lactate dehydrogenase-linked assay.[214] From these measurements an estimated K_i^{app} value was calculated; this parameter was measured rather than an IC_{50} value to account for the tight-binding kinetics displayed by STLC and its analogues.[129, 215] For each inhibitor, the ligand efficiency was calculated from the K_i^{app} to afford an additional means of comparison between structurally similar compounds of varying activities and size.[216] This metric relates the ratio of the free energy of binding over the number of heavy atoms in a molecule: more efficient ligands tend to be smaller and thus provide better starting points for further optimisation.[217] For all evaluated compounds, the physicochemical properties were calculated *in silico*, and where relevant this data is included in the discussion; the complete dataset is presented in appendix 1. The majority of inhibitors were assessed for growth inhibition activity against the K562 human leukaemia cell line, and this work is reported in context with the basal inhibitory activity SAR discussions. We subsequently evaluated particularly promising lead compounds across a panel of multiple tumour cell lines. For the selected lead candidates, the physicochemical and ADMET properties were then evaluated, prior to progression into *in vivo* xenograft models of cancer.

3.2. Structure activity relationship studies

3.2.1. Lipophilic modifications to the trityl head group

3.2.1.1. Inhibition of basal Eg5 ATPase activity by thioethers with a hydrophobic trityl substituent

STLC analogues incorporating a lipophilic *para* substituent on one ring in the trityl moiety had displayed increased potency against Eg5 in previous SAR studies.[130, 137, 141] The structure of the *p*-chlorophenyl derivative **7** in complex with Eg5 has been solved, and provided a structural explanation for these observations.[137] This established the *p*-chlorophenyl was positioned in the P3 pocket, surrounded predominantly by hydrophobic residues (Figure 15). To investigate this environment further, a series of analogues were prepared with a single hydrophobic substituent on one phenyl ring (**101-122**, Table 10). While the *o*-chloro substituent of **101** significantly reduced activity against Eg5 compared with STLC (**6**), a *m*-chloro (**103**) produced an approximately 2-fold improvement in K_i^{app} for basal inhibition of Eg5. To optimise this interaction, a series of *meta* substituted analogues of varying electronic and steric character was prepared (**104-115**, Table 10). Alkyl groups proved particularly beneficial for improving Eg5 inhibitory activity and the efficiency of inhibitors. A stepwise improvement was evident in K_i^{app} from **106** (Me, K_i^{app} = 80 ± 24 nM), **109** (*n*-Pr, K_i^{app} = 26.9 ± 11 nM), **108** (*i*-Pr, K_i^{app} = 10.3 ± 3.4 nM) to **107** (Et, K_i^{app} = 5.9 ± 2.3 nM), which illustrates this region of the inhibitor binding site is sensitive to steric bulk, with the increase in activity most likely reflecting an interaction between the proximal lipophilic Leu214 side chain. The electronic effects on the phenyl ring are also important: **110** with a *m*-CF_3 group, which can be considered as sterically comparable to a methyl substituent but electron-withdrawing (-*I*), proved 4-fold less active than **106**. In all the crystal structures of STLC and its analogues with Eg5, a C−H···π interaction is observed in the P3 pocket with the adjacent isopropyl side chain of Leu 214 (Figure 14).[132, 136, 137] This interaction has been calculated to be the most important contribution to the free energy of binding from a single residue in the P3 pocket.[139] As this interaction is mediated *via* the π-electron clouds of the phenyl ring, changes in its distribution will consequently affect the strength of interaction with local residues.

Table 10 – STLC analogues with one lipophilic trityl substituent

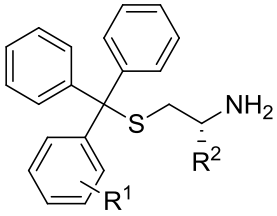

Cmpd	R^1	R^2	Inhibition of basal ATPase activity K_i^{app} (nM)	L.E.	K562 cells GI_{50} (nM)
6 (STLC)	H	(*R*)-CO_2H	135.9 ± 20.5	0.36	1452 ± 76
16	H	H	245.0 ± 1.8	0.39	2286 ± 213
101	2-Cl	*(R)*-CO_2H	1783.9 ± 384.0	0.29	n.d.
102	3-F	H	377.4 ± 38.4	0.36	n.d.
103	3-Cl	*(R)*-CO_2H	89.9 ± 18.5	0.36	2404± 222
104	3-Cl	H	297.8 ± 60.0	0.37	1045 ± 42
105	3-Br	H	293.9 ± 61.8	0.37	n.d.
106	3-Me	H	80.0 ± 23.9	0.40	698 ± 115
107	3-Et	H	5.9 ± 2.3	0.45	680 ± 84
108	3-*i*-Pr	H	10.3 ± 3.4	0.42	581 ± 68
109	3-*n*-Pr	H	29.6 ± 11.0	0.39	1760 ± 124
110	3-CF_3	H	352.7 ± 27.9	0.33	n.d.
111	3-OMe	H	149.8 ± 18.5	0.37	n.d.
112	3-SMe	H	520.4 ± 87.6	0.34	1474 ± 330
113	3-OCF_3	H	27.8 ± 5.0	0.37	1518 ± 164
114	3-COMe	*(R)*-CO_2H	519.8 ± 102.0	0.30	964 ± 82
115	3-COMe	H	185.8 ± 30.4	0.35	706 ± 47
116	4-Me	H	27.4 ± 6.5	0.43	731 ± 36
117	4-Et	H	57.5 ± 9.0	0.39	871 ± 59
10 (NSC123528)	4-OMe	*(R)*-CO_2H	15.7 ± 0.9	0.38	240 ± 17
118	4-OMe	H	21.5 ± 2.8	0.42	700 ± 27
119	4-OEt	H	17.3 ± 2.5	0.41	1901 ± 212
120	4-OCF_3	H	29.7 ± 3.8	0.37	2218 ± 198
121	4-COMe	*(R)*-CO_2H	271.7 ± 36.6	0.31	4266 ± 274
122	4-COMe	H	51.0 ± 21.6	0.38	705 ± 77

Note: n.d. = not determined; L.E. = ligand efficiency.

Several additional *para* substituted analogues were also prepared (**116-122**, Table 10). These results were in accord with the findings from the *meta* substituted series, with strong basal inhibition by both alkyl and ether substituted derivatives. Interestingly in the *para* position, ether substituents **118** and **119** displayed superior inhibitory activity against Eg5 to alkyl derivatives **116** and **117**, in contrast with the *meta* substituted series (e.g. **106** *c/f* **111**). However, the range of *para* substituted derivatives prepared was much narrower. Analysis of all results using a Craig plot[218] substantiated the optimal substituents in the *meta* and *para* positions as both electron-donating (+*I*) and hydrophobic relative to hydrogen (Figure 21).

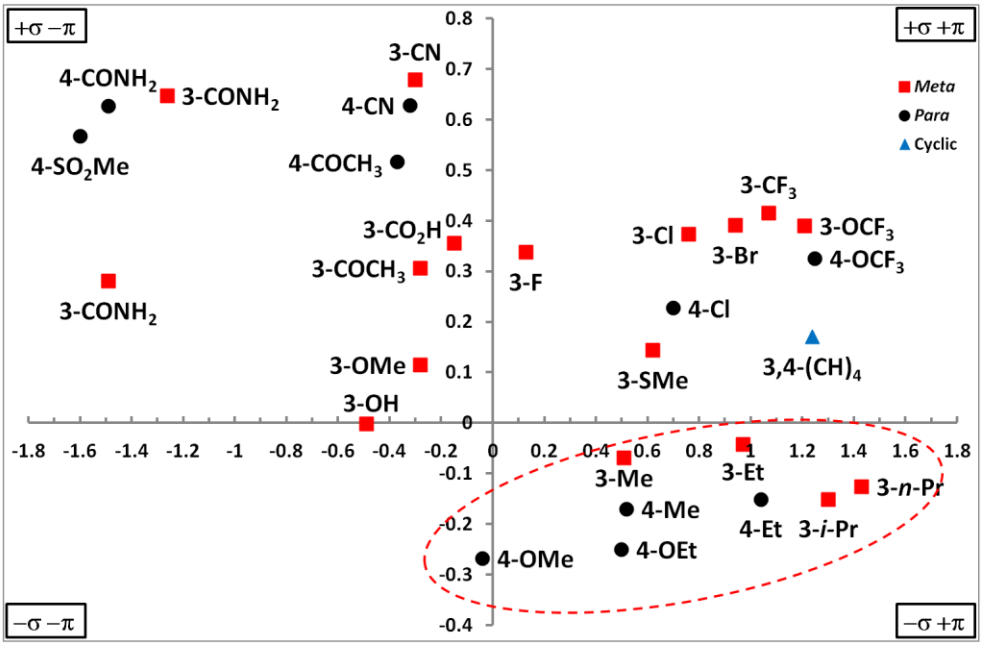

Figure 21 – Craig Plot for aromatic substituents of σ vs π.

π is the substituent hydrophobicity constant, and σ the Hammett substitution constant, a measure of the electronic influence of the substituent. Values obtained from model systems from the following references.[218-220] Modified from reference 138.

3.2.1.2. Evaluation of growth inhibition by thioethers with a hydrophobic trityl substituent

From the panel of derivatives prepared, submicromolar activity was evident against the K562 cell line for alkyl (**106-108** and **116-117**), acetate (**114**, **115**, **122**), and *p*-methoxy substituted analogues (**118**; Table 10). These in general yielded a ≥ 2-fold enhancement in potency *c/f* the benchmark compounds STLC (**6**) and its cysteamine analogue (**16**). Paradoxically, **109** and **119** with *n*-propyl and ethoxy substituents respectively both exhibited dramatic losses in cellular activity in comparison to their excellent basal inhibitory activity. This probably can be attributed to their limited aqueous solubility at physiological pH (turbidimetric solubility at pH 7.4: **109** = 3.75 µM; **119**: = 3.75 µM). Introduction of a carboxylic acid into the tail of **122** to produce **121** resulted in a 4-fold reduction in Eg5 activity, comparable to that seen with **115** and **114**, but produced a much more pronounced reduction in activity in the K562 cell line. This was a reversal of the pattern seen with STLC **6** and its cysteamine analogue **16** and the *p*-methoxy analogues **10** and **118**. From the comparable inhibitors prepared, two pairs with modified trityl moieties had better activity in the Eg5 basal assay when prepared without the carboxylic acid (**114** and **115**; **121** and **129**), while all modified *S*-trityl analogues with the carboxylic acid moiety exhibited lower activity in the cellular assay than their corresponding counterparts without the carboxylate (**103** and **104**; **114** and **115**; **121** and **122**) apart from the *p*-methoxy pair (**10** and **118**). This demonstrates the SAR role of the carboxylic acid is complex and its influence on efficacy required more investigation.

3.2.1.3. Crystal structure of the Eg5–**115** complex

The crystal structure of the Eg5·**115** complex was solved by Kristal Kaan to a resolution of 2.75 Å, with the modified trityl group of **115** adopting the same overall conformation as STLC (Figure 22).[138] This clearly demonstrated the *m*-acetate substituent binding in the hydrophobic P3 pocket: the ketone carbonyl appears to hydrogen bond with the main chain nitrogen in Ala218 and the side chain nitrogen (NH1) of Arg221. Removal of the carboxylic acid appears to afford increased conformational flexibility to the ethanamine tail. Although the hydrogen bonding interactions observed in the Eg5·STLC complex with the amide carbonyl and carboxylate of Glu117 and Glu116 respectively are maintained,[132] in one molecule in the unit cell the primary amine is positioned pointing towards Arg221 instead.[138] Interestingly in one of the seven Eg5 structures within the asymmetric unit cell, the neck linker remained undocked and the distal conformational adjustments at the switch II cluster were not fully propagated. This apparent transition state was previously also observed in the one molecule of the unit cell in the Eg5·STLC complex.[132] Together, these findings provide further support for the proposed biomechanical pathway of conformational changes that ultimately compromises Eg5 processivity (section 1.2.4.3).

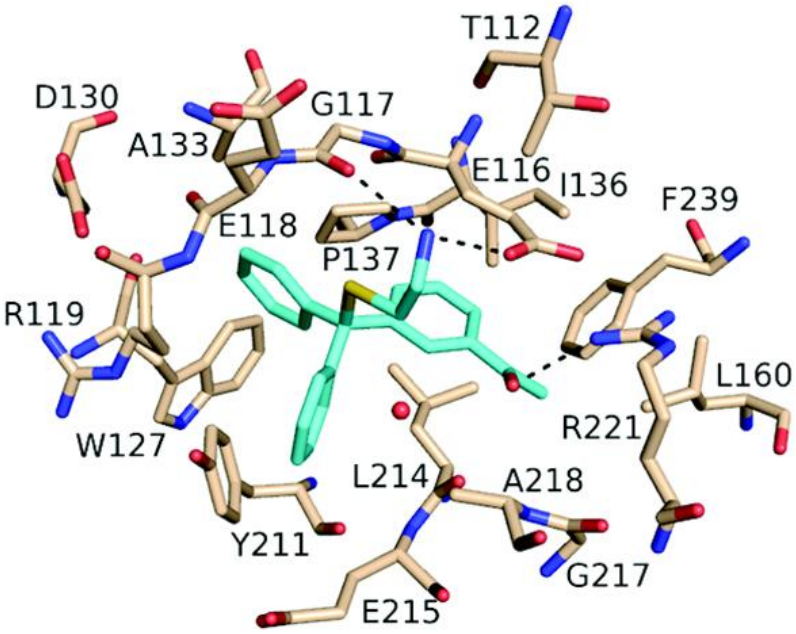

Figure 22 – Eg5-115 crystal structure showing 115 in the inhibitor-binding pocket.

Protein side chains are coloured by atom type: white (C), blue (N) and red (O). The ligand is coloured by atom type: turquoise (C), yellow (S), blue (N) and red (O). The dashed lines indicate hydrogen bonding interactions. Modified from reference 138.

3.2.2. Triphenylbutanamines

3.2.2.1. Introduction of the CH_2-trityl linker

In parallel to optimisation of the hydrophobic binding interactions of the trityl group in the P3 pocket, the effects of further SAR changes to the amino acid tail were examined by Dr. Fang Wang.[138] A crucial discovery from these investigations was that a methylene could serve as a replacement for the *S*-trityl linker in STLC (Figure 20).[138] Interestingly, although the activity of the CH_2-trityl analogue *rac*-**221** was lower against Eg5 *c/f* STLC **6**, in the growth inhibition assay the activity improved (Table 11). The *(R)*-**221** enantiomer proved more active than the *(S)*-enantiomer across both assays, in a reversal of the trend observed between STLC and STDC. Against Eg5, STLC is marginally more potent than its enantiomer STDC[129, 137] and *(R)*-**221** is in the opposite absolute configuration with respect to STLC.[138] In another contrast to the *S*-trityl analogues **6** and **16**, the CH_2-trityl analogue **222** without the terminal α-carboxylic acid exhibited improved activity against both Eg5 and in the cellular assay over the zwitterionic *rac*-**221**. Introduction of the CH_2-trityl bioisostere negated concerns regarding the possible susceptibility of the thioether to metabolism *via S*-oxidation.[221] Additionally both STLC and its CH_2-trityl analogue *rac*-**221** were demonstrated to be stable under acidic hydrolysis conditions comparable to those found in the stomach (pH = 1.0; $t_{½}$ > 24 h).[138] Drug candidates derived from either molecular skeleton could potentially therefore be administered orally.

Table 11 – Triphenylbutanamine analogues of STLC with one lipophilic trityl substituent

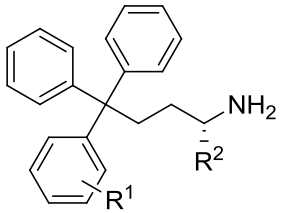

Cmpd	R^1	R^2	Inhibition of basal ATPase activity K_i^{app} (nM)	L.E.	K562 cells GI_{50} (nM)
rac-**221**	H	CO_2H	311.6 ± 53.9	0.34	865 ± 131
(*S*)-**221**	H	(*S*)-CO_2H	416.5 ± 64.2	0.33	2065 ± 168
(*R*)-**221**	H	(*R*)-CO_2H	173.5 ± 24.5	0.35	776 ± 26
222	H	H	214.7 ± 30.1	0.40	577 ± 61
223	3-Cl	H	120.6 ± 20.7	0.35	596 ± 68
rac-**224**	3-Me	CO_2H	12.2 ± 3.8	0.40	73 ± 3
(*S*)-**224**	3-Me	(*S*)-CO_2H	11.1 ± 3.9	0.40	128 ± 15
(*R*)-**224**	3-Me	(*R*)-CO_2H	6.4 ± 3.9	0.41	91 ± 9
225	3-Me	H	8.8 ± 1.8	0.46	200 ± 16
226	3-Et	H	3.6 ± 0.5	0.45	253 ± 13
227[a]	3-*i*-Pr	H	6.7 ± 1.3	0.43	305 ± 30
rac-**228**	4-Me	CO_2H	7.5 ± 1.7	0.41	95.5 ± 5
(*S*)-**228**	4-Me	(*S*)-CO_2H	16.7 ± 3.0	0.39	149 ± 6
(*R*)-**228**	4-Me	(*R*)-CO_2H	5.4 ± 1.7	0.42	82 ± 4
229	4-Me	H	16.4 ± 1.9	0.44	219 ± 21
230[a]	4-Et	H	9.7 ± 3.2	0.44	750 ± 34
rac-**231**	4-OMe	CO_2H	7.2 ± 2.2	0.40	94 ± 8
181	4-OMe	H	7.9 ± 3.4	0.44	83 ± 4

Notes: All compounds prepared by Fang Wang and modified from references 138 and 222 unless noted; [a] = prepared by Dawid Podgórski.[222]

3.2.2.2. Triphenylbutanamines containing a mono-substituted phenyl ring

The optimal phenyl substituents in the *meta* or *para* position were introduced to the CH_2-trityl based analogues, and across both assays a systematic increase in potency was evident relative to the comparable thioether analogues (**223-231**, Table 11).[138, 222] These analogues were prepared by Dr. Fang Wang and a visiting student under my supervision Dawid Podgórski. Multiple inhibitors displayed estimated K_i^{app} values ≤ 10 nM in the Eg5 basal activity assay; **226** was comparable in activity to the Phase II clinical candidate ispinesib (K_i^{app} ≈ 2 nM).[223] In the cell-based assay, a consistent improvement over the equivalent thioethers was found that ranged from ~ 2-fold (e.g. *m*-Cl: **104** and **223**; *m*-*i*-Pr: **108** and **227**) to a pronounced 8-fold enhancement (e.g. *m*-OMe **118** and **232**). The exception was **230**, which was comparable in growth inhibition activity to the thioether analogue **117**. However, **117** had exhibited poor aqueous solubility (turbidimetric solubility at pH 7.4 = 37.5 µM), which may have also been a limiting factor in the cellular activity of **230**. The SAR findings generally corresponded with those described for the thioether series (section 3.2.1.1): the most advantageous modifications in the *meta* position were small alkyl substituents, while in the *para* position a methyl or methoxy substituent was favoured. The most potent compounds were the carboxylic acid containing *rac*-**224**, *(R)*-**228** and *rac*-**231**, and the butan-1-amine **181**. *(R)*-Enantiomers consistently proved the more potent stereoisomer when racemates were resolved. The *m*-methyl and *p*-methyl substituted amino acid containing analogues *rac*-**224** and *rac*-**228** were 2-fold more active in the K562 assay than their comparable butan-1-amine analogues **225** and **229**. In contrast to this, the *p*-methoxyphenyl containing analogues *rac*-**231** and **181** were equipotent against Eg5, but in the cell-based assay **181** without the carboxylate displayed marginally more growth inhibition activity. However, in the majority of cases, translation of potent basal inhibition into cellular growth inhibition appeared to require the carboxylic acid.

3.2.2.3. Crystal structure of the Eg5–**224** complex

The structure of the Eg5·*rac*-**224** complex was solved by Kristal Kaan to a resolution of 2.75 Å, and demonstrated the new CH_2-trityl analogues bound to Eg5 in the same overall configuration as STLC (Figure 23).[138] The three phenyl rings are situated in the same distinct hydrophobic regions described for STLC (P1-P3, Figure 15),[132] with the *m*-tolyl ring positioned in the P3 pocket.[138] As the racemate was employed for crystallisation, electron density was observed for both enantiomers. The overall length of the amino acid tail was shortened by replacing the sulphur atom with a methylene (C−S−C bond = 4.5 Å; C−C−C bond = 3.9 Å);[138] however the interactions observed between (*S*)-**224** and Eg5 are

conserved with respect to those found in the Eg5·STLC complex.[132, 136] The primary amine in (*S*)-**224** forms hydrogen bonds with the backbone carbonyl of Gly117 and the carboxylate side chain of Glu116, and additionally the carboxylic acid hydrogen bonds to a guanidinium side chain nitrogen of Arg221.[138] Interestingly, the same interactions were not apparent in the more potent (*R*)-enantiomer: instead, the amino acid moiety appears to interact with the peptide backbone through a structural water molecule. The reason for the improved activity of the CH_2-trityl analogues *c/f* their *S*-trityl analogues is not evident, although recent MD calculations on the Eg5·STLC complex indicate the overall contribution to the free binding energy from the sulphur atom is positive and unfavourable.[139] However the disparity in cellular activity between the two series illustrates that the influence of other factors additionally contribute, and probably in fact predominate over the enthalpic changes to the free energy of binding.

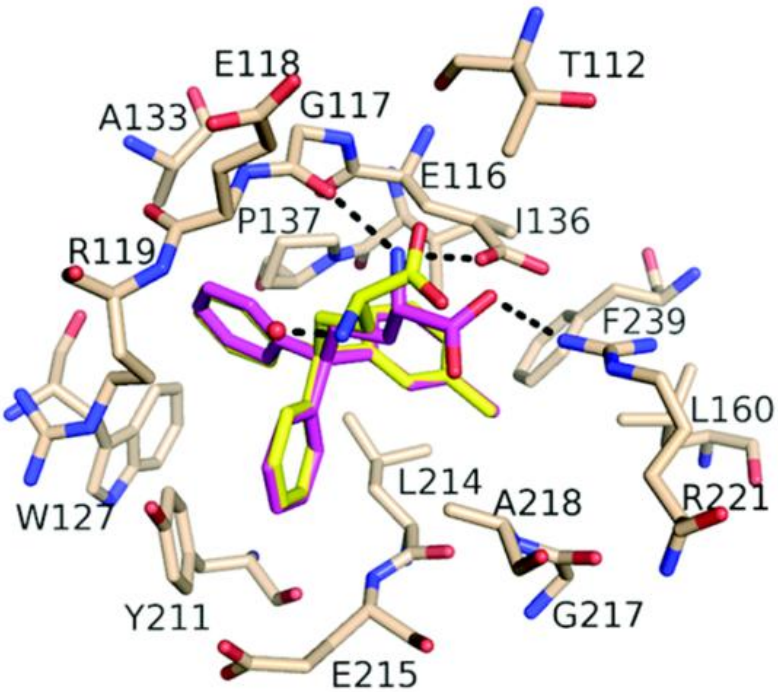

Figure 23 – Eg5-224 crystal structure showing *(S)*-224 (pink) and *(R)*-224 (yellow) in the inhibitor-binding pocket.

Protein side chains and ligands are coloured by atom type: white (C), blue (N) and red (O). The carbon atoms for *(S)*-224 are pink, whilst for *(R)*-224 enantiomer they are yellow. The dashed lines indicate hydrogen bonding interactions. Modified from reference 129.

3.2.3. Analogues containing a disubstituted phenyl ring

3.2.3.1. Thioethers with a fluorine and another hydrophobic phenyl substituent.

The data from our own SAR and previous studies suggested that further optimisation of the hydrophobic binding interactions in the P3 pocket was possible. Impressive increases in affinity with Eg5 had been recorded by scientists at Merck during the optimisation of their clinical candidate MK-0731 by situating a 2,5-difluorophenyl ring into the P3 pocket.[224] A *m*-fluoro substituent had proved detrimental to Eg5 affinity when present in the STLC scaffold (**102**, Table 10), however fluorine substituents in alternative positions in combination with the optimal *m*-alkyl or *p*-alkyl/methoxy substituents had not been investigated. An *o*-fluorine substituent diminished inhibitory activity against Eg5 substantially when combined with a methyl substituent in either the *meta* or *para* position (**152** and **153**, Table 12). However, when combined with a *p*-methoxy substituent (**154** and **155**), the *o*-fluorine modification afforded a ≥ 2-fold improvement in potency against Eg5 *c/f* the mono *p*-methoxy substituted analogue **118** (Table 10). Repositioning of the fluorine substituent in the *meta* position whilst retaining the *p*-methoxy substituent was not tolerated (**156**). In the cellular assay, **152**, **153**, **156** and **157** all proved weak inhibitors, but the improvements in **155** translated to a modest improvement in growth inhibition *c/f* the *p*-methoxyphenyl benchmark **111**. On incorporation of the carboxylic acid, a satisfying 3-fold improvement in growth inhibitory activity was realised in **154,** which demonstrated growth inhibition comparable to the lead triphenylbutanamine analogues prepared previously (GI_{50} ≈ 75 nM*; rac*-**224** and *rac*-**228**, Table 11).[138] Improved multi-polar contacts from the *o*-fluorine substituent may be partially responsible for the enhanced binding of **154** and **155** to Eg5;[225] the increases in cellular efficacy may additionally reflect a minor balancing of the physiochemical properties. The small size of the fluorine substituent also meant that these modest improvements were achieved with limited penalty to the efficiency of the ligand (**111**, L.E. = 0.42; **155**, L.E. = 0.42). Interestingly, the *o*-fluoro, *p*-methoxyphenyl analogue with a CH_2-trityl linker **232** proved 2-fold less potent against Eg5 than its *S*-trityl equivalent **155**, and this loss in activity was also evident in the cell-based assay.

Table 12 – STLC analogues containing a disubstituted phenyl trityl ring.

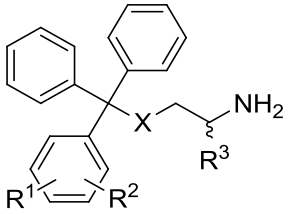

Cmpd	X	R^1	R^2	R^3	Inhibition of basal ATPase activity K_i^{app} (nM)	L.E.	K562 cells GI_{50} (nM)
152	S	2-F	3-Me	H	293.6 ± 23.2	0.36	2547 ± 141
153	S	2-F	4-Me	H	201.3 ± 18.7	0.37	2084 ± 109
154	S	2-F	4-OMe	(*R*)-CO_2H	10.4 ± 0.5	0.38	82 ± 3
155	S	2-F	4-OMe	H	11.6 ± 3.7	0.42	489 ± 26
156	S	3-F	4-OMe	H	162.2 ± 15.6	0.36	1892 ± 134
157	S	3-Cl	4-Cl	H	35.2 ± 4.9	0.41	1993 ± 343
158	S	3-Me	4-Me	(*R*)-CO_2H	1.2 ± 0.1	0.43	72 ± 8
159	S	3-Me	4-Me	H	25.7 ± 6.3	0.41	729 ± 43
160	S	3-Et	4-Me	(*R*)-CO_2H	4.6 ± 1.7	0.39	34 ± 2
161	S	3-Et	4-Me	H	6.9 ± 3.6	0.43	1045 ± 42
162	S	3,4-$(CH_2)_4$		(*R*)-CO_2H	2.1 ± 0.5	0.40	56 ± 2
163	S	3,4-$(CH_2)_4$		H	7.1 ± 2.6	0.41	934 ± 127
232[a]	CH_2	2-F	4-OMe	H	37.9 ± 4.7	0.39	764 ± 42
rac-**176**	CH_2	3-Me	4-Me	CO_2H	12.4 ± 0.4	0.38	23.4 ± 1.8

Notes: [a] = prepared by Dawid Podgórski.[222]

3.2.3.2. Thioethers with dialkyl phenyl substituents.

Crystallographic and SAR data also implied that further expansion was possible into the P3 pocket. A β-napthyl derivative of STLC had demonstrated strong activity against both Eg5 and HeLa cells, and docking studies had indicated the bicyclic ring was most likely to be situated in the P3 cavity (**11**, Table 1).[130] This compound had suffered from poor aqueous solubility (turbimetric solubility = 37.5 μM) and in addition naphthalene is a known toxicophore.[226] This observation correlated with the K_i^{app} estimates ≤ 30 nM displayed by thioethers substituted with *m-(i*-propyl) or *p*-ethoxy groups (**108** and **119**, Table 10); again however both these derivatives displayed weak cellular growth inhibition primarily due to poor aqueous solubility (section 3.2.1.2). Thioethers **152-156** with dialkylphenyl substitutents were prepared to investigate whether further pharmacodynamic improvements could be achieved, whilst maintaining a physicochemical profile conducive to overall efficacy (Table 12).[176] Excellent inhibitory activity was evident on combining *m*-ethyl and *p*-methyl substituents (**161**), and also in the tetralene analogue **163**: both of which demonstrated K_i^{app} estimates ≤ 10 nM. Substantial improvements were realised upon introduction of the terminal α-carboxylic acid, with an estimated K_i^{app} ≈ 1 nM for the dimethylphenyl analogue **158** against Eg5. In contrast to their potency in the Eg5 basal activity assay, the dialkylphenyl analogues **159**, **161** and **163** without the carboxylate were disappointingly weak inhibitors of cellular growth. Evaluation of the aqueous solubility of **38** and **40** demonstrated both were poorly soluble, implying physicochemical limitations were the cause of their reduced cellular efficacy (turbidimetric solubility at pH 7.4: **38** = 3.75 μM; **40** = 3.75 μM). The presence of the carboxylic acid ameliorated this: in addition to low nanomolar activity against Eg5, the amino acid containing analogues **158**, **160**, and **162** all exhibited GI_{50} values < 100 nM against the K562 cell line. The most potent of these contained both a *m*-ethyl and *p*-methyl substituent on the phenyl ring (**160**): the GI_{50} value reported (GI_{50}= 34 nM) represents an impressive ~ 30-fold improvement over **161** without the carboxylic acid, and is ~ 40-fold more active than STLC **6**. These are the most active *S*-trityl based inhibitors of Eg5 reported, thereby suggesting the optimal balance between lipophilicity and physicochemical properties has been achieved for this scaffold. The presence of the carboxylic acid is beneficial for both Eg5 inhibition and cellular activity in these examples: the main contribution of the carboxylate is apparently to enhance aqueous solubility. However, *S*-alkylated derivatives of cysteine were first designed as anticancer agents following the observation that radiolabelled cysteine was incorporated by leukemic white blood cells.[123, 124] Therefore the involvement of active transport cannot be discounted.

3.2.3.3. Triphenylbutanamines with dialkylphenyl substituents

To investigate whether further gains in binding affinity were achievable, the optimal dialkyl phenyl modifications were combined with the triphenylbutanamine scaffold. The poor aqueous solubility of tetralene analogue **162**, even with the addition of the carboxylic acid precluded continuing with this modification (turbidimetric solubility at pH 7.4 = 20 μM). While **160** was the most potent in the cellular assay, the superior physicochemical properties and exquisite enzymatic potency of **158** marked this as the optimal dialkylphenyl substitution pattern. The zwitterionic triphenylbutanamine analogue *rac*-**176** was less potent in the enzymatic assay, but significantly a 3-fold improvement in the cellular assay was afforded over the *S*-trityl analogue **158**, and the most active triphenylbutanamines previously reported (**224** and **228**, Table 11).[138]

3.2.4. Hydrophilic modifications to the trityl head group.

3.2.4.1. Rationale

All the modifications to the trityl group described so far increased its hydrophobicity, which in certain cases compromised cellular efficacy due to poor aqueous solubility (section 3.2.3). In addition to this immediate drawback, excessively lipophilic (i.e. log P/log $D_{7.4}$ > 3) compounds are more likely to possess unfavourable ADME properties, and bind more promiscuously, which is likely to result in greater side effects and general toxicity.[176] Therefore it was important to investigate parameters which were not based solely on improving the lead analogues through lipophilicity, but also through increasing the hydrophilicity of the trityl head group.[227]

3.2.4.2. Thioethers with hydrophilic phenyl substituents

On examining the available crystallographic data, several potential hydrophilic vectors emanating from the trityl group presented themselves. Crystallographic studies on STLC and related analogues had established that the phenyl ring in P1 π-stacked with the nearby phenol of Tyr 211, and that its leading edge both faced the nearby the acidic residue Glu215 and was exposed to the bulk solvent (Figure 14 and Figure 15).[132] Furthermore, the crystal structures of other ligands bound to Eg5 had revealed small polar substituents like the *m*-hydroxy group in (*S*)-monastrol **4** hydrogen bonds with the amide main chain oxygen of Glu118 in the P2 pocket.[97] A series of thioethers was prepared containing hydrophilic phenyl substituents designed to target these interactions (**123-142**, Table 13). The only compound to improve upon basal Eg5 inhibitory activity over STLC was the *m*-hydroxy STLC analogue **124**, which suggested hydrogen bonding similar to that observed in the crystal structures for dihydropyrimidine-Eg5 ternary complexes was being achieved.[24, 25] The direct analogue **125**, which differed only by the absence of the carboxylic acid in the tail, while 4-fold less potent in the basal assay, was 5-fold more potent than **124** in the cellular assay. This can be attributed to the difference in cell permeability resulting from the dual presence of the carboxylic acid and phenol. Evaluation of the passive *in vitro* cellular permeability by parallel artificial membrane permeability assays (PAMPA) demonstrated **125** to have higher permeability (P_{app} = 16.7 ± 2.6 x 10^{-6} cm s^{-1}), with no permeability recorded for **124**. All other compounds in this series displayed moderate inhibition of the basal activity of Eg5, but were generally similar in cellular activity to **16** which demonstrated a wide tolerance for polar substrates. Not surprisingly, aside from **124** and **125**, given the lower basal activities and relatively bulky

substituents all compounds were less efficient ligands than the comparative starting points **6** and **16**. A modest ~ 2-fold improvement in K562 cellular activity was observed for the *meta*-primary and secondary amides **131** and **132** *c/f* STLC, although their Eg5 inhibitory activity was reduced 2-fold and 4-fold respectively. Similarly, the *p*-CH_2OH containing compound **136** had improved cellular activity, but reduced Eg5 inhibitory activity. This could suggest their improved cellular activity is being expressed through an alternative mechanism to Eg5 inhibition. The *m*-primary amide derivative **130**, which has the carboxylic acid group in the tail had similar Eg5 inhibitory activity to **131**, but significantly reduced cellular activity (32-fold less than **131** and 18-fold less than STLC), probably due to a very low log D (log $D_{7.4}$ for **130** = 1.13; c/f log $D_{7.4}$ for **131** = 1.41). Measurement of the cell permeability by PAMPA assays found **131** to possess high permeability of (P_{app} = 42.8 ± 15.0 x 10^{-6} cm s^{-1}), while no membrane diffusion was detected for **130** when evaluated by this method. Thus, the dual presence of the trityl amide modification and carboxylate is incompatible with effective cell penetration, similar to the observations made for the phenol and carboxylate. In summary, although a penalty in basal activity and ligand efficiency is incurred, hydrophilic modifications to the trityl group such as *m*-primary or secondary amide substituents can potentially act as alternatives to the terminal carboxylic acid.

Table 13 – STLC analogues with one hydrophilic trityl substituent

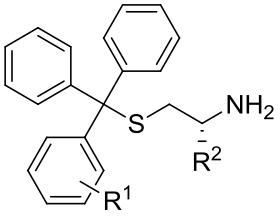

Cmpd	R^1	R^2	Inhibition of basal ATPase activity K_i^{app} (nM)	L.E.	K562 cells GI_{50} (nM)
123	2-OH	*(R)*-CO_2H	1978.5 ± 587.3	0.29	n.d.
124	3-OH	*(R)*-CO_2H	48.8 ± 22.0	0.37	2559 ± 302
125	3-OH	H	200.3 ± 51.9	0.38	555 ± 121
126	3-CN	H	450.6 ± 197.4	0.35	2128 ± 108
127	3-CH_2NH_2	H	838.2 ± 164.1	0.33	2018 ± 244
128	3-$CH_2NHCOMe$	H	829.2 ± 100.5	0.30	2133 ± 135
129	3-CO_2H	H	990.6 ± 156.9	0.31	2138 ± 241
130	3-$CONH_2$	*(R)*-CO_2H	329.9 ± 49.2	0.30	16749 ± 6112
131	3-$CONH_2$	H	419.7 ± 38.8	0.33	802 ± 51
132	3-CONHMe	H	887.8 ± 74.9	0.31	982 ± 72
133	3-$CONMe_2$	H	6055.6 ± 1123.0	0.25	2831 ± 171
134	3-SO_2Me	H	2089.6 ± 246.6	0.29	2559 ± 180
135	4-CN	H	432.4 ± 91.2	0.35	2178 ± 149
136	4-CH_2OH	H	311.2 ± 31.8	0.35	783 ± 50
137	4-CH_2NH_2	H	2942.4 ± 782.8	0.30	2594 ± 191
138	4-$CH_2NHCOMe$	H	1721.3 ± 294.5	0.28	2904 ± 150
139	4-$CONH_2$	H	3228.6 ± 447.4	0.29	4335 ± 341
140	4-CONHMe	H	2030.8 ± 671.6	0.29	3954 ± 293
141	4-$CONMe_2$	H	1526.7 ± 359.7	0.28	2911 ± 271
142	4-SO_2Me	H	1212.1 ± 179.9	0.30	2735 ± 482

3.2.4.3. Heterocycles in the trityl group

An alternate way to reduce lipophilicity was to replace a phenyl ring in the trityl group with small alkyl groups (**12-14**, Table 14).[130, 137] The structure of one such analogue complexed with Eg5 was solved and depicted the *sec*-butyl replacement for the phenyl ring positioned in the solvent exposed P1 pocket.[137] We postulated that a heterocyclic moiety situated in this region could undergo enthalpically favourable offset □-□-stacking with the proximal Tyr 211 phenol,[139] whilst improving the physicochemical attributes of the trityl group by reducing the overall lipophilicity and potentially interacting with water in the solvent exposed pocket. Unfortunately pyridyl, thiazole and oxazole derivatives prepared to investigate this premise were all weak inhibitors of Eg5 in the basal assay, and only modestly active in the cellular assay (**143-145**, Table 14). This corroborated with the weak activity recorded for a 2-thienyl STLC derivative from the NCI library, and 4-pyridyl analogues of STLC recently reported by Abualhasan *et al*.[137, 139] Collectively, these findings indicate that the tested heterocycles are not well tolerated in the Eg5 binding site when incorporated into the STLC scaffold.

Table 14 – STLC analogues with heterocycles in the trityl group

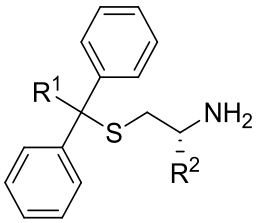

Cmpd	R^1	R^2	Inhibition of basal ATPase activity K_i^{app} (nM)	L.E.	K562 cells GI_{50} (nM)
143	3-Pyridyl	H	1460.7 ± 73.4	0.36	2442 ± 147
144	2-(1,3)-Thiazole	H	3584 ± 381.0	0.39	3750 ± 165
145	2-(1,3)-Oxazole	H	3013.3 ± 163.0	0.29	2312 ± 122

3.2.5. Analogues with two modified phenyl rings

3.2.5.1. Basal Eg5 activity inhibition by analogues with two modified phenyl rings

One potential explanation for the poor activity exhibited by the thioethers **123-142** with hydrophilic trityl substituents was that these analogues did not bind as proposed. If the hydrophilic substituents were situated in the hydrophobic P3 pocket, rather than either the solvent exposed P1 area or the P2 pocket with the potential to form hydrogen bonding interactions, this could explain the diminished affinity with Eg5. To investigate, a series of thioethers was prepared that incorporated a combination of the optimal hydrophobic and hydrophilic phenyl substituents onto discrete rings in the trityl group with the aim driving the more lipophilic phenyl into the P3 pocket (**146-151**, Table 15). This would leave the more hydrophilic phenyl group to bind in either of the remaining pockets and therefore potentially produce a synergistic increase in inhibitory activity. This was not the case for *rac*-**147** containing both *m*-phenol and *m*-chlorophenyl modifications, which exhibited poor basal inhibition, whereas related *m*-phenol analogues *rac*-**148** and *rac*-**149** with discrete *m*-ethyl and *p*-methyl substituents were ~ 2-fold and 4-fold more potent inhibitors of basal Eg5 activity, in comparison to their respective analogues **107** and **116**. This implied a synergistic binding motif was being realised through hydrogen bonding interactions in P2 from the phenol and improved hydrophobic interactions in P3 by the more hydrophobic phenyl ring. Improvements in Eg5 inhibitory activity were also seen when a *p*-tolyl was combined with a second phenyl containing either an *m*-cyano or *m*-primary amide substitiuents (*rac*-**150** and *rac*-**151**). The more hydrophilic phenyl group for these two compounds is more likely to be positioned in the solvent exposed P1 region because the relatively large hydrophilic substituents would not be accommodated in the P2 pocket, since this area is sterically restrained and can only accept a small hydroxyl group.[162, 224, 228]

Table 15 – STLC analogues with modifications to two phenyl rings.

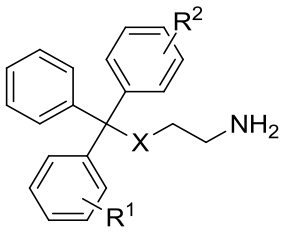

Cmpd	X	R^1	R^2	Inhibition of basal ATPase activity K_i^{app} (nM)	L.E.	K562 cells GI_{50} (nM)
125	S	3-OH	H	200.3 ± 51.9	0.38	555 ± 121
126	S	3-CN	H	450.6 ± 197.4	0.35	2128 ± 108
130	S	3-$CONH_2$	H	419.7 ± 38.8	0.33	802 ± 51
102	S	3-Cl	H	297.8 ± 60.0	0.37	1045 ± 42
107	S	3-Et	H	5.9 ± 2.3	0.45	680 ± 84
116	S	4-Me	H	27.4 ± 0.7	0.43	731 ± 36
229	CH_2	4-Me	H	16.4 ± 1.9	0.44	219 ± 21
146	S	4-Me	4-Me	56.0 ± 5.0	0.40	2174 ± 119
rac-**147**	S	3-OH	3-Cl	200.3 ± 35.3	0.37	1662 ± 77
rac-**148**	S	3-OH	3-Et	3.7 ± 0.8	0.44	260 ± 19
rac-**149**	S	3-OH	4-Me	7.1 ± 1.8	0.44	98 ± 6
rac-**150**	S	3-CN	4-Me	64.2 ± 5.2	0.38	1186 ± 34
rac-**151**	S	3-$CONH_2$	4-Me	55.6 ± 8.0	0.37	308 ± 16
rac-**233**[a]	CH_2	3-OH	4-Me	33.6 ± 6.4	0.41	232 ± 24

Notes: [a] = prepared by Fang Wang.[222]

3.2.5.2. Cellular growth inhibition by analogues with two modified phenyl rings

Reflective of its poor Eg5 inhibition, the *m*-chlorophenyl/*m*-phenol analogue *rac*-**147** was weakly active in the cellular assay (Table 15). However all analogues with modifications on two phenyl rings that exhibited improved basal inhibition over their comparable benchmarks were also more efficacious in the K562 assay. The *m*-phenol/*m*-ethylphenyl and *m*-phenol/*p*-tolyl analogues *rac*-**148** and *rac*-**149** improved ≥ 2-fold and ≥ 5-fold respectively over their comparable mono substituted counterparts **107**, **116** and **125**. With GI_{50} ≈ 100 nM, *rac*-**149** is the most potent thioethanamine analogue not including the terminal carboxylic acid in the cellular assay, and is ~ 15-fold more active than STLC **6** against the K562 cell line. Interestingly, the comparable CH_2-trityl analogue (*rac*-**233**) was less active against both Eg5 and the K562 cell line than either *rac*-**149** or the structurally related triphenylbutanamine **229**. These compounds (**147**-**151**) were prepared as racemic mixtures which suggested further gains in affinity were possible. However, the *m*-phenol modification was not pursued after concerns were raised over its metabolic stability. The high clearance[229] of *rac*-**149** *c/f* other lead candidates (section 3.4.1.2) was confirmed in an *in vitro* human hepatocyte assay (Cl_{int} = 50.1 ± 4.2 μL/min/million cells; $t_{½}$ = 27.7 min). The cyano-substituted *rac*-**150** demonstrated a 2-fold improvement over the comparable mono-substituted derivative **126**, but was still only active in the micromolar range. A similar improvement was also displayed by *m*-primary amide substituted *rac*-**151** over its mono-substituted counterparts **116** and **130**. The synergistic increases in activity support the proposed binding mode with the *p*-tolyl occupying the P3 pocket and the *m*-amide situated in the P1 region for *rac*-**151**, and confirm this amide substituent as a potential alternative hydrophilic modification to the terminal α-carboxylate in STLC.

3.2.5.3. Crystal structure of the Eg5 – *rac*-**148** complex

The crystal structure of *rac*-**148** complexed to Eg5 was solved to a resolution of 2.65 Å by Kristal Kaan, and provided structural confirmation for the proposed binding mode (Figure 24).[222] The inhibitor adopts the same overall conformation seen in STLC and related analogues, with the three phenyl rings occupying the defined P1-P3 pockets.[132, 137, 138] Interestingly, although the racemic mixture of **148** was employed, electron density was only observed for the *(R)*-enantiomer, implying this is more stable. The two phenyl substituents could be easily identified, and a structural rationale provided for the increased potency of *rac*-**148**. In the P2 pocket, the *m*-hydroxy substituted phenol forms a hydrogen bond with the main chain carbonyl of Glu118, in an identical manner to that observed in the structures of monastrol (**4**) and structurally related dihydropyrimidines.[97, 230] The *m*-ethyl substituent is situated into the P3 pocket bounded by Leu160, Gly217, Ala218, Arg221, with the terminal CH_3 occupying previously unutilised space between the methyl of Ala218 and the aliphatic chain of Arg221. These improved hydrophobic contacts may explain the improved activity against Eg5 by ligands incorporating this substituent (e.g. **107** and **160**). In the thioethanamine chain, the primary amine maintains the crucial hydrogen bonds exhibited in all STLC analogues with the carboxylate of Glu116 and the main chain amide carbonyl of Gly117.[132, 136] In summary, this crystal structure provides a valuable structural validation for the rationale beneath the SAR improvements implemented.

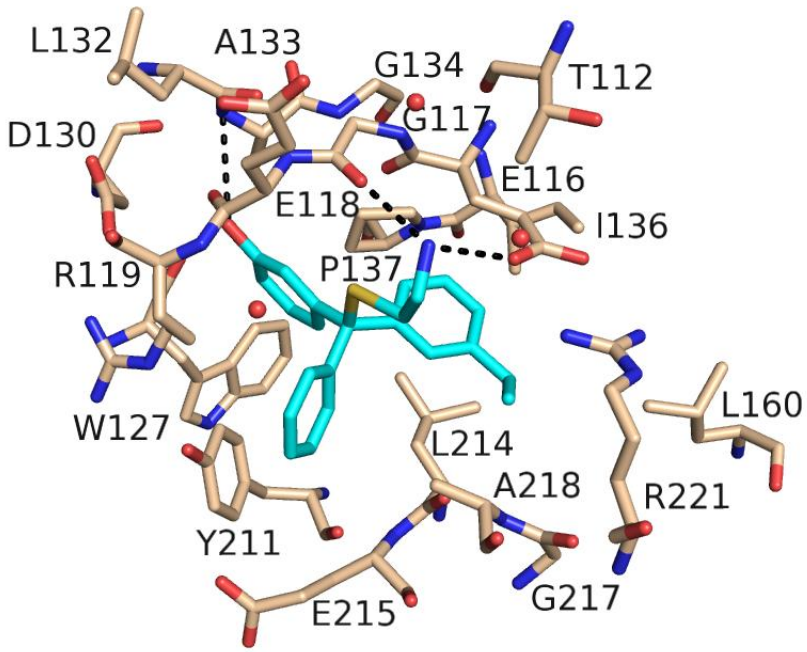

Figure 24 – Eg5-*rac*-148 crystal structure showing (*R*)-148 in the inhibitor-binding pocket.

The protein side chains are coloured by atom type: white (C), blue (N) and red (O). The (*R*)-148 ligand is coloured by atom type: turquoise (C), blue (N), red (O) and yellow (S). Hydrogen bond interactions between the protein and inhibitor are represented by dashed lines. Modified from reference 222.

3.2.6. Modifications to the amino acid tail

3.2.6.1. β-Fluorination to modulate amine basicity

The *p*-methoxy triphenylbutanamine analogue **181** without the carboxylic acid had exhibited excellent potency in both the basal and cellular assays (Table 11), and was a potential backup candidate to the lead dialkylphenyl analogues (Table 12). However, profiling of the comparable *m*-methylphenyl analogue **225** revealed several potentially significant toxicological interactions in analogues without the carboxylic acid, such as hERG and inhibition of common CYP isoforms.[138] Therefore, we examined whether in the DMPK profile for this analogue could be improved by modulating the basicity of the primary amine through β-fluorination.[231, 232] Although a common strategy to overcome hERG liabilities is alkylation of a primary amine, the necessity of the primary amine in the STLC scaffold to form three hydrogen bonds had already been demonstrated.[137] β-Fluorination represented a more subtle approach, and **182-184** were prepared as tool compounds to investigate this strategy (Table 16). While good inhibitory activity was retained in the basal assay for the mono-fluorinated analogue **182**, a > 10-fold reduction was recorded for the difluorinated **183** and activity abolished to micromolar levels for the α-trifluoro containing **184**. Evaluation in the cellular assay revealed an ~ 8-fold drop in activity for the mono-fluorinated **182** *c/f* the benchmark **181**, with micromolar activity for the difluorinated **183** and no apparent inhibition by **184**. Measurement of the pK_a values of **181-184** revealed a variation of over 5 log units as the number of fluorine atoms in the β-position increased. While these results reinforced the importance of the protonation state of the amine, and its subsequent ability to form three hydrogen bonds, the pK_a of the NH_2 group in the zwitterionic amino acid moiety of **158** is equivalent to that in the β-difluorinated primary amine **183** (section 3.4.1.1.). This indicates that additional factors contributed to the reduced cellular efficacy. However, as useful efficacy was not demonstrated by these analogues, this was not investigated further.

Table 16 – β-Fluorinated analogues of 4-(4-methoxyphenyl)-4,4-diphenylbutan-1-amine 181.

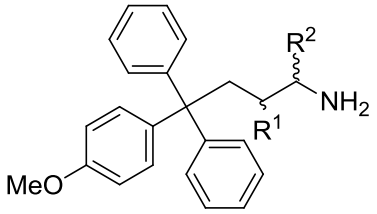

Cmpd	R^1	R^2	pK_a	Inhibition of basal ATPase activity K_i^{app} (nM)	L.E.	K562 cells GI_{50} (nM)
181[a]	H	H	9.86 ± 0.05	7.9 ± 3.4	0.44	83 ± 4
rac-**182**	F	H	7.86 ± 0.07	27.3 ± 1.2	0.40	652 ± 61
183[a]	F_2	H	7.11 ± 0.05	88.4 ± 1.9	0.36	2624 ± 379
rac-**184**	H	CF_3	4.63 ± 0.10	2268 ± 39.1	0.27	>100000

Notes: [a] = prepared by Fang Wang.[222]

3.2.6.2. Bioisosteric replacements for the carboxylic acid to overcome Pgp efflux

At the onset of lead optimisation, a known liability of STLC and related analogues was their efflux by the MDR related Pgp transporter.[137, 139] The physiological relevance of Pgp efflux to cancer therapy has yet to be fully deciphered, and it is not as likely to play as important a role in drug efficacy as intrinsic activity and advantageous DMPK characteristics (section 1.3.4.2).[32, 145] However, it is a pathway of resistance known to affect several classes of existing chemotherapy drugs and for Eg5 inhibitors to provide therapeutic benefits over existing treatments, it was therefore desirable to develop strategies to circumvent or reduce efflux by the Pgp transporter. The carboxylic acid had been identified in preceding investigations as the critical structural feature in STLC for determining whether uptake and efflux by Pgp would occur.[137, 139] A direct approach to ameliorating extracellular Pgp-mediated efflux was therefore to replace the carboxylic acid with a suitable bioisostere. In the crystal structure of STLC, the carboxylate forms a hydrogen bonding interactions with the Arg221 guanadinium and to the bulk solvent.[132, 136] MD calculations had contrastingly demonstrated that the enthalpy from binding with Eg5 was unfavourable for the carboxylate because of repulsion from the anionic diphosphate of the neighbouring nucleotide.[139] In combination with the SAR established for the most active ligands (section 3.2.3), this supported the hypothesis that the principle contribution of the carboxylic acid to enhancing efficacy is by improving physiochemical parameters. To investigate whether improved interactions with Eg5 could be achieved through optimising interactions in this region, a number of analogues incorporating amide replacements for the carboxylic acid were prepared (Table 17). Replacement of the entire amino acid zwitterion with a primary amide in **210** resulted in an abolition of inhibitory activity, reinforcing the prerequisite of the amine moiety to form three hydrogen bonds.[132, 137] The primary amide replacements for the carboxylate (**215)** proved equivalent to STLC in the basal assay, and improved in the cellular assay. This result agrees with the findings of Ogo *et al.* who evaluated this isostere against Hela cells and found **215** more active than STLC.[141] This perhaps surprising result suggests a primary amide replacement for the carboxylate can function as a bioisostere in the Eg5 binding site. Other bulkier secondary, tertiary and Weinreb amide replacements for the carboxylate (**216-218)** were less active against Eg5 than STLC, and whilst a reduction in intrinsic affinity was tolerable if improved activity was accomplished in Pgp overexpressing systems, these analogues were also disappointingly weak in the cellular assay. A number of conventional isosteres for a carboxylic acid were also tested.[233] Whilst the hydroxamic acid derivative **220** displayed reasonable basal Eg5 inhibition, only weak activity in the cellular assay was apparent. The

tetrazole CH_2-trityl based analogue *rac*-**235** demonstrated reasonable inhibition in the enzymatic assay; again however this did not translate into the cellular assay, with an 8-fold decrease in potency when compared to the amino acid *rac*-**231**. Similar levels of basal inhibition to *rac*-**231** were displayed by the amino alcohol *rac*-**234**. Satisfyingly, *rac*-**234** did maintain reasonable levels of growth inhibition in the cellular assay, in agreement with recent findings for cysteinol based STLC derivatives reported by Rodriguez *et al.*[234]

Table 17 – STLC analogues incorporating carboxylate isosteres.

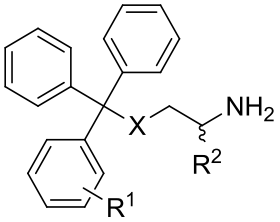

Cmpd	X	R^1	R^2	Inhibition of basal ATPase activity K_i^{app} (nM)	L.E.	K562 cells GI_{50} (nM)
6 (STLC)	S	H	(*R*)-COOH	135.9 ± 20.5	0.36	1452 ± 76
rac-**231**	C	4-OMe	(*R*)-COOH	7.2 ± 2.2	0.35	94 ± 8
210	S	H	⁓=O	n.i.	n/a	>100,000
215	S	H	(*R*)-$CONH_2$	133.2 ± 1.6	0.36	1064 ± 48
216	S	H	(*R*)-CONHMe	359.2 ± 26.6	0.33	5012 ± 218
217	S	H	(*R*)-$CONMe_2$	249.3 ± 7.2	0.32	5916 ± 319
218	S	H	(*R*)-CONMeOMe	429.3 ± 27.2	0.30	6918 ± 601
220	S	H	(*R*)-CONHOH	298.2 ± 19.3	0.30	13152 ± 575
rac-**234**[a]	CH_2	4-OMe	CH_2OH	4.5 ± 2.9	0.42	192 ± 18
rac-**235**[a]	CH_2	4-OMe	Tetrazole	20.6 ± 3.1	0.35	826 ± 55

Notes: n.i. = no inhibition; n/a = not applicable; [a] = prepared by Fang Wang.[222]

3.3. Further *in vitro* characterization

3.3.1. Inhibition of microtubule stimulated Eg5 ATPase activity

A selection of the most active compounds were evaluated for their inhibition of the microtubule-stimulated (MT-stimulated) ATPase activity of Eg5 (Table 18). This assay provides a more accurate estimate of the K_i^{app}, since the activity of Eg5 is increased in the presence of microtubules which allows lower concentrations of Eg5 to be employed than in the basal assay (~ 5 nM *c/f* ~ 80 nM).[235] Differences were apparent for the dimethylphenyl thioethanamine analogue **158**, which was much less potent than was observed in the basal assay (MT-stimulated K_i^{app} ≈ 50 nM *c/f* basal K_i^{app} ≈1 nM). In general however, the results are in good agreement with the strong inhibitory activity demonstrated in the basal assay, with the most potent analogue **160** (K_i^{app} 2.4 ± 0.4).

Table 18 – Evaluation of MT-stimulated inhibitory activity of lead inhibitors.

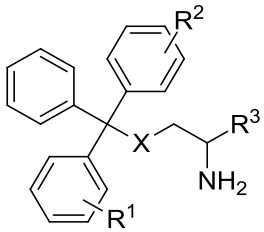

Cmpd	X	R^1	R^2	R^3	Inhibition of basal ATPase activity K_i^{app} (nM)	Inhibition of MT-stimulated ATPase activity K_i^{app} (nM)
6 (STLC)	S	H	H	(*R*)-COOH	135.9 ± 20.5	143.8 ± 21.6
154	S	2-F, 4-OMe	H	(*R*)-COOH	10.4 ± 0.5	28.8 ± 1.0
158	S	3-Me, 4-Me	H	(*R*)-COOH	1.2 ± 0.1	49.9 ± 2.6
160	S	3-Et, 4-Me	H	(*R*)-COOH	4.6 ± 1.7	2.4 ± 0.4
162	S	3,4-$(CH_2)_4$	H	(*R*)-COOH	2.1 ± 0.5	13.9 ± 1.3
rac-**176**	CH_2	3-Me, 4-Me	H	COOH	12.4 ± 0.4	7.3 ± 0.9
rac-**149**	S	4-Me	3-OH	H	7.1 ± 1.8	9.7 ± 1.8

*3.3.2. Specificity of rac-**176** amongst kinesins*

To evaluate the specificity of the new analogues amongst human kinesins, one of the most active, the triphenylbutanamine *rac*-**176** which incorporated a dimethylphenyl, was examined against a panel involved in both mitosis and intracellular transport (Table 19).[51, 59] Significant inhibition was not recorded of any of the kinesins examined at the concentrations tested, in agreement with the reported selectivity by STLC for Eg5 (section Table 19).[104, 129]

Table 19 – Effect of *rac*-176 on the activity of other human kinesins.

Kinesin	Kinesin family	Inhibition of basal ATPase activity K_i^{app} (μM) [MIA (%)]	Inhibition of MT-stimulated ATPase activity K_i^{app} (μM) [MIA (%)]
Kif5A[a]	Kinesin 1	n.i. (10)	n.i. (10)
Kif5B[b]	Kinesin 1	n.i. (5)	n.i. (5)
Kif3B	Kinesin 2	n.i. (5)	n.i. (20)
MKLP-2[c]	Kinesin 6	n.i. (5)	n.i. (10)
MPP1[d]	Kinesin 6	n.i. (10)	n.i. (15)
Kif7	Kinesin 7	n.i. (5)	n.i. (5)
Kif9	Kinesin 9	n.i. (5)	n.i. (20)

Notes: MIA = maximum inhibitory activity observed. n.i. = no inhibition. [a] = a.k.a. neuronal kinesin heavy chain; [b] = a.k.a. conventional kinesin, kinesin heavy chain; [c] = a.k.a. Kif20A, RabK6; [d] = Kif20B, MPHOSPH1, KRMP1.

3.3.3. Evaluation of lead analogues across multiple cell lines

The most promising lead compounds were evaluated in a panel of five additional tumour cell lines derived from colon, breast, pancreatic and prostate cancers (Table 20). STLC was included as a control, and selected triphenylbutanamines from the study by Wang *et al*,[138] whilst to benchmark against external controls the Phase II clinical candidate ispinesib (**21**) and its second generation analogue SB-743921 (**22**) were evaluated. The activity of the CH_2-trityl linker was broadly comparable to STLC, apart from in the K562 cell line, reinforcing the observation that the most significant gains in potency were realised on incorporation of lipophilic trityl substituents (e.g. *(R)*-**228** *c/f* **6**). The most potent triphenylbutanamine analogue *(R)*-**228** with a *p*-methyl substituent was ~ 10 fold more active across comparable cell lines than the unsubstituted **6**. The *S*-trityl analogues **158**, **160** and **162** containing a dialkylphenyl displayed excellent potency across all cell lines: the *m*-ethyl, *p*-methylphenyl analogue **160** was the most potent STLC analogue in the pancreatic and LNCap prostate cancer derived cell lines. Its activity was only surpassed by the CH_2-trityl dimethylphenyl *rac*-**176**, which was more active in the HCT116, K562 and PC3 cell lines. Between them, **160** and *rac*-**176** bettered or matched the activity of the Phase II clinical candidates **21** and **22** in all of the cell lines, except HCT116. The *m*-phenol containing *rac*-**149** also displayed good potency across most cell lines demonstrating that increases in activity were achievable through discrete modifications to the trityl group.

Table 20 – Testing of selected analogues for growth inhibition of colon (HCT116), human leukaemia (K562), lung (NCI-H1299), pancreas (BxPC3) and prostate (LNCap and PC3) tumour cell lines.

Cmpd	HCT116 GI_{50} (nM)	K562 GI_{50} (nM)	NCI-H1299 GI_{50} (nM)	BxPC3 GI_{50} (nM)	LNCap GI_{50} (nM)	PC3 GI_{50} (nM)
1 (STLC)	553 ± 57	1452 ± 76	1549 ± 111	1563 ± 155	811 ± 116	1371 ± 96
(*R*)-**221**[a]	472 ± 20	776 ± 26	1324 ± 55	1119 ± 138	n.d.	n.d.
(*R*)-**228**	40 ± 2	82 ± 4	111 ± 6	85 ± 12	32 ± 2	58 ± 4
181	33 ± 2	83 ± 4	158 ± 10	168 ± 12	60 ± 6	158 ± 11
154	114 ± 8	82 ± 3	325 ± 45	77 ± 15	93 ± 8	94 ± 10
158	63 ± 9	72 ± 8	111 ± 10	124 ± 29	34 ± 6	73 ± 8
160	34 ± 3	34 ± 2	39 ± 2	26 ± 6	9.2 ± 1.2	27.3 ± 2.3
162	39 ± 2	56 ± 2	101 ± 9	53 ± 5	31 ± 2	43 ± 5
rac-**176**	28 ± 2	23.4 ± 1.8	41 ± 3	44 ± 10	11.4 ± 0.8	21 ± 1
rac-**149**	91 ± 10	98 ± 6	221 ± 16	427 ± 85	97 ± 10	258 ± 24
21 (Ispinesib)[a]	25 ± 3	48 ± 4	82 ± 10	80 ± 15	22 ± 4	50 ± 5
22 (SB743921)	9.7 ± 0.8	24 ± 1	35 ± 7	25 ± 4	15 ± 3.5	21.2 ± 2.4

Notes: n.d. = not determined; [a] = from reference 138. All other data modified from reference 222.

3.3.4. Evaluation of the MDR ratio for selected new inhibitors

3.3.4.1. The effect of the CH_2-trityl linker

The MDR ratios of a representative panel of inhibitors were evaluated to compile an SAR portfolio for Pgp efflux (Table 21). As a positive control, the known Pgp substrate vinblastine was included, and STLC and the thioethanamine analogue **16** were included as internal control compounds. In agreement with previous results obtained from LLC-PK1 and MDCKII and matched Pgp overexpressing cell lines L-MDR1 and MDCKII-MDR1, STLC had an MDR ratio of 42, whereas **16** without the carboxylic acid had an MDR ratio of 1.1.[137] The CH_2-trityl modification proved detrimental to activity in the Pgp overexpressing KB-V1 cell line: the zwitterionic *rac*-**221,** *rac*-**224** and *rac*-**228** exhibited 2-fold worse MDR ratios than STLC, both displaying decreases in activity from < 100 nM in the parental cell line to > 5 μM in the Pgp overexpressing cell line. The higher ratios evident for CH_2-trityl *versus S*-trityl analogues may reflect the increase in the respective strengths of the acid and amine moieties.[138] The increase in the ionised population would decrease the passive membrane diffusion, which may allow for the efficiency of Pgp mediated efflux to be increased resulting in a greater MDR ratio for these analogues.[144] Whilst Pgp is not intrinsically stereospecific,[142, 144] selectivity was evident in the triphenylbutanamine series, with the *(S)*-enantiomers exhibiting greater decreases in activity in the KB-V1 assay than their *(R)*-enantiomers [e.g. (*R)*-**228**, MDR ratio = 92; *(S)*-**228**, MDR ratio = 69], in agreement with prior observations made for STLC and STDC.[137] Removal of the α-carboxylic acid from the amino acid tail in the CH_2-trityl series restored activity in the KB-V1 cell line, with submicromolar activity evident for **181** and **225**. This data illustrates that whilst the CH_2-trityl linker contributes to the MDR ratio, it is not intrinsically incompatible with avoiding efflux. The presence of the carboxylate remains the decisive factor in determining the overall rate efficacy of Pgp efflux in the overexpressing KB-V1 cell line.

3.3.4.2. Modifications to the trityl group

While the *S*-trityl analogue **160** displayed a comparable MDR ratio to STLC, the other dialkylphenyl substituted analogues **158** and **160** with the carboxylic acid had improved MDR ratios. Thus the increased lipophilicity of **158** and **160** *c/f* **6** appeared to reduce their uptake through increased passive diffusion through the cell membrane, although why the same did not apply to **160** is not clear. Interestingly, the excellent potency of the *m*-ethyl, *p*-methylphenyl analogue **160** meant that even with > 35 fold reduced activity, it still

registered ~ 1 μM growth inhibition activity against the KB-V1 cell line. This indicates that even small reductions in the MDR ratio for the most potent compounds would restore activity to acceptable levels and render Pgp efflux less of an issue for STLC based inhibitors. The CH_2-trityl dimethylphenyl analogue *rac*-**176** exhibited the highest measured MDR ratio of all, confirming the CH_2 modification as detrimental. Although alkyl trityl substituents had a limited effect on the MDR ratio, the *p*-methoxy trityl substituent appeared to substantially increase the MDR ratio: e.g. **181** has an MDR ratio ~ 3-fold worse than the comparable *m*-methyl substituted **225**. This agrees with prior SAR studies on Pgp which highlighted ethers as a common motif in accentuating recognition and transport.[144] This may relate to increased aqueous solubility through the increased polar surface area slowing passive membrane diffusion and allowing increased uptake by Pgp. The *meta*-primary amide analogue **131**, which had been investigated as a potential replacement for the terminal α-terminal acid, had a greater MDR ratio than STLC. Phenol containing analogues *rac*-**148** and *rac*-**149** proved moderate substrates, with MDR ratios of 9.1 and 12.0 respectively.

3.3.4.3. Modifications to the amino acid tail

The strategies designed to modulate the properties of the amino acid tail proved generally successful at ameliorating Pgp efflux. β-Fluorinated amine analogue **182** displayed comparable potency across both the parental KB-3-1 and overexpressing KB-V1 cell lines. This confirmed proximal fluorination of the primary amine in STLC as a valid strategy to modulate DMPK properties, and one which could be employed to reduce Pgp efflux. For the carboxylate isosteres and replacements, the activity of the tetrazole *rac*-**234** was abolished, and the β-amino alcohol analogue *rac*-**135** similarly was subject to a high MDR ratio. The weakly active amide analogues **216-218** were not subject to Pgp efflux, but their weak activity precluded their further use. Most notably, the primary amide isostere **215** displayed a low MDR ratio of 4. Whilst still only weakly active in the KB-V1 cell line (~ 2 μM), this represents a 10-fold improvement in activity on its direct analogue STLC. Thus, a primary amide represents a viable bioisosteric replacement for the carboxylic acid to alleviate Pgp-mediated efflux.

Table 21 – Determination of MDR ratios of STLC analogues with modifications to the trityl group.

Cmpd	KB-3-1` EC_{50} (nM)	KB-3-1+Z EC_{50} (nM)	KB-V1 EC_{50} (nM)	KB-V1+Z EC_{50} (nM)	MDR ratio
6	1094 ± 212	1002 ± 195	36982 ± 5200	922 ± 62	42
16	1910 ± 364	1932 ± 537	2037 ± 516	1268 ± 296	1.1
rac-**221**	1202 ± 47	1117 ± 102	> 50000	1109 ± 163	> 40
(R)-**221**	748 ± 40	736 ± 94	> 50000	708 ± 124	> 65
(S)-**221**	2213 ± 359	2009 ± 255	> 50000	2223 ± 600	> 25
222	561 ± 92	587 ± 164	1972 ± 388	373 ± 29	3.5
rac-**224**	81 ± 8	73 ± 6	6471 ± 808	46 ± 4	80
(R)-**224**	70 ± 6	74 ± 5	5768 ± 748	69 ± 12	82
(S)-**224**	207 ± 29	200 ± 21	12474 ± 1202	161 ± 39	60
225	257 ± 42	208 ± 37	927 ± 186	188 ± 27	3.6
rac-**228**	86 ± 5	78 ± 13	7145 ± 1482	71 ± 9	83
(R)-**228**	73 ± 4	62 ± 5	6683 ± 998	68 ± 13	92
(S)-**228**	161 ± 32	153 ± 15	11117 ± 1726	117 ± 26	69
rac-**231**	105 ± 5	99 ± 9	12853 ± 2030	107 ± 16	122
181	79 ± 5	72 ± 11	767 ± 73	71 ± 11	9.7
154	108 ± 5	105 ± 5	8511 ± 997	96 ± 6	79
158	245 ± 14	213 ± 16	3899 ± 376	100 ± 11	15.9
160	28 ± 4	29 ± 4	1028 ± 66	27 ± 2	36.7
162	92 ± 9	95 ± 14	2148 ± 233	70 ± 10	23.3
rac-**176**	19.0 ± 2.2	23.0 ± 0.6	3304 ± 125	29 ± 2	174
rac-**148**	229 ± 60	195 ± 24	2074 ± 327	188 ± 30	9.1
rac-**149**	152 ± 13	160 ± 29	1820 ± 405	117 ± 21	12.0
131	1138 ± 88	1010 ± 87	> 50000	740 ± 97	> 45
182	670 ± 94	685 ± 116	855 ± 71	661 ± 248	1.3
215	2028 ± 157	2344 ± 169	8279 ± 1166	1019 ± 332	4
216	13677 ± 1283	12106 ± 852	9705 ± 757	4539 ± 841	n.d.
217	5861 ± 812	6053 ± 891	5916 ± 672	5715 ± 894	1.0
218	6516 ± 635	9120 ± 557	7709 ± 1604	5395 ± 661	1.2
rac-**234**	1426 ± 153	1132 ± 86	>50000	587 ± 97	> 40
rac-**235**	171 ± 41	163 ± 38	3311 ± 213	69 ± 6	19.4
Vinblastine	12.6 ± 2.0	12.4 ± 1.8	2037 ± 135	13.0 ± 0.7	163

Notes: MDR ratios were determined by dividing the GI_{50} value obtained in the Pgp over-expressing cell line KB-V1, with the GI_{50} determined in isogenic parental KB-3-1 cells. A further control experiment was conducted in the presence of the specific Pgp inhibitor Zosuquidar trihydrochloride (Z).

3.4. Profiling of lead inhibitors

3.4.1.1. Physicochemical properties

The lead dialkylphenyl *S*-trityl analogues **158** and **160** and the CH_2-trityl based *rac*-**176** were profiled to ascertain their drug-like properties in a series of *in vitro* and *in vivo* assays. The physicochemical properties of *S*-trityl analogues **158** and **160** were at the upper limit of the typically described range for achieving optimal drug-like properties.[236] With molecular weights ~ 400, **158** and **160** were partially soluble, with a non-optimal LogP for **160**.[176] In contrast, the smaller CH_2-trityl based analogue demonstrated good aqueous solubility (> 100 μM) and an optimal Log P.[176] The Log D at pH 7.4 for all three candidates was around 3 and favourable, although the inaccuracy associated with these readings diminishes their relative utility. Interestingly, one significant difference evident between all three was the relative strengths of the acid/base moieties as reflected by their pK_a, with the *S*-trityl analogues **158** and **160** much weaker acids/bases than the CH_2-trityl analogue *rac*-**176**.

3.4.1.2. ADME assays

In mouse microsomal stability assays, both **160** and *rac*-**176** were stable over the time course of the experiment, while **158** was cleared at a moderate rate ($t_{½}$ ≈ 80 min); all three were stable in human microsomes. In human hepatocytes, **158** and *rac*-**176** exhibited low clearance, while a moderate rate of clearance was observed for **160** ($t_{½}$ ≈ 60 min). Another factor which is an important influence on distribution, clearance and overall pharmacological efficacy is the proportion bound to plasma protein: while both **158** and *rac*-**176** had a comparable fraction unbound (*fu* ≈ 5.0%), a higher proportion of the more lipophilic analogue **160** was bound (*fu* ≈ 1.6%). This compound was also demonstrated to possess good oral bioavailability of 62%, higher than the value reported for ispinesib, with a rapid onset of peak concentration (t_{max} = 0.5 h, Table 23).[138] However, **160** is more rapidly cleared from the systemic circulation than ispinesib.

3.4.1.3. Toxicology

An important safety consideration which has emerged in recent years for drugs is the potential for interactions with hERG potassium channels which are involved in modulating electrical activity in the heart, as their disruption can cause cardiac arrhythmia.[169] None of the lead inhibitors demonstrated interactions at the maximum concentration examined.

Screening was also performed against CYP isoforms from the five main families.[237] Metabolism by CYP enzymes accounts for the majority of degradation pathways encountered by known drugs in the body, and their inhibition can lead to adverse reactions resulting from drug-drug interactions.[238, 239] This is therefore an important consideration for Eg5 inhibitors given the likelihood that they would be administered in combination chemotherapies. The dimethyl *S*-trityl analogue **158** moderately inhibited the CYP2C19 isoform, whilst **160** weakly interacted with the CYP2C9 isoform, whose activities account for 12% and 16% respectively of the overall CYP-mediated metabolism of drugs.[237] No inhibition of the isoforms from the five main families was evident for the dimethyl CH_2-trityl analogue *rac*-**176**.

Table 22 – DMPK profiles of lead analogues 158, and 160 and *rac*-176.

Assay / Compounds	**158**	**160**	***rac*-176**
Molecular Weight (Da)	391.53	405.55	373.49
Turbidimetric Solubility [**pH 2.0, 6.0, 7.4** (μM)]	65, 65, 65	> 100, 65, 65	>100, >100, >100
Log P	2.94 ± 0.03	4.13 ± 0.03	1.955 ± 0.51
p*K*$_a$	p*K*$_a$ 1: 8.21 ± 0.09 p*K*$_a$ 2: 2.51 ± 0.11	p*K*$_a$ 1: 7.10 ± 0.10 p*K*$_a$ 2: 3.28 ± 0.07	p*K*$_a$ 1: 9.36 ± 0.05 p*K*$_a$ 2: 1.69 ± 0.46
Log D$_{7.4}$	3.17 ± 0.20	3.08 ± 0.15	3.28 ± 0.367
Microsomal Stability [Clint (μL/min/mg protein)]			
Human	stable	stable	stable
t$_{½}$ (min)	--	--	--
Mice	17.8 ± 3.67	stable	stable
t$_{½}$ (min)	77.8	--	--
Human Hepatocytes (μL/min/million cells)	7.9 ± 3.4	24.4 ± 4.7	5.91 ± 1.89
t$_{½}$ (min)	176	56.9	235
Human Plasma Protein Binding (%)	95.5	98.4	94.9
[*fu*(%)]	(4.5 ± 1.1)	(1.6 ± 1.1)	(5.1 ± 1.2)
Recovery (%)	79.6	70.7	78.9
CYP450 Inhibition (μM)			
1A2	> 25	> 25	> 25
2C9	> 25	14.0 ± 4.9	> 25
2C19	7.9 ± 1.3	> 25	> 25
2D6	> 25	> 25	> 25
3A4	> 25	> 25	> 25
hERG (μM)	> 25	> 25	> 25

Table 23 – Bioavailability and pharmacokinetics of 160 compared to ispinesib

Cmpd	F (%)	Oral Dosing (PO)			Intravenous Dosing (iv)					Comments
		C_{max} (µg/mL)	t_{max} (h)	AUC_{last} [µg/(mL x h)]	$C_{(0)}$ (µg/mL)	$t_{1/2}$ (h)	V_D (L/kg)	Cl (mL/min/kg)	AUC_{last} [µg/(mL x h)]	
Ispinesib	45	0.25	2.7	1.50	2.15	4.14	2.53	20.49	3.11	Moderate clearance, good PO levels
160	63	1.25	0.5	4.43	13.55	2.06	0.37	11.38	7.07	High clearance, good PO levels

3.5. Xenograft Studies

*3.5.1. Anti-tumour efficacy of **158**, **160** and rac-**176***

On the basis of these profiles we advanced **158**, **160** and *rac*-**176** into *in vivo* experiments with lung cancer patient explants (LXFS 538) passaged as subcutaneous xenografts in nude mice. Explanted xenograft models provide a better model for predicting clinical outcomes over solid tumours derived from *in vitro* cell lines as the transplanted tumours retain the histological complexity from the patient and reflect prior treatment. Earlier studies have shown that explants correctly replicate the response of the donor patient to standard anticancer drugs in > 90% of the cases, and they were also shown to be more accurate predictors of clinical outcome for the Eg5 drug candidate ARRY-520.[240, 241] For **160** weak tumour growth inhibition was observed with *T/C* = 44% on day 32, corresponding to reduced tumour growth rate (Figure 25). Two key factors may have contributed to this. The relatively short plasma t½ of **160** may have meant that maintenance of sufficient concentration of the drug to induce a pharmacodynamic response was not achieved with the employed dosing schedule (Table 23). More pertinently, evaluation of the phase 2 clearance of **160** in mice hepatocytes revealed high rates of clearance (Cl_{int} = 58.7 ± 5.64 μL/min/million cells; $t_{½}$ = 23.6 min). For **158**, no tumour growth inhibition activity was recorded, and a similar explanation applied for the lack of activity (Figure 26). Although **158** was stable or showed low clearance in human microsomes and hepatocytes respectively, in mice medium clearance was evident in microsomes (17.8 ± 3.7 μL/min/mg protein) and extremely quick clearance in hepatocytes (170 ± 9.4 μL/min/million cells; $t_{½}$ = 8.2 min). Mice xenografts therefore may not have been the most appropriate *in vivo* model for assessing the potential of **158** and **160**, and in the future alternative models such as nude rats will have to be employed. In contrast to the reduced efficacy of thioethanamines **158** and **160**, the strong activity of the most potent butanamine *rac*-**176** translated into the xenograft model (Figure 26). Total tumour regression was achieved by day 21 on a dosage of 15 mg/kg every 3-4 days administered intraperitoneally.

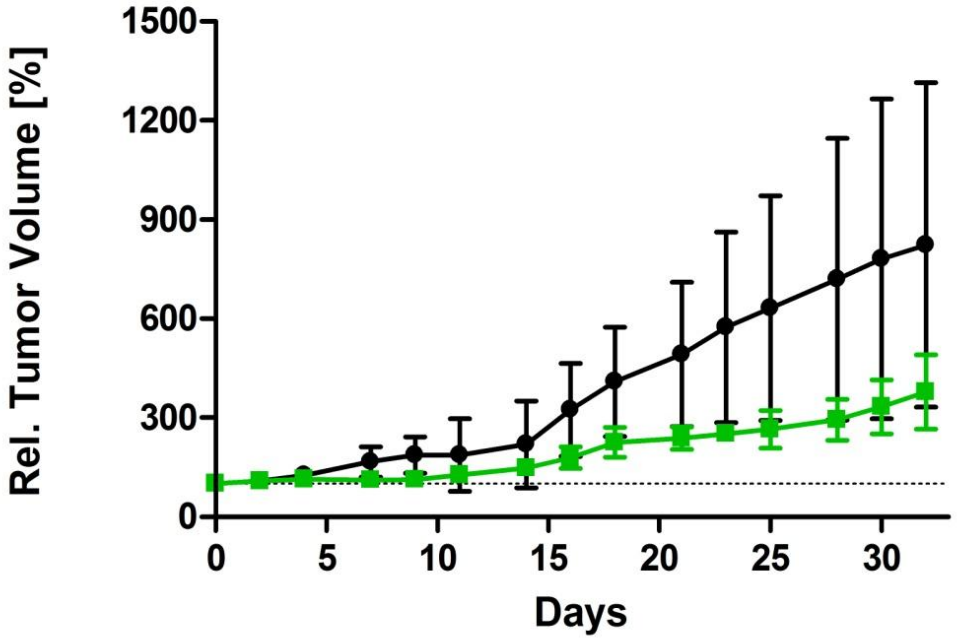

Figure 25 – Anticancer efficacy of 160 in a subcutaneous tumour xenograft model with LXFS 538.

The 160 treatment group (■) received 15 mg/kg on days 0, 2, and 4; 17 mg/kg on days 7, 18, 21 and 23; 14 mg/kg on days 11, 14 and 16; 20 mg/kg on days 25 and 28; 22.5 mg/kg on days 30 and 32. The control group (●) received vehicle only on the same days. The data are plotted as the mean of the RTV ± standard deviation. The difference between the treated group and vehicle is statistically significant (p = 0.0124).

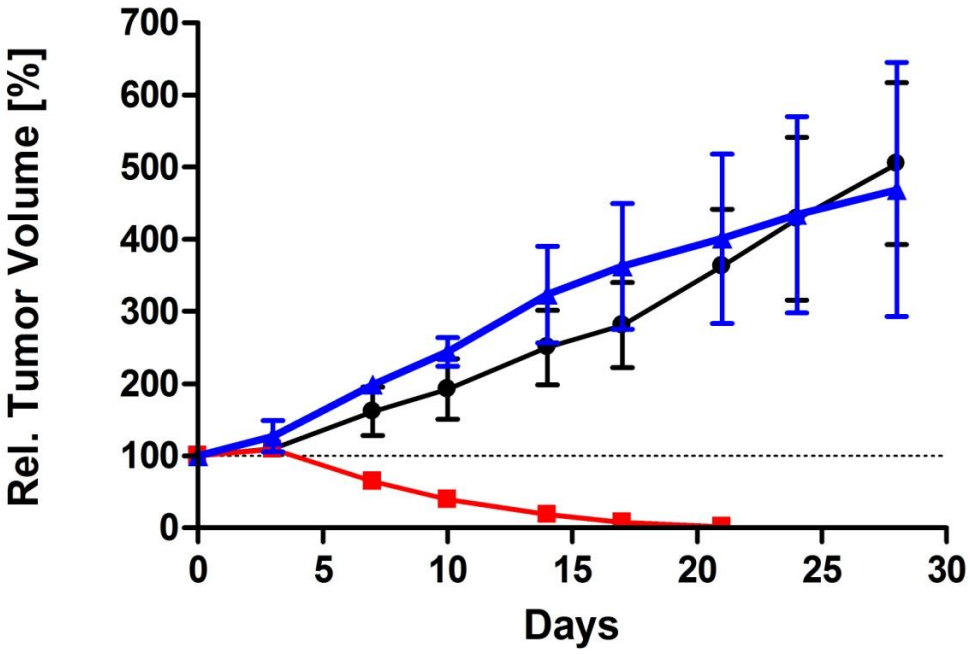

Figure 26 – Differing responses of tumour xenografts to 158 and *rac*-176.

Treatment with *rac*-176 in a subcutaneous tumour xenograft model with lung cancer patient explants (LXFS 538) resulted in complete tumour regression within 21 days (*T/C* = 0% on day 21), but no response was recorded for 158. The *rac*-176 treatment group (■) received 15 mg/kg on days 0, 3, 7, 10 and 14, while the 158 treatment group (▲) received 15 mg/kg 34 on days 0, 3, 7, 10 and 14 and up to 30 mg/kg during later treatment, without indications of toxicity at this dose. The control group (●) received only vehicle on the same days. Data are plotted as the mean of the RTV ± standard deviation. The difference between the treated group (*rac*-176, ■) and vehicle is statistically significant (p = 0.0003).

Chapter 4. Conclusions

4.1. Key conclusions

The optimisation of STLC based inhibitors by rational, structure based drug design has been reported. A number of modifications have been identified to dramatically increase *in vitro* efficacy, primarily focussed on substituents to the trityl group which were hydrophobic and electron-donating. In the most active compounds, the role of the carboxylate was delineated to be balancing the physicochemical attributes of the lipophilic trityl head by enhancing the aqueous solubility of the amino acid tail. Metabolic stability and potency was increased further by replacement of the *S*-trityl linker with a methylene group, whilst a number of effective hydrophilic vectors from the trityl group were also investigated. Strategies to alleviate and eliminate the potential for Pgp efflux from certain resistant tumours were also considered, and produced two modifications which may prove effective in the future: proximal fluorination of the primary amine aliphatic chain and bioisosteric replacement of the carboxylate with a primary amide. The activity of the optimised inhibitors has transferred to *in vivo* models. While thioethanamine based analogues **158** and **160** evaluated displayed poor metabolic stability and limited efficacy in the chosen mouse model, the butanamine *rac*-**176** induced tumour regression. This lead compound displays strong drug-like properties conducive to further investigation, and represents an excellent candidate for cancer chemotherapy as either monotherapy or in combination.

4.2. Future Work

*4.2.1. Separation of rac-**176** and improvements to synthesis.*

Limitations of time and material prevented further attempts at resolving the racemate of the most active compound prepared *rac*-**176**. The problems encountered with separation (section 2.3.1.2) could readily be circumvented through resolving at an earlier stage in the synthesis, such as the α-aminonitrile *rac*-**174**. Additionally, although effective, the linear nature of the synthesis of zwitterionic triphenylbutanamines such as *rac*-**176** analogues precludes rapid generation of analogues. A more convergent synthetic approach or employment of asymmetric syntheses such as the Schöllkopf method[242] would therefore be welcome improvements.

4.2.2. Identification of optimal substituent pattern

Excellent *in vitro* potency has been achieved with the developed lead analogues. To successfully translate this into strong *in vivo* efficacy will require a more detailed understanding of the metabolism and pharmacokinetics of the lead compounds. A selection of combinations of substituents which can effectively increase *in vitro* potency have been developed; further ADMET and pharmacokinetic profiling will reveal which is optimal. Additionally, only one triphenylbutanamine analogue of the most efficacious trityl modifications has been prepared so far (*rac*-**176**).

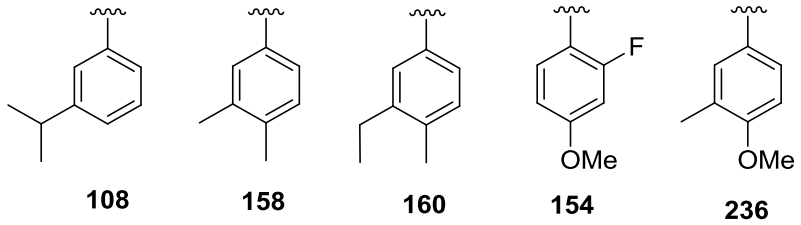

Figure 27 – Selected optimal lipophilic trityl modifications and proposed further modification (236).

4.2.3. Development of Pgp-efflux resistant candidates

4.2.3.1. Primary amide analogues

The terminal carboxylic acid provides physicochemical balance to the scaffold, and can contribute to Eg5 affinity. However, given the propensity for the carboxylate moiety to induce efflux by the Pgp transporter, it may be desirable to replace this feature, particularly given the likelihood of Eg5 therapy being given in combination with existing treatments. One bioisosteric alternative which emerged to the carboxylate was a primary amide (section 3.2.6.2). To fully examine the potential of this modification, it would be interesting to combine it with the triphenylbutanamine scaffold (Figure 28).

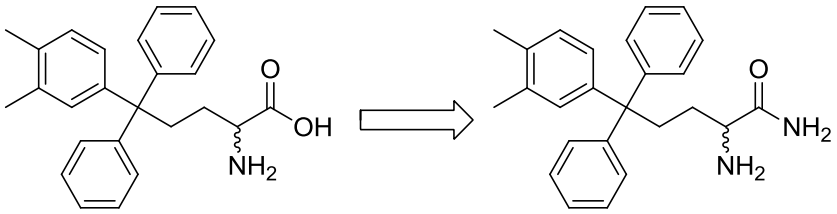

rac-**176** *rac*-**237**

Figure 28 – Proposed terminal primary amide triphenylbutanamine *rac*-237

The improved activity of the amide suggests we do not fully understand the electronic influences of the carboxylate with the Eg5 backbone; thus further structural modifications and investigation of isosteres[233] may reveal more potent alternatives to the carboxylate which are not subject to Pgp efflux.

4.2.3.2. Use of proximal fluorination

Another strategy which emerged was the use of β-fluorination of a primary amine to attenuate Pgp-mediated efflux (sections 3.2.6.1 and 3.3.4.3). Although the efficacy of the prepared examples was compromised, the effect of proximal fluorination on the MDR ratio of a zwitterionic candidate is intriguing (Figure 29). However, diastereoselectively preparing the enantiomers of **238** is synthetically complex and makes this prospect unlikely.

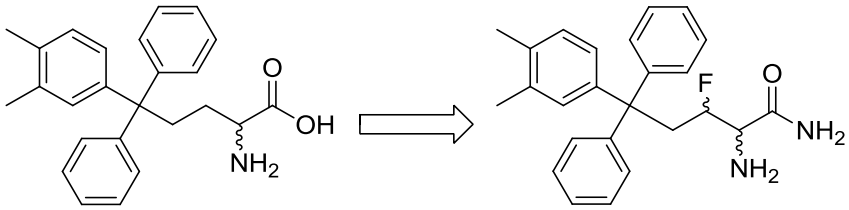

rac-**176** *rac*-**238**

Figure 29 – Proposed β-fluorinated amino acid 238

4.2.4. Investigation into uptake mechanisms of lead candidates

The initial observations that radiolabelled L-cysteine was incorporated into leukemic white blood cells, which led to the synthesis of STLC strongly suggest that active transport mechanisms are involved in the uptake of the lead amino acid based compounds. When combined with the observations of dramatic increases in cellular efficacy on incorporation of the amino acid moiety in the lead series (section 3.2.3.2), that the natural amino acid enantiomers were more potent (section 3.2.2.1), and the excellent bioavailability of **160** (section 3.4.1.2), it is clear further investigation is necessary. A variety of *in vitro* assays are available to determine the level of involvement of membrane transporters and which specifically are involved.[243, 244] As a first step, a Caco-2 assay to investigate intestinal absorption in comparison to the expected rates achieved by passive diffusion could be performed. Alternatively, comparisons of the rate of passive diffusion into cells as measured by a PAMPA assay contrasted with the observed rate of uptake in cells could also provide compelling evidence for the involvement or lack of active transport.

4.2.5. Investigation of combination therapy in haematological malignancies

The data from multiple clinical trials has indicated only limited efficacy when Eg5 inhibitors are administered as a monotherapy (section 1.4). One of the postulated reasons for this is that the *in vivo* preclinical models have artificially high cell division rates, not reflective of tumour growth rates found in patients.[44] Therefore more selective novel anti-mitotic therapies, such as Eg5 inhibitors are actually likely to be more effective against more rapidly dividing cancers. There has been some corroboration of this hypothesis in the successes recorded for SB-743921and ARRY-520 in clinical studies focused on lymphomas and multiple myeloma.[154, 168] Therefore, an intriguing prospect for the lead STLC-based exemplars would be to test these in haematological related xenograft models, and perform *in vitro* combination screening to identify potential synergy with existing therapeutic agents for haematological malignancies.

Chapter 5. Experimental

5.1. Biology

5.1.1. General

Eg5 protein was expressed and purified by Dr. Kristal Kaan and Sandeep Talapatra. The evaluation of the basal inhibition of Eg5 ATPase activity with new compounds was performed by Prof. Frank Kozielski and Sandeep Talapatra. All cellular assays were conducted by Dr. Oliver Rath. ADME and toxicology related assays were conducted by Cyprotex (Macclesfield, UK). Tumour xenografts were carried out by Oncotest GmbH (Freiburg, Germany).

5.1.2. Measurement of the inhibition of the basal and MT-stimulated Eg5 ATPase activities.

$Eg5_{1\text{-}368}$ was cloned, expressed and purified for use in ATPase assays as previously described.[132] The inhibition of the basal Eg5 ATPase activity was determined as previously described.[137, 235] In brief, ATPase rates were recorded using the pyruvate kinase/lactate dehydrogenase-linked assay.[214] This assay couples the ADP turnover of Eg5 with NADH oxidation, whose fluorescence can be monitored to allow measurement of the steady state ATPase rate. These measurements were performed at 25 °C in 96-well μclear plates using a 96-well Tecan Sunrise photometer to monitor fluorescence at 340 nm. ATPase rate assays were conducted utilising a salt concentration of 150 mM NaCl for the inhibition of the basal ATPase activity. No salt was employed in the measurement of the MT-stimulated ATPase activity. It is noteworthy that the K_i^{app} estimates can vary dependent on the ionic strength of the buffer for this Eg5 construct.[223] The Eg5 concentration was ~ 80 nM and ~ 5 nM in the basal and MT-stimulated assays respectively. All data were measured at least in triplicate. Estimates for the K_i^{app} values were calculated by fitting data to the Morrison equation.[245]

$$\frac{v_i}{v_o} = 1 - \frac{\left[(v_{max} - v_{min}) \left(([E] + [I] + K_i^{app}) - \sqrt{([E] + [I] + K_i^{app})^2 - 4[E][I]} \right) \right] + v_{min}}{2[E]}$$

whereby v_i/v_0 is the fractional activity, v_{max} is the uninhibited protein activity, v_{min} is the remaining activity at the highest inhibitor concentration used, [E] and [I] represent the enzyme and inhibitor concentrations used in the assays respectively, and K_i^{app} is the determined apparent K_i value.

5.1.3. Measurement of the inhibition of the basal and MT-stimulated ATPase activities of other human kinesins.

Assays were performed as described in section 5.1.2 with *rac*-**176** by Sandeep Talapatra with human kinesin constructs expressed and purified by Dr. Kristal Kaan and Sandeep Talapatra. The salt concentrations were optimised for each kinesin.[223] The highest concentration of *rac*-**176** used against each kinesin was 200 μM.

5.1.4. Cellular assays

5.1.4.1. Tissue culture

Tissue culture was performed as described previously by Dr. Oliver Rath.[138] In brief, HCT116 (ATCC CCL-247) cells were cultured in DMEM, supplemented with 10% fetal bovine serum. K562 (ATCC CCL-243), LNCaP (ATCC CRL-1740) and NCI-H1299 (CRL-5803) cells were cultured in RPMI, supplemented with 10% fetal bovine serum. BxPC-3 (ATCC CRL-1687) cells were cultured in RPMI, supplemented with 1% non-essential amino acids, 1% sodium pyruvate, 1% glutamine and 10% fetal bovine serum. All cells were maintained at 37 °C, 95% humidity and 5% carbon dioxide in a humidified incubator and used for experiments for 6-8 weeks, before being replaced with fresh stocks that had been stored in liquid nitrogen.

5.1.4.2. Proliferation assays

Cell proliferation assays were conducted as described previously by Dr. Oliver Rath.[138] Cells were seeded in triplicates in 96-well assay plates at 1.250 cells (BxPC-3, HCT116), 2.500 cells (hTERT-HME1, NCI-H1299), or 5.000 cells (K562) per well in 100 µL of the respective growth medium. Medium blanks and cell blanks for every cell line were also prepared. The following day, inhibitors were added with a starting concentration of 100 µM in a 3-fold serial dilution series. 72 h post inhibitor addition, 10% Alamar Blue was added and depending on the cell line, 2-12 h later the absorbance was measured at 570 nm and 600 nm. All values were corrected for the absorbance of the medium blank and the corrected cell blanks were set to 100%. Calculations for determining the relative proliferation were performed using equations described in the manufacturer's manual. Finally, the GI_{50} values were determined using a sigmoidal dose-response fitting (variable slope) with GraphPad Prism 5.03 for Windows (GraphPad Software, San Diego, USA).

5.1.5. Tumour xenografts

5.1.5.1. Protocols

Tumour xenograft experiments were performed as described previously at Oncotest GmbH with female NMRI nu/nu mice (Charles River, Sulzfeld, Germany).[138] Tumour fragments were obtained from xenografts in serial passage in nude mice. After removal from donor mice, tumours were cut into fragments (4-5 mm diameter) and placed in PBS until subcutaneous implantation. The recipient mice were anaesthetized by inhalation of isoflurane, a small incision was made and one tumour fragment per animal was transplanted with tweezers. The approximate age at implantation was 5-7 weeks. At 10-12 weeks, mice were randomized to the various groups and dosing started when the required number of mice carried a tumour of 50-250 mm^3 volume, preferably 80-200 mm^3. The vehicle for all compounds was a solution of DMSO (8%), Tween 80 (2%), distilled water (pH 5). All treatments were given intraperitoneally.

Experiment 1: Vehicle control mice (group 1) were treated with 10 ml/kg vehicle on days 0, 2, 4, 7, 11, 14, 16, 18, 21, 23, 25, 28, 30 and 32. The **160** treatment group (group 2) received 15 mg/kg on days 0, 2, and 4; 17 mg/kg on days 7, 18, 21 and 23; 14 mg/kg on days 11, 14 and 16; 20 mg/kg on days 25 and 28; 22.5 mg/kg on days 30 and 32. The experiment was terminated on day 34 and tumour samples were collected.

Experiment 2: Vehicle control mice (group 1) were treated with 10 mL/kg vehicle on days 0, 3, 7, 10 and 14. The *rac*-**176** treatment group (group 2) received 15 mg/kg *rac*-**176** on days 0, 3, 7, 10 and 14. The **158** treatment group (group 3) received 15 mg/kg **158** on days 0, 3, 7, 10 and 14 and up to 30 mg/kg during later treatment, without indications of toxicity at this dose.

Mortality checks were conducted at least daily during routine monitoring. Body weight was used as means of determining toxicity, with mice weighed twice a week. The tumour volume was determined by two-dimensional measurement with a calliper on the day of randomization (day 0) and then twice weekly (i.e. on the same days on which mice were weighed). Tumour volumes were calculated according to the formula $(a \times b^2) \times 0.5$, where a represents the largest and b the perpendicular tumour diameter.

5.1.5.2. Interpretation of data

Tumour inhibition for a particular day (*T/C* in %) was calculated from the ratio of the median RTV values of test versus control groups multiplied by 100%, as illustrated by the following equation:

$$T/C_x\,[\%] = \frac{\text{median } RTV_x \text{ treated group}}{\text{median } RTV_x \text{ control group}} \times 100$$

For the evaluation of the statistical significance of tumour inhibition, the Mann-Whitney U-Test was performed. Individual RTVs were compared on days on which the minimum T/C value was achieved, as long as sufficient animals were left for statistical analysis or otherwise on days as indicated. By convention, p-values ≤ 0.05 indicate significance of tumour inhibition. Statistical calculations were performed using GraphPad Prism 5.01 (GraphPad Software, San Diego, USA).

5.1.6. ADME profiling

All ADME and toxicology related profiling was carried out by Cyprotex (Macclesfield, UK) as described previously.[138]

5.1.6.1. Microsomal stability

Human and mouse microsomal stability was measured at a compound concentration of 3 μM and a microsome concentration of 0.5 mg/ml at time points of 0.5,15,30 and 45 min. The final DMSO concentration was 0.25%. NADPH was included as a cofactor to initiate the reaction. Dextromethorphan and verapamil and diazepam and diphenydramine were included as controls for human and mouse microsomes, respectively. The disappearance of compounds was monitored using LC-MS/MS. The stability is expressed as the intrinsic clearance (Cl_{int}) ± its standard error and the half-life ($t_{½}$). Compounds with Cl_{int} values < 8.6 (mouse: 8.8) or > 47.0 (mouse 48.0) were classified as showing low and high clearance, respectively.[229] Compounds with negative values are considered stable in microsomal stability assays.

5.1.6.2. Hepatocyte stability

Human hepatocyte stability was measured at a compound concentration of 3 μM using cryopreserved hepatocytes. Incubation time was 0, 5, 10, 20, 40 and 60 min. The final DMSO concentration was 0.25%. Compounds with known activity were included as controls. Data were analyzed using LC-MS/MS. The stability is expressed as the intrinsic clearance ± its standard error and the half-life.

5.1.6.3. Plasma binding

The extent of binding to human plasma was determined by equilibrium dialysis at 50% plasma at compound concentrations of 5 μM. The experiments were performed as duplicates. Quantifications were performed in each compartment by LC-MS/MS equilibration at 37 °C. Plasma protein binding is expressed as fraction unbound ($fu_{100\%}$) in 100% plasma and the recovery (%Recovery) is given.

5.1.6.4. hERG inhibition

Inhibition of hERG was investigated using the Ionworks HT system (Molecular Devices). CHO-hERG cells were used with amphotericin B as the perforating agent. The compound

concentrations for the calculation of the IC_{50} values were 0.008, 0.04, 0.2, 1, 5, and 25 μM (4 replicates). The final DMSO concentration was 0.25%. Quinidine was used as a positive control.

5.1.6.5. Cytochrome P450 inhibition

To assess whether the compounds inhibit one of the main cytochrome P450 isoforms CYP1A, CYP2C9, CYP2C19, CYP2D6 or CYP3A4, which might lead to adverse drug reactions or toxicity, cytochrome P450 inhibition assays were performed. Assays were performed at a range of compound concentrations (0, 0.1, 0.25, 1, 2.5, 10, 25 μM) in the presence of isoform-specific substrates. Known isoform-specific inhibitors (α-naphthoflavone, sulphaphenazole, tranylcypromine, quinidine, and ketoconazole) were used as controls. The formation of metabolites was monitored using LC-MS/MS and IC_{50} values and their standard errors were calculated.

5.1.6.6. Bioavailability

To determine bioavailability, the compounds are administered by intravenous and by oral routes to mice at 5 mg/kg. The vehicle used was 17.5-21.3 mM sodium citrate, pH 5.0, 15% DMSO, 0.5-1.0% Tween 80 and either **160** or ispinesib. Up to eight blood samples were taken over a period of up to 8 h. The compound concentrations were quantified using LC-MS/MS. Pharmacokinetic parameters were extracted for oral (C_{max}, t_{max}, AUC_{last}) and intravenous ($C_{(0)}$, AUC_{last}, $t_{½}$, V_D, and Cl) dosing.

5.2. Chemistry

5.2.1. General

5.2.1.1. Materials and methods

All reagents and solvents were of commercial quality and used without further purification. STLC (**6**), the primary acid isostere **215** and SB-743921 were purchased from Nova Biochem, Sigma Aldrich and Selleck Chemicals respectively and used without further purification. The following compounds were prepared by Dr. Fang Wang as described previously: **181, 183, 221-226**, **228-229, 231,** and **233-235**.[138, 222] Compounds **227**, **230** and **232** were prepared by Dawid Podgórski.[222] Compound **10** (NSC123528) was obtained from the NCI/DTP Open Chemical Repository (http://dtp.cancer.gov) of the National Cancer Institute. All other tested compounds were synthesised as described by myself. Anhydrous reactions were carried out in oven dried glassware under a nitrogen atmosphere unless otherwise noted. Thin-layer chromatography (TLC) was carried out on aluminium backed SiO_2 plates (silica gel 60, F_{254}), and visualized using ultraviolet light (254 nm), and by staining with phosphomolybdic acid (alcohols) or ninhydrin (amines). Flash column chromatography was performed on silica gel [SNAP KP-Sil, 60 Å, 40−63 μm cartridges] using a Biotage SP4 automated chromatography system (detection wavelength, 254 nm; monitoring, 280 nm).

5.2.1.2. Analysis and characterisation

Melting points were determined using a Stuart Scientific SMP1 melting point apparatus and are uncorrected. ^{1}H and ^{13}C NMR spectra were recorded on a JEOL ECX-400 (400 MHz), Avance DPX400 (400 MHz), or Avance DPX500 (500 MHz) spectrometer. ^{19}F NMR spectra were recorded on an Avance AV400 (400 MHz) instrument equipped with a multinuclear probe. ^{1}H chemical shifts (δ) are reported in ppm relative to the residual signal of the deuterated solvent [7.26 in $CDCl_3$, 3.31 in CD_3OD (denoted as MeOD), and 2.50 in DMSO-d_6]. Multiplicities are indicated by s (singlet), d (doublet), t (triplet), q (quartet), p (pentet), m (unresolved multiplet), and br (broad). ^{13}C chemical shifts (δ) are reported in ppm relative to the carbon resonance of the deuterated solvent (77.16 in $CDCl_3$, 49.00 in CD_3OD, and 39.52 in DMSO-d_6). ^{19}F spectra are referenced relative to $CFCl_3$. High resolution mass spectra were recorded on a Thermo Electron LTQ ORBITRAP mass spectrometer using electrospray ionisation. Gas chromatography mass spectra (GC-MS) using electron ionisation (EI) were recorded on a Thermo Scientific Focus GC with DSQ2 single quadrupole mass spectrometer. GC-MS using chemical ionisation (CI) were recorded on an Agilent Technologies 7890A GC system and an Agilent 5975C Inert XL EI/CI MSD with DSQ2 single quadrupole mass spectrometer, equipped with an Agilent Technologies DB5-MS column (30 m x 0.25 mm x 0.25 μm). Helium was the carrier gas (flow rate = 1 mL/min^{-1}). Elemental analysis was performed on a Perkin-Elmer 2400 series 2 CHN analyzer. LC−MS analyses were performed with an Agilent Quaternary 1200 series pump and an Agilent 6130 dual source mass spectrometer with UV detection at 254 nM. Retention times (t_R) were in minutes, and purity was calculated as percentage of total area. The method for determining purity consisted of the following: Zorbax Eclipse XDB-C18 reverse phase column (15 cm x 4.3 μm, particle size 5 μm); column temperature 40 °C; solvent A: H_2O (5 mM ammonium acetate); solvent B: MeCN (5 mM ammonium acetate); gradient of A:B, 95:5 (0 – 3 min), A:B, 95:5 → B, 100% (3 – 17 min), B, 100% (17- 27 min), B, 100% → A:B, 95:5 (27-33 min), A:B, 95:5 (33 – 36 min); flow rate 1 ml min^{-1}. All assayed compounds were ≥ 95% pure by either elemental analysis or LC-MS. New compounds are named according to IUPAC nomenclature using ACD ChemSketch 12.01 (Windows, Advanced Chemistry Development, Toronto, Canada).

5.2.2. Measurement of physicochemical properties

Physicochemical measurements were made by Cyprotex (turbidimetric solubility and Log $D_{7.4}$; Macclesfield, UK) and Sai Advantium (Log P and pK_a; Pune, India).

5.2.2.1. Turbidimetric Solubility

To determine turbidimetric solubility, compounds were measured at 1 μM, 3 μM, 10 μM, 30 μM and 100 μM at a final DMSO concentration of 1% in 10 mM phosphate buffered saline at pH 7.4, and optionally at pH 2.0 and 6.0. Pyrene and Nicardipine were used as controls. The temperature was 37 °C with an incubation time of 2 h, and the turbidimetry was measured at a wavelength of 620 nm. The number of replicates was n = 7.

5.2.2.2. Log P and pK_a

The acid dissociation constant (pK_a) and the partition coefficient (log P) were determined using the potentiometric method on a Sirius GL-pK_a under standard conditions.

5.2.2.3. Log $D_{7.4}$

Log D (distribution coefficient) is used as a measure of lipophilicity. The log $D_{7.4}$ was measured using the miniaturized shake flask method. The partition solvent was *n*-octanol with ratios of buffer:octanol of 50:1, 5:1 and 1:2 (*v/v*). Acetobutolol and ketoconazole were used as positive controls. LC-MS/MS was used to quantify the samples.

*5.2.3. Enantiomeric separation of rac-**176***

Attempts to separate *rac*-**176** were performed on a Dionex P680 HPLC system using a 10 mm × 250 mm ChiralPack IC column containing cellulose *tris*(3,5-dichlorophenylcarbamate) immobilized on 5 μm silica gel as the chiral stationary phase with UV detection at 254 nM. The method consisted of the following: solvent A: *n*-heptane (0.1% triethylamine/0.1% TFA *v/v*); solvent B: ethanol; gradient of A:B 95:5 → A:B 85:15 (0 – 30 min), A:B 85:15 → A:B 80:20 (30 – 40 min), A:B 80:20 (40 – 47 min), A:B 80:20 → A:B 95:5 (47 – 47.1 min), A:B 95:5 (47.1 min – 55 min); flow rate 4 ml min^{-1}.

5.2.4. General procedures

5.2.4.1. General procedure (i): Preparation of trityl alcohols by Grignard mediated reduction of substituted benzophenones.

Intermediate trityl alcohols **31-38** were synthesised by the reaction of commercially available substituted benzophenones with phenylmagnesium bromide. A representative procedure is provided for the synthesis of **31** (Scheme 21).

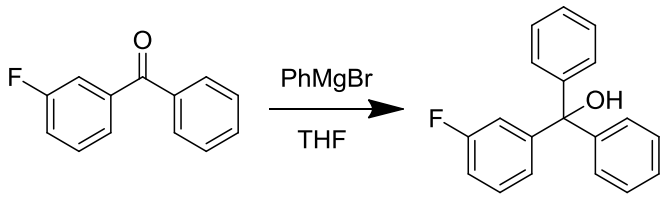

31

Scheme 21 – Reduction of (3-fluorophenyl)(phenyl)methanone with PhMgBr.

5.2.4.2. (3-Fluorophenyl)(diphenyl)methanol (**31**)

To a solution of (3-fluorophenyl)(phenyl)methanone (2.00 g, 10 mmol) in anhydrous THF (5 mL) was added PhMgCl (2.0 M in THF, 12.5 ml, 25 mmol) and stirred at reflux for 20.5 h. The reaction was quenched with saturated aqueous NH_4Cl solution (15 mL) and extracted with EtOAc (3 x 25 mL). The organic extracts were washed with brine (75 mL), dried ($MgSO_4$) and concentrated *in vacuo*. Purification of the crude residue by flash chromatography [SiO_2; 0-18% EtOAc in hexane] afforded the trityl alcohol **31** as a white solid (1.79 g, 64%). Mpt. 112-113 °C (lit.[246] 117 °C). ^{1}H NMR (500 MHz, $CDCl_3$) δ = 2.80 (s, 1H, OH), 6.96-7.00 (m, 1H), 7.05-7.10 (m, 1H), 7.26-7.36 (m, 11H). ^{13}C NMR (125 MHz, $CDCl_3$) δ = 81.86, 114.26 (d, *J* = 21.9 Hz), 115.24 (d, *J* = 22.7 Hz), 123.77, 127.68, 127.98, 128.23, 129.47 (d, *J* = 8.7 Hz), 146.49, 149.60 (d, *J* = 6.0 Hz), 162.71 (d, *J* = 245.7 Hz). HRMS (ESI+) calcd. for $C_{19}H_{14}F$ $[M\text{-}OH]^+$: 261.10741; found: 261.10742. Anal. Calcd. for $C_{19}H_{15}FO$: C, 81.99; H, 5.43. Found: C, 82.06; H, 5.45.

5.2.4.3. General procedure (ii): Preparation of trityl alcohols by reduction of benzophenone with lithiated aryl bromides.

Intermediate trityl alcohols **47**-**70** were synthesised by the reaction benzophenone with lithiated aryl bromides incorporating a variety of substituents. A representative procedure is provided for the synthesis of **53** (Scheme 22).

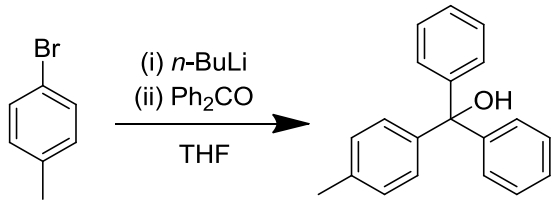

xx

Scheme 22 – Synthesis of 4-methylphenyl)(diphenyl)methanol *via* lithium bromine exchange.

5.2.4.4. (4-Methylphenyl)(diphenyl)methanol (**53**).

n-Butyllithium (2.5 M in hexane, 2.4 mL, 6.00 mmol) was added by slow dropwise addition over 2 min to a cooled (-78 °C) solution of 1-bromo-4-methylbenzene (855 mg, 5.00 mmol) in anhydrous THF (5 mL) and stirred for 30 min at ≤ -70 °C. A solution of benzophenone (1.05 g, 5.75 mmol) in anhydrous THF (5.75 mL) was added by slow dropwise addition over 5 min, and the reaction mixture stirred with the temperature maintained ≤ -70 °C for 6 h, before allowing the reaction to warm to room temperature and stirring for a further 17 h. The reaction was quenched with saturated aqueous NH_4Cl solution (10 mL) and extracted with EtOAc (3 x 10 mL). The combined organic layers were then washed successively with H_2O and brine (30 mL each), dried ($MgSO_4$) and concentrated *in vacuo*. Purification by flash chromatography [SiO_2; 0-9% EtOAc in hexane] afforded the trityl alcohol **53** as a white solid (707 mg, 43%). Mpt. 65-66 °C (lit.[247] 68-69 °C). ^{1}H NMR (400 MHz, $CDCl_3$) δ = 2.34 (s, 3H, CH_3), 2.75 (s, 1H, OH), 7.10-7.17 (m, 4H), 7.24-7.34 (m, 10H). ^{13}C NMR (100 MHz, $CDCl_3$) δ = 21.17, 82.03, 127.32, 128.00, 128.03, 128.78, 137.09, 144.19, 147.15. HRMS (ESI+) calcd. for $C_{20}H_{17}$ = $[M\text{-}OH]^+$: 257.1317; found: 257.1325. Anal. calcd. for $C_{20}H_{18}O$: C, 87.56; H, 6.61. Found: C, 87.32; H, 6.72.

5.2.4.5. General procedure (iii): Thioetherification of trityl alcohols

Thioethers were prepared from trityl alcohols by dehydration in trifluoroacetic acid and subsequent thioetherification with L-cysteine or cysteamine hydrochloride unless otherwise noted, in an adaptation of the procedure reported by Maltese *et al.*[190] A representative procedure is provided for the synthesis of **126**.

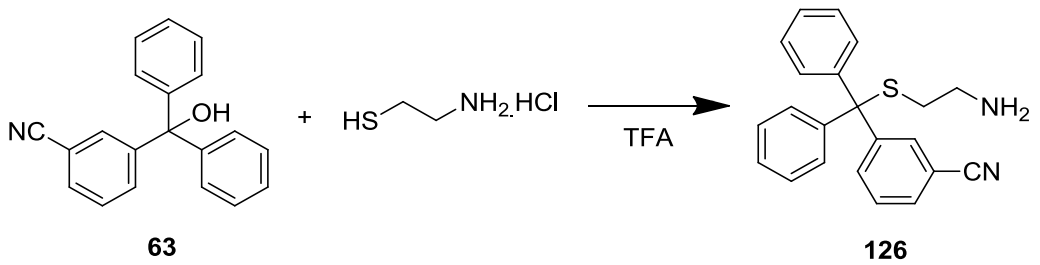

Scheme 23 – Thioetherification of 3-(hydroxy(diphenyl)methyl)benzonitrile with cysteamine hydrochloride.

5.2.4.6. 3-(((2-Aminoethyl)sulfanyl)(diphenyl)methyl)benzonitrile (**126**).

A solution of the tertiary alcohol **63** (1.0 mmol) with cysteamine hydrochloride (125 mg, 1.1 mmol) in trifluoroacetic acid (1.0 mL) was stirred for 3 h at room temperature. The volatiles were removed *in vacuo*, and the residue basified (*circa.* pH 10) with saturated aqueous sodium carbonate solution. The aqueous mixture was extracted with CH_2Cl_2 (3 x 10 mL) and the organic layer dried ($MgSO_4$) and concentrated *in vacuo*. Purification by flash chromatography [SiO_2; 0-20% MeOH in CH_2Cl_2] afforded thioether **126** as a colorless oil (324 mg, 94%). ^{1}H NMR (400 MHz, MeOD) δ = 2.33 (t, *J* = 6.9 Hz, 2H, CH_2), 2.46 (t, *J* = 6.9 Hz, 2H, CH_2), 7.24-7.29 (m, 2H), 7.30-7.36 (m, 4H), 7.38-7.43 (m, 4H), 7.46-7.51 (m, 1H), 7.59-7.62 (m, 1H), 7.73-7.78 (m, 2H). ^{13}C NMR (100 MHz, MeOD) δ = 35.97, 41.46, 67.16, 82.00, 113.12, 119.57, 128.31, 129.30, 130.23, 130.60, 131.65, 133.86, 145.23, 148.32. HRMS (ESI+) calcd. for $C_{22}H_{21}N_2S$ $[M+H]^+$: 345.1420; found: 345.1417. Anal. calcd. for $C_{22}H_{20}N_2S \cdot ⅕CH_2Cl_2$: C, 73.77; H, 5.69; N, 7.75. Found: C, 74.01; H, 5.63; N, 7.45.

5.2.5. Characterisation and synthetic procedures for all other compounds

5.2.5.1. (2-Chlorophenyl)(diphenyl)methanol (**30**)

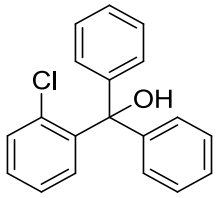

The tertiary trityl alcohol **30** was prepared using an adaptation of the method reported by Hatano *et al.*[179] Zinc chloride (284 mg, 2.1 mmol) was added to a solution of PhMgBr (1.0 M in THF, 45 mL, 45 mmol) and the mixture stirred at room temperature for 1 h. A solution of (2-chlorophenyl)(phenyl)methanone (4.33g, 20 mmol) in anhydrous THF (8 mL) was added, and the reaction heated at reflux for 120 h. The reaction was quenched with saturated aqueous NH_4Cl solution (30 mL) and extracted with EtOAc (4 x 30 mL). The organic extracts were washed with brine (2 x 100 mL), dried ($MgSO_4$) and concentrated *in vacuo*. The crude product was purified by flash chromatography [SiO_2; 0-10% EtOAc in hexane] to afford trityl alcohol **30** as a white solid (3.432g, 58%). Mpt. 83 °C (lit.[248] 89-91 °C). ^{1}H NMR (500 MHz, $CDCl_3$) δ = 4.42 (s, 1H, OH), 6.71 (dd, *J* = 1.6, 7.9 Hz, 1H), 7.09-7.13 (m, 1H), 7.23-7.35 (m, 11H), 7.40 (dd, *J* = 1.2, 7.9 Hz, 1H). ^{13}C NMR (125 MHz, $CDCl_3$) δ = 82.73, 126.54, 127.52, 127.91, 128.14, 129.24, 131.50, 131.64, 133.38, 143.88, 145.69. HRMS (ESI+) calcd. for $C_{19}H_{14}Cl$ $[M\text{-}OH]^+$: 277.07785; found: 277.07770. Anal. calcd. for $C_{19}H_{15}ClO$: C, 77.42; H, 5.13. Found: C, 77.86; H, 5.21.

5.2.5.2. (3-Chlorophenyl)(diphenyl)methanol (**32**)

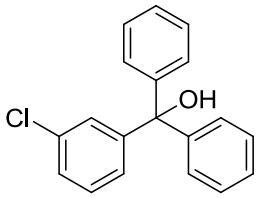

The title compound was prepared using an adaptation of the method described for **30** with (3-chlorophenyl)(phenyl)methanone (4.33 g, 20 mmol), zinc chloride (284 mg, 2.1 mmol) and PhMgCl (2.0 M in THF, 25 mL, 50 mmol) and 22 h at reflux. Aqueous workup and purification by flash chromatography [SiO_2; 0-15% EtOAc in hexane] afforded the trityl alcohol **32** a white solid (4.05 g, 69%). Mpt. 42 °C (lit.[246] 53-55 °C). ^{1}H NMR (500 MHz, $CDCl_3$) δ = 2.80 (s, 1H, OH), 7.16-7.18 (m, 1H), 7.23-7.38 (m, 13H). ^{13}C NMR (125

MHz, $CDCl_3$) δ = 81.86, 126.37, 127.55, 127.72, 127.99, 128.16, 128.27, 129.62, 134.19, 146.41, 149.01. HRMS (ESI+) calcd. for $C_{19}H_{14}Cl$ $[M\text{-}OH]^+$: 277.07785; found: 277.07764. Anal. calcd. for $C_{19}H_{15}ClO$: C, 77.42; H, 5.13. Found: C, 77.08; H, 4.98.

5.2.5.3. (3-Bromophenyl)(diphenyl)methanol (**33**).

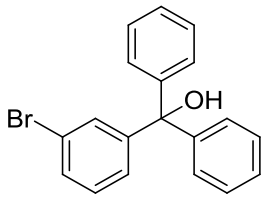

The title compound was prepared using general procedure (i) with (3-bromophenyl)(phenyl)methanone (2.61 g, 10 mmol) and PhMgCl (2.0 M in THF, 12.5 ml, 25 mmol) in anhydrous THF (5 mL). Purification by flash chromatography [SiO_2; 0-15% EtOAc in hexane] afforded the tertiary alcohol **33** as a colorless oil (1.55 g, 46%). ^{1}H NMR (500 MHz, DMSO-d_6) δ = 6.61-6.66 (m, 1H), 7.10-7.16 (m, 1H), 7.18-7.36 (m, 10H), 7.41-7.50 (m, 2H). ^{13}C NMR (125 MHz, DMSO-d_6) δ = 810.25, 21.22, 126.92, 127.00, 127.67, 127.70, 129.57, 129.74, 130.22, 147.00, 150.55. HRMS (ESI+) calcd. for $C_{19}H_{14}{}^{79}Br$ $[M\text{-}OH]^+$: 321.02734; found: 321.02750. Anal. calcd. for $C_{19}H_{15}BrO$: C, 67.27; H, 4.46. Found: C, 68.65; H, 4.32.

5.2.5.4. (3-Methylphenyl)(diphenyl)methanol (**34**).

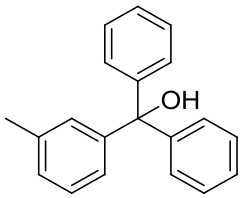

The title compound was prepared using general procedure (i) with (3-methylphenyl)(phenyl)methanone (1.84 mL, 10 mmol) and PhMgCl (2.0 M in THF, 12.5 ml, 25 mmol) in anhydrous THF (5 mL). Purification by flash chromatography [SiO_2; 0-15% EtOAc in petroleum ether (40/60)] afforded the tertiary alcohol **34** as a white solid (1.61 g, 59%). Mpt. 58 °C (lit.[249] 62-63 °C). ^{1}H NMR (500 MHz, $CDCl_3$) δ = 2.33 (s, 3H, CH_3), 2.80 (s, 1H, OH), 7.03 (d, J = 7.8 Hz, 1H), 7.11 (d, J = 7.4 Hz, 1H), 7.16 (s, 1H), 7.20 (t, J = 7.7 Hz, 1H), 7.28-7.35 (m, 10H). ^{13}C NMR (125 MHz, $CDCl_3$) δ = 21.74, 82.15, 125.32, 127.35, 127.89, 128.04, 128.08, 128.18, 128.61, 137.13, 146.98, 147.09. HRMS (ESI+) calcd. for $C_{20}H_{17}$ $[M\text{-}OH]^+$: 257.13248; found: 257.13235. Anal. calcd. for $C_{20}H_{18}O$: C, 87.56; H, 6.61. Found: C, 87.91; H, 6.51.

5.2.5.5. Diphenyl(3-(trifluoromethyl)phenyl)methanol (**35**).

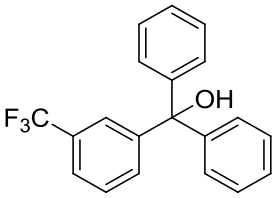

The title compound was prepared using general procedure (i) with phenyl-(3-(trifluoromethyl)phenyl)methanone (2.50 g, 10 mmol) and PhMgCl (2.0 M in THF, 12.5 ml, 25 mmol) in anhydrous THF (5 mL). Purification by flash chromatography [SiO_2; 0-15% EtOAc in petroleum ether (40/60)] afforded the tertiary alcohol **35** as a pale yellow oil (1.38 g, 42%). ^{1}H NMR (500 MHz, $CDCl_3$) δ = 2.83 (s, 1H, OH), 7.25-7.27 (m, 4H), 7.32-7.37 (m, 6H), 7.41-7.49 (m, 2H), 7.55-7.57 (m, 1H), 7.70-7.71 (m, 1H). ^{13}C NMR (125 MHz, $CDCl_3$) δ = 81.92, 124.24 (q, J_{CF} = 3.5 Hz), 124.30 (q, J_{CF} = 272.8 Hz), 124.57 (q, J_{CF} = 3.6Hz), 127.84, 127.97, 128.36, 128.42, 130.51 (q, J_{CF} = 31.9 Hz), 131.58, 146.35, 147.89. HRMS (ESI+) calcd. for $C_{20}H_{14}F_3$ $[M\text{-}OH]^+$: 257.13248; found: 257.13235. Anal. calcd. for $C_{20}H_{15}F_3O$·½EtOAc: C, 70.96; H, 5.14. Found: C, 70.21; H, 4.40.

5.2.5.6. (4-Ethylphenyl)(diphenyl)methanol (**36**).

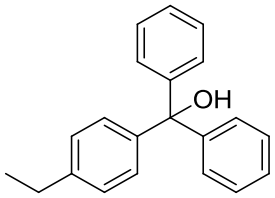

The title compound was prepared using general procedure (i) with (4-ethylphenyl)(phenyl)methanone (1.18 ml, 6.0 mmol) and PhMgCl (2.0 M in THF, 7.50 ml, 15.0 mmol) in anhydrous THF (10 mL). Purification by flash chromatography [SiO_2; 0-10% EtOAc in hexane] afforded the tertiary alcohol **36** as a white solid (1.51 g, 87%). Mpt. 58-60 °C. ^{1}H NMR (400 MHz, $CDCl_3$) 1.24 (t, 3H, J = 7.6 Hz, CH_3), 2.65 (q, 2H, J = 7.7 Hz, CH_2), 2.78 (s, 1H, OH), 7.12-7.20 (m, 4H), 7.25-7.35 (m, 10H). ^{13}C NMR (125 MHz, $CDCl_3$) δ = 15.54, 28.55, 82.06, 127.30, 127.56, 128.02, 128.05, 143.40, 144.39, 147.18. HRMS (ESI+) calcd. for $C_{21}H_{19}$ $[M\text{-}OH]^+$: 271.1481; found: 271.1475. Anal. calcd. for $C_{21}H_{20}O$: C, 87.46; H, 6.99. Found: C, 87.48; H, 7.03.

5.2.5.7. (3,4-Dimethylphenyl)(diphenyl)methanol (**37**).

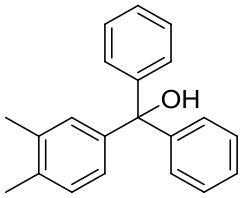

The title compound was prepared using general procedure (i) with 3,4-dimethylbenzophenone (3.15 g, 15.0 mmol) and PhMgBr (1.0 M in THF, 22.5 ml, 22.5 mmol) in anhydrous THF (5 mL). Purification by flash chromatography [SiO_2; 0-8% EtOAc in hexane] afforded the trityl alcohol **37** as a colourless oil (3.90 g, 90%). ^{1}H NMR (500 MHz, $CDCl_3$) δ = 2.21 (s, 3H, CH_3), 2.25(s, 3H, CH_3), 2.75 (s, 1H, OH), 6.92 (dd, *J* = 2.0, 7.9 Hz, 1H), 7.04-7.09 (m, 2H), 7.24-7.32 (m, 10H). ^{13}C NMR (125 MHz, $CDCl_3$): 19.51, 20.12, 82.03, 125.64, 127.27, 128.00, 128.05, 129.16, 129.25, 135.77, 136.30, 144.61, 147.22. HRMS (ESI+) calcd. for $C_{21}H_{19}$ $[M\text{-}OH]^+$: 271.1481; found: 271.1478. Anal. calcd. for $C_{21}H_{20}O$: C, 87.46; H, 6.99. Found: C, 87.01; H, 6.86.

5.2.5.8. Bis(4-methylphenyl)(phenyl)methanol (**38**).

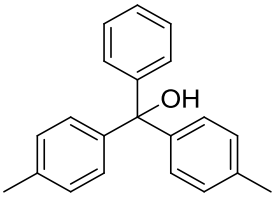

The title compound was prepared using general procedure (i) with bis(4-methylphenyl)methanone (2.10 g, 10 mmol) and PhMgCl (2.0 M in THF, 12.5 ml, 25 mmol) in anhydrous THF (10 mL), with the following modifications. The reaction was stirred for 1 h at 0 °C, and then for a further 74 h at room temperature. After aqueous workup, purification by flash chromatography [SiO_2; 0-10% EtOAc in pet. ether (60/80)] afforded the trityl alcohol **38** as a white solid (1.33 g, 46%). Mpt. 70-71 (lit.[250] 75.5-76.4 ^{o}C). ^{1}H NMR ($CDCl_3$, 500 MHz) δ 2.35 (s, 6H, 2 x CH_3), 7.10-7.13 (m, 4H), 7.15-7.18 (m, 4H), 7.46-7.33 (m, 5H). ^{13}C NMR ($CDCl_3$, 125 MHz) δ 21.16, 81.90, 127.23, 127.98, 128.74, 136.98, 144.34, 147.31. HRMS (ESI+) calcd. for $C_{21}H_{19}$ $[M\text{-}OH]^+$: 271.1481; found: 271.1479. Anal. calcd. for $C_{21}H_{20}O$: C, 87.46; H, 6.99; Found: C, 87.40; H, 7.06.

5.2.5.9. Methyl 3-methoxybenzoate (**41**).

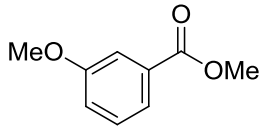

The title compound was prepared using a modification of the procedure reported by Ulrik *et al.*[177] Methyl 3-hydroxybenzoate (3.80 g, 25 mmol), NaH (60% in mineral oil, 660 mg, 27.5 mmol) in anhydrous DMF (41 mL) and subsequent treatment with iodomethane (1.71 mL, 27.5 mmol) after stirring for 22.5 h at room temperature, aqueous workup and purification by flash chromatography [SiO_2; 0-16% EtOAc in hexane] afforded **41** as a colorless oil (2.60 g, 63%). ^{1}H NMR (400 MHz, $CDCl_3$) δ = 3.85 (s, 3H), 3.91 (s, 3H), 7.08-7.11 (m, 1H), 7.32-7.36 (m, 1H), 7.55-7.56 (m, 1H), 7.62-7.64 (m, 1H). ^{13}C NMR (125 MHz, $CDCl_3$) δ = 52.29, 55.56, 114.11, 119.65, 122.13, 129.52, 131.60, 159.71, 167.13. HRMS (ESI+) calcd. for $C_{19}H_{11}O_3$ $[M+H]^+$: 167.07027; found: 167.07028. Anal. calcd. for $C_9H_{10}O_3$: C, 65.05; H, 6.07. Found: C, 64.75; H, 6.06.

5.2.5.10. 2-(Hydroxy(diphenyl)methyl)phenol (**42**).

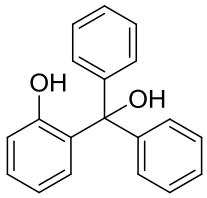

Phenyllithium (1.8 M in Et_2O, 17.7 mL, 32 mmol) was added to a solution of methyl 2-hydroxybenzoate (699 μL, 8 mmol) in anhydrous THF (12 mL) at -78 °C, and stirred for 1 h, whilst maintaining the temperature below -70 °C. The reaction mixture was allowed to warm to room temperature, stirred for 2 h, then quenched with saturated aqueous NH_4Cl solution (25 mL) and extracted EtOAc (2 x 30 mL). The combined organic extracts were washed with brine (25 mL), dried ($MgSO_4$) and concentrated *in vacuo*. Purification by flash chromatography [SiO_2; 5-20% EtOAc in hexane] yielded the trityl alcohol **42** as an off-white solid (1.26 g, 57%). Mpt. 133-134 °C (lit.[251] 135.5-138.5 °C). ^{1}H NMR (500 MHz, $CDCl_3$) δ = 3.68 (br s, 1H, OH), 6.53 (dd, J = 1.6, 7.8 Hz, 1H), 6.73-6.76 (m, 1H), 6.90 (dd, J = 1.0, 8.1 Hz, 1H), 7.20-7.24 (m, 5H), 7.32-7.36 (m, 6H), 8.09 (br s, 1H, OH). ^{13}C NMR (125 MHz, $CDCl_3$) δ = 84.61, 117.76, 119.22, 125.97, 127.91, 128.10, 128.35, 129.74, 130.15, 145.01, 156.02. HRMS (ESI-) calcd. for $C_{19}H_{15}O$ $[M-H]^-$: 275.10775; found: 275.10791. Anal. calcd. for $C_{19}H_{16}O_2$: C, 82.58; H, 5.84. Found: C, 82.65; H, 5.94.

5.2.5.11. 3-(Hydroxy(diphenyl)methyl)phenol (**43**).

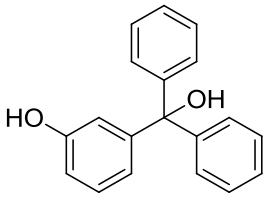

The title compound was prepared using an adaptation of the procedure for **42** using methyl 3-hydroxybenzoate (1.52g, 10 mmol) and phenyllithium (1.8 M in Et_2O, 22.2 mL, 40 mmol) in anhydrous THF (16.6 mL) with the following modifications. The reaction mixture was allowed to stir for 4.5 h after warming to room temperature. Purification by flash chromatography [SiO_2; 0-20% EtOAc in hexane] afforded the tertiary alcohol **43** as an off-white powder (1.55g, 56%). Mpt. 139-142 °C (lit.[252] 148 °C from benzene). ^{1}H NMR (500 MHz, $CDCl_3$) δ = 2.85 (s, 1H, OH), 4.94 (br s, 1H, OH), 6.73-6.77 (m, 2H), 6.81 (dd, *J* = 0.8, 7.9 Hz, 1H), 7.17 (t, *J* = 7.9 Hz, 1H), 7.26-7.32 (m, 10H). ^{13}C NMR (125 MHz, $CDCl_3$) δ = 82.07, 114.42, 115.24, 120.72, 127.49, 128.05, 128.10, 129.33, 146.73, 148.66, 155.37. HRMS (ESI-) calcd. for $C_{19}H_{15}O$ $[M-H]^-$: 275.10775; found: 275.10793. Anal. calcd. for $C_{19}H_{16}O_2$: C, 82.58; H, 5.84. Found: C, 82.46; H, 5.89.

5.2.5.12. (3-Methoxyphenyl)(diphenyl)methanol (**44**).

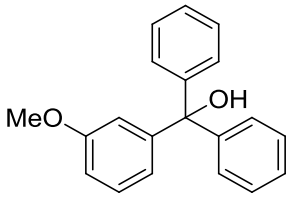

Phenyllithium (1.8 M in Et_2O, 22.2 mL, 40 mmol) was added to a solution of methyl 3-methoxybenzoate **41** (1.52g, 10 mmol) in anhydrous THF (16.6 mL) at -78 °C, and stirred for 1 h whilst maintaining the temperature below -70 °C. The reaction mixture was allowed to warm to room temperature and stirred for 20 h, then quenched with saturated aqueous NH_4Cl solution (25 mL) and extracted EtOAc (2 x 30 mL). The combined organic extracts were washed with brine (2 x 50 mL), dried ($MgSO_4$) and concentrated *in vacuo*. Purification of the crude material by flash chromatography [SiO_2; 0-20% EtOAc in hexane] afforded the tertiary alcohol **44** as a pale yellow solid (3.52 g, 84%). Mpt. 80-81 °C (lit.[253] 88-89 °C from Et_2O). ^{1}H NMR (500 MHz, $CDCl_3$) δ = 2.81 (s, 1H, OH), 3.75 (s, 3H, CH_3), 6.82-6.84 (m, 2H), 6.89-6.90 (m, 1H), 7.21-7.25 (m, 1H), 7.27-7.33 (m, 10H). ^{13}C NMR (125 MHz, $CDCl_3$) δ = 55.12, 82.13, 112.61, 114.13, 120.70, 127.43, 128.06, 129.01, 146.89, 148.66, 159.44. HRMS (ESI+) calcd. for $C_{19}H_{17}O$ $[M-OH]^+$:

273.12739; found: 273.12738. Anal. calcd. for $C_{20}H_{18}O_2$: C, 82.73; H, 6.25. Found: C, 82.75; H, 6.23.

5.2.5.13. Methyl 5,6,7,8-tetrahydronaphthalene-2-carboxylate (**239**).

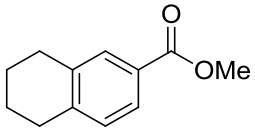

A solution of 5,6,7,8-tetrahydronaphthalene-2-carboxylic acid (3.52 g, 20 mmol) and conc. sulphuric acid (1 mL) in anhydrous MeOH (20 mL) was refluxed for 17 h. After cooling to room temperature, the reaction mixture was concentrated *in vacuo*, the crude residue dissolved in EtOAc (50 mL), and washed successively with saturated aqueous $NaHCO_3$, water, brine (50 mL each), dried ($MgSO_4$) and concentrated *in vacuo* to yield the crude product **236** as a colourless oil (3.45 g, 91%), which was used without further purification. ^{1}H NMR ($CDCl_3$, 400 MHz) δ 1.79-1.83 (m, 4H, 2 x CH_2), 2.78-2.82 (m, 4H, 2 x CH_2), 3.89 (s, 3H, CH_3), 7.11 (d, J = 7.6 Hz, 1H), 7.72-7.75 (m, 2H). ^{13}C NMR ($CDCl_3$, 100 MHz) δ 22.98, 23.08, 29.40, 29.73, 52.01, 126.63, 127.44, 129.27, 130.53, 137.40, 142.94, 167.54. HRMS (ESI+) calcd. for $C_{12}H_{15}O_2$ $[M+H]^+$: 191.10666; found: 191.10661. Anal. calcd. for $C_{12}H_{14}O_2 \cdot ⅓H_2O$: C, 73.47; H, 7.53. Found: C, 73.31; H, 7.39.

5.2.5.14. Diphenyl(5,6,7,8-tetrahydronaphthalen-2-yl)methanol (**46**).

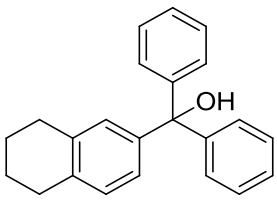

Phenyllithium solution (1.8 M in Et_2O, 13.8 mL, 25 mmol) was added to a solution of **239** (1.90 g, 10 mmol) in anhydrous Et_2O (3.5 ml) at -84 °C, and stirred for 1 h whilst maintaining the temperature below -70 °C. The reaction mixture was allowed to warm to room temperature and stirred for 20 h, then quenched with saturated aqueous NH_4Cl solution (25 mL) and extracted EtOAc (3 x 20 mL). The combined organic extracts were washed successively with H_2O and brine (50 mL each), dried ($MgSO_4$) and concentrated *in vacuo*. Purification of the crude material by flash chromatography [SiO_2; 0-16% EtOAc in hexane] afforded the tertiary alcohol **46** as a white solid (1.76 g, 56%). Mpt. 101-103 °C. ^{1}H NMR ($CDCl_3$, 500 MHz) δ 1.77-1.82 (m, 4H, 2 x CH_2), 2.69-2.72 (m, 2H, CH_2), 2.74-2.78 (m, 3H), 6.92 (dd, J = 1.9, 8.0 Hz, 1H), 7.00 (d, J = 8.1 Hz, 1H), 7.26-7.34 (m, 10H).

^{13}C NMR ($CDCl_3$, 125 MHz) 23.33, 29.19, 29.71, 82.02, 125.39, 127.24, 127.98, 128.05, 128.52, 128.74, 136.35, 136.84, 144.19, 147.22. HRMS (ESI+) calcd. for $C_{23}H_{21}$ [M-OH]$^+$: 297.16378; found: 297.16373. Anal. calcd. for $C_{23}H_{22}O{\cdot}¼H_2O$: C, 86.62; H, 7.11. Found: C, 86.62; H, 7.23.

5.2.5.15. (3-Ethylphenyl)(diphenyl)methanol (**47**).

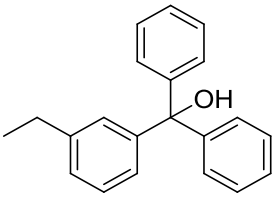

The title compound was prepared using an adaptation of general procedure (ii) with 1-bromo-3-ethylbenzene (1.11 g, 6 mmol) and *n*-butyllithium (2.5 M in hexane, 2.90 mL, 7.2 mmol) in anhydrous THF:toluene (1:4, 11.4 mL) and subsequently benzophenone (1.33 g, 7.30 mmol) in anhydrous toluene (7.2 mL).[254] The reaction was maintained at ≤ -70 °C for 1 h after addition of *n*-butyllithium, and for 4 h after the addition of benzophenone. Purification by flash chromatography [SiO_2; 0-12% EtOAc in petroleum ether (60/80)] afforded the trityl alcohol **47** as a colorless oil (0.86 g, 50%). ^{1}H NMR (500 MHz, $CDCl_3$) δ = 1.20 (t, *J* = 7.6 Hz, 3H, CH_3), 2.62 (q, *J* = 7.6 Hz, 2H, CH_3), 2.80 (s, 1H, OH), 7.02-7.04 (m, 1H), 7.13-7.14 (m, 1H), 7.18-7.19 (m, 1H), 7.23 (t, *J* = 7.7 Hz, 1H), 7.27-7.34 (m, 10H). ^{13}C NMR (125 MHz, $CDCl_3$) δ = 15.70, 29.07, 125.60, 126.90, 127.33, 127.55, 127.94, 128.02, 128.08, 144.11, 146.99, 147.13. HRMS (ESI+) calcd. for $C_{22}H_{19}$ [M+H]$^+$: 271.14813; found: 271.14758. Anal. calcd. for $C_{21}H_{20}O$: C, 87.46; H, 6.99. Found: C, 87.41; H, 6.99.

5.2.5.16. Diphenyl(3-(propan-2-yl)phenyl)methanol (**48**).

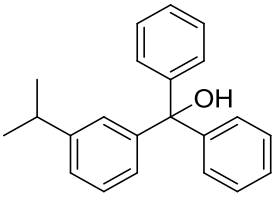

The title compound was prepared using an adaptation of the procedures described by Zhang *et al*. and Deshpande *et al*.[254, 255] *n*-Butyllithium (2.5 M in hexane, 4.8 mL, 12.2 mmol) was added to a cooled (-78 °C) solution of 1-bromo-3-(propan-2-yl)benzene (1.55 mL, 10 mmol) in anhydrous THF (10 mL). The reaction mixture was stirred for 1 h at -78 °C, treated with a solution of benzophenone (2.10 g, 11.5 mmol) in anhydrous THF (10

mL) and stirred for a further 3 h at ≤ -70 °C. The mixture was allowed to warm to room temperature, stirred for 17 h, quenched with saturated aqueous NH_4Cl solution (10 mL) and extracted with EtOAc (3 x 10 mL). The combined organic layers were then washed successively with H_2O and brine (75 mL each), dried ($MgSO_4$) and concentrated in vacuo. Purification by flash chromatography [SiO_2; 0-12% EtOAc in petroleum ether (40/60)] afforded the trityl alcohol **48** as a white solid (1.41 g, 47%). Mpt. 51-54 °C. ^{1}H NMR (500 MHz, $CDCl_3$) δ = 1.22 (d, *J* = 7.0 Hz, 6H, 2 x CH_3), 2.83-2.92 (m, 2H), 7.03-7.05 (m, 1H), 7.17-7.19 (m, 1H), 7.22-7.26 (m, 2H), 7.29-7.35 (m, 10H). ^{13}C NMR (125 MHz, $CDCl_3$) δ = 24.11, 34.29, 82.28, 125.29, 125.76, 126.36, 127.30, 127.90, 128.00, 128.08, 146.90, 147.17, 148.73. HRMS (ESI+) calcd. for $C_{22}H_{21}$ $[M\text{-}OH]^+$: 285.16378; found: 285.16408. Anal. calcd. for $C_{22}H_{22}O{\cdot}½H_2O$: C, 84.85; H, 7.44 Found: C, 85.02; H, 7.24.

5.2.5.17. Diphenyl(3-propylphenyl)methanol (**49**).

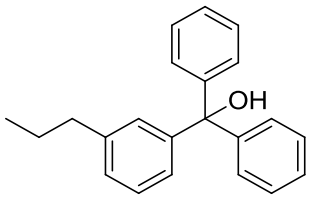

The title compound was prepared using an adaptation of the procedure for **48** using 1-bromo-3-propylbenzene **80** (1.78 g, 8.92 mmol) and *n*-butyllithium (2.5 M in hexane, 4.28 mL, 10.71 mmol) in anhydrous THF (8.92 mL), and subsequently benzophenone (1.79 g, 9.81 mmol) in anhydrous THF (9.81 mL), with the following modifications. The reaction was maintained at ≤ -70 °C for 2 h after the addition of benzophenone. Purification by flash chromatography [SiO_2; 0-15% EtOAc in hexane] afforded the trityl alcohol **49** as a white solid (1.12 g, 41%). Mpt 42-43 °C. ^{1}H NMR ($CDCl_3$, 500 MHz) δ = 0.90 (t, *J* = 7.4 Hz, 3H, CH_3), 1.59 (p, *J* = 7.5 Hz, 2H, CH_2), 2.55 (t, *J* = 7.6 Hz, 2H, CH_2), 2.78 (s, 1H, OH), 7.02-7.04 (m, 1H), 7.10-7.11 (m, 1H), 7.13-7.14 (m, 1H), 7.21 (t, *J* = 7.6 Hz, 1H), 7.27-7.34 (m, 10H). ^{13}C NMR ($CDCl_3$, 125 MHz) δ 13.92, 24.69, 38.25, 82.20, 125.56, 127.32, 127.54, 127.87, 128.02, 128.08, 128.18, 142.56, 146.90, 147.14. HRMS (ESI+) calcd. for $C_{22}H_{21}$ $[M\text{-}OH]^+$: 285.16378; found: 285.16354. Anal. calcd. for $C_{22}H_{22}O$: C, 87.38; H, 7.33. Found: C, 87.05; H, 7.60.

5.2.5.18. (3-(2-Methyl-1,3-dioxolan-2-yl)phenyl)(diphenyl)methanol (**50**).

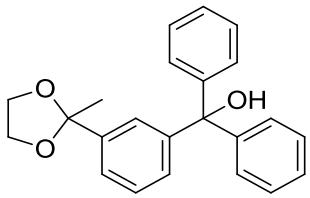

The title compound was prepared using general procedure (ii) with dioxolane **77** (1.82 g, 7.50 mmol) and *n*-butyllithium (2.5 M in hexane, 3.60 mL, 9.00 mmol) in anhydrous THF (7.5 mL), and subsequently benzophenone (1.57 g, 8.63 mmol) in anhydrous THF (8.63 mL), with the following modifications. The reaction was maintained at ≤ -70 °C for 1 h after addition of *n*-butyllithium, and for 5 h after the addition of benzophenone. Purification by flash chromatography [SiO_2; 0-30% EtOAc in hexane with 1% NH_4OH] afforded the trityl alcohol **50** as a white solid (1.82 g, 70%). Mpt. 104-105 °C. ^{1}H NMR (400 MHz, $CDCl_3$) δ = 1.62 (s, 3H, CH_3), 2.82 (s, 1H, OH), 3.69-3.73 (m, 2H, CH_2), 3.97-4.01 (m, 2H, CH_2), 7.15-7.18 (m, 1H), 7.25-7.34 (m, 11H), 7.39-7.43 (m, 1H), 7.49 (t, *J* = 1.8 Hz, 1H). ^{13}C NMR (100 MHz, $CDCl_3$) δ = 27.58, 64.53, 82.16, 108.95, 124.45, 124.81, 127.42, 127.66, 127.89, 128.04, 128.07, 143.08, 147.02. HRMS (ESI+) calcd. for $C_{23}H_{23}O_3S$ $[M+H]^+$: 347.1642; found: 363.1639. Anal. calcd. for $C_{22}H_{22}O_3$: C, 79.74; H, 6.40. Found: C, 79.55; H, 6.15.

5.2.5.19. Diphenyl(3-(trifluoromethoxy)phenyl)methanol (**51**).

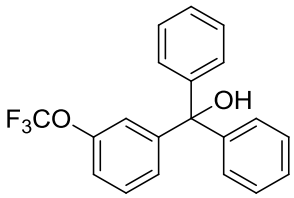

The title compound was prepared using an adaptation of the procedure for **48** using 1-bromo-3-(trifluoromethoxy)benzene (1.49 mL, 10 mmol) and *n*-butyllithium (2.5 M in hexane, 4.80 mL, 12.2 mmol) in anhydrous THF (10 mL), and subsequently benzophenone (2.10 g, 11.5 mmol) in anhydrous THF (10 mL). Purification by flash chromatography [SiO_2; 0-12% EtOAc in petroleum ether (40/60)] afforded the trityl alcohol **51** as a colourless oil (0.80 g, 23%). ^{1}H NMR (500 MHz, $CDCl_3$) δ = 2.85 (s, 1H, OH), 7.13-7.15 (m, 1H), 7.21-7.35 (m, 13H). ^{13}C NMR (125 MHz, $CDCl_3$) δ = 81.82, 119.61, 120.61 (q, J_{CF} = 257.8 Hz), 120.81, 121.64, 126.51, 127.77, 127.96, 128.29, 129.27, 146.37, 149.17, 149.37. ^{19}F NMR (376.5MHz, DMSO-d_6) δ = -57.75. HRMS (ESI+) calcd. for $C_{20}H_{14}OF_3$

[M-OH]$^+$: 327.09913; found: 327.09950. Anal. calcd. for $C_{20}H_{15}F_3O_2 \cdot ¼H_2O$: C, 68.86; H, 4.48. Found: C, 68.90; H, 4.53.

5.2.5.20. (3-(Methylsulfanyl)phenyl)(diphenyl)methanol (**52**).

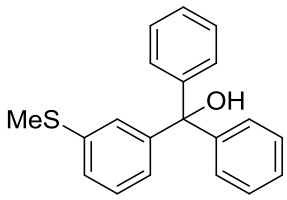

The title compound was prepared using an adaptation of the procedure for **48** using (3-bromophenyl)(methyl)sulfane (1.35 mL, 10 mmol) and *n*-butyllithium (2.5 M in hexane, 4.80 mL, 12.2 mmol) in anhydrous THF (10 mL), and subsequently benzophenone (2.10 g, 11.5 mmol) in anhydrous THF (10 mL). Purification by flash chromatography [SiO_2; 0-15% EtOAc in petroleum ether (40/60)] afforded the tertiary alcohol **52** as a colorless oil (1.67 g, 54%). ^{1}H NMR (500 MHz, $CDCl_3$) δ = 2.40 (s, 3H, CH_3), 2.83 (s, 1H, OH), 7.01-7.03 (m, 1H), 7.16-7.18 (m, 1H), 7.21-7.33 (m, 12H). ^{13}C NMR (125 MHz, $CDCl_3$) δ = 15.81, 82.08, 125.05, 125.34, 126.01, 127.51, 128.03, 128.12, 128.42, 138.37, 146.72, 147.65. HRMS (ESI+) calcd. for $C_{20}H_{17}S$ [M-OH]$^+$: 289.10455; found: 289.104581. Anal. calcd. for $C_{20}H_{18}O_2S$: C, 78.39; H, 5.92. Found: C, 77.42; H, 5.87.

5.2.5.21. (4-(2-Methyl-1,3-dioxolan-2-yl)phenyl)(diphenyl)methanol (**54**).

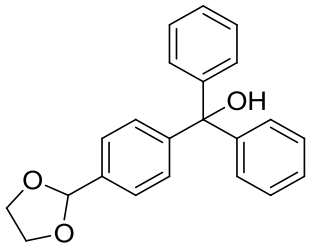

The title compound was prepared using general procedure (ii) with dioxolane **78** (1.46 g, 6.0 mmol) and *n*-butyllithium (2.5 M in hexane, 2.52 mL, 6.3 mmol) in anhydrous THF (6 mL), and subsequently benzophenone (1.20 g, 6.6 mmol in anhydrous THF (6 mL) with the following modifications. The reaction was cooled initially to -84 °C, and following *n*-butyllithium addition maintained at ≤ -70 °C for 1 h. After addition of benzophenone, the reaction was stirred at ≤ -70 °C for 2 h. Purification by flash chromatography [SiO_2; EtOAc/Hexane with 1% NH_4OH; 0-30%] afforded the tertiary alcohol **54** as a white solid (1.01 g, 49%). Mpt. 129-130 °C (lit.[256] 128 °C). ^{1}H NMR (400 MHz, $CDCl_3$) δ = 1.65 (s, 3H, CH_3), 2.76 (s, 1H, OH), 3.75-3.84 (m, 2H, CH_2), 3.99-4.07 (m, 2H, CH_2), 7.22-7.33

(m, 12H), 7.39-7.43 (m, 2H). ^{13}C NMR (100 MHz, $CDCl_3$) δ = 27.65, 64.64, 108.89, 125.00, 127.42, 127.93, 128.02, 128.08, 142.40, 146.54, 146.92. HRMS (ESI+) calcd. for $C_{23}H_{23}O_3$ $[M+H]^+$: 347.1642; found: 347.1639. Anal. calcd. for $C_{23}H_{22}O_3$: C, 79.74; H, 6.40. Found: C, 79.63; H, 6.34.

5.2.5.22. (4-Ethoxyphenyl)(diphenyl)methanol (**55**).

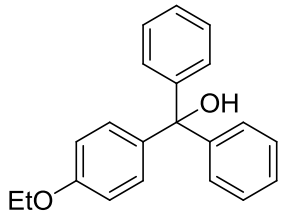

The title compound was prepared using general procedure (ii) with 1-bromo-4-ethoxybenzene (715 μL, 5.00 mmol) and *n*-butyllithium (2.5 M in hexane, 2.40 mL, 6.00 mmol) in anhydrous THF (5.00 mL), and subsequently benzophenone (1.050 g, 5.75 mmol) in anhydrous THF (5.75 mL). Purification by flash chromatography [SiO_2; 0-14% EtOAc in hexane] afforded the trityl alcohol **55** as a white solid (0.967 g, 64%). Mpt. 69-71 °C. ^{1}H NMR (400 MHz, $CDCl_3$) δ = 1.40 (t, *J* = 7.0 Hz, 3H, CH_3), 2.75 (s, 1H, OH), 4.02 (q, *J* = 7.0 Hz, 2H, CH_2), 6.80-6.84 (m, 2H), 7.13-7.17 (m, 2H), 7.24-7.33 (m, 10H). ^{13}C NMR (100 MHz, $CDCl_3$) δ = 14.98, 63.56, 81.89, 113.91, 127.29, 128.01, 129.36, 139.23, 147.29, 158.26. HRMS (ESI+) calcd. for $C_{21}H_{19}O$ $[M-OH]^+$: 287.14304; found: 287.14252. Anal. calcd. for $C_{20}H_{20}O_2$: C, 82.86; H, 6.62. Found: C, 81.38; H, 6.70.

5.2.5.23. Diphenyl(4-(trifluoromethoxy)phenyl)methanol (**56**).

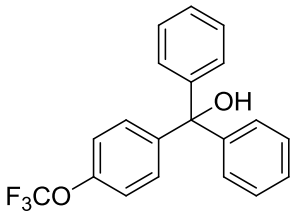

The title compound was prepared using general procedure (ii) with 1-bromo-4-(trifluoromethoxy)benzene (743 μL, 5.00 mmol) and *n*-butyllithium (2.5 M in hexane, 2.40 mL, 6.00 mmol) in anhydrous THF (5.00 mL), and subsequently benzophenone (1.050 g, 5.75 mmol) in anhydrous THF (5.75 mL). Purification by flash chromatography [SiO_2; 0-15% EtOAc in hexane] afforded the trityl alcohol **56** as a white solid (655 mg, 38%). Mpt. 38-39 °C. ^{1}H NMR (400 MHz, $CDCl_3$) δ = 2.78 (s, 1H, OH), 7.12-7.17 (m, 2H), 7.23-7.36 (m, 12H). ^{19}F NMR (376.5 MHz, $CDCl_3$) δ = -57.77. ^{13}C NMR (100 MHz, $CDCl_3$) δ =

81.78, 120.33, 120.61 (q, J_{CF} = 257.3 Hz), 127.70, 127.94, 128.27, 129.58, 145.53, 146.56, 148.42 (q, J_{CF} = 1.6 Hz). HRMS (ESI+) calcd. for $C_{20}H_{14}F_3O$ $[M\text{-}OH]^+$: 327.09913; found: 327.09848. Anal. calcd. for $C_{20}H_{15}F_3O_2$: C, 69.76; H, 4.39. Found: C, 69.63; H, 4.44.

5.2.5.24. (4-(Methylsulfanyl)phenyl)(diphenyl)methanol (**57**).

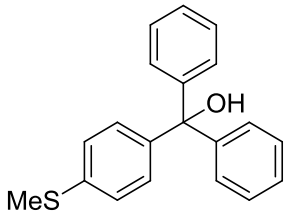

The title compound was prepared using general procedure (ii) with 1-bromo-4-(methylsulfanyl)benzene (1.625 g, 8.0 mmol) and *n*-butyllithium (2.5 M in hexane, 3.84 mL, 9.6 mmol)) in anhydrous THF (8.00 mL), and subsequently benzophenone (1.676 g, 9.2 mmol) in anhydrous THF (9.20 mL) with the following modifications. The reaction was maintained at ≤ -70 °C for 1 h following addition of *n*-butyllithium, and 2 h after the addition of benzophenone. Purification by flash chromatography [SiO_2; 0-25% EtOAc in hexane;] afforded the tertiary alcohol **57** as an opaque white oil (1.860 g, 76%). ^{1}H NMR (400 MHz, $CDCl_3$) δ = 2.47 (s, 3H, CH_3), 2.75 (s, 1H, OH), 7.16-7.21 (m, 4H), 7.24-7.34 (m, 10H). ^{13}C NMR (100 MHz, $CDCl_3$) δ = 15.80, 81.92, 126.04, 127.47, 128.01, 128.12, 128.58, 137.65, 143.91, 146.89. HRMS (ESI+) calcd. for $C_{20}H_{17}S$ $[M\text{-}OH]^+$: 289.1045; found: 289.1043. Anal. calcd. for $C_{20}H_{18}OS$: C, 78.39; H, 5.92. Found: C, 78.05; H, 5.69.

5.2.5.25. (2-Fluoro-3-methylphenyl)(diphenyl)methanol (**58**).

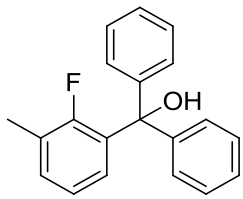

The title compound was prepared using general procedure (ii) with 1-bromo-2-fluoro-3-methylbenzene (1.70 g, 9.0 mmol) and *n*-butyllithium (2.5 M in hexane, 3.96 mL, 9.9 mmol) in anhydrous THF (15.0 mL), and subsequently benzophenone (1.37 g, 7.5 mmol) in anhydrous THF (7.5 mL) with the following modifications. The reaction was maintained at ≤ -70 °C for 1 h following addition of *n*-butyllithium, and 2 h after the addition of benzophenone. Purification by flash chromatography [SiO_2; 0-10% EtOAc in

hexane] afforded the trityl alcohol **58** as a white solid (1.74 g, 80%). Mpt. 64-67 °C. ^{1}H NMR (400 MHz, $CDCl_3$) δ = 2.26 (m, 3H, CH_3), 3.61-3.66 (m, 1H, OH), 6.53-6.58 (m, 1H), 6.88-6.92 (m, 1H), 7.14-7.19 (m, 1H), 7.27-7.39 (m, 10H). ^{19}F NMR (376.5 MHz, $CDCl_3$) δ = -114.90. ^{13}C NMR (400 MHz, MeOD) δ = 14.60 (d, J_{CF} = 5.6 Hz), 81.27, 123.19 (d, J_{CF} = 3.6 Hz), 125.74 (d, J_{CF} = 18.4 Hz), 127.59, 127.73, 128.09, 131.49 (d, J_{CF} = 5.3 Hz), 134.11(d, J_{CF} = 11.0 Hz), 145.85, 159.68 (d, J_{CF} = 250.3 Hz). HRMS (ESI+) calcd. for $C_{20}H_{16}F$ $[M\text{-}OH]^+$: 275.1231; found: 275.1229. Anal. calcd. for $C_{20}H_{17}FO$: C, 82.17; H, 5.86. Found: C, 81.55; H, 5.81.

5.2.5.26. (2-Fluoro-4-methylphenyl)(diphenyl)methanol (**59**).

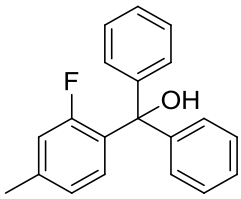

The title compound was prepared using general procedure (ii) with 1-bromo-2-fluoro-4-methylbenzene (1.14 mL, 9.0 mmol) and *n*-butyllithium (2.5 M in hexane, 3.96 mL, 9.9 mmol) in anhydrous THF (15.0 mL), and subsequently benzophenone (1.37 g, 7.5 mmol) in anhydrous THF (7.5 mL) with the following modifications. The reaction was maintained at ≤ -70 °C for 2.5 h after the addition of benzophenone. Purification by flash chromatography [SiO_2; 0-10% EtOAc in hexane] afforded the trityl alcohol **59** as a colourless oil (1.47 g, 67%). ^{1}H NMR (400 MHz, $CDCl_3$) δ = 2.34 (s, 3H, CH_3), 3.54 (d, J = 10.0 Hz, 1H), 6.62 (t, J = 8.4 Hz, 1H), 6.80-6.84 (m, 1H), 6.90 (dd, J = 0.9, 13.0 Hz, 1H), 7.25-7.36 (m, 10H). ^{19}F NMR (376.5 MHz, $CDCl_3$) δ = -111.20. ^{13}C NMR (100 MHz, $CDCl_3$) δ = 21.03, 81.01, 116.92 (d, J_{CF} = 29.3 Hz) 124.4 (d, J_{CF} = 2.7 Hz), 127.59, 127.72, 128.09, 130.2 (d, J_{CF} = 3.4 Hz), 131.4 (d, J_{CF} = 9.7 Hz), 140.4 (d, J_{CF} = 8.7 Hz), 145.80, 160.96 (d, J_{CF} = 243.4 Hz). HRMS (ESI+) calcd. for $C_{20}H_{16}F$ $[M\text{-}OH]^+$: 275.1231; found: 275.1228. Anal. calcd. for $C_{20}H_{17}FO$: C, 82.17; H, 5.86. Found: C, 82.27; H, 5.78.

5.2.5.27. (2-Fluoro-4-methoxyphenyl)(diphenyl)methanol (**60**).

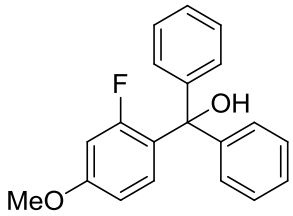

The title compound was prepared using general procedure (ii) with 1-bromo-2-fluoro-4-methoxybenzene (645 μL, 5.00 mmol) and *n*-butyllithium (2.5 M in hexane, 2.40 mL, 6.00 mmol) in anhydrous THF (5.00 mL), and subsequently benzophenone (1.048 g, 5.75 mmol) in anhydrous THF (5.75 mL). Purification by flash chromatography [SiO_2; 0-20% EtOAc in hexane] afforded the trityl alcohol **60** as a white solid (1.165 g, 76%). Mpt. 84-87 °C. ^{1}H NMR (400 MHz, $CDCl_3$) δ = 2.74 (s, 1H, OH), 3.87 (s, 3H, CH_3), 6.85-6.90 (m, 1H), 6.94-6.97 (m, 1H), 7.02-7.07 (m, 1H), 7.23-7.34 (m, 10H). ^{19}F NMR (376.5 MHz, $CDCl_3$) δ = -107.90. ^{13}C NMR (100 MHz, $CDCl_3$) δ = 56.38, 81.61 (d, J_{CF} = 1.5 Hz), 112.62, (d, J_{CF} = 2.4 Hz), 116.22 (d, J_{CF} = 19.7 Hz), 123.84 (d, J_{CF} = 3.6 Hz), 127.59, 127.91, 128.18, 140.17 (d, J_{CF} = 5.1 Hz), 146.70, 146.81 (d, J_{CF} = 10.8 Hz), 151.90 (d, J_{CF} = 245.4 Hz). HRMS (ESI+) calcd. for $C_{20}H_{16}FO$ $[M-OH]^+$: 290.11797; found: 290.11737. Anal. calcd. for $C_{20}H_{17}FO_2 \cdot ⅓H_2O$: C, 76.43; H, 5.66. Found: C, 76.21; H, 5.44.

5.2.5.28. (3-Fluoro-4-methoxyphenyl)(diphenyl)methanol (**61**).

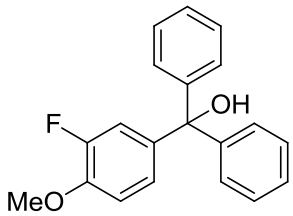

The title compound was prepared using general procedure (ii) with 4-bromo-2-fluoro-1-methoxybenzene (1.03 g, 5.00 mmol) and *n*-butyllithium (2.5 M in hexane, 2.40 mL, 6.00 mmol) in anhydrous THF (5.00 mL), and subsequently benzophenone (1.05 g, 5.75 mmol) in anhydrous THF (5.75 mL). Purification by flash chromatography [SiO_2; 0-20% EtOAc in hexane] afforded the trityl alcohol **61** as an off-white solid (0.93 g, 60%). Mpt. 54-55 °C. ^{1}H NMR (400 MHz, $CDCl_3$) δ = 3.43-3.48 (m, 1H), 3.78 (s, 3H, CH_3), 6.52-6.55 (m, 1H), 6.60-6.67 (m, 2H), 7.24-7.35 (m, 10H). ^{19}F NMR (376.5 MHz, $CDCl_3$) δ = -134.90. ^{13}C NMR (100 MHz, $CDCl_3$) δ = 55.73, 80.85, 102.78 (d, J_{CF} = 26.5 Hz), 108.81 (d, J_{CF} = 2.6 Hz), 126.60 (d, J_{CF} = 10.7 Hz), 127.58, 127.69, 128.10, 130.90 (d, J_{CF} = 5.1 Hz), 160.70 (d, J_{CF} = 11.7 Hz), 161.60 (d, J_{CF} = 245.6 Hz). HRMS (ESI+) calcd. for $C_{20}H_{16}FO$

[M-OH]$^+$: 290.11797; found: 290.11758. Anal. calcd. for $C_{20}H_{17}FO_2 \cdot ¼H_2O$: C, 76.78; H, 5.64. Found: C, 76.94; H, 5.72.

5.2.5.29. (3-Ethyl-4-methylphenyl)(diphenyl)methanol (**62**).

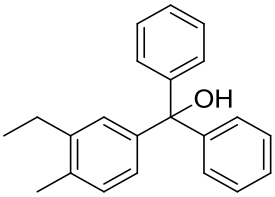

The title compound was prepared using general procedure (ii) with 4-bromo-2-ethyl-1-methylbenzene **84** (918 mg, 4.61 mmol) and *n*-butyllithium (2.5 M in hexane, 2.21 mL, 5.53 mmol) in anhydrous THF (4.61 mL), and subsequently benzophenone (966 mg, 5.30 mmol) in anhydrous THF (5.30 mL) with the following modifications. The reaction was maintained at ≤ -70 °C for 1 h after addition of *n*-butyllithium, and for 5 h after the addition of benzophenone. Purification by flash chromatography [SiO_2; 0-10% EtOAc in hexane] afforded the trityl alcohol **62** as a yellow oil (1.263 g, 91%). ^{1}H NMR ($CDCl_3$, 500 MHz) 1.14 (t, J = 7.6 Hz, 3H, CH_3), 2.31 (s, 3H, CH_3), 2.59 (q, J = 7.6 Hz, 2H, CH_2), 2.77 (s, 1H, OH), 6.93 (dd, J = 2.0, 7.9 Hz, 1H), 7.07 (d, J = 7.9 Hz, 1H), 7.12 (d, J = 1.9 Hz, 1H), 7.26-7.32 (m, 10H). ^{13}C NMR ($CDCl_3$, 125 MHz) δ 14.60, 18.92, 82.11, 125.60, 127.24, 127.66, 127.98, 128.06, 129.67, 134.96, 142.11, 144.77, 147.26. HRMS (ESI$^+$) calcd. for $C_{21}H_{21}$ [M-OH]$^+$: 285.16378; found: 285.16348. Anal. calcd. for $C_{22}H_{22}O$: C, 87.38; H, 7.33. Found: C, 87.23; H, 6.81.

5.2.5.30. 3-(Hydroxy(diphenyl)methyl)benzonitrile (**63**).

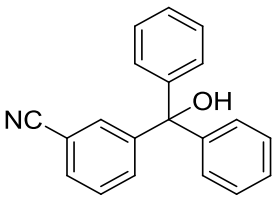

The title compound was prepared using an adaptation of the reverse addition method developed by Luliński *et al.* and the procedure reported by Neumann *et al.*[180, 181] A solution of 3-bromobenzonitrile (1.82 g, 10.0 mmol) in anhydrous THF (10 mL) was added by slow dropwise addition over 5 min to a solution of *n*-butyllithium (2.5 M in hexane, 4.2 mL, 10.5 mmol) at -94 °C, and stirred for 1 h maintaining the temperature ≤ -80 °C. After cooling again to -94 °C, a solution of benzophenone (2.00 g, 11.0 mmol) in anhydrous THF was added by slow dropwise addition over 6 min and stirred with the temperature

maintained ≤ -50 °C for 4 h. The reaction mixture was allowed to warm to room temperature and stirred for a further 19 h, then quenched with saturated aqueous NH_4Cl solution (25 mL) and extracted with EtOAc (3 x 25 mL). The combined organic layers were washed successively with H_2O and brine (75 mL each), dried ($MgSO_4$) and concentrated *in vacuo*. Purification by flash chromatography [SiO_2; 0-25% EtOAc in hexane;] afforded the trityl alcohol **63** as a white solid (2.30 g, 81%). Mpt. 90-92 °C (lit.[257] 96.5-97 °C). ^{1}H NMR (400 MHz, $CDCl_3$) δ = 2.85 (s, 1H, OH), 7.20-7.25 (m, 4H), 7.30-7.38 (m, 6H), 7.42 (t, *J* = 7.8 Hz, 1H), 7.55-7.62 (m, 2H), 7.65 (s, 1H). ^{13}C NMR (100 MHz, $CDCl_3$) δ = 81.70, 112.18, 119.05, 127.90, 128.03, 128.47, 128.86, 131.02, 131.60, 132.48, 145.91, 148.41. HRMS (ESI+) calcd. for $C_{20}H_{16}NO$ $[M+H]^+$: 286.1226; found: 286.1224. Anal. calcd. for $C_{20}H_{15}NO$: C, 84.19; H, 5.30; N, 4.91. Found: C, 83.71; H, 5.13; N, 4.80.

5.2.5.31. 4-(Hydroxy(diphenyl)methyl)benzonitrile (**64**).

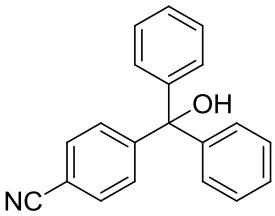

The title compound was prepared using an adaptation of the reverse addition method developed by Luliński *et al.* and the procedure reported by Neumann *et al.*[180, 181] A solution of 4-bromobenzonitrile (3.64 g, 20 mmol) in anhydrous THF (20 mL) was added by slow dropwise addition over 5 min to a solution of *n*-butyllithium (2.5 M in hexane, 8.40 mL, 21 mmol) at -94 °C and stirred for 30 min, maintaining the temperature ≤ -85 °C. After cooling again to -94 °C, a solution of benzophenone (4.01g, 22 mmol) in anhydrous THF (17 mL) was added by slow dropwise addition over 15 min and stirred for 5 h with the temperature maintained ≤ -80 °C. The mixture was allowed to warm to room temperature and stirred for a further 23 h, then quenched with saturated aqueous NH_4Cl solution (40 mL) and extracted with EtOAc (3 x 40 mL). The combined organic layers were washed successively with H_2O (100 mL) and brine (100 mL), dried ($MgSO_4$) and concentrated *in vacuo*. Purification by flash chromatography [SiO_2; 0-30% EtOAc in hexane] afforded the tertiary alcohol **64** as an off-white solid (3.86 g, 68%). Mpt. 85-87 °C (lit.[257] 92-93.5 °C). ^{1}H NMR (500 MHz, $CDCl_3$) δ = 2.85 (s, 1H, OH), 7.22-7.25 (m, 4H), 7.30-7.36 (m, 6H), 7.46-7.49 (m, 2H), 7.59-7.61 (m, 2H). ^{13}C NMR (125 MHz, $CDCl_3$) δ = 81.92, 111.19, 118.92, 127.93, 128.00, 128.44, 128.72, 131.89, 145.90, 152.00.

HRMS (ESI+) calcd. for $C_{20}H_{16}NO$ $[M+H]^+$: 286.1226; found: 286.1226. Anal. calcd. For $C_{20}H_{15}NO$: C, 84.19; H, 6.30; N, 4.91. Found: C, 83.91; H, 5.35; N, 4.81.

5.2.5.32. 3-(Hydroxy(4-methylphenyl)phenylmethyl)benzonitrile (*rac*-**65**).

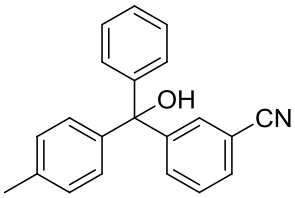

The title compound was prepared using an adaptation of the reverse addition method developed by Luliński *et al.* and the procedure reported by Neumann *et al.*[180, 181] A solution of 3-bromobenzonitrile (1.18g, 6.50 mmol) in anhydrous THF (6.5 mL) was added by slow dropwise addition over 18 min to a solution of *n*-butyllithium (2.5 M in hexane, 2.73 mL, 6.80 mmol) at -94 °C, and stirred for 1 h whilst maintaining the temperature ≤ -90°C. After cooling to -94 °C, a solution of (4-methylphenyl)(phenyl)methanone (1.40 g, 7.15 mmol) in anhydrous THF was added by slow dropwise addition over 10 min, and the reaction mixture stirred with the temperature maintained ≤ -75 °C for 5 h. The reaction was allowed to warm to room temperature and stirred for a further 16 h, then with saturated aqueous NH_4Cl solution (15 mL) and extracted with EtOAc (3 x 15 mL). The combined organic layers were washed successively with H_2O and brine (50 mL each), dried ($MgSO_4$) and concentrated *in vacuo*. Purification by flash chromatography [SiO_2; 0-18% EtOAc in hexane] afforded the trityl alcohol *rac*-**65** as a colourless oil (1.31 g, 67%). ^{1}H NMR (500 MHz, $CDCl_3$) δ = 2.36 (s, 3H, CH_3), 2.81 (s, 1H, OH), 7.08-7.11 (m, 2H), 7.13-7.16 (m, 2H), 7.22-7.24 (m, 2H), 7.29-7.36 (m, 3H), 7.39-7.43 (m, 1H), 7.54-7.57 (m, 1H), 7.59-7.61 (m, 1H), 7.64-7.65 (m, 1H). ^{13}C NMR (125 MHz, $CDCl_3$) δ = 21.16, 81.56, 112.13, 119.09, 127.84, 127.88, 127.92, 128.38, 128.41, 128.81, 129.16, 130.94, 131.60, 132.46, 137.84, 143.10, 146.08, 148.60. HRMS (ESI+) calcd. for $C_{21}H_{16}N$ $[M-OH]^+$: 282.1277; found: 282.1276. Anal. calcd. for $C_{21}H_{17}NO$: C, 84.25; H, 5.72; N 4.68. Found: C, 82.52; H, 5.33; N, 5.32.

5.2.5.33. 3-((3-Chlorophenyl)(hydroxy)phenylmethyl)phenol (*rac*-**66**).

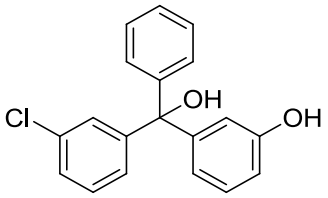

The title compound was prepared using an adaptation of the procedure for **48** using 1-bromo-3-chlorobenzene (2.11 mL, 18.00 mmol) and *n*-butyllithium (2.5 M in hexane, 8.42 mL, 21.05 mmol) in anhydrous THF (9 mL), and subsequently (3-hydroxyphenyl)(phenyl)methanone (1.19 g, 6.00 mmol) in anhydrous THF (6 mL), with the following modifications. The reaction was maintained at ≤ -70 °C for 2 h after addition of (3-hydroxyphenyl)(phenyl)methanone. Purification by flash chromatography [SiO_2; 0-25% EtOAc in pet. ether (40/60)] afforded the racemic trityl alcohol *rac*-**66** as a pale yellow solid (0.73 g, 39%). Mpt 95-96 °C. ^{1}H NMR (500 MHz, $CDCl_3$) δ = 2.77 (s, 1H, OH), 4.81 (br s, 1H, OH), 6.74-6.75 (m, 1H), 6.77 (ddd, *J* = 0.9, 2.5, 8.0 Hz, 1H), 6.79-6.82 (m, 1H), 7.15-7.27 (m, 5H), 7.30-7.35 (m, 5H). ^{13}C NMR (125 MHz, $CDCl_3$) δ = 81.71, 114.71, 115.16, 120.61, 126.33, 127.64, 127.80, 127.96, 128.12, 128.29, 129.29, 129.54, 134.19, 146.15, 148.28, 148.75, 155.46. HRMS (ESI-) calcd. for $C_{19}H_{14}ClO_2$ [M-H]$^-$: 309.06878; found: 309.06894. Anal. calcd. for $C_{19}H_{15}ClO_2$: C, 73.43; H, 4.86. Found: C, 73.55; H, 5.03.

5.2.5.34. 3-((3-Ethylphenyl)(hydroxy)phenylmethyl)phenol (*rac*-**67**).

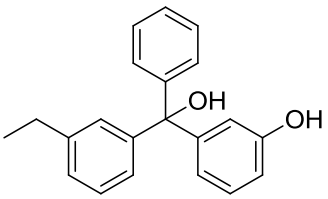

The title compound was prepared using general procedure (ii) with 1-bromo-3-ethylbenzene (2.08 ml, 15 mmol) and *n*-butyllithium (2.5 M in hexane, 6.20 mL, 15.6 mmol) in anhydrous THF (15.6 mL), and subsequently (3-hydroxyphenyl)(phenyl)methanone (1.19 g, 6 mmol) in anhydrous THF (6.0 mL) with the following modifications. The reaction was performed at at -84 °C and maintained at the same temperature for 1 h after addition of *n*-butyllithium, and after addition of (3-hydroxyphenyl)(phenyl)methanone for 5 h at ≤ -70 °C. Purification by flash chromatography [SiO_2; 0-20% EtOAc in hexane] afforded the racemic trityl alcohol *rac*-**67** as a yellow oil (1.09 g, 59 %). ^{1}H NMR ($CDCl_3$, 500 MHz) δ 1.19 (t, *J* = 7.6 Hz, 3H,

CH_3), 2.61 (q, J = 7.6 Hz, 2H, CH_2), 2.81 (s, 1H, OH), 4.80 (s, 1H, OH), 6.73-6.75 (m, 1H), 6.77-6.78 (m, 1H), 6.81-6.83 (m, 1H), 7.01-7.03 (m, 1H), 7.11-7.13 (m, 1H), 7.16-7.23 (m, 2H), 7.27-7.33 (m, 5H). ^{13}C NMR (MeOD, 125 MHz) δ 15.69, 29.06, 82.09, 114.33, 115.24, 120.76, 125.57, 126.99, 127.42, 127.51, 127.97, 128.05, 129.28, 144.15, 146.72, 146.85, 149.01, 155.30. HRMS (ESI+) calcd. for $C_{21}H_{19}O$ $[M\text{-}OH]^+$: 287.14304; found: 287.14307. Anal. calcd. for $C_{21}H_{20}O_2$: C, 82.86; H, 6.62. Found: C, 82.14; H, 6.69.

5.2.5.35. 3-(Hydroxy(4-methylphenyl)phenylmethyl)phenol (*rac*-**68**).

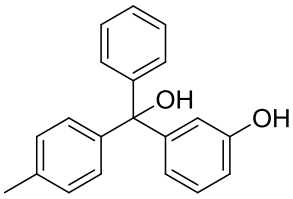

The title compound was prepared using an adaptation of the procedure for **48** using 1-bromo-4-methylbenzene (3.08 g, 18 mmol) and *n*-butyllithium (2.5 M in hexane, 8.42 mL, 21.6 mmol) in anhydrous THF (10 mL), and subsequently (3-hydroxyphenyl)(phenyl)methanone (1.19 g, 6 mmol) in anhydrous THF (6 mL), with the following modifications. The reaction was maintained at ≤ -70 °C for 2 h after addition of (3-hydroxyphenyl)(phenyl)methanone. Purification by flash chromatography [SiO_2; 0-28% EtOAc in pet. ether (60/80)] afforded the racemic trityl alcohol *rac*-**68** as a white solid (0.65 g, 37%). Mpt. 119-122 °C. ^{1}H NMR (500 MHz, $CDCl_3$) δ = 2.35 (s, 3H, CH_3), 2.85 (s, 1H, OH), 5.05 (br s, 1H, OH), 6.73-6.75 (m, 1H), 6.78-6.79 (m, 1H), 6.80-6.82 (m, 1H), 7.11-7.19 (m, 5H), 7.27-7.33 (m, 5H). ^{13}C NMR (125 MHz, $CDCl_3$) δ = 21.15, 81.95, 114.34, 115.20, 120.67, 127.40, 127.97, 128.01, 128.04, 128.79, 129.27, 137.18, 143.89, 146.87, 148.97, 155.36. HRMS (ESI-) calcd. for $C_{20}H_{17}O_2$ $[M\text{-}H]^-$: 289.12350; found: 289.12340. Anal. calcd. for $C_{20}H_{18}O_2$: C, 82.73; H, 6.25. Found: C, 82.09; H, 6.21.

5.2.5.36. Diphenyl(pyridin-3-yl)methanol (**69**).

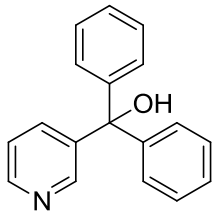

n-Butyllithium (2.5 M in hexane, 3.96 mL, 9.96 mmol) was added by slow dropwise addition over 8 min to a cooled (-94 °C) solution of 3-bromopyridine (722 μL, 7.5 mmol) in anhydrous THF (15 mL) stirred for 1 h at ≤ -70 °C. A solution of benzophenone (1.50 g, 8.25 mmol) in anhydrous THF (8.25 mL) was then added by slow dropwise addition over 10 min, and the reaction mixture stirred with the temperature maintained ≤ -85 °C for 3 h, before allowing the reaction to warm slowly to room temperature and stirring for a further 15 h. The reaction was quenched with aqueous HCl (1.0 M, 15 mL) and washed with Et_2O (50 mL). The organic washings were extracted with aqueous HCl (1.0 M, 3 x 20 mL), and the combined aqueous layers basified (*circa.* pH 9) with saturated aqueous sodium carbonate solution, and extracted with Et_2O (3 x 100 mL). These organic extracts were washed with brine (100 mL), dried ($MgSO_4$) and concentrated *in vacuo*. Purification by flash chromatography [SiO_2; 20-60% EtOAc in hexane] afforded the tertiary alcohol **69** as a white solid (565 mg, 29%). Mpt. 105-107 °C (lit.[258] 115-116 °C from EtOAc). ^{1}H NMR (400 MHz, $CDCl_3$) δ = 3.62 (br s, 1H, OH), 7.17-7.35 (m, 11H), 7.62-7.66 (m, 1H), 8.39-8.48 (m, 2H). ^{13}C NMR (400 MHz, $CDCl_3$) δ = 80.79, 122.89, 127.77, 127.94, 128.33, 135.62, 142.56, 146.20, 148.27, 149.47. HRMS (ESI+) calcd. for $C_{18}H_{16}NO$ $[M+H]^+$: 262.1226; found: 262.1224. Anal. calcd. for $C_{18}H_{15}NO$: C, 82.73; H, 5.79; N, 5.36. Found: C, 82.54; H, 5.47; N, 5.12.

5.2.5.37. Diphenyl(1,3-thiazol-2-yl)methanol (**70**).

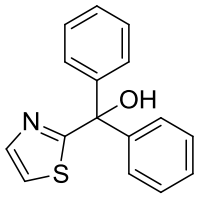

The title compound was prepared using general procedure (ii) with 2-bromo-1,3-thiazole (676 μL, 7.50 mmol) and *n*-butyllithium (2.5 M in hexane, 3.15 mL, 7.88 mmol) in anhydrous THF (30 mL), and subsequently benzophenone (1.05 g, 5.75 mmol) in anhydrous THF (5.75 mL) with the following modifications. The reaction was maintained

at ≤ -70 °C for 1 h after addition of *n*-butyllithium, and for 2 h after the addition of benzophenone. Purification by flash chromatography [SiO_2; 0-20% EtOAc in hexane] afforded the trityl alcohol **70** as a pale brown solid (825 mg, 41%). Mpt. 107-108 °C (lit.[259] 114-115 °C from pet. ether). ^{1}H NMR (400 MHz, $CDCl_3$) δ = 4.20 (s, 1H, OH), 7.29-7.37 (m, 6H), 7.38-7.44 (m, 4H), 7.81 (d, *J* = 3.3 Hz, 1H). ^{13}C NMR (400 MHz, $CDCl_3$) δ = 80.84, 120.19, 127.58, 128.12, 128.28, 142.81, 145.46, 177.39. HRMS (ESI+) calcd. for $C_{16}H_{12}NS$ $[M\text{-}OH]^+$: 250.0685; found: 250.0683. Anal. calcd. for $C_{16}H_{13}NOS$: C, 71.88; H, 4.90; N, 5.24. Found: C, 70.85; H, 4.48; N, 5.06.

5.2.5.38. 1,3-Oxazol-2-yl)(diphenyl)methanol (**71**).

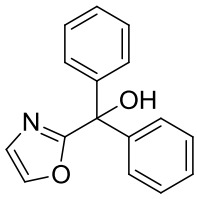

n-Butyllithium (2.5 M in hexane, 3.96 mL, 9.96 mmol) was added by slow dropwise addition over 15 min to a cooled (-94 °C) solution of oxazole (0.59 mL, 9 mmol) in anhydrous THF (25 mL) stirred for 30 min. A solution of benzophenone (1.37 g, 7.50 mmol) in anhydrous THF (7.5 mL) was then added by slow dropwise addition, and the reaction mixture stirred with the temperature maintained ≤ -85 °C for 1.5 h, before allowing the reaction to warm slowly to room temperature and stirring for a further 16 h. The reaction was quenched with saturated aqueous NH_4Cl solution (15 mL) and extracted with Et_2O (3 x 40 mL). The combined organic layers were washed with aqueous HCl (1.0 M, 3 x 10 mL), dried ($MgSO_4$) and concentrated *in vacuo*. Purification by flash chromatography [SiO_2; 0-15% EtOAc in hexane] afforded the tertiary alcohol **71** as a white solid (507 mg, 27%). Mpt. 97.5-98.5 °C (lit.[183] 100-102 °C). ^{1}H NMR (400 MHz, $CDCl_3$) δ = 4.59 (br s, 1H, OH), 7.05 (d, *J* = 0.8 Hz, 1H). 7.31-7.36 (m, 10H), 7.65 (d, *J* = 0.8 Hz, 1H). ^{13}C NMR (400 MHz, $CDCl_3$) δ = 78.43, 126.91, 127.32, 128.19, 128.28, 139.78, 143.67, 166.94. HRMS (ESI+) calcd. for $C_{16}H_{12}NO$ $[M+H]^+$: 234.0913; found: 234.0909. Anal. calcd. for $C_{16}H_{13}NO_2$: C, 76.48; H, 5.21; N 5.57. Found: C, 76.64; H, 4.95; N, 5.34.

5.2.5.39. 2-(3-Bromophenyl)-2-methyl-1,3-dioxolane (**77**).

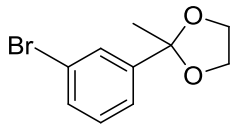

Anhydrous ethylene glycol (2.31 mL, 42.0 mmol) and a catalytic amount of *p*-toluenesulfonic acid monohydrate (114 mg, 0.6 mmol) were added to a solution of 1-(4-bromophenyl)ethanone (1.59 mL, 12.0 mmol) in anhydrous toluene (80 mL) and the reaction mixture refluxed, using a Dean-Stark trap, for 20 h. The reaction was cooled to room temperature, washed with brine (40 mL) and concentrated *in vacuo* to give the crude acetal **77** as a colourless oil, which was taken to the next step without further purification (2.64 g, 90%). ^{1}H NMR (400 MHz, $CDCl_3$) δ = 1.63 (s, 3H, CH_3), 3.73-3.81 (m, 2H, CH_2), 4.00-4.08 (m, 2H, CH_2), 7.21-7.37 (t, *J* = 7.9 Hz, 1H), 7.39-7.44 (m, 2H), 7.63-7.65 (m, 1H). ^{13}C NMR (100 MHz, CDCl) δ = 27.70, 64.68, 108.30, 124.14, 128.68, 130.04, 131.07, 145.98.

5.2.5.40. 2-(4-Bromophenyl)-2-methyl-1,3-dioxolane (**78**).

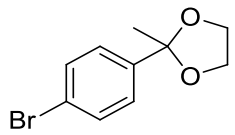

Anhydrous ethylene glycol (1.32 mL, 24.0 mmol) and a catalytic amount of *p*-toluenesulfonic acid monohydrate (114 mg, 0.6 mmol) were added to a solution of 1-(4-bromophenyl)ethanone (2.39 g, 12.0 mmol) in anhydrous toluene (80 mL) and the reaction mixture refluxed, using a Dean-Stark trap, for 20 h. The reaction was cooled to room temperature, washed with brine (40 mL) and concentrated *in vacuo*. Purification by flash chromatography [SiO_2; 0-12% EtOAc in hexane with 1% NH_4OH] yielded acetal **78** as a white solid (1.88 g, 65% yield), which was used directly in the next reaction. ^{1}H NMR (400 MHz, $CDCl_3$) δ = 1.64 (s, 3H, CH_3), 3.73-3.77 (m, 2H, CH_2), 4.01-4.05 (m, 2H, CH_2), 7.33-7.37 (m, 2H), 7.4 3-7.49 (m, 2H). ^{13}C NMR (100 MHz, CDCl) δ = 27.74, 64.70, 108.67, 122.10, 127.39, 131.55, 142.67.

5.2.5.41. 1-Bromo-3-propylbenzene (**80**).

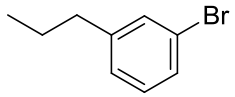

The title compound was prepared using an adaptation of the procedure reported by Chackal-Catoen *et al.*[260] Hydrazine hydrate monohydrate (2.18 mL, 45 mmol) was added to a solution of 1-(3-bromophenyl)propan-1-one (3.20 g, 15 mmol) and powdered KOH (2.53 g, 45 mmol) in anhydrous ethylene glycol (18.6 mL) and refluxed for 4 h. After cooling to room temperature, the reaction was quenched was aqueous HCl (1.0 M, 70 mL) and extracted with CH_2Cl_2 (3 x 50 mL). The organics were washed successively with water and brine (100 mL each), dried ($MgSO_4$) and concentrated *in vacuo* and the residue purified by flash chromatography [SiO_2; hexane] to afford the alkane **80** as a colorless oil (2.03 g, 68%). ^{1}H NMR ($CDCl_3$, 400 MHz) δ = 0.94 (t, *J* = 7.5 Hz, 3H, CH_3), 1.63 (p, *J* = 7.5 Hz, 2H, CH_2), 2.56 (t, 2H, *J* = 7.5 Hz, 2H, CH_2), 7.09-7.16 (m, 2H), 7.30-7.34 (m, 2H). ^{13}C NMR ($CDCl_3$, 125 MHz) δ 13.85, 24.47, 37.81, 122.46, 127.28, 128.88, 129.92, 131.66, 145.17. GC-MS (EI, 70 eV) t_R = 4.72 min (*m/z* = 197.9, [M^+]).

5.2.5.42. 5-Bromo-*N*-methoxy-*N*,2-dimethylbenzamide (**82**).

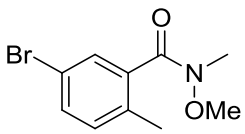

Oxalyl chloride (3.43 ml, 40 mmol) was added to a solution of 5-bromo-2-methylbenzoic acid (4.30 g, 20 mmol) in anhydrous CH_2Cl_2 (20 ml), with a catalytic amount of DMF (1 drop), and stirred at room temperature for 2 h. The reaction mixture was concentrated *in vacuo,* and the residual oil added by slow dropwise addition over 5 min to a cooled (0 °C) solution of *N,O*-dimethylhydroxylamine hydrochloride (2.24 g, 23 mmol) and triethylamine (3.67 mL, 50 mmol) in anhydrous CH_2Cl_2 (20 ml). After stirring for 1 h, the reaction mixture was warmed to room temperature, stirred for 20.5 h, then quenched with water followed by aqueous HCl (0.5 M, 25 mL), and extracted with CH_2Cl_2 (3 x 25 mL). The combined organic extracts were dried ($MgSO_4$), concentrated *in vacuo*, and purified by flash chromatography [SiO_2; 0-50% EtOAc in hexane] to afford amide **82** as a colourless oil (3.63 g, 70%). ^{1}H NMR ($CDCl_3$, 500 MHz) δ 2.26 (s, 3H, CH_3), 3.30 (br s, 3H, CH_3), 3.48 (br s, 3H, CH_3), 7.07 (d, *J* = 8.6 Hz, 2H), 7.38-7.40 (m, 2H). ^{13}C NMR ($CDCl_3$, 125 MHz) δ 18.77, 61.33, 118.95, 129.13, 131.95, 132.23, 134.06, 137.20.

HRMS (ESI+) calcd. for $C_{10}H_{13}BrNO_2$ $[M+H]^+$: 258.01242; found: 258.01244. Anal. calcd. for $C_{10}H_{12}BrNO_2$: C, 46.53; H, 4.69; N, 5.43. Found: C, 45.03; H, 4.78; N, 5.60.

5.2.5.43. 1-(5-Bromo-2-methylphenyl)ethanone (**83**).

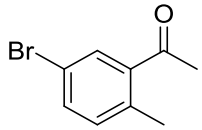

The title compound was prepared using an adaptation of the procedure reported by Hirashima *et al.*[261] MeMgCl (3.0 M in THF, 8.27 mL, 24.8 mmol) was added by slow dropwise addition over 10 min to a cooled (0 °C) solution of Weinreb amide **82** (3.27 g, 12.4 mmol) in THF (12.4 mL) and stirred for 2 h. The reaction mixture was warmed to room temperature, stirred for 2 h, before quenching with saturated aqueous NH_4Cl solution (20 mL) and extracting with EtOAc (3 x 25 mL). The organics were washed successively with water and brine (75 ml each), dried ($MgSO_4$) and concentrated *in vacuo* to afford ketone **83** as a clear pale brown oil (2.40 g, 91%), which was used without further purification. ^{1}H NMR ($CDCl_3$, 500 MHz) δ 2.45 (s, 3H, CH_3), 2.56 (s, 3H, CH_3), 7.11 (d, J = 8.2 Hz, 1H), 7.48 (dd, J = 2.1, 8.2 Hz, 1H), 7.77 (d, J = 2.1 Hz, 1H). ^{13}C NMR ($CDCl_3$, 125 MHz) δ 22.10, 29.62, 119.24, 132.11, 133.77, 134.39, 137.29, 139.46. GC-MS (EI, 70 eV) t_R = 4.68 min (m/z = 211.9, $[M^+]$). Anal. calcd. for C_9H_9BrO C, 50.73; H, 4.26. Found: C, 50.44; H, 4.30.

5.2.5.44. 4-Bromo-2-ethyl-1-methylbenzene (**84**).

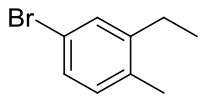

The title compound was prepared using an adaptation of the method described for **80**. Ketone **83** (2.13 g, 10 mmol) in anhydrous ethylene glycol (10 ml) afforded after refluxing for 4 h, aqueous workup and purification by flash chromatography [SiO_2; hexane] afforded alkane **84** as a colourless oil (1.10 g, 55 %). ^{1}H NMR ($CDCl_3$, 400 MHz) δ 1.20 (t, J = 7.5 Hz, 3H, CH_3), 2.24 (s, 3H, CH_3), 2.59 (q, J = 7.5 Hz, 2H, CH_2), 7.00 (d, J = 8.0 Hz, 1H), 7.22 (dd, J = 2.0, 8.0 Hz, 1H), 7.28 (d, J = 1.9 Hz, 1H). ^{13}C NMR ($CDCl_3$, 100 MHz) δ 14.21, 18.84, 26.18, 119.63, 128.72, 130.80, 131.71, 134.83, 144.68. GC-MS (EI, 70 eV) t_R = 4.90 min (m/z = 199.8, $[M^+]$).

5.2.5.45. 3-(Hydroxy(diphenyl)methyl)benzamide (**85**).

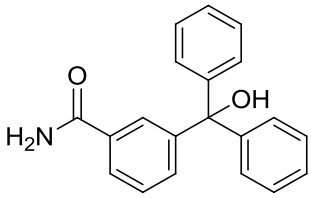

This hydrolysis protocol is a modification of the literature procedure reported by Iso *et al.*[262] Hydrogen peroxide (30% in H_2O, 536 µl, 5.25 mmol) and aqueous NaOH (6.0 M, 350 µL, 2.1 mmol) were added to a solution of benzonitrile **63** (494 mg, 1.75 mmol) in EtOH (7.69 mL) and stirred at 60 °C for 4 h. After cooling to room temperature, the reaction mixture was partitioned between CH_2Cl_2 (75 mL) and aqueous HCl (0.25 M, 25mL). The organic layer was washed successively with H_2O (and brine (75 mL each), dried ($MgSO_4$) and concentrated *in vacuo.* Purification of the crude by flash chromatography [SiO_2; 40-100% EtOAc in hexane] afforded the amide **85** as a white solid (440 mg, 83%). Mpt. 168-169 °C. ^{1}H NMR (400 MHz, MeOD) δ = 7.23-7.32 (m, 10H), 7.35-7.43 (m, 2H), 7.73-7.76 (m, 1H), 7.88-7.90 (m, 1H). ^{13}C NMR (100 MHz, MeOD) δ = 82.70, 127.06, 128.15, 128.46, 128.79, 129.26, 132.78, 134.57, 148.46, 149.61, 172.52. HRMS (ESI+) calcd. for $C_{22}H_{23}N_2OS$ $[M+H]^+$: 363.1526; found: 363.1522. Anal. calcd. for $C_{20}H_{17}NO_2$: C, 79.19; H, 5.65; N, 4.62. Found: C, 78.99; H, 5.57; N, 4.49.

5.2.5.46. 4-(Hydroxy(diphenyl)methyl)benzamide (**86**).

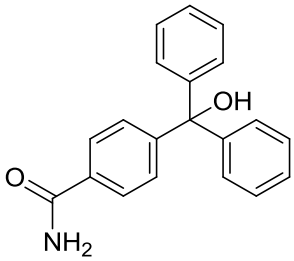

The title compound was prepared using an adaptation of the procedure for **85** with benzonitrile **64** (571 mg, 2.0 mmol)**,** hydrogen peroxide (30% in H_2O, 612 µl, 6.0 mmol) and aqueous NaOH (6.0 M, 400 µL, 2.4 mmol) in EtOH (15 mL) at 60 °C for 3 h. Purification by flash chromatography [SiO_2; 50-90% EtOAc in hexane] afforded amide **86** as a white solid (502 mg, 83%). Mpt. 176-179 °C (lit.[263] 188 °C from MeOH). ^{1}H NMR (500 MHz, MeOD) δ = 7.23-7.32 (m, 10H), 7.35-7.39 (m, 2H), 7.89-7.92 (m, 2H). ^{13}C NMR (125 MHz, MeOD) δ = 82.68, 128.03, 128.20, 128.79, 128.79, 129.23, 129.33, 133.48, 148.35, 152.91, 172.18. HRMS (ESI+) calcd. for $C_{20}H_{18}NO_2$ $[M+H]^+$: 304.1332;

found: 304.1330. Anal. calcd. for $C_{20}H_{17}NO_2$: C, 79.19; H, 5.65; N, 4.62. Found: C, 79.01; H, 5.60; N, 4.56.

5.2.5.47. 3-(Hydroxy(4-methylphenyl)phenylmethyl)benzamide (*rac*-**87**)

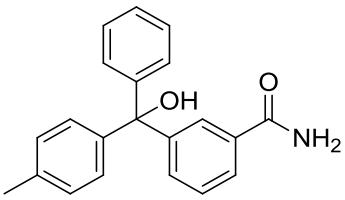

The title compound was prepared using an adaptation of the procedure for **85** with benzonitrile *rac*-**65** (400 mg, 1.34 mmol), hydrogen peroxide (30% in H_2O, 409 µl, 4.01 mmol) and aqueous NaOH (6.0 M, 400 µL, 2.4 mmol) in EtOH (10 mL). Purification by flash chromatography [SiO_2; 0-27% MeOH in CH_2Cl_2] afforded amide *rac*-**87** as a white solid (262 mg, 62%). Mpt. 77-80 °C. ^{1}H NMR (500 MHz, MeOD) δ = 2.32 (s, 3H, CH_3), 4.57 (s, 1H, OH), 7.09-7.12 (m, 4H), 7.22-7.31 (m, 5H), 7.34-7.42 (m, 2H), 7.72-7.75 (m, 1H), 7.86-7.88 (m, 1H), 7.61-7.64 (m, 1H), 7.74-7.79 (m, 2H). ^{13}C NMR (125 MHz, MeOD) δ = 21.02, 82.61, 127.01, 128.10, 128.42, 128.75, 129.22, 129.38, 129.41, 132.77, 134.50, 137.95, 145.50, 148.56, 149.74, 172.57. HRMS (ESI+) calcd. for $C_{21}H_{18}NO$ [M-OH]$^+$: 300.1383; found: 300.1380. Anal. calcd. for $C_{21}H_{19}NO_2 \cdot ⅓H_2O$: C, 78.01; H, 6.13; N 4.33. Found: C, 77.70; H, 5.90; N, 4.21.

5.2.5.48. 3-(Hydroxy(diphenyl)methyl)benzoic acid (**88**).

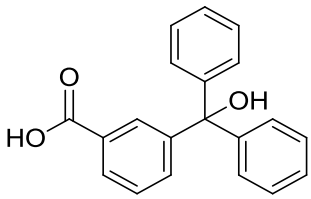

A solution of benzonitrile **63** (1.25 g, 4.37 mmol) and potassium hydroxide (2.728 g, 48.60 mmol) was refluxed in an EtOH/H_2O mixture (1:1, 49 mL) for 24 h. After cooling to room temperature, the EtOH was removed under reduced pressure, the solution washed with Et_2O (30 mL), acidified (*circa* pH 1) with aqueous HCl (1.0 M) and extracted with CH_2Cl_2 (3 x 50 mL). The organic extracts were dried ($MgSO_4$) and concentrated *in vacuo* to yield as a white solid **88**, which was used without further purification (1.25 g, 94%). Mpt. 166-168 °C. ^{1}H NMR (400 MHz, DMSO-d_6) δ = 6.60 (s, 1H, OH), 7.19-7.22 (m, 4H), 7.24-7.28 (m, 2H), 7.29-7.34 (m, 4H), 7.41-7.44 (m, 2H), 7.81-7.85 (m, 1H), 7.86-7.88 (m, 1H), 12.82 (br s, 1H, COOH). ^{13}C NMR (100 MHz, DMSO-d_6) δ = 80.40, 126.82, 127.69,

127.58, 130.20, 132.19, 147.33, 148.29, 167.40. HRMS (ESI-) calcd. for $C_{20}H_{15}O_3$ $[M-H]^-$: 303.1027; found: 303.1028. Anal. calcd. for $C_{20}H_{16}O_3 \cdot ⅓CH_2Cl_2$: C, 73.42; H, 5.05. Found: C, 73.48; H, 5.06.

5.2.5.49. (4-(Hydroxymethyl)phenyl)(diphenyl)methanol (**90**).

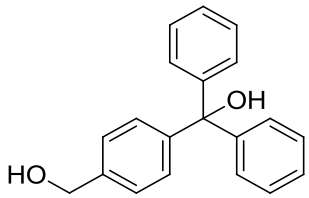

The title compound was prepared using a modification of the procedure reported by Zee-Cheng *et al.*[127] A solution of 4-(hydroxy(diphenyl)methyl)benzoic acid (304 mg, 1.0 mmol) in anhydrous THF (4 mL) was added by slow dropwise addition over 3 min to a cooled (0 °C) solution of lithium aluminium hydride (1.0 M in THF, 4.5 mL, 4.5 mmol). The reaction mixture was allowed to warm to room temperature and stirred for 20.5 h, then heated at 65 °C for 1 h. The reaction was cooled to 0 °C, and quenched with EtOAc (5 mL), H_2O (0.17 mL), aqueous NaOH (15% *w/v*, 0.17 mL) and H_2O (3 x 0.17 mL) and stirred for 45 min at room temperature. After filtering and washing the precipitate with EtOAc, the filtrate was washed successively with saturated aqueous $NaHCO_3$ solution, H_2O and brine (50 mL each), dried ($MgSO_4$) and concentrated *in vacuo*. Purification by flash chromatography [SiO_2; 0-40% EtOAc in hexane] yielded **90** as a white solid (182 mg, 63%). Mpt. 112-115 °C (lit.[127] 115-117 °C). ^{1}H NMR (400 MHz, $CDCl_3$) δ = 4.67 (s, 2H, CH_2), 7.25-7.33 (m, 14H). ^{13}C NMR (100 MHz, $CDCl_3$) δ = 65.23, 82.11, 126.80, 127.52, 128.11, 128.18, 128.36, 140.01, 146.59, 147.02. HRMS (ESI+) calcd. for $C_{20}H_{17}O$ $[M-OH]^+$: 273.1274; found: 273.1272. Anal. calcd. for $C_{20}H_{18}O_2$: C, 82.73; H, 6.25. Found: C, 82.17; H, 6.23.

5.2.5.50. 3-(Hydroxy(diphenyl)methyl)-*N*-methylbenzamide (**91**).

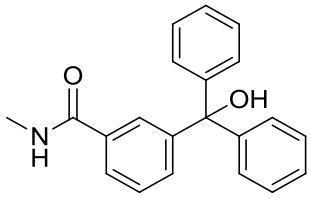

Methanamine hydrochloride (203 mg, 3.0 mmol), followed by triethylamine (1.26 mL, 9.0 mmol) and T3P® (50% in DMF, 876 µL, 1.5 mmol) were added to a cooled (0 °C) solution of **88** (304 mg, 1.0 mmol) in anhydrous THF (2 mL), and stirred at room temperature for 44 h. The reaction was quenched with saturated aqueous $NaHCO_3$ (10 mL) and stirred for 45 min. The volatiles were removed *in vacuo* and the pH was adjusted (*circa.* pH 7) with aqueous HCl (1.0 M) and extracted with CH_2Cl_2 (3 x 30 mL). The organic extracts were washed successively with H_2O and brine (75 mL each), dried ($MgSO_4$), then concentrated *in vacuo* to afford 3-(hydroxy(diphenyl)methyl)-*N*-methylbenzamide **91** as a white solid, which was taken to the next step without further purification (248 mg, 78%). Mpt. 137-138 °C. ^{1}H NMR (400 MHz, $CDCl_3$) δ = 2.90 (d, *J* = 4.9 Hz, 3H, CH_3), 3.15 (br s, OH), 6.18 (br s, NH), 7.22-7.36 (m, 12H), 7.67-7.70 (m, 1H), 7.78-7.80 (m, 1H). ^{13}C NMR (100 MHz, $CDCl_3$) δ = 26.90, 82.03, 125.88, 126.25, 127.65, 128.03, 128.24, 131.17, 134.58, 146.59, 147.45, 168.32. HRMS (ESI+) calcd. for $C_{21}H_{20}NO_2$ $[M+H]^+$: 318.1487; found: 318.1489. Anal. calcd. for $C_{21}H_{19}NO_2$: C, 79.47; H, 6.03; N, 4.41. Found: C, 78.44; H, 6.07; N, 5.12.

5.2.5.51. 3-(Hydroxy(diphenyl)methyl)-*N,N*-dimethylbenzamide (**92**).

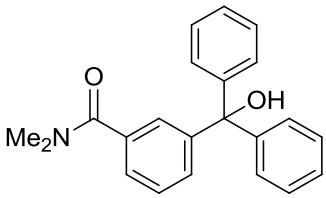

N-methylmethanamine hydrochloride (245 mg, 3.0 mmol), followed by triethylamine (1.25 mL, 9.0 mmol) and T3P® (50% in DMF, 876 µL, 1.5 mmol) were added to a cooled (0 °C) solution of **88** (304 mg, 1.0 mmol) in anhydrous THF (2 mL) and stirred at room temperature for 44 h. The reaction was quenched with saturated aqueous $NaHCO_3$ (10 mL) and stirred for 1.5 h. The volatiles were removed *in vacuo*, and the mixture extracted with CH_2Cl_2 (3 x 30 mL). The organic extracts were washed successively with H_2O and brine (75 mL each), dried ($MgSO_4$), then concentrated *in vacuo* to the amide **92** as a white solid, which was taken to the next step without further purification (259 mg, 78%). Mpt.

165-167 °C. ^{1}H NMR (500 MHz, $CDCl_3$) δ = 2.87 (s, 3H, CH_3), 3.05 (s, 3H, CH_3), 7.26-7.37 (m, 14H). ^{13}C NMR (125 MHz, $CDCl_3$) δ = 35.48, 39.65, 82.00, 126.34, 126.75, 127.58, 128.03, 128.18, 128.28, 129.23, 135.96, 146.65, 147.10, 171.60. HRMS (ESI+) alcd. for $C_{22}H_{22}NO_2$ $[M+H]^+$: 332.1645; found: 332.1643. Anal. calcd. for $C_{22}H_{21}NO_2 \cdot ⅕H_2O$: C, 78.58; H, 6.09; N, 4.36. Found: C, 78.87; H, 6.39; N, 4.57.

5.2.5.52. 4-(Hydroxy(diphenyl)methyl)-*N*-methylbenzamide (**93**).

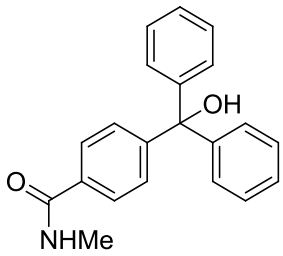

Methanamine hydrochloride (203 mg, 3.0 mmol), followed by triethylamine (1.26 mL, 9.0 mmol) and T3P® (50% in DMF, 876 µL, 1.5 mmol) were added to a cooled (0 °C) solution of 4-(hydroxy(diphenyl)methyl)benzoic acid (304 mg, 1.0 mmol) in anhydrous THF (2 mL) and stirred at room temperature for 44 h. The reaction was quenched with saturated aqueous $NaHCO_3$ (10 mL) and stirred for 45 min. The volatiles were removed *in vacuo* and the pH was adjusted (*circa.* pH 7) with aqueous HCl (1.0 M) and extracted with CH_2Cl_2 (3 x 30 mL). The organic extracts were washed successively with H_2O and brine (75 mL each) then concentrated *in vacuo*. Purification by flash chromatography [SiO_2; 25-90% EtOAc in hexane] afforded amide **93** as an off-white solid (181 mg, 57%). Mpt. 62-64 °C. ^{1}H NMR (400 MHz, $CDCl_3$) δ = 2.97 (d, J = 4.9 Hz, 3H, CH_3), 3.01 (s, 1H, OH), 6.17 (br s, 1H, NH), 7.22-7.33 (m, 10H), 7.36-7.38 (m, 2H), 7.65-7.68 (m, 2H). ^{13}C NMR (100 MHz, $CDCl_3$) δ = 26.96, 81.97, 126.59, 127.65, 128.01, 128.21, 128.23, 133.60, 146.53, 150.28, 168.15. HRMS (ESI+) calcd. for $C_{21}H_{20}NO_2$ $[M+H]^+$: 318.1489; found: 318.1487. Anal. calcd. for $C_{21}H_{19}NO_2$: C, 79.47; H, 6.03; N, 4.41. Found: C, 79.27; H, 5.99; N, 4.33.

5.2.5.53. 4-(Hydroxy(diphenyl)methyl)-*N,N*-dimethylbenzamide (**94**).

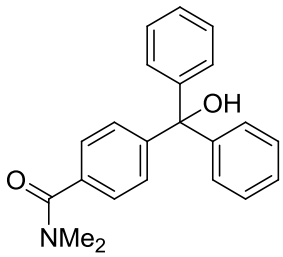

N-Methylmethanamine hydrochloride (245 mg, 3.0 mmol), followed by triethylamine (1.25 mL, 9.0 mmol) and T3P® (50% in DMF, 876 µL, 1.5 mmol) were added to a cooled (0 °C) solution of 4-(hydroxy(diphenyl)methyl)benzoic acid (304 mg, 1.0 mmol) in anhydrous THF (2.5 mL) and stirred at room temperature for 45 h. The volatiles were removed *in vacuo* and the residue suspended in saturated aqueous NaHCO3 (10 mL) and stirred for 1 h at room temperature. The pH was adjusted (*circa.* pH 7) with aqueous HCl (1.0 M) and extracted with EtOAc (3 x 30 mL). The organic extracts were washed successively with H_2O and brine (75 mL each) then concentrated *in vacuo* to afford tertiary amide **94** as a white solid, which was used without further purification (246 mg, 74%). Mpt. 142-143 °C. ^{1}H NMR (500 MHz, MeOD) δ = 3.00 (s, 3H, CH_3), 3.09 (s, 3H, CH_3), 7.23-7.32 (m, 10H), 7.34-7.38 (m, 4H). ^{13}C NMR (125 MHz, MeOD) δ = 35.64, 40.06, 82.64, 127.48, 128.17, 128.78, 129.23, 129.38, 135.81, 148.42, 150.91, 173.70. HRMS (ESI+) calcd. for $C_{22}H_{22}NO_2$ $[M+H]^+$: 332.1645; found: 332.1642. Anal. calcd. for $C_{22}H_{21}NO_2$: C, 79.73; H, 6.39; N, 4.23. Found: C, 79.25; H, 6.27; N, 4.02.

5.2.5.54. (3-(Aminomethyl)phenyl)(diphenyl)methanol (**95**).

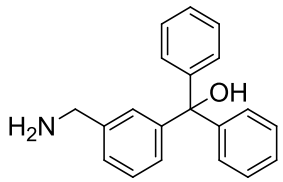

A solution of lithium aluminium hydride (1.0 M in THF, 7.87 mL, 7.87 mmol) was added by slow dropwise addition over 8 min to a cooled solution (0 °C) of benzonitrile **63** (936 mg, 3.28 mmol) in anhydrous THF (10.90 mL). The reaction mixture was allowed to warm to room temperature and stirred for 22 h, and then cooled to 0 °C and quenched by slow dropwise addition of H_2O (10 mL), followed by aqueous NaOH solution (15% *w/v*, 5 mL) and H_2O (15 mL). The suspension was filtered and the precipitate washed with CH_2Cl_2, and the filtrate washed successively with H_2O and brine (50 mL each), dried ($MgSO_4$) and concentrated *in vacuo*. Purification by flash chromatography [SiO_2; 0-18% MeOH in CH_2Cl_2 with 1% NH_4OH] afforded the tertiary alcohol **95** as a white solid (643 mg, 68%). Mpt. 136-138 °C. ^{1}H NMR (500 MHz, DMSO-d_6) δ = 3.66 (s, 2H, CH_2), 6.38 (br s, 1H, OH), 6.97-6.99 (m, 1H), 7.19-7.34 (m, 13H). ^{13}C NMR (125 MHz, DMSO-d_6) δ = 45.72, 80.58, 125.35, 125.87, 126.35, 126.55, 127.17, 127.46, 127.78, 143.19, 147.55, 147.87. HRMS (ESI+) calcd. for $C_{20}H_{20}NO$ $[M+H]^+$: 290.1539; found: 290.1537. Anal. calcd. for $C_{20}H_{19}NO$: C, 83.01; H, 6.62; N, 4.84. Found: C, 82.23; H, 6.43; N, 4.29.

5.2.5.55. (4-(Aminomethyl)phenyl)(diphenyl)methanol (**96**).

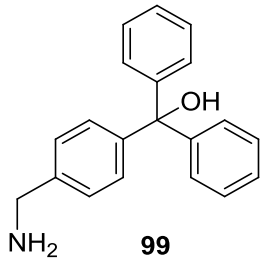

99

A solution of lithium aluminium hydride (1.0 M in THF, 19.2 mL, 19.2 mmol) was added by slow dropwise addition over 10 min to a solution of benzonitrile **64** (2.28 g, 8.0 mmol) in anhydrous THF (25 mL) at 0 °C. The reaction mixture was allowed to warm to room temperature stirred for 22 h. It was then cooled to 0 °C and quenched by slow dropwise addition of H_2O (40 mL), followed by aqueous NaOH solution (15% *w/v*, 20 mL) and H_2O (20 mL). As this failed to break up the aluminium salt emulsion, saturated aqueous Na_2SO_4 solution (250 mL) was added and the mixture stirred for 30 min at room temperature. The mixture was filtered, the precipitate washed with CH_2Cl_2 and MeOH, and the filtrate concentrated to ~50 mL *in vacuo*, diluted with saturated aqueous Na_2SO_4 solution (50 mL) and extracted with CH_2Cl_2 (3 x 50 mL). The organic extracts were washed with brine (100 mL), dried ($MgSO_4$) and and concentrated *in vacuo*. Purification by flash chromatography [SiO_2; 0-22% MeOH in CH_2Cl_2 with 1% NH_4OH] afforded the title compound **96** as an off-white solid (1.34 g, 59%). Mpt. 138-140 °C. ^{1}H NMR (500 MHz, DMSO-d_6) δ = 3.68 (s, 2H, CH_2), 6.36 (br s, 1H, OH), 7.11-7.14 (m, 2H), 7.19-7.25 (m, 8H), 7.27-7.31 (m, 4H). ^{13}C NMR (125 MHz, DMSO-d_6) δ = 45.29, 80.43, 126.13, 126.55, 127.45, 127.52, 127.75, 142.49, 145.69, 147.92**.** HRMS (ESI+) calcd. for $C_{20}H_{20}NO$ $[M+H]^+$: 290.1539; found: 290.1536. Anal. calcd. for $C_{20}H_{19}NO$: C, 83.01; H, 6.62; N, 4.84. Found: C, 82.54; H, 6.52; N, 4.66.

5.2.5.56. *N*-(3-(Hydroxy(diphenyl)methyl)benzyl)acetamide (**97**).

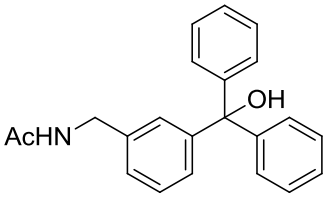

Acetic anhydride (97 µL, 1.02 mmol) was added to a solution of **95** (270 mg, 0.93 mmol) in anhydrous DMF (1.17 mL) and stirred at room temperature for 4 h. The reaction mixture was diluted with aqueous HCl (0.25 M, 5 mL) and extracted with CH_2Cl_2 (3 x 10 mL). The organic extracts were washed successively with saturated aqueous $NaHCO_3$ solution (20 mL), H_2O (2 x 20 mL) and brine (20 mL), dried (MgSO4), and concentrated *in vacuo* to afford amide **97** as a white solid (290 mg, 88%), which was used in the next step without further purification. Mpt. 170-172 °C. ^{1}H NMR (500 MHz, DMSO-d_6) δ = 1.81 (s, 3H, CH_3), 4.19 (d, J = 6.0 Hz, 2H, CH_2), 6.42 (s, 1H, OH), 7.01-7.03 (m, 1H), 7.11-7.13 (m, 1H), 7.17-7.32 (m, 12H), 8.29 (t, J = 6.0 Hz, 1H, NH). ^{13}C NMR (125 MHz, DMSO-d_6) δ = 22.48, 42.14, 80.51, 125.50, 126.36, 126.43, 126.61, 127.35, 127.48, 127.77, 147.75, 168.89. HRMS (ESI+) calcd. for $C_{22}H_{20}NO$ $[M\text{-}OH]^+$: 314.1539; found: 314.1538. Anal. calcd. for $C_{22}H_{21}NO_2 \cdot ¼H_2O$: C, 78.66; H, 6.45; N, 4.17. Found: C, 78.72; H, 6.23; N, 3.98.

5.2.5.57. *N*-(4-(Hydroxy(diphenyl)methyl)benzyl)acetamide (**98**).

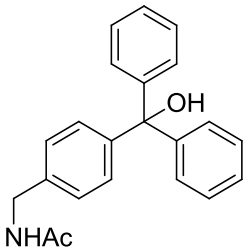

Acetic anhydride (104 µL, 1.1 mmol) was added to a solution of **96** (289 mg, 1.0 mmol) in anhydrous DMF (1.25 mL) and stirred at room temperature for 3 h. The reaction mixture was diluted with aqueous HCl (0.25 M, 10 mL) and extracted with CH_2Cl_2 (3 x 10 mL). The organic extracts were washed successively with saturated aqueous $NaHCO_3$ solution (30 mL), H_2O (2 x 30 mL) and brine (30 mL), dried (MgSO4), and concentrated *in vacuo* to afford amide **98** as a white solid (286 mg, 86%), which was taken to the next step without further purification. Mpt. 166-168.5 °C. ^{1}H NMR (500 MHz, DMSO-d_6) δ = 1.85 (s, 3H, CH_3), 4.22 (d, J = 6.0 Hz, 2H, CH_2), 6.39 (s, 1H, OH), 7.13-7.25 (m, 10H), 7.27-7.31 (m, 4H), 7.17-7.32 (m, 12H), 8.29 (t, J = 6.0 Hz, 1H, NH). ^{13}C NMR (125 MHz,

DMSO-d_6) δ = 22.53, 41.78, 80.39, 126.48, 126.61, 127.49, 127.68, 127.74, 137.82, 146.34, 147.78, 169.05. HRMS (ESI+) calcd. for $C_{22}H_{22}NO_2$ $[M+H]^+$: 332.1645; found: 332.1643. Anal. calcd. for $C_{22}H_{21}NO_2 \cdot ½H_2O$: C, 77.62; H, 6.51; N, 4.11. Found: C, 77.66; H, 6.42; N, 3.87.

5.2.5.58. (3-(Methylsulfonyl)phenyl)(diphenyl)methanol (**99**).

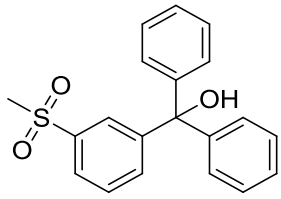

Intermediate sulfone **99** was prepared by adaptation of the procedure reported by Yeon Hwang *et al.*[264] *m*-CPBA (68% pure, 620 mg, 3.59 mmol) was added to a cooled (0 °C) solution of **52** (500 mg, 1.63 mmol) in anhydrous CH_2Cl_2 (4.26 mL) and stirred at the same temperature for 3 h. The reaction was poured into H_2O (10 mL) and extracted with CH_2Cl_2 (3 x 10 mL). The organic extracts were washed successively with saturated aqueous $NaHCO_3$ solution (3 x 30 mL), brine (30 mL), dried ($MgSO_4$), and concentrated *in vacuo*. Purification by flash chromatography [SiO_2; 10-75% EtOAc in hexane] afforded the sulfone **99** as a white solid (445 mg, 81%). Mpt. 143-146 °C. ^{1}H NMR (500 MHz, $CDCl_3$) δ = 3.02 (s, 3H, CH_3), 7.20-7.37 (m, 10H), 7.51 (t, *J* = 7.8 Hz, 1H), 7.58 (ddd, *J* = 1.2, 1.8, 7.8 Hz, 1H), 7.87 (ddd, *J* = 1.2, 1.8, 7.7 Hz, 1H), 8.06-8.07 (m, 1H). ^{13}C NMR (125 MHz, $CDCl_3$) δ = 44.58, 81.93, 126.27, 126.49, 128.01, 128.06, 128.52, 129.04, 133.51, 140.64, 146.14, 148.96. HRMS (ESI+) calcd. for $C_{20}H_{17}O_2S$ $[M-OH]^+$: 322.0944; found: 322.0941.

5.2.5.59. (4-(Methylsulfonyl)phenyl)(diphenyl)methanol (**100**).

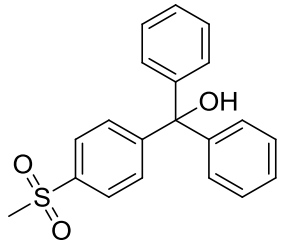

The title compound was prepared using an adaptation of the procedure for **99** with **57** (759 mg, 2.50 mmol) and *m*-CPBA (68% pure, 1.12 g, 4.41 mmol) in anhydrous CH_2Cl_2 (8 mL) for 7 h. Purification by flash chromatography [SiO_2; 10-100% EtOAc in hexane] afforded sulfone **100** as a white solid (395 mg, 58%). Mpt. 179-180 °C. ^{1}H NMR (500

MHz, DMSO-d_6) δ = 3.20 (s, 3H, CH_3), 6.72 (s, 1H, OH), 7.20-7.24 (m, 4H), 7.25-7.36 (m, 6H), 7.49-7.53 (m, 2H), 7.86-7.89 (m, 2H). ^{13}C NMR (125 MHz, DMSO-d_6) δ = 43.52, 80.41, 126.41, 127.02, 127.73, 127.79, 128.53, 139.14, 146.82, 153.37. HRMS (ESI+) calcd. for $C_{20}H_{17}O_2S$ $[M\text{-}OH]^+$: 322.0944; found: 322.0941. Anal. calcd. for $C_{20}H_{18}O_3S$: C, 70.98; H, 5.36. Found: C, 70.35; H, 5.39.

5.2.5.60. 2-(Tritylsulfanyl)ethanamine (**16**).

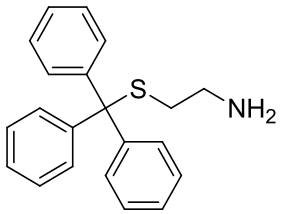

The title compound was prepared following general procedure (iii) with triphenylmethanol (1.95 g, 7.5 mmol) and cysteamine hydrochloride (937 mg, 8.25 mmol) in trifluoroacetic acid (7.5 mL). Purification by flash chromatography [SiO_2; 0-16% MeOH in CH_2Cl_2 with 1% NH_4OH] afforded the thioether **16** as a white solid (1.94 g, 81%). Mpt. 87-90 °C [lit 90-93°C from petroleum ether (40/60)].[265] ^{1}H NMR (500 MHz, MeOD) δ = 2.32-2.36 (m, 2H, CH_2), 2.41-2.45 (m, 2H, CH_2), 7.19-7.24 (m, 3H), 7.25-7.31 (m, 6H), 7.39-7.41 (m, 6H). ^{13}C NMR (125 MHz, MeOD) δ = 36.11, 41.56, 67.77, 127.79, 128.89, 130.78, 146.34. HRMS (ESI+) calcd. for $C_{21}H_{22}NS$ $[M+H]^+$: 320.1467; found: 320.1466. Anal. calcd. for $C_{21}H_{21}NS$: C, 78.95; H, 6.63; N, 4.38. Found: C, 78.96; H, 6.63; N, 4.20.

5.2.5.61. (2*R*)-2-Amino-3-(((2-chloroxyphenyl)(diphenyl)methyl)sulfanyl)propanoic acid (**101**).

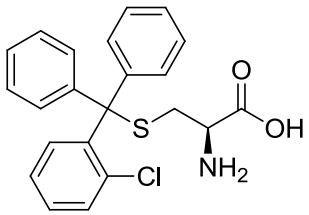

The title compound was then prepared by an adaptation of the procedure reported by DeBonis *et al.*[130] To a solution of **30** (325 mg, 1.1 mmol) and L-cysteine (121 mg, 1 mmol) in AcOH (1 mL) was added $BF_3{\cdot}Et_2O$ solution (214 µL, 1.70 mmol) and stirred for 3 h at room temperature. A solution of aqueous NaOAc (10% *w/v*, 3 mL) was added, followed by H_2O (3 mL), and the solution extracted with EtOAc (3 x 10 mL). The combined organic extracts were dried ($MgSO_4$), concentrated *in vacuo* and the crude residue purified by flash chromatography [SiO_2; 10-20% MeOH in (CH_2Cl_2 with 1%

NH_4OH)] to give **101** as a white solid (117 mg, 29%). Mpt. 159-161 °C. ^{1}H NMR (500 MHz, DMSO-d_6) δ = 2.24-2.29 (dd, J = 8.8, 12.4 Hz, 1H, CH_2), 2.24-2.29 (dd, J = 4.5, 12.4 Hz, CH_2), 2.37-2.41 (dd, J = 4.5, 8.7 Hz, 1H, CH_2), 2.91-2.94 (m, 1H, CH), 7.21-7.26 (m, 2H), 7.30-7.39 (m, 10H), 7.47-7.50 (m, 1H), 8.12-8.13 (m, 1H). ^{13}C NMR (125 MHz, DMSO-d_6) δ = 34.51, 53.18, 66.60, 126.73, 126.75, 127.30, 127.72, 127.80, 129.26, 129.40, 131.81, 131.99, 134.26, 140.00, 140.83, 141.32, 168.74. HRMS (ESI+) calcd. for $C_{22}H_{21}ClNO_2S$ $[M+H]^+$: 398.09761; found: 398.09760. Anal. calcd. for $C_{22}H_{20}ClNO_2S{\cdot}H_2O$: C, 63.53; H, 5.33; N, 3.37. Found: C, 63.24; H, 5.28; N, 3.60.

5.2.5.62. 2-(((3-Fluorophenyl)(diphenyl)methyl)sulfanyl)ethanamine (**102**).

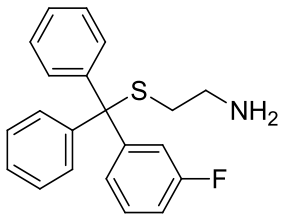

The title compound was prepared using general procedure (iii) with **31** (278 mg, 1 mmol) and cysteamine hydrochloride (114 mg, 1 mmol) in trifluoroacetic acid (1 mL) with the following modifications. Basification of the crude residue (*circa* pH 9) was performed with aqueous NaOH (1.0 M) and EtOAc was used for extraction of the aqueous mixture (3 x 10mL). Purification by flash chromatography [SiO_2; 0-18% MeOH in CH_2Cl_2 with 1% NH_4OH] afforded the amine **102** as a white solid (79 mg, 24%). Mpt. 62-63 °C. ^{1}H NMR (500 MHz, DMSO-d_6) δ = 2.14-2.18 (m, 2H, CH_2), 2.42-2.46 (m, 2H, CH_2), 7.06-7.17 (m, 3H), 7.24-7.29 (m, 2H), 7.31-7.41 (m, 9H). ^{13}C NMR (125 MHz, DMSO-d_6) δ = 35.65, 40.78, 65.35, 113.57 (d, J = 20.6 Hz), 115.78 (d, J = 23.0 Hz), 125.37, 126.85, 128.09, 129.00, 129.91 (d, J = 8.3 Hz), 144.12, 147.66 (d, J = 6.4 Hz), 161.7 (d, J = 242.7 Hz). HRMS (ESI+) calcd. for $C_{21}H_{21}NFS$ $[M+H]^+$: 338.13733; found: 338.13739. Anal. calcd. for $C_{21}H_{20}FNS$: C, 74.74; H, 5.97; N 4.15. Found: C, 74.29; H, 5.92; N, 4.15.

5.2.5.63. (2*R*)-2-Amino-3-(((3-chloroxyphenyl)(diphenyl)methyl)sulfanyl)propanoic acid (**103**).

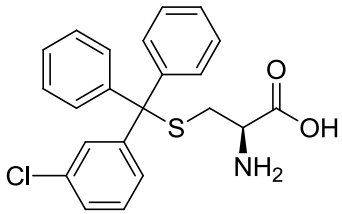

In a procedure analogous to **101**, the trityl alcohol **32** (325 mg, 1.1 mmol) and L-cysteine (121 mg, 1 mmol) in AcOH (1 mL) was treated with $BF_3{\cdot}Et_2O$ (214 µl, 1.70 mmol). After stirring for 1 h a further portion of $BF_3.Et_2O$ (214 µl, 1.70 mmol) was added and the mixture stirred for a further 1.5 h. Aqueous workup and purification by flash chromatography [SiO_2; 8-20% MeOH in CH_2Cl_2 with 1% NH_4OH] afforded **103** as an off-white solid (74 mg, 19%). Mpt. 160-163 °C. ^{1}H NMR (500 MHz, DMSO-d_6) δ = 2.43 (dd, J = 8.6, 12.4 Hz, 1H, CH_2), 2.56 (dd, J = 4.6, 12.4 Hz, 1H, CH_2), 3.01 (dd, J = 4.7, 8.6 Hz, 1H, CH), 7.26-7.40 (m, 14H). ^{13}C NMR (125 MHz, DMSO-d_6) δ = 34.41, 53.25, 65.62, 126.91, 127.04, 127.93, 128.27, 128.67, 129.03, 130.01, 132.78, 143.52, 143.55, 146.87, 168.37. HRMS (ESI+) calcd. for $C_{22}H_{21}ClNO_2S$ $[M+H]^+$: 398.09761; found: 398.09827. Anal. calcd. for $C_{22}H_{20}ClNO_2S{\cdot}⅓CH_2Cl_2$: C, 62.97; H, 4.89; N, 3.29. Found: C, 62.87; H, 4.80; N, 3.31.

5.2.5.64. 2-(((3-Chlorophenyl)(diphenyl)methyl)sulfanyl)ethanamine (**104**).

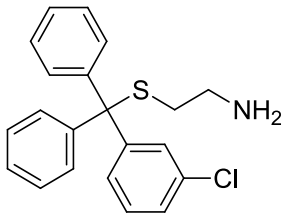

The title compound was prepared using general procedure (iii) with **32** (295 mg, 1 mmol) and cysteamine hydrochloride (125 mg, 1.1 mmol) in trifluoroacetic acid (1 mL) with the following modifications. Basification of the crude residue (*circa* pH 9) was performed with aqueous NaOH (1.0 M) and EtOAc was used for extraction of the aqueous mixture (3 x 10mL). Purification by flash chromatography [SiO_2; 0-18% MeOH in CH_2Cl_2 with 1% NH_4OH] afforded the amine **104** as a colorless oil (231 mg, 65%). ^{1}H NMR (MeOD, 500 MHz) 2.33-2.36 (m, 2H, CH_2), 2.45-2.48 (m, 2H, CH_2), 7.23-7.36 (m, 3H), 7.28-7.36 (m, 6H), 7.39-7.41 (m, 5H). ^{13}C NMR (MeOD, 125 MHz) δ 36.00, 41.50, 67.35, 127.91, 128.10, 129.11, 129.19, 130.44, 130.63, 130.67, 134.93, 145.64, 148.84. HRMS (ESI+)

calcd. for $C_{21}H_{21}ClNS$ $[M+H]^+$: 354.10777; found: 354.10754. Anal. calcd. for $C_{21}H_{20}ClNS \cdot ⅕H_2O$: C, 70.09; H, 5.79; N, 3.89. Found: C, 70.39; H, 5.86; N, 3.51.

5.2.5.65. 2-(((3-Bromophenyl)(diphenyl)methyl)sulfanyl)ethanamine (**105**).

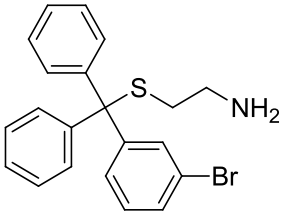

The title compound was prepared using general procedure (iii) with **33** (339 mg, 1 mmol) and cysteamine hydrochloride (136 mg, 1.2 mmol) in trifluoroacetic acid (1 mL) with the following modifications. Basification of the crude residue (*circa* pH 9) was performed with aqueous NaOH (1.0 M) and EtOAc was used for extraction of the aqueous mixture (3 x 10 mL). Purification by flash chromatography [SiO_2; 0-18% MeOH in CH_2Cl_2 with 1% NH_4OH] afforded the amine **105** as a colorless oil which solidified on standing to a white solid (192 mg, 48%). Mpt. 59-61 °C. ^{1}H NMR (500 MHz, DMSO-d_6) δ = 2.16 (t, J = 7.0 Hz, 2H, CH_2), 2.45 (t, J = 7.1 Hz, 2H, CH_2), 7.24-7.37 (m, 12H), 7.45-7.47 (m, 2H). ^{13}C NMR (125 MHz, DMSO-d_6) δ = 35.64, 40.78, 65.33, 121.29, 126.89, 128.14, 128.31, 128.98, 129.62, 130.17, 131.50, 143.98, 147.50. HRMS (ESI+) calcd. for $C_{21}H_{21}BrNS$ $[M+H]^+$: 398.05726; found: 398.05716. Anal. calcd. for $C_{21}H_{20}BrNS$: C, 63.32; H, 5.06; N, 3.52. Found: C, 63.36; H, 4.96; N, 3.44.

5.2.5.66. 2-(((3-Methylphenyl)(diphenyl)methyl)sulfanyl)ethanamine (**106**).

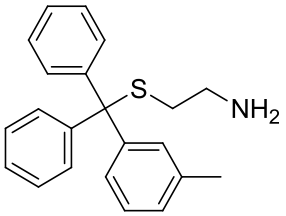

The title compound was prepared following general procedure (iii) **34** (275 mg, 1 mmol) and cysteamine hydrochloride (136 mg, 1.2 mmol) in trifluoroacetic acid (1 mL) with the following modifications. Basification of the crude residue (*circa* pH 9) was performed with aqueous NaOH (1.0 M) and EtOAc was used for extraction (3 x 10mL). Purification by flash chromatography [SiO_2; 0-18% MeOH in CH_2Cl_2 with 1% NH_4OH] afforded the amine **106** as a colorless oil (184 mg, 55%). ^{1}H NMR (500 MHz, DMSO-d_6) δ = 2.15 (t, J = 7.2 Hz, 2H, CH_2), 2.25 (s, 3H, CH_3), 2.43 (t, J = 7.1 Hz, 2H, CH_2), 7.04-7.06 (m, 1H),

7.09-7.11 (m, 1H), 7.17-7.25 (m, 4H), 7.31-7.34 (m, 8H). ^{13}C NMR (125 MHz, DMSO-d_6) δ = 21.24, 35.62, 40.82, 65.74, 126.27, 126.56, 127.28, 127.80, 127.89, 129.13, 129.51, 136.94, 144.69, 144. 76. HRMS (ESI+) calcd. for $C_{22}H_{24}NS$ $[M+H]^+$: 334.16240; found: 334.16226. Anal. calcd. for $C_{22}H_{23}NS \cdot ⅕H_2O$: C, 78.39; H, 7.00; N, 4.16. Found: C, 78.38; H, 6.65; N, 3.95.

5.2.5.67. 2-(((3-Ethylphenyl)(diphenyl)methyl)sulfanyl)ethanamine (**107**).

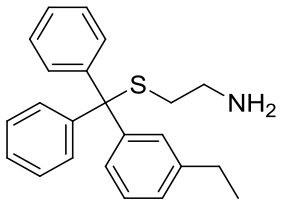

The title compound was prepared following general procedure (iii) with **47** (298 mg, 1 mmol) and cysteamine hydrochloride (129 mg, 1.1 mmol) in trifluoroacetic acid (1 mL) with the following modifications. The reaction time was 2 h, basification of the crude residue (*circa* pH 9) was performed with aqueous NaOH (1.0 M) and EtOAc was used for extraction (3 x 10 mL). Purification by flash chromatography [SiO_2; 0-18% MeOH in CH_2Cl_2 with 1% NH_4OH] afforded the amine **107** a colorless oil (157 mg, 44%). ^{1}H NMR (500 MHz, DMSO-d_6) δ = 1.11 (t, J = 7.5 Hz, 3H, CH_3), 2.16 (t, J = 7.1 Hz, 2H, CH_2), 2.42 (t, J = 7.1 Hz, 2H, CH_2), 2.54 (q, J = 7.5 Hz, 2H, CH_2), 7.07-7.10 (m, 2H), 7.21-7.25 (m, 4H), 7.30-7.34 (m, 8H). ^{13}C NMR (125 MHz, DMSO-d_6) δ = 15.52, 28.23, 35.66, 40.85, 65.83, 126.02, 126.57, 127.88, 128.48, 129.12, 143.23, 144.68, 144.75. HRMS (ESI+) calcd. for $C_{23}H_{26}NS$ $[M+H]^+$: 348.17805; found: 348.17786. Anal. calcd. for $C_{23}H_{25}NS \cdot ⅕H_2O$: C, 78.73; H, 7.35; N, 3.96. Found: C, 78.90; H, 7.10; N, 3.70.

5.2.5.68. 2-(((3-(Propan-2-yl)phenyl)diphenylmethyl)sulfanyl)ethanamine (**108**).

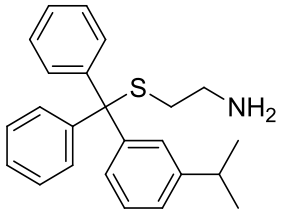

The title compound was prepared following general procedure (iii) with **48** (302 mg, 1 mmol) and cysteamine hydrochloride (125 mg, 1.1 mmol) in trifluoroacetic acid (1 mL) with the following modifications. The reaction time was 2 h, basification of the crude residue (*circa* pH 9) was performed with aqueous NaOH (1.0 M) and EtOAc was used for extraction (3 x 10 mL). Purification by flash chromatography [SiO_2; 0-18% MeOH in CH_2Cl_2 with 1% NH_4OH] afforded the amine **108** as a colorless oil (249 mg, 69%). ^{1}H NMR (500 MHz, DMSO-d_6) δ = 1.13 (d, J = 6.9 Hz, 6H, 2 x CH_3), 2.17 (t, J = 7.0 Hz, 2H, CH_2), 2.42 (t, J = 7.0 Hz, 2H, CH_2), 2.81 (p, J = 6.9 Hz, 1H, CH), 7.06-7.08 (m, 1H), 7.11-7.12 (m, 1H), 7.21-7.26 (m, 4H), 7.31-7.33 (m, 8H). ^{13}C NMR (125 MHz, DMSO-d_6) δ = 23.78, 33.36, 35.68, 40.87, 65.92, 124.44, 126.57, 126.74, 127.26, 127.82, 127.88, 129.09, 144.48, 144.82. HRMS (ESI+) calcd. for $C_{22}H_{28}NS$ $[M+H]^+$: 362.19370; found: 362.19351. Anal. calcd. for $C_{24}H_{27}NS{\cdot}¼H_2O$: C, 78.75; H, 7.57; N, 3.83. Found: C, 78.63; H, 7.42; N, 3.59.

5.2.5.69. 2-(((3-Propylphenyl)(diphenyl)methyl)sulfanyl)ethanamine (**109**).

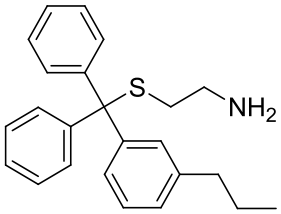

The title compound was prepared following general procedure (iii) with **49** (302 mg, 1 mmol) and cysteamine hydrochloride (125 mg, 1.1 mmol) in trifluoroacetic acid (1 mL) with the following modifications. Basification of the crude residue (*circa* pH 9) was performed with aqueous NaOH (1.0 M) and EtOAc was used for extraction (3 x 10 mL). Purification by flash chromatography [SiO_2; 0-18% MeOH in CH_2Cl_2 with 1% NH_4OH] afforded the thioether **109** as a pale clear yellow oil (227 mg, 63%). ^{1}H NMR (MeOD, 500 MHz) δ = 0.87 (t, J = 7.4 Hz, 3H, CH_3), 1.56 (p, J = 7.4 Hz, 2H, CH_2), 2.33-2.36 (m, 2H, CH_2), 2.41-2.44 (m, 2H, CH_2), 2.51 (t, J = 7.5 Hz, 2H, CH_2), 7.03-7.05 (m, 1H), 7.16-7.24 (m, 9H), 7.40-7.42 (m, 4H). ^{13}C NMR (MeOD, 125 MHz) δ 13.96, 25.69, 36.00, 39.04,

41.55, 67.83, 127.75, 127.94, 128.16, 128.78, 128.85, 130.77, 131.06, 143.06, 146.17, 146.42. HRMS (ESI+) calcd. for $C_{24}H_{28}NS$ $[M+H]^+$: 362.19370; found: 362.19293. Anal. calcd. for $C_{24}H_{27}NS \cdot ¼H_2O$: C, 78.75; H, 7.57; N, 3.83. Found: C, 78.64; H, 7.31; N, 3.95.

5.2.5.70. 2-((Diphenyl(3-(trifluoromethyl)phenyl)methyl)sulfanyl)ethanamine (**110**).

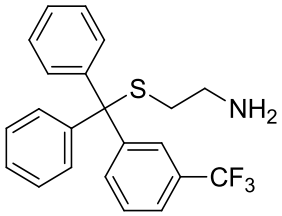

The title compound was prepared following general procedure (iii) with **35** (298 mg, 1 mmol) and cysteamine hydrochloride (125 mg, 1.1 mmol) in trifluoroacetic acid (1 mL) with the following modifications. The reaction time was 2 h, basification of the crude residue (*circa* pH 9) was performed with aqueous NaOH (1.0 M) and EtOAc was used for extraction (3 x 10 mL). Purification by flash chromatography [SiO_2; 0-18% MeOH in CH_2Cl_2 with 1% NH_4OH] afforded the amine **110** as a colorless oil (125 mg, 32%). ^{1}H NMR (500 MHz, DMSO-d_6) δ = 2.16 (t, J = 7.0 Hz, 2H, CH_2), 2.44 (t, J = 7.0 Hz, 2H, CH_2), 7.26-7.29 (m, 2H), 7.32-7.38 (m, 8H), 7.57-7.66 (m, 4H). ^{13}C NMR (125 MHz, DMSO-d_6) δ = 35.61, 40.77, 65.46, 123.63 (q, J_{CF} = 3.7 Hz, CH), 124.08 (q, J_{CF} = 271.8 Hz), 125.06 (q, J_{CF} = 3.6 Hz, CH), 127.00, 128.24, 128.68 (q, J_{CF} = 31.2 Hz), 128.95, 129.26, 133.43, 143.91, 146.12. ^{19}F NMR (376.5 MHz, DMSO-d_6) δ = -61.18. HRMS (ESI+) calcd. for $C_{22}H_{21}NF_3S$ $[M+H]^+$: 388.13413; found: 388.13388. Anal. calcd. for $C_{22}H_{20}F_3NS$: C, 68.20; H, 5.20; N, 3.61. Found: C, 67.97; H, 5.41; N, 2.87.

5.2.5.71. 2-(((3-Methoxyphenyl)(diphenyl)methyl)sulfanyl)ethanamine (**111**).

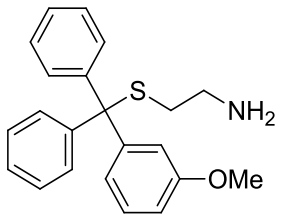

The title compound was prepared following general procedure (iii) with **44** (290 mg, 1 mmol and cysteamine hydrochloride (114 mg, 1 mmol) in trifluoroacetic acid (1 mL) with the following modifications. The reaction time was 2.5 h, basification of the crude residue (*circa* pH 9) was performed with aqueous NaOH (1.0 M) and EtOAc was used for extraction (3 x 10mL). Purification by flash chromatography [SiO_2; 0-18% MeOH in

CH_2Cl_2 with 1% NH_4OH] afforded the thioether **111** as a pale brown oil (282 mg, 81%). ^{1}H NMR (500 MHz, DMSO-d_6) δ = 2.18 (t, J = 7.0 Hz, 2H, CH_2), 2.45 (t, J = 7.1 Hz, 2H, CH_2), 6.81-6.90 (m, 3H), 7.22-7.35 (m, 11H). ^{13}C NMR (125 MHz, DMSO-d_6) δ = 35.47, 40.74, 54.96, 65.70, 111.23, 115.66, 121.62, 126.66, 127.92, 129.02, 129.10, 144.53, 146.23, 158.73. HRMS (ESI+) calcd. for $C_{22}H_{24}NOS$ $[M+H]^+$: 350.15731; found: 350.15817. Anal. calcd. for $C_{22}H_{23}NOS{\cdot}¼H_2O$: C, 74.65; H, 6.71; N, 3.94. Found: C, 74.69; H, 6.69; N, 3.96.

5.2.5.72. 2-(((3-(Methylsulfanyl)phenyl)diphenylmethyl)sulfanyl)ethanamine (**112**).

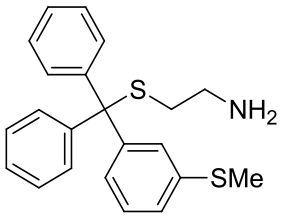

The title compound was prepared following general procedure (iii) with **52** (306 mg, 1 mmol) and cysteamine hydrochloride (125 mg, 1.1 mmol) in trifluoroacetic acid (1 mL) with the following modifications. The reaction time was 2 h, basification of the crude residue (*circa* pH 9) was performed with aqueous NaOH (1.0 M) and EtOAc was used for extraction (3 x 10 mL). Purification by flash chromatography [SiO_2; 0-18% MeOH in CH_2Cl_2 with 1% NH_4OH] afforded the thioether **112** as a clear pale yellow oil (280 mg, 77%). ^{1}H NMR (500 MHz, MeOD) δ = 2.33-2.37 (m, 5H), 2.43-2.46 (m, 2H, CH_2), 7.11-7.13 (m, 1H), 7.15-7.18 (m, 1H), 7.20-7.24 (m, 3H), 7.27-7.32 (m, 5H), 7.39-7.42 (m, 4H). ^{13}C NMR (125 MHz, MeOD) δ = 15.67, 36.11, 41.57, 67.69, 125.80, 127.58, 127.92, 128.80, 128.96, 129.39, 130.74, 139.83, 146.04, 147.08. HRMS (ESI+) calcd. for $C_{22}H_{24}NS_2$ $[M+H]^+$: 366.13447; found: 366.13452. Anal. calcd. for $C_{22}H_{23}NS_2$: C, 72.78; H, 6.34; N, 3.83. Found: C, 72.28; H, 6.29; N, 3.44.

5.2.5.73. 2-((Diphenyl(3-(trifluoromethoxy)phenyl)methyl)sulfanyl)ethanamine (**113**).

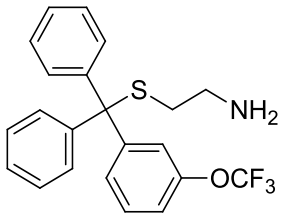

The title compound was prepared following general procedure (iii) with **51** (344 mg, 1 mmol) and cysteamine hydrochloride (125 mg, 1.1 mmol) in trifluoroacetic acid (1 mL) with the following modifications. Basification of the crude residue (*circa* pH 9) was performed with aqueous NaOH (1.0M) and EtOAc was used for extraction (3 x 10 mL). Purification by flash chromatography [SiO_2; 0-18% MeOH in CH_2Cl_2 with 1% NH_4OH] afforded the thioether **113** as a pale clear yellow oil (313 mg, 78%). ^{1}H NMR (500 MHz, DMSO-d_6) δ = 2.17 (t, J = 7.0 Hz, 2H, CH_2), 2.43 (t, J = 7.0 Hz, 2H, CH_2), 7.24-7.29 (m, 4H), 7.31-7.39 (m, 9H), 7.48 (t, J = 8.0 Hz, 1H). ^{13}C NMR (125 MHz, DMSO-d_6) δ = 35.61, 40.77, 65.32, 119.12, 120.03 (q, J_{CF} = 257.7 Hz), 121.45, 126.95, 128.17, 128.32, 128.92, 129.96, 143.96, 147.44, 147.92. ^{19}F NMR (376.5 MHz, DMSO-d_6) δ = -56.87. HRMS (ESI+) calcd. for $C_{22}H_{21}F_3NS$ $[M+H]^+$: 404.12905; found: 404.12881. Anal. calcd. for $C_{22}H_{20}F_3NOS{\cdot}½H_2O$: C, 64.06; H, 5.13; N, 3.40. Found: C, 64.61; H, 4.91; N, 2.90.

5.2.5.74. (*R*)-3-(((3-Acetylphenyl)diphenylmethyl)sulfanyl)-2-aminopropanoic acid (**114**).

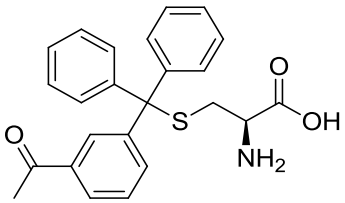

A solution of **50** (346 mg, 1.0 mmol) and L-cysteine (133 mg, 1.1 mmol) in (1 mL) was stirred at room temperature for 4.5 h. The volatiles were removed *in vacuo*, and the residue suspended in aqueous HCl (0.5 M, 2.5 mL) and stirred at room temperature for 2.5 h, during which time a colourless gum precipitated. The aqueous layer was poured off, and the gum washed with H_2O (10 mL). The combined aqueous layers were extracted with CH_2Cl_2 (3 x 10 mL), the gum dissolved in CH_2Cl_2 (5 mL), and the combined organic extracts concentrated *in vacuo*. Purification by flash chromatography [SiO_2; 0-20% MeOH in CH_2Cl_2] afforded the thioether **114** as a white solid (290 mg, 72%). Mpt. 109.5-112 °C. ^{1}H NMR (400 MHz, MeOD) δ = 2.54 (s, 3H, CH_3), 2.68 (dd, J = 9.1, 13.3 Hz, 1H, CH_2), 2.80 (dd, J = 4.2, 13.2 Hz, 1H, CH_2), 3.09 (dd, J = 4.2, 9.0 Hz, 1H, CH), 7.24-7.29 (m,

2H), 7.31-7.37 (m, 4H), 7.43-7.50 (m, 5H), 7.70-7.73 (m, 1H), 7.89-7.92 (m, 1H), 8.08-8.09 (m, 1H). ^{13}C NMR (125 MHz, MeOD) δ = 26.76, 34.09, 54.96, 67.95, 128.32, 129.38, 129.69, 130.11, 130.65, 135.54, 138.19, 145.09, 145.19, 146.54, 172.06, 200.11. HRMS (ESI+) Calcd. for $C_{24}H_{24}NO_3S$ $[M+H]^+$: 406.1471; found: 406.1466. Anal. calcd. for $C_{24}H_{23}NO_3S{\cdot}H_2O$: C, 68.06; H, 5.95; N, 3.32. Found: C, 68.32; H, 5.55; N, 3.02.

5.2.5.75. 1-(3-(((2-Aminoethyl)thio)diphenylmethyl)phenyl)ethanone hydrochloride (**115**).

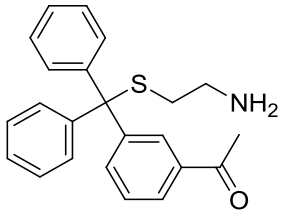

A solution of the tertiary alcohol **50** (346 mg, 1.0 mmol) with cysteamine hydrochloride (125 mg, 1.1 mmol) in trifluoroacetic acid (1 mL) was stirred for 3 h at room temperature. The volatiles were removed *in vacuo*, and the crude basified (*circa.* pH 10) with saturated aqueous sodium carbonate solution. The aqueous mixture was extracted with CH_2Cl_2 (3 x 10 mL) and the organic layer dried ($MgSO_4$) and concentrated *in vacuo*. The crude residue was suspended in aqueous HCl (1.0 M, 30 mL), stirred at room temperature for 62 h, basified (*circa.* pH 10) with saturated aqueous sodium carbonate solution and extracted with CH_2Cl_2 (3 x 50 mL). The organic extracts were dried ($MgSO_4$) and concentrated *in vacuo*. Purification by flash chromatography [SiO_2; 0-15% MeOH in CH_2Cl_2 with 1% NH_4OH] yielded a white solid, which to generate the hydrochloride salt, was suspended in aqueous HCl (1.0 M, 10 mL) and stirred at room temperature for 65 h. A white precipitate formed, which was filtered and washed successively with aqueous HCl (1.0 M), petroleum ether (60/80) and Et_2O, and dried *in vacuo* to yield the hydrochloride salt **25** as a white solid (122 mg, 31%). Mpt. 96-98 °C. ^{1}H NMR (400 MHz, DMSO-d_6) δ = 2.40-2.44 (m, 2H, CH_2), 2.51-2.58 (m, 5H), 7.28-7.41 (m, 10H), 7.52-7.60 (m, 2H), 7.80 (br s, 3H, NH_3^+), 7.92-7.95 (m, 2H). ^{13}C NMR (125 MHz, DMSO-d_6) δ = 26.76, 28.39, 37.63, 66.26, 127.14, 127.55, 127.73, 128.37, 128.79, 128.97, 133.83, 136.56, 143.55, 144.69, 197.60. HRMS (ESI+) Calcd. for $C_{23}H_{24}NOS$ $[M+H]^+$: 362.1573; found: 362.1572. Anal. calcd. for $C_{23}H_{23}NOS{\cdot}1.5$ HCl: C, 66.38; H, 5.93; N, 3.37. Found: C, 66.31; H, 5.90; N, 3.24.

5.2.5.76. 2-(((4-Methylphenyl)(diphenyl)methyl)sulfanyl)ethanamine (**116**).

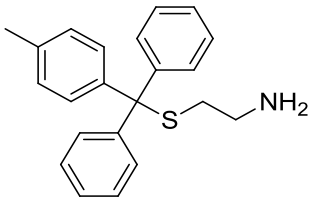

The title compound was prepared following general procedure (iii) with **53** (274 mg, 1.0 mmol) and cysteamine hydrochloride (125 mg, 1.1 mmol) in trifluoroacetic acid (1 mL). Purification by flash chromatography [SiO_2; 0-12% MeOH in CH_2Cl_2 with 1% NH_4OH] afforded the thioether **116** as a white solid (229 mg, 69%). Mpt. 72-74 °C. ^{1}H NMR (400 MHz, MeOD) δ = 2.28-2.36 (m, 5H), 2.40-2.45 (m, 2H, CH_2), 7.07-7.11 (m, 2H), 7.17-7.22 (m, 2H), 7.23-7.29 (m, 6H), 7.37-7.42 (m, 4H). ^{13}C NMR (100 MHz, MeOD) δ = 20.93, 36.13, 41.57, 67.54, 127.70, 128.84, 129.48, 130.73, 137.59, 143.31, 146.52. HRMS (ESI+) calcd. for $C_{22}H_{24}NS$ $[M+H]^+$: 334.1624; found: 334.1624. Anal. calcd. for $C_{22}H_{23}NS$: C, 79.23; H, 6.95; N, 4.13. Found: C, 78.84; H, 7.03; N, 4.13.

5.2.5.77. 2-(((4-Methylphenyl)(diphenyl)methyl)sulfanyl)ethanamine (**117**).

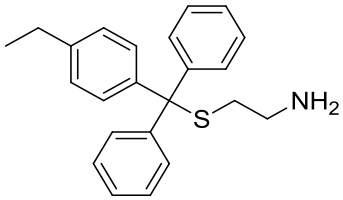

The title compound was prepared following general procedure (iii) with **36** (288 mg, 1.0 mmol) and cysteamine hydrochloride (125 mg, 1.1 mmol) in trifluoroacetic acid (1 mL). Purification by flash chromatography [SiO_2; 0-12% MeOH in CH_2Cl_2 with 1% NH_4OH] afforded the thioether **117** as a colourless oil (296 mg, 85%). 1H NMR (500 MHz, MeOD) δ = 1.22 (t, J = 7.6 Hz, 3H, CH_3), 2.32-2.36 (m, 2H, CH_2), 2.41-2.46 (m, 2H, CH_2), 2.62 (q, J = 7.6 Hz, 2H, CH_2), 7.10-7.14 (m, 2H), 7.18-7.22 (m, 2H), 7.25-7.32 (m, 6H), 7.39-7.43 (m, 4H). 13C NMR (125 MHz, MeOD) δ = 16.02, 29.29, 36.12, 41.58, 67.57, 127.71, 128.30, 128.84, 130.75, 130.79, 143.58, 144.06, 146.54. HRMS (ESI+) calcd. for $C_{23}H_{26}NS$ $[M+H]^+$: 348.1780; found: 348.1775. Anal. calcd. for $C_{23}H_{25}NS \cdot ⅓H_2O$: C, 78.16; H, 7.32; N, 3.96. Found: C, 78.11; H, 7.03; N, 3.66.

5.2.5.78. 2-(((4-Methoxyphenyl)(diphenyl)methyl)sulfanyl)ethanamine (**118**).

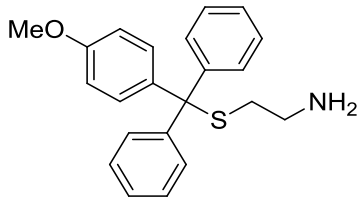

The title compound was prepared following general procedure (iii) with (4-methoxyphenyl)(diphenyl)methanol (291 mg, 1.0 mmol) and cysteamine hydrochloride (125 mg, 1.1 mmol) in trifluoroacetic acid (1 mL). Purification by flash chromatography [SiO_2; 0-15% MeOH in CH_2Cl_2] afforded the thioether **118** as a colourless oil (63 mg, 18%). ^{1}H NMR (500 MHz, MeOD) δ = 2.32-2.36 (m, 2H, CH_2), 2.41-2.45 (m, 2H, CH_2), 3.77 (s, 3H, CH_3), 6.81-6.84 (m, 2H), 7.17-7.21 (m, 2H), 7.24-7.31 (m, 6H), 7.38-7.42 (m, 4H). ^{13}C NMR (125 MHz, MeOD) δ = 36.14, 41.60, 55.72, 67.33, 114.13, 127.70, 128.86, 130.67, 131.99, 138.21, 146.70, 159.78. HRMS (ESI+) calcd. for $C_{22}H_{24}NOS$ $[M+H]^+$: 350.1573; found: 350.1565. Anal. calcd. for $C_{22}H_{23}NOS$: C, 75.61; H, 6.63; N, 4.01. Found: C, 74.77; H, 6.22; N, 3.19.

5.2.5.79. 2-(((4-Ethoxyphenyl)(diphenyl)methyl)sulfanyl)ethanamine (**119**).

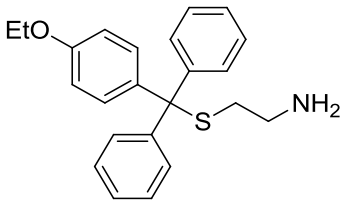

The title compound was prepared following general procedure (iii) with **55** (305 mg, 1.0 mmol) and cysteamine hydrochloride (125 mg, 1.1 mmol) in trifluoroacetic acid (1 mL). Purification by flash chromatography [SiO_2; 0-15% MeOH in CH_2Cl_2 with NH_4OH] afforded the thioether **119** as a clear pale brown oil (209 mg, 58%). ^{1}H NMR (500 MHz, MeOD) δ = 1.37 (t, 3H, J = 7.0 Hz, CH_3), 2.32-2.37 (m, 2H, CH_2), 2.41-2.45 (m, 2H, CH_2), 4.01 (q, 2H, J = 7.0 Hz, CH_2), 6.79-6.84 (m, 2H), 7.17-7.22 (m, 2H), 7.24-7.30 (m, 6H), 7.38-7.42 (m, 4H). ^{13}C NMR (125 MHz, MeOD) δ = 15.15, 36.13, 41.60, 64.50, 67.34, 114.67, 127.69, 128.85, 130.67, 131.98, 138.09, 146.72, 159.07. HRMS (ESI+) calcd. for $C_{23}H_{26}NOS$ $[M+H]^+$: 364.1730; found: 364.1727. Anal. calcd. for $C_{23}H_{26}NOS{\cdot}½H_2O$: C, 74.56; H, 6.53; N, 3.78. Found: C, 74.48; H, 6.93; N, 4.18.

5.2.5.80. 2-((Diphenyl(4-(trifluoromethoxy)phenyl)methyl)sulfanyl)ethanamine (**120**).

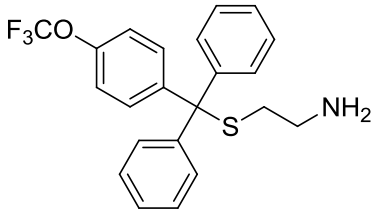

The title compound was prepared following general procedure (iii) with **56** (344 mg, 1.0 mmol) and cysteamine hydrochloride (125 mg, 1.1 mmol) in trifluoroacetic acid (1 mL). Purification by flash chromatography [SiO_2; 0-15% MeOH in CH_2Cl_2 with NH_4OH] afforded the thioether **120** as a colourless oil (145 mg, 36%). ^{1}H NMR (400 MHz, MeOD) δ = 2.34 (t, 2H, *J* = 6.9 Hz), 2.46 (t, 2H, *J* = 6.9 Hz), 7.17-7.34 (m, 8H), 7.35-7.44 (m, 4H), 7.50-7.54 (m, 2H). ^{19}F NMR (376.5 MHz, MeOD) δ = -59.42. ^{13}C NMR (100 MHz, MeOD) δ = 36.01, 41.48, 67.17, 121.25, 121.92 (q, J_{CF} = 255.4 Hz), 123.18, 128.05, 129.11, 130.66, 132.44, 145.60, 145.85, 149.04. HRMS (ESI+) calcd. for $C_{22}H_{21}F_3NOS$ $[M+H]^+$: 404.1290; found: 404.1291. Anal. calcd. for $C_{22}H_{20}F_3NOS$: C, 65.49; H, 5.00; N, 3.47. Found: C, 65.44; H, 5.04; N, 3.95.

5.2.5.81. (*R*)-3-(((4-Acetylphenyl)diphenylmethyl)sulfanyl)2-aminopropanoic acid (**121**).

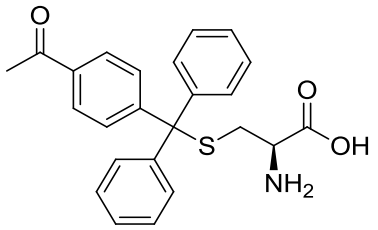

A solution of **54** (346 mg, 1.0 mmol) and L-cysteine (133 mg, 1.1 mmol) in trifluoroacetic acid (1 mL) was stirred at room temperature for 4 h. The volatiles were removed *in vacuo*, and the residue suspended in aqueous HCl (0.5 M, 2.5 mL) and stirred at room temperature for 30 min, during which time a white gum precipitated. The aqueous layer was separated, and extracted with CH_2Cl_2 (3 x 5 mL). The precipitated gum was washed with H_2O (5 mL), dissolved in CH_2Cl_2 (5 mL), and combined with the combined organic extracts concentrated *in vacuo*. Purification by flash chromatography [SiO_2; 0-25% MeOH in CH_2Cl_2] afforded the thioether **121** as a white solid (221 mg, 55%). Mpt. 116-119 °C. ^{1}H NMR (500 MHz, MeOD) δ = 2.58 (s, 3H, CH_3), 2.66-2.72 (m, 1H, CH_2), 2.80 (dd, *J* = 3.6, 13.3 Hz, 1H, CH_2) 3.13 (dd, *J* = 3.6, 13.3 Hz, 1H, CH), 7.24-7.29 (m, 2H), 7.30-7.36 (m, 4H), 7.42-7.47 (m, 4H), 7.58-7.62 (m, 2H), 7.92-7.96 (m, 2H). ^{13}C NMR (125 MHz,

MeOD) δ = 26.73, 34.06, 54.87, 68.01, 128.34, 129.32, 129.36, 130.62, 130.66, 130.99, 136.86, 144.91, 145.03, 151.06, 171.97. HRMS (ESI+) Calcd. for $C_{24}H_{24}NO_3S$ $[M+H]^+$: 406.1471; found: 406.1468. Anal. calcd. for $C_{24}H_{23}NO_3S \cdot ⅓CH_2Cl_2$: C, 67.41; H, 5.50; N, 3.23. Found: 67.84; H, 5.73; N, 3.20.

5.2.5.82. 1-(4-(((2-Aminoethyl)thio)diphenylmethyl)phenyl)ethanone hydrochloride (**122**).

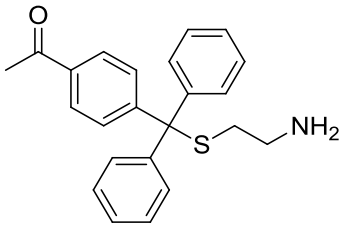

A solution of tertiary alcohol **54** (346 mg, 1.0 mmol) with cysteamine hydrochloride (125 mg, 1.1 mmol) in trifluoroacetic acid (1 mL) was stirred for 3 h at room temperature. The volatiles were removed *in vacuo*, and the residue suspended in aqueous HCl (1.0 M, 10 mL) and stirred at room temperature for 18 h, during which time a white precipitate formed. The mixture was filtered, and the precipitate washed successively with HCl (1.0 M, 10 mL), petroleum ether (60/80) and Et_2O, and dried *in vacuo* to yield the hydrochloride salt **122** as a white solid (378 mg, 95%). Mpt. 186-188 °C. ^{1}H NMR (500 MHz, DMSO-d_6) δ = 2.40-2.43 (m, 2H, CH_2), 2.52-2.56 (m, 5H), 7.28-7.31 (m, 2H), 7.33-7.40 (m, 10H), 7.47-7.49 (m, 2H), 7.77 (br s, 3H, NH_3^+), 7.93-7.96 (m, 2H). ^{13}C NMR (125 MHz, DMSO-d_6) δ = 27.61, 28.36, 37.58, 66.29, 127.16, 128.17, 128.36, 128.96, 129.31, 135.21, 143.40, 149.04, 197.30. HRMS (ESI+) Calcd. for $C_{23}H_{24}NOS$ $[M+H]^+$: 362.1573; found: 362.1571. Anal. calcd. for $C_{23}H_{23}NOS \cdot 1.75HCl$: C, 64.95; H, 5.87; N, 3.29. Found: C, 65.08; H, 5.80; N, 3.13.

5.2.5.83. (2*R*)-2-Amino-3-(((2-hydroxyphenyl)(diphenyl)methyl)sulfanyl)propanoic acid (**123**).

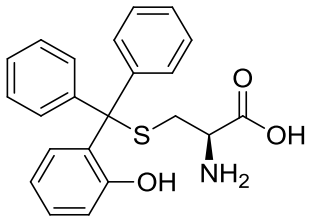

The title compound was then prepared by an adaptation of the procedure reported by DeBonis *et al.*[130] A solution of phenol **42** (532 mg, 1.93 mmol) and L-cysteine (212 mg, 1.75 mmol) in AcOH (1.75 mL) was treated with $BF_3{\cdot}Et_2O$ (376 µL, 2.99 mmol) at 0 °C. After stirring for 2 h at room temperature the reaction was quenched with aqueous NaOAc (10% *w/v*, 5.3 mL), diluted with H_2O (5.3 mL) and the resulting white precipitate collected by filtration. The crude precipitate was dissolved in hot MeOH, filtered whilst hot and then concentrated *in vacuo*. The crude product was purified by flash chromatography [SiO_2; 10-20% MeOH in CH_2Cl_2 with 1% NH_4OH] to afford thioether **123** as a white solid (35 mg, 5%). Mpt. 156-159 °C. ^{1}H NMR (400 MHz, DMSO-d_6) δ = 2.20-2.25 (m, 1H), 2.40-2.44 (m, 1H), 2.81-2.84 (m, 1H), 6.71-6.73 (m, 1H), 6.85-6.88 (m, 1H), 7.12-7.36 (m, 11H), 7.73-7.75 (m, 1H). ^{13}C NMR (100 MHz, DMSO-d_6) δ = 35.32, 53.79, 65.12, 116.40, 118.49, 125.85, 126.99, 128.52, 128.99, 129.89, 142.92, 143.17, 155.09, 171.89. HRMS (ESI+) calcd. for $C_{22}H_{22}NO_3S$ $[M+H]^+$: 380.13149; found: 380.13141. Anal. calcd. for $C_{22}H_{21}NO_3S{\cdot}½CH_2Cl_2$: C, 64.05; H, 5.26; N, 3.32. Found: C, 63.64; H, 5.53; N, 4.09.

5.2.5.84. (2*R*)-2-Amino-3-(((3-hydroxyphenyl)(diphenyl)methyl)sulfanyl)propanoic acid (**124**).

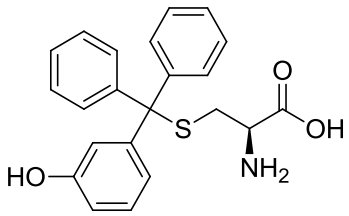

The title compound was prepared by an adaptation of the procedure for **101** using **43** (304 mg, 1.1 mmol) and L-cysteine (121 mg, 1 mmol) in AcOH (1 mL) followed by $BF_3{\cdot}Et_2O$ solution (214 µL, 1.70 mmol), with a reaction time of 2 h. Purification by flash chromatography [SiO_2; 0-20% MeOH in CH_2Cl_2 with 1% NH_4OH] afforded the thioether **124** as a white solid (161 mg, 62%). Mpt. 178-180 °C. ^{1}H NMR (500 MHz, DMSO-d_6) δ = 1.88 (s, 1H, OH), 2.40 (dd, *J* = 9.0, 12.4 Hz, 1H, CH_2), 2.58 (dd, *J* = 4.4, 12.4 Hz, 1H, CH_2), 2.99 (dd, *J* = 4.4, 9.0 Hz, 1H, CH), 6.64 (dd, *J* = 1.8, 8.0 Hz, 1H), 6.70 (d, *J* = 7.9

Hz, 1H), 6.78 (br s, 1H). 7.09 (t, J = 7.9 Hz, 1H), 7.22-7.26 (m, 2H), 7.30-7.34 (m, 8H). ^{13}C NMR (125 MHz, DMSO-d_6) δ = 34.02, 53.57, 65.94, 113.78, 116.39, 119.75, 126.64, 127.92, 128.80, 129.21, 144.30, 144.35, 145.83, 157.08, 169.26. HRMS (ESI+) calcd. for $C_{22}H_{22}NO_3NaS$ $[M+Na]^+$: 402.1134; found: 402.11453. Anal. calcd. for $C_{22}H_{21}NO_3S{\cdot}⅓CH_2Cl_2$: C, 65.82; H, 5.36; N, 3.44. Found: C, 65.83; H, 5.36; N, 3.43.

5.2.5.85. 3-(((2-Aminoethyl)sulfanyl)(diphenyl)methyl)phenol (**125**).

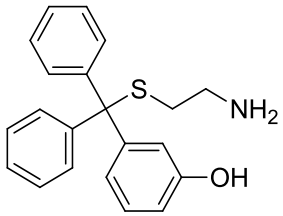

The title compound was prepared following general procedure (iii) with **43** (276 mg, 1 mmol) and cysteamine hydrochloride (114 mg, 1 mmol) in trifluoroacetic acid (1 mL) with the following modifications. Basification of the crude residue (*circa* pH 9) was performed with aqueous NaOH (1.0 M) and EtOAc was used for extraction (3 x 10mL). Purification by flash chromatography [SiO_2; 0-16% MeOH in CH_2Cl_2 with 1% NH_4OH] afforded the thioether **125** as a white solid (259 mg, 77%). Mpt. 143 °C. ^{1}H NMR (400 MHz, DMSO-d_6) δ = 2.16 (t, J = 7.0 Hz, 2H, CH_2), 2.44 (t, J = 7.1 Hz, 2H, CH_2), 6.62 (ddd, J = 0.7, 2.4, 8.0 Hz, 1H), 6.71-6.73 (m, 1H), 6.78-6.79 (m, 1H), 7.10 (t, J = 8.0 Hz, 1H), 7.21-7.26 (m, 2H), 7.30-7.34 (m, 8H). ^{13}C NMR (100 MHz, DMSO-d_6) δ = 35.58, 40.81, 65.75, 113.64, 116.34, 119.88, 126.60, 127.90, 128.83, 129.18, 144.72, 146.20, 156.89. HRMS (ESI+) calcd. for $C_{21}H_{22}NOS$ $[M+H]^+$: 336.14166; found: 336.14172. Anal. calcd. for $C_{21}H_{21}NOS{\cdot}⅕H_2O$: C, 74.39; H, 6.36; N 4.13. Found: C, 74.33; H, 6.33; N, 4.07.

5.2.5.86. 2-(((3-(Aminomethyl)phenyl)(diphenyl)methyl)sulfanyl)ethanamine (**127**).

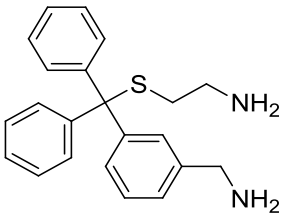

The title compound was prepared following general procedure (iii) with **95** (250 mg, 0.86 mmol) and cysteamine hydrochloride (108 mg, 0.95 mmol) in trifluoroacetic acid (1 mL). Purification by flash chromatography [SiO_2; 0-25% MeOH in CH_2Cl_2 with 1% NH_4OH] afforded the thioether **127** as a clear yellow oil (250 mg, 72%). ^{1}H NMR (500 MHz, DMSO-d_6) δ = 2.15 (t, J = 7.1 Hz, 2H, CH_2), 2.42 (t, J = 7.0 Hz, 2H, CH_2), 3.67 (s, 2H, CH_2), 7.10-7.12 (m, 1H), 7.20-7.26 (m, 4H), 7.30-7.34 (m, 8H), 7.36-7.38 (m, 1H). ^{13}C NMR (125 MHz, DMSO-d_6) δ = 35.70, 40.85, 45.64, 65.87, 125.35, 126.54, 127.11, 127.62, 127.88, 129.16, 143.80, 144.52, 144.78. HRMS (ESI+) calcd. for $C_{22}H_{25}N_2S$ $[M+H]^+$: 349.1733; found: 349.1731. Anal. calcd. for $C_{22}H_{24}N_2S{\cdot}½H_2O$: C, 73.91; H, 7.05; N, 7.84. Found: C, 73.93; H, 6.97; N, 8.39.

5.2.5.87. *N*-(3-(((2-aminoethyl)sulfanyl)(diphenyl)methyl)benzyl)acetamide (**128**).

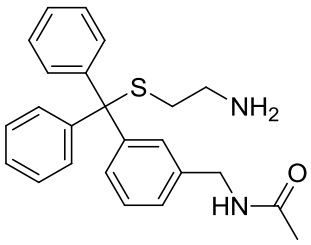

The title compound was then prepared following general procedure (iii) with **97** (166 mg, 0.50 mmol) and cysteamine hydrochloride (63 mg, 0.55 mmol) in trifluoroacetic acid (0.5 mL). Purification by flash chromatography [SiO_2; 0-18% MeOH in CH_2Cl_2 with 1% NH_4OH] afforded the amine **128** as a colourless oil (169 mg, 82%). ^{1}H NMR (500 MHz, DMSO-d_6) δ = 1.81 (s, 3H, CH_3), 2.16 (d, J = 7.0 Hz, 2H, CH_2), 2.42 (d, J = 7.0 Hz, 2H, CH_2), 4.19 (d, J = 6.0 Hz, m, NHC$\underline{H}_2$), 7.10-7.15 (m, 2H), 7.22-7.35 (m, 12H), 8.32 (t, J = 6.0 Hz, 1H, NH). ^{13}C NMR (125 MHz, DMSO-d_6) δ = 22.45, 35.48, 40.75, 42.08, 65.77, 125.33, 126.61, 127.68, 127.74, 127.83, 127.91, 129.12, 139.37, 144.16, 169.05. HRMS (ESI+) calcd. for $C_{24}H_{27}N_2OS$ $[M+H]^+$: 391.1839; found: 391.1836. Anal. calcd. for $C_{24}H_{26}N_2OS{\cdot}H_2O$: C, 70.56; H, 6.91; N, 6.86. Found: C, 70.87; H, 6.97; N, 6.84.

5.2.5.88. 3-(((2-Aminoethyl)sulfanyl)(diphenyl)methyl)benzoic acid hydrochloride (**129**).

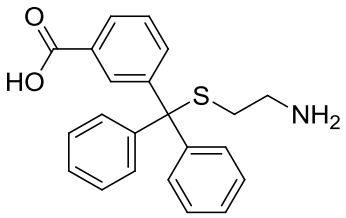

A solution of the tertiary alcohol **88** (346 mg, 1.0 mmol) with cysteamine hydrochloride (125 mg, 1.1 mmol) in trifluoroacetic acid (1 mL) was stirred for 3.5 h at room temperature. The volatiles were removed *in vacuo*, and the residue suspended in aqueous HCl (1.0 M, 10 mL) and stirred at room temperature for 18 h, during which time a white precipitate formed. The mixture was filtered, and the precipitate washed successively with HCl (1.0 M, 10 mL), petroleum ether (60/80) and Et_2O, and dried *in vacuo* to yield thioether **129** as a white solid (145 mg, 36%). Mpt. 218-220 °C. ^{1}H NMR (500 MHz, DMSO-d_6) δ = 2.43 (m, 2H, CH_2), 2.50-2.55 (m, 2H, CH_2), 7.28-7.31 (m, 2H), 7.33-7.40 (m, 8H), 7.50 (t, J = 7.8 Hz, 1H), 7.58 (ddd, J = 1.2, 2.0, 7.9 Hz, 1H), 7.85-7.87 (m, 1H), 7.88-8.05 (m, 4H), 13.06 (br s, 1H, COOH). ^{13}C NMR (125 MHz, DMSO-d_6) δ = 28.42, 37.65, 66.23, 127.15, 127.96, 128.39, 128.63, 128.96, 129.73, 130.67, 133.48, 143.59, 144.62, 167.01. HRMS (ESI+) calcd. for $C_{22}H_{22}NO_2S$ $[M+H]^+$: 364.1366; found: 364.1363. Anal. calcd. for $C_{21}H_{21}NO_2S{\cdot}1.1HCl$: C, 64.42; H, 5.69; N, 3.58. Found: C, 64.12; H, 5.57; N, 3.37.

5.2.5.89. (*R*)-2-Amino-3-(((3-carbamoylphenyl)diphenylmethyl)sulfanyl)propanoic acid (**130**).

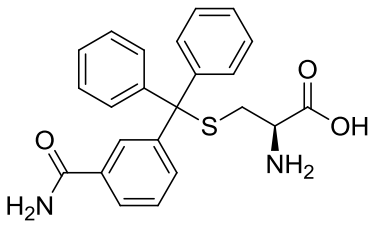

The title compound was prepared following general procedure (iii) with **85** (303 mg, 1.0 mmol) and L-cysteine (133 mg, 1.1 mmol) in trifluoroacetic acid (1 mL). Purification by flash chromatography [SiO_2; 0-35% MeOH in CH_2Cl_2] afforded the title compound **130** as a white solid (139 mg, 34%). Mpt. 154-157 °C. ^{1}H NMR (500 MHz, MeOD) δ = 2.69 (dd, J = 8.5, 13.2 Hz, 1H, CH_2), 2.77 (dd, J = 4.3, 13.2 Hz, 1H, CH_2), 3.09 (dd, J = 4.3, 8.5 Hz, 1H, CH), 7.22-7.27 (m, 2H), 7.30-7.35 (m, 4H), 7.40 (t, J = 7.8 Hz, 1H), 7.43-7.56 (m,

4H), 7.54-7.59 (m, 1H), 7.74-7.76 (m, 1H), 8.11-8.13 (m, 1H). ^{13}C NMR (125 MHz, MeOD) δ = 34.16, 55.01, 67.95, 127.24, 128.22, 129.33, 129.75, 130.53, 130.71, 134.42, 135.09, 145.24, 145.49, 146.22, 172.24, 172.31. HRMS (ESI-) calcd. for $C_{23}H_{21}NO_3S$ $[M-H]^-$: 405.1278; found: 405.1280. Anal. calcd. for $C_{23}H_{22}N_2O_3S \cdot ⅓CH_2Cl_2$: C, 64.49; H, 5.26; N, 6.45. Found: C, 64.73; H, 5.20; N, 6.48.

5.2.5.90. 3-(((2-Aminoethyl)sulfanyl)(diphenyl)methyl)benzamide hydrochloride (**131**).

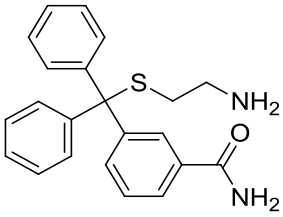

A solution of the tertiary alcohol **85** (131 mg, 0.43 mmol) with cysteamine hydrochloride (54 mg, 0.48 mmol) in trifluoroacetic acid (0.86 mL) was stirred for 2.5 h at room temperature. The volatiles were removed *in vacuo*, and the crude basified (*circa.* pH 10) with aqueous NaOH (1.0 M). The aqueous mixture was extracted with CH_2Cl_2 (3 x 10 mL) and the organic layer dried ($MgSO_4$) and concentrated *in vacuo*. Purification by flash chromatography [SiO_2; 0-18% MeOH in CH_2Cl_2 with 1% NH_4OH] yielded a white solid, which was suspended in aqueous HCl (1.0 M, 10 mL) and stirred at room temperature for 18 h, during which time a white precipitate formed. The mixture was filtered, and the precipitate washed successively with HCl, petroleum ether (60/80) and Et_2O, and dried *in vacuo* to afford the hydrochloride salt **131** as a white solid (48 mg, 28%). Mpt. 202-205 °C. ^{1}H NMR (500 MHz, DMSO-d_6) δ = 2.43-2.47 (m, 2H, CH_2), 7.26-7.31 (m, 2H), 7.33-7.49 (m, 11H), 7.78-7.81 (m, 1H), 7.91-7.98 (m, 4H), 7.99-8.03 (br s, 1H, $CONH_2$). ^{13}C NMR (125 MHz, DMSO-d_6) δ = 28.38, 37.65, 66.36, 125.73, 127.03, 128.08, 128.29, 128.39, 129.02, 131.76, 134.17, 143.73, 144.40, 167.57. HRMS (ESI+) calcd. for $C_{22}H_{23}N_2OS$ $[M+H]^+$: 363.1526; found: 363.1522. Anal. calcd. for $C_{22}H_{22}N_2OS \cdot 1.75HCl$: C, 61.99; H, 5.62; N, 6.57. Found: C, 62.39; H, 5.39; N, 6.38.

5.2.5.91. 3-(((2-Aminoethyl)sulfanyl)(diphenyl)methyl)-*N*-methylbenzamide hydrochloride (**132**).

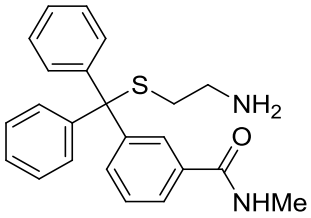

A solution of the tertiary alcohol **91** (220 mg, 0.69 mmol) with cysteamine hydrochloride (87 mg, 0.76 mmol) in trifluoroacetic acid (692 µL) was stirred for 3 h at room temperature. The volatiles were removed *in vacuo* and the crude basified (*circa.* pH 10) with saturated aqueous sodium carbonate solution. The aqueous mixture was extracted with CH_2Cl_2 (3 x 10 mL), and the organic layer dried ($MgSO_4$) and concentrated *in vacuo*. After purification by flash chromatography [SiO_2; 0-15% MeOH in CH_2Cl_2 with 1% NH_4OH], the crude product was suspended in aqueous HCl (1.0 M, 10 mL) and stirred at room temperature for 18 h, during which time a white precipitate formed. The mixture was filtered, the precipitate washed successively with CH_2Cl_2 and H_2O, and dried *in vacuo* to yield the hydrochloride salt **132** as a white solid (69 mg, 24%). Mpt. 197-200 °C. ^{1}H NMR (500 MHz, DMSO-d_6) δ = 2.43-2.48 (m, 2H, CH_2), 2.74 (d, J = 4.5 Hz, 3H, CH_3), 7.26-7.47 (m, 12H), 7.74-7.77 (m, 2H), 7.88-7.99 (m, 4H), 8.51 (d, J = 4.5 Hz, 3H, NH_3). ^{13}C NMR (125 MHz, DMSO-d_6) δ = 26.23, 28.38, 37.64, 66.35, 125.31, 127.03, 128.02, 128.14, 128.29, 129.01, 131.59, 134.40, 143.74, 144.40, 166.24. HRMS (ESI+) calcd. for $C_{23}H_{25}N_2OS$ $[M+H]^+$: 377.1682; found: 377.1679. Anal. calcd. for $C_{23}H_{24}N_2OS{\cdot}2.5HCl$: C, 59.07; H, 5.71; N, 5.99. Found: C, 58.67; H, 5.42; N, 5.90.

5.2.5.92. 3-(((2-Aminoethyl)sulfanyl)(diphenyl)methyl)benzamide (**133**).

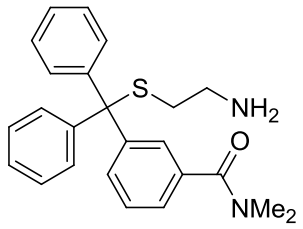

The title compound was prepared following general procedure (iii) with **92** (199 mg, 0.6 mmol) and cysteamine hydrochloride (75 mg, 0.66 mmol) in trifluoroacetic acid (0.6 mL). Purification by flash chromatography [SiO_2; 0-20% MeOH in CH_2Cl_2 with 1% NH_4OH] afforded the thioether **133** as a colourless oil (201 mg, 86%). ^{1}H NMR (500 MHz, MeOD) δ = 2.33-2.38 (m, 2H, CH_2), 2.43-2.48 (m, 2H, CH_2), 2.89-2.93 (m, 3H, CH_3), 3.03-3.07 (m, 3H, CH_3), 7.21-7.34 (m, 7H), 7.38-7.46 (m, 6H), 7.55-7.59 (m, 1H). ^{13}C NMR (100 MHz, MeOD) δ = 35.64, 35.92, 40.03, 41.51, 67.56, 126.51, 128.06, 129.11, 129.30, 129.37, 130.72, 132.17, 136.86, 145.80, 147.03, 173.51. HRMS (ESI+) calcd. for $C_{24}H_{27}N_2OS$ $[M+H]^+$: 391.1839; found: 391.1836. Anal. calcd. for $C_{24}H_{26}N_2OS{\cdot}\frac{1}{3}CH_2Cl_2$: C, 70.73; H, 6.49; N, 6.80. Found: C, 70.87; H, 6.44; N, 6.69.

5.2.5.93. 2-(((3-(Methylsulfonyl)phenyl)(diphenyl)methyl)sulfanyl)ethanamine (**134**).

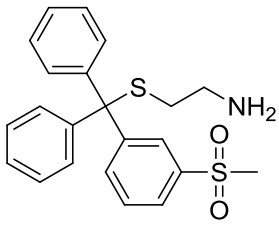

The title compound was prepared following general procedure (iii) with **99** (169 mg, 0.5 mmol) and cysteamine hydrochloride (63 mg, 0.55 mmol) in trifluoroacetic acid (0.6 mL). Purification by flash chromatography [SiO_2; 0-15% MeOH in CH_2Cl_2 with 1% NH_4OH] afforded thioether **134** as a colourless oil (163 mg, 82%). ^{1}H NMR (500 MHz, DMSO-d_6)) δ = 2.17 (t, J = 7.0 Hz, 3H, CH_3), 2.43 (t, J = 7.0 Hz, 3H, CH_3), 3.19 (s, 3H, CH_3), 7.26-7.30 (m, 2H), 7.33-7.40 (m, 8H), 7.62-7.64 (m, 2H), 7.84-7.88 (m, 1H), 7.92-7.93 (m, 1H). ^{13}C NMR (125 MHz, DMSO-d_6) δ = 35.33, 40.73, 43.56, 65.53, 125.55, 126.73, 126.99, 128.26, 128.95, 129.35, 134.40, 140.59, 143.86, 146.23. HRMS (ESI+) calcd. for $C_{22}H_{24}NO_2S_2$ $[M+H]^+$: 398.1243; found: 398.1241. Anal. calcd. for $C_{22}H_{23}NO_2S_2{\cdot}\frac{1}{5}CH_2Cl_2$: C, 64.32; H, 5.69; N, 3.38. Found: C, 64.42; H, 5.67; N, 3.32.

5.2.5.94. 4-(((2-Aminoethyl)sulfanyl)(diphenyl)methyl)benzonitrile (**135**).

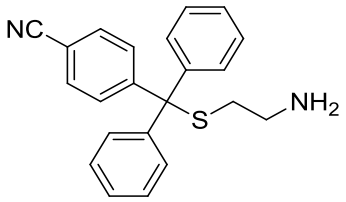

The title compound was prepared following general procedure (iii) with **64** (285 mg, 1 mmol) and cysteamine hydrochloride (125 mg, 1.1 mmol) in trifluoroacetic acid (1 mL). Purification by flash chromatography [SiO_2; 0-20% MeOH in CH_2Cl_2 with 1% NH_4OH] afforded the thioether **135** as a yellow oil (253 mg, 68%). ^{1}H NMR (500 MHz, DMSO-d_6) δ = 2.15 (t, J = 7.1 Hz, 2H, CH_2), 2.44 (t, J = 7.1 Hz, 2H, CH_2), 7.24-7.30 (m, 2H), 7.31-7.39 (m, 8H), 7.49-7.53 (m, 2H), 7.80-7.84 (m, 2H). ^{13}C NMR (125 MHz, DMSO-d_6) δ = 35.38, 40.66, 54.88, 65.60, 109.46, 118.58, 127.01, 128.25, 130.08, 131.98, 143.65, 150.12. HRMS (ESI+) Calcd. for $C_{22}H_{21}N_2S$ $[M+H]^+$: 345.1420; found: 345.1418. Anal. calcd. for $C_{22}H_{20}N_2S{\cdot}\frac{1}{3}CH_2Cl_2$: C, 71.96; H, 5.59; N, 7.51. Found: C, 71.95; H, 5.54; N, 7.39.

5.2.5.95. (4-(((2-Aminoethyl)sulfanyl)(diphenyl)methyl)phenyl)methanol (**136**).

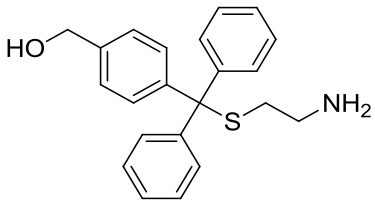

The title compound was prepared following general procedure (iii) with **90** (154 mg, 0.53 mmol) and cysteamine hydrochloride (66 mg, 0.58 mmol) in trifluoroacetic acid (0.53 mL). Purification by flash chromatography [SiO_2; 0-25% MeOH in CH_2Cl_2 with 1% NH_4OH] afforded the thioether **136** as a yellow oil (54 mg, 29%). ^{1}H NMR (500 MHz, MeOD) δ = 2.35 (t, J = 6.7 Hz, 2H, CH_2), 2.43 (t, J = 6.7 Hz, 2H, CH_2), 4.58 (s, 2H, CH_2), 7.18-7.31 (m, 8H), 7.36-7.44 (m, 6H). ^{13}C NMR (125 MHz, MeOD) δ = 35.94, 41.50, 64.75, 67.61, 127.55, 127.80, 128.90, 130.74, 141.31, 145.33, 146.33. HRMS (ESI+) calcd. for $C_{22}H_{24}NOS$ $[M+H]^+$: 350.1573; found: 350.1571. Anal. calcd. for $C_{22}H_{23}NOS{\cdot}\frac{1}{4}CH_2Cl_2$: C, 72.09; H, 6.39; N, 3.78. Found: C, 72.36; H, 6.19; N, 3.50.

5.2.5.96. 2-(((4-(Aminomethyl)phenyl)(diphenyl)methyl)sulfanyl)ethanamine (**137**).

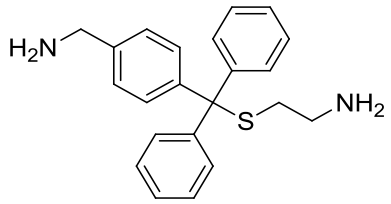

The title compound was prepared following general procedure (iii) using **96** (145 mg, 0.5 mmol) and cysteamine hydrochloride (63 mg, 0.55 mmol) in trifluoroacetic acid (0.5 mL). Purification by flash chromatography [SiO_2; 0-25% MeOH in CH_2Cl_2 with 1% NH_4OH] afforded the thioether **137** as an off-white solid (250 mg, 72%). Mpt. 70-72 °C. ^{1}H NMR (500 MHz, DMSO-d_6) δ = 2.15 (t, J = 7.1 Hz, 2H, CH_2), 2.43 (t, J = 7.1 Hz, 2H, CH_2), 3.69 (s, 2H, CH_2), 7.21-7.34 (m, 14H). ^{13}C NMR (100 MHz, DMSO-d_6) δ = 35.67, 40.86, 45.16, 65.58, 126.55, 127.90, 128.82, 129.09, 142.52, 142.60, 144.85. HRMS (ESI+) calcd. for $C_{22}H_{25}N_2S$ $[M+H]^+$: 349.1733; found: 349.1731. Anal. calcd. for $C_{22}H_{24}N_2S{\cdot}½H_2O$: C, 73.91; H, 7.05; N, 7.84. Found: C, 73.91; H, 6.76; N, 7.57.

5.2.5.97. *N*-(4-(((2-Aminoethyl)sulfanyl)(diphenyl)methyl)benzyl)acetamide (**138**).

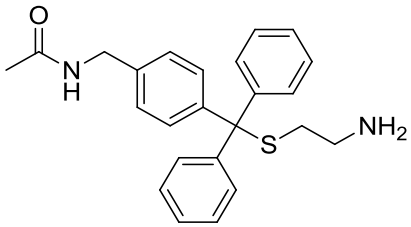

The title compound was then prepared following general procedure (iii) using **98** (166 mg, 0.50 mmol) and cysteamine hydrochloride (63 mg, 0.55 mmol) in trifluoroacetic acid (0.5 mL). Purification by flash chromatography [SiO_2; 0-18% MeOH in CH_2Cl_2 with 1% NH_4OH] afforded thioether **138** as a pale yellow solid (143 mg, 73%). Mpt. 74-77 °C. ^{1}H NMR (400 MHz, MeOD) δ = 1.97 (s, 3H, CH_3), 2.31-2.35 (m, 2H, CH_2), 2.40-2.45 (m, 2H, CH_2), 4.33 (s, NHC$\underline{H}_2$), 7.18-7.31 (m, 8H), 7.36-7.43 (m, 6H). ^{13}C NMR (100 MHz, MeOD) δ = 22.52, 35.92, 41.50, 43.77, 67.54, 127.82, 128.15, 128.91, 130.74, 130.91, 138.51, 145.37, 146.26, 173.13. HRMS (ESI+) calcd. for $C_{24}H_{27}NO_2S$ $[M+H]^+$: 391.1839; found: 391.1835. Anal. calcd. for $C_{24}H_{26}N_2OS{\cdot}¼CH_2Cl_2$: C, 70.73; H, 6.49; N, 6.80. Found: C, 70.47; H, 6.35; N, 6.64.

5.2.5.98. 4-(((2-Aminoethyl)sulfanyl)(diphenyl)methyl)benzamide (**139**).

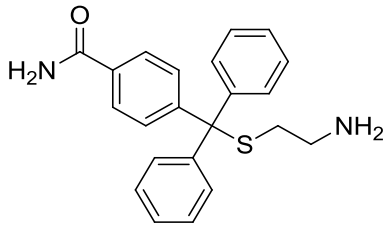

A solution of the tertiary alcohol **86** (303.4 mg, 1.0 mmol) with cysteamine hydrochloride (125 mg, 1.1 mmol) in trifluoroacetic acid (1 mL) was stirred for 2 h at room temperature. The volatiles were removed *in vacuo* and the residue suspended in aqueous HCl (1.0 M, 10 mL) and stirred at room temperature for 18.5 h, during which time a precipitate formed. The mixture was filtered, and the precipitate washed successively with HCl (1.0 M, 10 mL), petroleum ether (60/80) and Et_2O, and dried *in vacuo* to yield the crude hydrochloride salt as an off-white solid. This was basified (*circa.* pH 10) with saturated sodium carbonate solution, extracted with CH_2Cl_2 (3 x 10 mL) and the organic layer dried ($MgSO_4$) and concentrated *in vacuo*. Purification by flash chromatography [SiO_2; 0-15% MeOH in CH_2Cl_2 with 1% NH_4OH] afforded the title compound **139** as a white solid (252 mg, 70%). Mpt. 62-65 °C. ^{1}H NMR (500 MHz, MeOD) δ = 2.32-2.37 (m, 2H, CH_2), 2.42-2.47 (m, 2H, CH_2), 7.21-7.26 (m, 2H), 7.26-7.33 (m, 4H), 7.40-7.44 (m, 4H), 7.50-7.54 (m, 2H), 7.79-7.82 (m, 2H). ^{13}C NMR (125 MHz, MeOD) δ = 36.04, 41.51, 67.55, 128.04, 128.29, 129.08, 130.71, 130.84, 133.31, 145.76, 150.38, 171.86. HRMS (ESI+) calcd. for $C_{22}H_{23}N_2OS$ $[M+H]^+$: 363.1526; found: 363.1523. Anal. calcd. for $C_{22}H_{22}N_2OS{\cdot}½H_2O$: C, 71.13; H, 6.24; N, 7.54. Found: C, 70.73; H, 5.96; N, 7.33.

5.2.5.99. 4-(((2-Aminoethyl)sulfanyl)(diphenyl)methyl)-*N*-methylbenzamide (**140**).

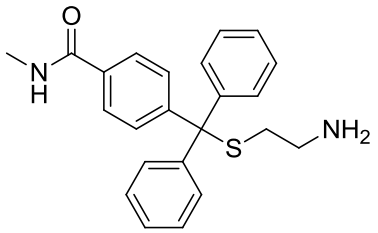

The title compound was prepared following general procedure (iii) using **93** (150 mg, 0.47 mmol) with cysteamine hydrochloride (59 mg, 0.52 mmol) in trifluoroacetic acid (0.5 mL) and CH_2Cl_2 (2 mL). Purification by flash chromatography [SiO_2; 0-15% MeOH in CH_2Cl_2 with 1% NH_4OH] afforded thioether **140** as a white solid (122 mg, 69%). Mpt. 62-64 °C. ^{1}H NMR (400 MHz, MeOD) δ = 2.32-2.36 (m, 2H, CH_2), 2.41-2.46 (m, 2H, CH_2), 2.91 (s,

3H, CH_3), 7.21-7.26 (m, 2H), 7.27-7.33 (m, 4H), 7.39-7.44 (m, 4H), 7.49-7.54 (m, 2H), 7.71-7.76 (m, 2H). ^{13}C NMR (100 MHz, MeOD) δ = 26.89, 35.99, 41.49, 67.54, 127.80, 128.03, 129.07, 130.71, 130.86, 133.92, 145.77, 150.01, 170.22. HRMS (ESI+) calcd. for $C_{23}H_{25}N_2OS$ $[M+H]^+$: 377.1682; found: 377.1679. Anal. calcd. for $C_{23}H_{24}N_2OS \cdot ½H_2O$: C, 71.66; H, 6.54; N, 7.27. Found: C, 71.50; H, 6.19; N, 7.12.

5.2.5.100. 4-(((2-Aminoethyl)sulfanyl)(diphenyl)methyl)-*N,N*-dimethylbenzamide (**141**).

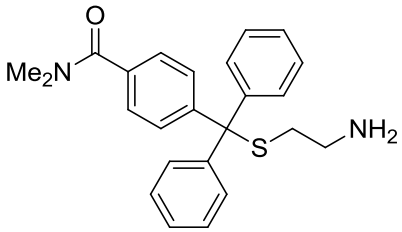

The title compound was then prepared following general procedure (iii) using **94** (125 mg, 0.37 mmol) with cysteamine hydrochloride (51 mg, 0.42 mmol) in trifluoroacetic acid (0.5 mL) and CH_2Cl_2 (2 mL). Purification by flash chromatography [SiO_2; 0-15% MeOH in CH_2Cl_2 with 1% NH_4OH] afforded the thioether **141** as a clear yellow crystalline solid (129 mg, 88%). Mpt. 60-62 °C. ^1H NMR (400 MHz, MeOD) δ = 2.32-2.38 (m, 2H, CH_2), 2.42-2.48 (m, 2H, CH_2), 3.01 (s, 3H, CH_3), 3.09 (s, 3H, CH_3), 7.21-7.26 (m, 2H), 7.27-7.33 (m, 4H), 7.35-7.45 (m, 6H), 7.50-7.55 (m, 2H). ^{13}C NMR (100 MHz, MeOD) δ = 35.65, 36.01, 40.07, 41.52, 67.56, 127.73, 128.02, 129.06, 130.74, 130.87, 135.66, 145.82, 148.40, 173.41. HRMS (ESI+) calcd. for $C_{24}H_{27}N_2OS$ $[M+H]^+$: 391.1839; found: 391.1835. Anal. calcd. for $C_{24}H_{26}N_2OS \cdot ⅓CH_2Cl_2$: C, 69.82; H, 6.42; N, 6.69. Found: C, 69.78; H, 6.10; N, 6.56.

5.2.5.101. 2-(((4-(Methylsulfonyl)phenyl)(diphenyl)methyl)sulfanyl)ethanamine (**142**).

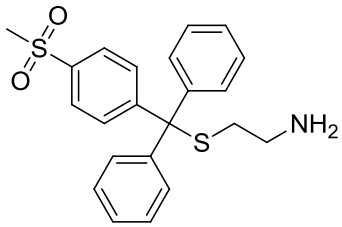

The title compound was then prepared following general procedure (iii) using **100** (197 mg, 0.58 mmol) and cysteamine hydrochloride (73 mg, 0.64 mmol) in trifluoroacetic acid (1 mL). Purification by flash chromatography [SiO_2; 0-20% MeOH in CH_2Cl_2 with 1% NH_4OH] afforded the thioether **142** as a colourless oil (143 mg, 62%). ^{1}H NMR (400 MHz, MeOD) δ = 2.32-2.37 (m, 2H, CH_2), 2.43-2.48 (m, 2H, CH_2), 3.12 (s, 3H, CH_3), 7.23-7.28 (m, 2H), 7.30-7.36 (m, 4H), 7.41-7.45 (m, 4H), 7.70-7.74 (m, 2H), 7.87-7.91 (m, 2H). ^{13}C NMR (125 MHz, DMSO-d_6) δ = 35.50, 40.71, 43.45, 65.54, 126.79, 126.97, 128.23, 129.02, 129.95, 138.97, 143.97, 150.38. HRMS (ESI+) calcd. for $C_{22}H_{24}NO_2S_2$ $[M+H]^+$: 398.1243; found: 398.1239. Anal. calcd. for $C_{22}H_{23}NO_2S_2 \cdot ⅕CH_2Cl_2$: C, 64.32; H, 5.69; N, 3.38. Found: C, 64.98; H, 5.55; N, 2.90.

5.2.5.102. 2-((Diphenyl(pyridin-3-yl)methyl)sulfanyl)ethanamine (**143**).

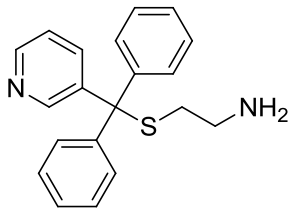

The title compound was prepared following general procedure (iii) with **69** (274 mg, 1.05 mmol) and cysteamine hydrochloride (131 mg, 1.15 mmol) in trifluoroacetic acid (1 mL). Purification by flash chromatography [SiO_2; 0-25% MeOH in CH_2Cl_2] afforded the thioether **143** as a yellow oil (187 mg, 59%). ^{1}H NMR (400 MHz, MeOD) δ = 2.35-2.40 (m, 2H, CH_2), 2.45-2.50 (m, 2H, CH_2), 7.25-7.30 (m, 2H), 7.32-7.37 (m, 4H), 7.38-7.44 (m, 5H), 7.92 (ddd, J = 1.6, 2.5, 8.2 Hz, 1H), 8.40-8.42 (m, 1H), 8.56 (dd, J = 0.7, 2.5 Hz, 1H). ^{13}C NMR (400 MHz, MeOD) δ = 35.36, 41.31, 65.73, 124.58, 128.39, 129.38, 130.52, 139.18, 143.04, 145.05, 148.15, 151.05. HRMS (ESI+) calcd. for $C_{20}H_{21}N_2S$ $[M+H]^+$: 321.1431; found: 321.1424. Anal. calcd. for $C_{20}H_{20}N_2S \cdot ⅓CH_2Cl_2$: C, 70.07; H, 5.98; N, 8.04. Found: C, 70.14; H, 5.88; N, 7.75.

5.2.5.103. 2-((Diphenyl(1,3-thiazol-2-yl)methyl)sulfanyl)ethanamine (**144**).

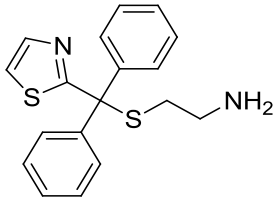

The title compound was prepared following general procedure (iii) with **70** (267 mg, 1.0 mmol) and cysteamine hydrochloride (125 mg, 1.1 mmol) in trifluoroacetic acid (1 mL). Purification by flash chromatography [SiO_2; 0-25% MeOH in CH_2Cl_2] afforded the thioether **144** as a brown solid (98 mg, 30%). Mpt 59-61 °C. ^{1}H NMR (400 MHz, MeOD) δ = 2.62-2.66 (m, 2H, CH_2), 2.73-2.77 (m, 2H, CH_2), 7.31-7.40 (m, 6H), 7.39-7.43 (m, 4H), 7.54 (d, *J* = 3.4 Hz, 1H), 7.83 (d, *J* = 3.4 Hz, 1H). ^{13}C NMR (400 MHz, MeOD) δ = 33.99, 40.87, 65.08, 122.16, 128.98, 129.25, 130.46, 143.81, 144.82, 178.61. HRMS (ESI+) calcd. for $C_{18}H_{19}N_2S_2$ $[M+H]^+$: 327.0984; found: 327.0981. Anal. calcd. for $C_{18}H_{18}N_2S_2 \cdot ½CH_2Cl_2$: C, 60.23; H, 5.19; N, 7.59. Found: C, 60.70; H, 4.75; N, 7.63.

5.2.5.104. 2-((1,3-Oxazol-2-yl(diphenyl)methyl)sulfanyl)ethanamine (**145**).

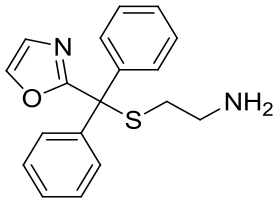

The title compound was prepared following general procedure (iii) with **71** (201 mg, 0.8 mmol) and cysteamine hydrochloride (100 mg, 0.88 mmol) in trifluoroacetic acid (1 mL). Purification by flash chromatography [SiO_2; 0-25% MeOH in CH_2Cl_2] afforded the thioether **145** as an orange solid (55 mg, 27%). Mpt. 59-61 °C. ^{1}H NMR (400 MHz, MeOD) δ = 2.62-2.70 (m, 4H, 2 x CH_2), 7.21 (d, *J* = 0.7 Hz, 1H), 7.91 (d, *J* = 0.7 Hz, 1H), 7.28-7.37 (m, 10H). ^{13}C NMR (400 MHz, MeOD) δ = 34.40, 40.95, 62.24, 127.76, 129.00, 129.34, 130.05, 141.38, 142.55, 167.68. HRMS (ESI+) calcd. for $C_{18}H_{19}N_2OS$ $[M+H]^+$: 311.1213; found: 311.1210. Anal. calcd. for $C_{18}H_{18}N_2OS \cdot ½CH_2Cl_2$: C, 62.97; H, 5.43; N, 7.94. Found: C, 62.65; H, 4.79; N, 8.04.

5.2.5.105. 2-((Bis-(4-methylphenyl)(phenyl)methyl)sulfanyl)ethanamine (**146**).

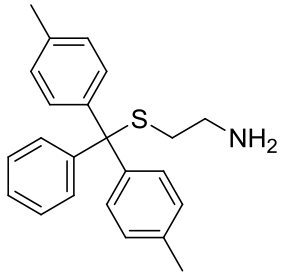

The title compound was prepared using general procedure (iii) with bis **37** (289 mg, 1.0 mmol) and cysteamine hydrochloride (125 mg, 1.1 mmol) in trifluoroacetic acid (1 mL) with the following modifications. Basification of the crude residue (*circa* pH 9) was performed with aqueous NaOH (1.0 M) and EtOAc was used for extraction of the aqueous mixture (3 x 10 mL). Purification by flash chromatography [SiO_2; 0-18% MeOH in CH_2Cl_2 with 1% NH_4OH] afforded the thioether **146** as a yellow solid (271 mg, 79%). Mpt. 64-67 °C. ^{1}H NMR (MeOD, 500 MHz) δ 2.30 (s, 6H, 2 x CH_3), 2.32-2.35 (m, 2H, CH_2), 2.41-2.44 (m, 2H, CH_2), 7.07-7.09 (m, 4H), 7.17-7.20 (m, 1H), 7.24-7.27 (m, 5H), 7.38-7.40 (m, 2H). ^{13}C NMR (MeOD, 125 MHz) δ 19.30, 20.05, 36.08, 41.56, 67.55, 127.66, 128.21, 128.79, 130.00, 130.76, 131.94, 136.13, 136.97, 143.71, 146.56. HRMS (ESI+) calcd. for $C_{23}H_{26}NS$ $[M+H]^+$: 348.17805; found: 348.17805. Anal. calcd. for $C_{23}H_{25}NS{\cdot}¼H_2O$: C, 78.48; H, 7.30; N, 3.98. Found: C, 78.41; H, 7.49; N, 3.65.

5.2.5.106. 3-(((2-Aminoethyl)thio)(3-chlorophenyl)phenylmethyl)phenol (*rac*-**147**).

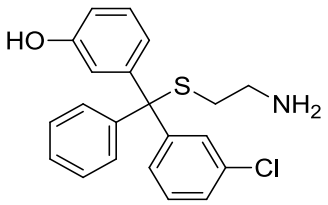

The title compound was prepared following general procedure (iii) with *rac*-**66** (311 mg, 1.0 mmol) and cysteamine hydrochloride (125 mg, 1.1 mmol) in trifluoroacetic acid (1 mL) with the following modifications. Basification of the crude residue (*circa* pH 9) was performed with aqueous NaOH (1.0 M) and EtOAc was used for extraction (3 x 10mL). Purification by flash chromatography [SiO_2; 0-16% MeOH in CH_2Cl_2 with 1% NH_4OH] afforded thioether *rac*-**147** as a pale yellow solid (253 mg, 68%). Mpt. 74 °C. ^{1}H NMR (500 MHz, MeOD) δ = 2.36 (t, J = 6.9 Hz, 2H, CH_2), 2.48 (t, J = 6.9 Hz, 2H, CH_2), 6.67 (ddd, J = 0.7, 2.4, 8.1 Hz, 1H), 6.82-6.84 (m, 1H), 6.87-6.88 (m, 1H), 7.12 (t, J = 8.0 Hz, 1H), 7.22-7.33 (m, 5H), 7.34-7.36 (m, 1H), 7.39-7.41 (m, 3H). ^{13}C NMR (125 MHz,

MeOD) δ = 36.00, 41.48, 67.29, 115.02, 117.08, 121.93, 127.85, 128.05, 129.04, 129.21, 130.00, 130.36, 130.64, 130.70, 134.85, 145.67, 147.04, 148.88, 158.35. HRMS (ESI-) calcd. for $C_{21}H_{19}Cl_2NOS$ $[M-H]^-$: 368.08814; found: 368.08881. Anal. calcd. for $C_{21}H_{20}ClNOS$: C, 68.19; H, 5.45; N, 3.79. Found: C, 68.83; H, 5.45; N, 3.40.

5.2.5.107. 3-(((2-Aminoethyl)sulfanyl)(3-ethylphenyl)phenylmethyl)phenol (*rac*-**148**).

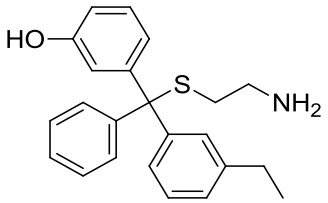

The title compound was prepared following general procedure (iii) with *rac*-**67** (305 mg, 1.0 mmol) and cysteamine hydrochloride (125 mg, 1.1 mmol) in trifluoroacetic acid (1 mL) with the following modifications. Basification of the crude residue (*circa* pH 9) was performed with aqueous NaOH (1.0 M) and EtOAc was used for extraction (3 x 10mL). Purification by flash chromatography [SiO_2; 0-18% MeOH in CH_2Cl_2 with 1% NH_4OH] afforded thioether *rac*-**148** as an off-white solid (186 mg, 51%). Mpt. 50-52 °C. ^{1}H NMR (500 MHz, MeOD) δ = 1.16 (t, *J* = 7.6 Hz, 3H, CH_3), 2.35-2.38 (m, 2H, CH_2), 2.43-2.46 (m, 2H, CH_2), 2.57 (q, *J* = 7.6 Hz, 2H, CH_2), 6.65 (ddd, *J* = 0.8, 2.4, 8.1 Hz, 1H), 6.84-6.86 (m, 1H), 6.90-6.91 (m, 1H), 7.05-7.07 (m, 1H), 7.09 (t, *J* = 8.0 Hz, 1H), 7.16-7.21 (m, 3H), 7.26-7.29 (m, 3H), 7.41-7.43 (m, 2H). ^{13}C NMR (125 MHz, MeOD) δ = 16.15, 29.93, 36.09, 41.56, 67.80, 118.04, 122.13, 127.21, 127.69, 128.22, 128.78, 129.71, 130.39, 130.82, 144.99, 146.33, 146.47, 147.89, 158.12. HRMS (ESI-) calcd. for $C_{23}H_{24}NOS$ $[M-H]^-$: 362.15841; found: 362.15860 *m/z*. Anal. calcd. for $C_{23}H_{25}NOS{\cdot}¼H_2O$: C, 75.06; H, 6.98; N, 3.81. Found: C, 75.04; H, 6.90; N, 3.88.

5.2.5.108. 3-(((2-Aminoethyl)sulfanyl)(4-methylphenyl)phenyl methyl)phenol (*rac*-**149**).

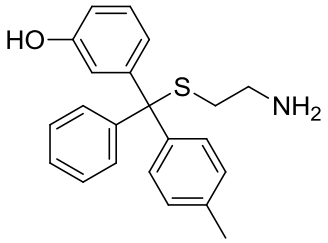

The title compound was prepared following general procedure (iii) with *rac*-**68** (290 mg, 1 mmol) and cysteamine hydrochloride (125 mg, 1.1 mmol) in trifluoroacetic acid (1 mL) with the following modifications. Basification of the crude residue (*circa* pH 9) was performed with aqueous NaOH (1.0 M) and EtOAc was used for extraction (3 x 10mL). Purification by flash chromatography [SiO_2; 0-18% MeOH in CH_2Cl_2 with 1% NH_4OH] afforded thioether *rac*-**149** as an off-white solid (291 mg, 83%). Mpt. 68 °C. ^{1}H NMR (500 MHz, MeOD) δ = 2.30 (CH_3), 2.34-2.37 (m, 2H, CH_2), 2.44-2.47 (m, 2H, CH_2), 6.63-6.65 (m, 1H), 6.83-6.85 (m, 1H), 6.88-6.89 (m, 1H), 7.06-7.10 (m, 3H), 7.18-7.21 (m, 1H), 7.25-7.29 (m, 4H), 7.39-7.42 (m, 2H). ^{13}C NMR (125 MHz, MeOD) δ = 20.93, 36.00, 41.52, 67.51, 114.60, 117.98, 122.09, 127.67, 128.78, 129.41, 129.71, 130.76, 137.55, 143.34, 146.56, 147.99, 158.10. HRMS (ESI+) calcd. for $C_{22}H_{24}NOS$ $[M+H]^+$: 348.14276; found: 348.14307. Anal. calcd. for $C_{22}H_{23}NOS \cdot ¼H_2O$: C, 74.65; H, 6.69; N, 3.96. Found: C, 74.73; H, 6.96; N, 3.73.

5.2.5.109. 3-(((2-Aminoethyl)sulfanyl)(4-methylphenyl)phenylmethyl)benzonitrile (*rac*-**150**).

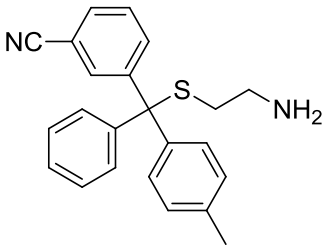

The title compound was prepared following general procedure (iii) with *rac*-**65** (299 mg, 1.0 mmol) and cysteamine hydrochloride (125 mg, 1.1 mmol) in trifluoroacetic acid (1 mL). Purification by flash chromatography [SiO_2; 0-17% MeOH in CH_2Cl_2] afforded thioether *rac*-**150** as an off-white solid (254 mg, 71%). Mpt. 46-48 °C. ^{1}H NMR (500 MHz, MeOD) δ = 2.33 (s, 3H, CH_3), 2.48-2.52 (m, 2H, CH_2), 2.54-2.58 (m, 2H, CH_2), 7.16-7.19 (m, 2H), 7.26-7.30 (m, 3H), 7.33-7.37 (m, 2H), 7.40-7.43 (m, 2H), 7.48-7.52 (m, 1H), 7.61-7.64 (m, 1H), 7.74-7.79 (m, 2H). ^{13}C NMR (125 MHz, MeOD) δ = 20.93,

31.44, 39.98, 67.46, 113.30, 119.50, 128.52, 129.45, 130.07, 130.39, 130.52, 131.83, 133.64, 135.36, 138.64, 141.68, 144.89, 147.98. HRMS (ESI+) calcd. for $C_{23}H_{23}N_2S_2$ $[M+H]^+$: 359.1587; found: 359.1574. Anal. calcd. for $C_{23}H_{22}N_2S{\cdot}CH_2Cl_2$: C, 65.01; H, 5.46; N, 6.32. Found: C, 64.57; H, 5.06; N, 5.99.

5.2.5.110. 3-(((Aminomethyl)sulfanyl)(4-methylphenyl)phenylmethyl)benzamide (*rac*-**151**).

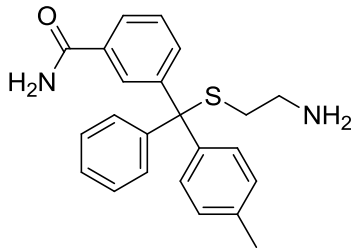

The title compound was prepared following general procedure (iii) with *rac*-**87** (224 mg, 0.71 mmol) and cysteamine hydrochloride (88 mg, 0.77 mmol) in trifluoroacetic acid (1 mL). Purification by flash chromatography [SiO_2; 0-25% MeOH in CH_2Cl_2] afforded thioether *rac*-**151** as a white solid (254 mg, 71%). Mpt. 95-97 °C. ^{1}H NMR (400 MHz, MeOD) δ = 2.32 (s, 3H, CH_3), 2.47-2.55 (m, 4H, 2 x CH_2), 7.12-7.17 (m, 2H), 7.22-7.35 (m, 5H), 7.37-7.45 (m, 3H), 7.55-7.58 (m, 1H), 7.72-7.76 (m, 1H), 8.07-8.10 (m, 1H). ^{13}C NMR (400 MHz, MeOD) δ = 20.94, 31.97, 40.19, 67.85, 126.86, 128.16, 129.22, 129.25, 129.85, 130.62, 134.26, 134.87, 138.17, 142.43, 145.63, 146.84, 172.14. HRMS (ESI+) calcd. for $C_{23}H_{25}N_2OS_2$ $[M+H]^+$: 377.1682; found: 377.1678. Anal. calcd. for $C_{23}H_{24}N_2OS{\cdot}CH_2Cl_2$: C, 62.47; H, 5.68; N, 6.07. Found: C, 61.92; H, 5.01; N, 5.40. LC-MS t_R = 11.43 min (*m/z* = 350.2, $[M+H]^+$; purity = 97.6%).

5.2.5.111. 2-((2-Fluoro-3-methylphenyl)(diphenyl)methyl)sulfanyl)ethanamine (**152**).

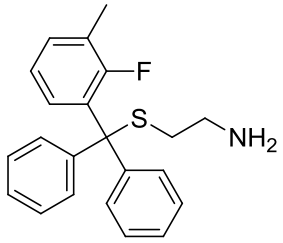

The title compound was prepared following general procedure (iii) with **58** (292 mg, 1.0 mmol) and cysteamine hydrochloride (125 mg, 1.1 mmol) in trifluoroacetic acid (1 mL). Purification by flash chromatography [SiO_2; 0-25% MeOH in CH_2Cl_2] afforded thioether **152** as a white solid (226 mg, 64%). Mpt. 165-168 °C. ^{1}H NMR (400 MHz, MeOD) δ = 2.14-2.17 (m, 3H, CH_3), 2.35-2.40 (m, 4H, 2 x CH_2), 7.14-7.19 (m, 1H), 7.23-7.35 (m, 7H), 7.46-7.49 (m, 1H), 7.71-7.76 (m, 1H). ^{19}F NMR (376.5 MHz, $CDCl_3$) δ = -105.84. ^{13}C NMR (400 MHz, MeOD) δ = 14.48 (d, J_{CF} = 5.8 Hz), 31.27, 39.81, 66.39, 124.74 (d, J_{CF} = 4.2 Hz), 127.26 (d, J_{CF} = 19.2 Hz), 128.16, 128.92, 129.13 (d, J_{CF} = 3.6 Hz), 130.27, 131.72 (d, J_{CF} = 10.8 Hz), 132.67 (d, J_{CF} = 5.3 Hz), 143.95, 160.09 (d, J_{CF} = 250.3 Hz). HRMS (ESI+) calcd. for $C_{22}H_{23}FNS$ $[M+H]^+$: 352.1541; found: 352.1528. Anal. calcd. for $C_{22}H_{22}FNS{\cdot}CH_2Cl_2$: C, 63.30; H, 5.54; N, 3.21. Found: C, 62.61; H, 5.11; N, 3.05.

5.2.5.112. 2-((2-Fluoro-4-methylphenyl)(diphenyl)methyl)sulfanyl)ethanamine (**153**).

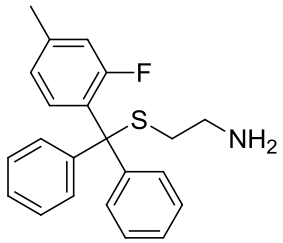

The title compound was prepared following general procedure (iii) with **59** (292 mg, 1.0 mmol) and cysteamine hydrochloride (125 mg, 1.1 mmol) in trifluoroacetic acid (1 mL). Purification by flash chromatography [SiO_2; 0-20% MeOH in CH_2Cl_2] afforded the thioether **153** as a white solid (170 mg, 48%). Mpt. 74-76 °C. ^{1}H NMR (400 MHz, $CDCl_3$) δ = 2.23-2.28 (m, 2H, CH_2), 2.32-2.38 (m, 5H), 6.78-6.83 (m, 1H), 7.03-7.06 (m, 1H), 7.17-7.30 (m, 6H), 7.38-7.44 (m, 4H), 7.69-7.74 (m, 1H). ^{19}F NMR (376.5 MHz, $CDCl_3$) δ = -102.04. ^{13}C NMR (100 MHz, $CDCl_3$) δ = 20.73, 36.05, 41.38, 65.54 (d, J_{CF} = 2.6 Hz), 117.98 (d, J_{CF} = 23.0 Hz), 125.61 (d, J_{CF} = 2.74 Hz), 127.81, 128.70, 129.60 (d, J_{CF} = 10.6 Hz), 130.25, 131.63 (d, J_{CF} = 3.3 Hz), 141.71 (d, J_{CF} = 8.0 Hz), 144.60, 161.68 (d, J_{CF} = 250.2 Hz). HRMS (ESI+) calcd. for $C_{44}H_{45}F_2N_2S_2$ $[2M+H]^+$: 703.2987; found:

703.2991. Anal. calcd. for $C_{22}H_{22}FNS \cdot ¼H_2O$: C, 74.23; H, 6.37; N, 3.93. Found: C, 74.27; H, 6.23; N, 3.58.

5.2.5.113. (2*R*)-2-Amino-3-(((2-fluoro-4-methoxyphenyl)(diphenyl)methyl)sulfanyl)propanoic acid (**154**).

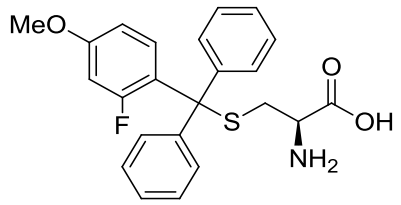

The title compound was prepared following general procedure (iii) with **60** (308 mg, 1.0 mmol) and L-cysteine (133 mg, 1.1 mmol) in trifluoroacetic acid (1 mL). Purification by flash chromatography [SiO_2; 0-25% MeOH in CH_2Cl_2 with 1% NH_4OH] afforded the thioether **154** as a white solid (204 mg, 50%). Mpt. 152-154.5 °C. ^{1}H NMR (400 MHz, MeOD) δ = 2.68 (dd, 1H, *J* = 8.9, 13.1 Hz), 2.81 (dd, 1H, *J* = 4.3, 13.1 Hz), 3.17 (dd, 1H, *J* = 4.2, 8.9 Hz), 3.87 (s, 3H, CH_3), 7.00-7.06 (m, 1H), 7.12-7.20 (m, 2H), 7.23-7.30 (m, 2H), 7.30-7.36 (m, 4H), 7.41-7.46 (m, 4H). ^{19}F NMR (376.5 MHz, MeOD) δ = -136.39. ^{13}C NMR (100 MHz, MeOD) δ = 34.75, 55.17, 56.70, 67.31, 114.20 (d, J_{CF} = 1.4 Hz), 118.42 (d, J_{CF} = 20.1 Hz), 126.69 (d, J_{CF} = 3.2 Hz), 128.15, 129.22, 130.54, 138.63 (d, J_{CF} = 4.9 Hz), 145.54, 145.57, 147.91 (d, J_{CF} = 11.0 Hz), 152.96 (d, J_{CF} = 244.6 Hz), 173.11. HRMS (ESI+) calcd. for $C_{23}H_{23}NO_3FS$ $[M+H]^+$: 412.1377; found: 412.1377. Anal. calcd. for $C_{23}H_{22}NO_3FS \cdot H_2O$: C, 64.32; H, 5.63; N, 3.26. Found: C, 64.03; H, 5.59; N, 3.26.

5.2.5.114. 2-(((2-Fluoro-4-methoxyphenyl)(diphenyl)methyl)sulfanyl)ethanamine (**155**).

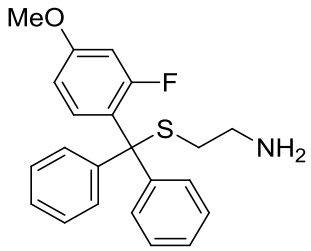

The title compound was prepared following general procedure (iii) with **60** (308 mg, 1.0 mmol) and cysteamine hydrochloride (125 mg, 1.1 mmol) in trifluoroacetic acid (1 mL). Purification by flash chromatography [SiO_2; 0-15% MeOH in CH_2Cl_2] afforded the thioether **155** as a brown solid (280 mg, 76%). Mpt. 68-70 °C. ^{1}H NMR (400 MHz, MeOD) δ = 2.32-2.37 (m, 2H, CH_2), 2.43-2.48 (m, 2H, CH_2), 3.85 (s, 3H, CH_3), 6.96-7.02 (m, 1H), 7.08-7.15 (m, 2H), 7.19-7.25 (m, 2H), 7.26-7.33 (m, 4H), 7.37-7.42 (m, 4H). ^{19}F

NMR (376.5 MHz, MeOD) δ = -136.78. ^{13}C NMR (100 MHz, MeOD) δ = 36.08, 41.55, 56.74, 67.01, 113.79, 118.43 (d, J_{CF} = 20.2 Hz), 126.69 (d, J_{CF} = 2.8 Hz), 127.94, 129.00, 130.61, 139.38 (d, J_{CF} = 5.5 Hz), 146.12, 147.73 (d, J_{CF} = 10.8 Hz), 152.86 (d, J_{CF} = 244.5 Hz). HRMS (ESI+) calcd. for $C_{22}H_{23}FNOS$ $[M+H]^+$: 368.1479; found: 368.1475. Anal. calcd. for $C_{22}H_{22}FNOS \cdot ½H_2O$: C, 70.19; H, 6.16; N, 3.72. Found: C, 70.37; H, 5.80; N, 3.40.

5.2.5.115. 2-(((3-Fluoro-4-methoxyphenyl)(diphenyl)methyl)sulfanyl)ethanamine (**156**).

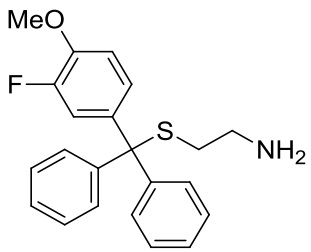

The title compound was prepared following general procedure (iii) with **61** (308 mg, 1.0 mmol) and cysteamine hydrochloride (125 mg, 1.1 mmol) in trifluoroacetic acid (1 mL). Purification by flash chromatography [SiO_2; 0-14% MeOH in CH_2Cl_2 with NH_4OH] afforded thioether **156** as a pale yellow oil (247 mg, 67%). ^{1}H NMR (400 MHz, MeOD) δ = 2.24-2.29 (m, 2H, CH_2), 2.35-2.40 (m, 2H, CH_2), 3.79 (s, 3H, CH_3), 6.58 (dd, J = 2.6, 13.3 Hz, 1H), 6.78 (dd, J = 2.6, 8.7 Hz, 1H), 7.17-7.29 (m, 6H), 7.39-7.44 (m, 4H), 7.68-7.74 (m, 1H). ^{19}F NMR (376.5 MHz, MeOD) δ = -99.28. ^{13}C NMR (100 MHz, MeOD) δ = 36.10, 41.43, 56.14, 65.33 (d, J_{CF} = 2.6 Hz), 103.75 (d, J_{CF} = 27.1 Hz), 110.06 (d, J_{CF} = 2.5 Hz), 124.68 (d, J_{CF} = 11.2 Hz), 127.77 128.70 130.21, 132.42 (d, J_{CF} = 4.1 Hz), 144.83, 162.35 (d, J_{CF} = 250.2 Hz), 162.36 (d, J_{CF} = 11.0 Hz). HRMS (ESI+) calcd. for $C_{22}H_{23}FNOS$ $[M+H]^+$: 368.1479; found: 368.1474. Anal. calcd. for $C_{22}H_{22}FNOS$: C, 71.90; H, 6.03; N, 3.81. Found: C, 72.04; H, 6.05; N, 3.84.

5.2.5.116. 2-(((3,4-Dichlorophenyl)(diphenyl)methyl)sulfanyl)ethanamine (**157**).

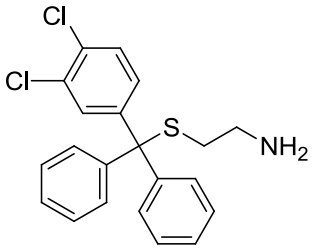

The title compound was prepared following general procedure (iii) with (3,4-dichlorophenyl)(diphenyl)methanol (165 mg, 0.5 mmol) and cysteamine hydrochloride (57 mg, 0.5 mmol) in trifluoroacetic acid (0.5 mL) with the following modifications. Basification of the crude residue (*circa* pH 9) was performed with aqueous NaOH (1.0 M) and EtOAc was used for extraction (3 x 6 mL). Purification by flash chromatography [SiO_2; 0-18% MeOH in CH_2Cl_2 with NH_4OH] afforded thioether **157** as white solid (91 mg, 47%). Mpt. 99-102 °C. ^{1}H NMR (400 MHz, DMSO-d_6) δ = 2.16 (t, J = 7.0 Hz, 2H, CH_2), 2.45 (t, J = 7.1 Hz, 2H, CH_2), 7.25-7.37 (m, 11H), 7.46 (m, 1H), 7.61-7.63 (m, 1H). ^{13}C NMR (100 MHz, DMSO-d_6) δ = 35.60, 40.78, 64.96, 127.09, 128.23, 128.93 129.49, 129.73, 130.27, 130.64, 130.74, 143.74, 145.90. HRMS (ESI+) calcd. for $C_{21}H_{120}Cl_2NS$ $[M+H]^+$: 388.0688; found: 388.0683. Anal. calcd. for $C_{21}H_{19}Cl_2NS \cdot ⅓H_2O$: C, 63.97; H, 5.03; N 3.55. Found: C, 63.99; H, 5.01; N, 3.61.

5.2.5.117. (2*R*)-2-Amino-3-(((3-,4-dimethylphenyl)(diphenyl)methyl)sulfanyl)propanoic acid (**158**).

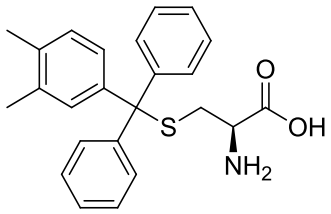

The title compound was prepared following general procedure (iii) with **37** (500 mg, 1.73 mmol) and L-cysteine (231 mg, 1.1 mmol) in trifluoroacetic acid (1.7 mL). Purification by flash chromatography [SiO_2; 0-25% MeOH in CH_2Cl_2] afforded the thioether **158** as a white solid (464 mg, 68%). Mpt. 148-150 °C. ^{1}H NMR (400 MHz, MeOD) δ = 2.19 (s, 3H, CH_3), 2.23 (s, 3H, CH_3), 2.68 (dd, 1H, J = 9.2, 13.3 Hz), 2.81 (dd, 1H, J = 4.1, 13.3 Hz), 3.05 (dd, 1H, J = 4.1, 9.2 Hz), 7.06 (d, 1H, J = 8.0 Hz), 7.12 (dd, 1H, J = 2.0, 8.0 Hz), 7.17-7.24 (m, 3H), 7.26-7.32 (m, 4H), 7.41-7.46 (m, 4H). ^{13}C NMR (125 MHz, MeOD) δ = 19.30, 20.02, 34.41, 55.12, 67.93, 127.90, 128.17, 129.04, 130.23, 130.69, 130.72, 131.86, 136.45, 137.29, 143.09, 145.92, 145.96, 172.62. HRMS (ESI+) calcd. for

$C_{48}H_{51}O_4N_2S_2$ $[2M+H]^+$: 783.3286; found: 783.3295. Anal. calcd. for $C_{24}H_{25}NO_2S{\cdot}H_2O$: C, 70.39; H, 6.65; N, 3.42. Found: C, 70.31; H, 6.25; N, 3.25.

5.2.5.118. 2-(((3,4-Dimethylphenyl)(diphenyl)methyl) sulfanyl)ethanamine (**159**).

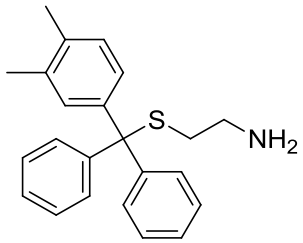

The title compound was prepared following general procedure (iii) with **37** (289 mg, 1.0 mmol) and cysteamine hydrochloride (125 mg, 1.1 mmol) in trifluoroacetic acid (1 mL) with the following modifications. Basification of the crude residue (*circa* pH 9) was performed with aqueous NaOH (1M) and EtOAc was used for extraction (3 x 10mL). Purification by flash chromatography [SiO_2; 0-18% MeOH in CH_2Cl_2 with 1% NH_4OH] afforded the thioether **159** a pale yellow oil (273 mg, 79%). ^{1}H NMR (MeOD, 500 MHz) δ 2.17 (s, 3H, CH_3), 2.22 (s, 3H, CH_3), 2.32-2.35 (m, 2H, CH_2), 2.41-2.44 (m, 2H, CH_2), 7.02 (d, *J* = 8.0 Hz, 1H), 7.09 (dd, *J* = 2.0, 8.0 Hz, 1H), 7.16-7.21 (m, 3H), 7.24-7.27 (m, 4H), 7.38-7.41 (m, 4H). ^{13}C NMR (MeOD, 125 MHz) δ 19.30, 20.05, 36.08, 41.56, 67.55, 127.66, 128.21, 128.79, 130.00, 130.76, 131.94, 136.13, 136.97, 143.71, 146.56. HRMS (ESI+) calcd. for $C_{23}H_{26}NS$ $[M+H]^+$: 348.17805; found: 348.17886. Anal. calcd. for $C_{23}H_{25}NS{\cdot}¼H_2O$: C, 78.48; H, 7.30; N, 3.98. Found: C, 78.47; H, 7.38; N, 3.82.

5.2.5.119. (2*R*)-2-Amino-3-(((3-ethyl-4-methylphenyl)(diphenyl)methyl)sulfanyl)propanoic acid (**160**).

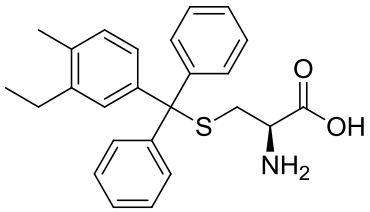

The title compound was prepared following general procedure (iii) with **62** (254 mg, 0.84 mmol) and L-cysteine (112 mg, 0.93 mmol) in trifluoroacetic acid (1 mL). Purification by flash chromatography [SiO_2; 0-25% MeOH in CH_2Cl_2] afforded thioether **160** as a white solid (242 mg, 71%). Mpt. 149-152 °C. ^{1}H NMR (500 MHz, MeOD) δ = 1.10 (t, 3H, *J* = 7.6 Hz), 2.27 (s, 3H), 2.56 (q, 2H, *J* = 7.6 Hz), 2.69 (dd, 1H, *J* = 9.2, 13.4 Hz), 2.82 (dd, 1H, *J* = 4.2, 13.4 Hz), 3.05 (dd, 1H, *J* = 4.2, 9.2 Hz), 7.06 (d, 1H, *J* = 8.0 Hz), 7.14 (dd,

1H, J = 2.1, 8.0 Hz), 7.18-7.24 (m, 3H), 7.27-7.32 (m, 4H), 7.42-7.46 (m, 4H). ^{13}C NMR (125 MHz, MeOD) δ = 14.94, 18.73, 27.28, 34.36, 55.13, 68.05, 127.92, 128.07, 129.04, 130.47, 130.70, 130.74, 135.60, 143.16, 143.29, 145.91, 145.95, 172.53. HRMS (ESI+) calcd. for $C_{25}H_{28}NO_2S$ $[M+H]^+$: 406.1835; found 406.1843. Anal. calcd. for $C_{25}H_{27}NO_2S \cdot ½H_2O$: C, 72.43; H, 6.81; N, 3.38. Found: C, 72.18; H, 6.37; N, 3.14.

5.2.5.120. 2-(((3-Ethyl-4-methylphenyl)(diphenyl)methyl)sulfanyl)ethanamine (**161**).

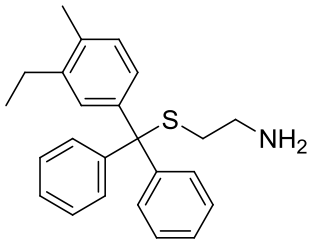

The title compound was prepared following general procedure (iii) with **62** (302 mg, 1.0 mmol) and cysteamine hydrochloride (125 mg, 1.1 mmol) in trifluoroacetic acid (1 mL) with the following modifications. Basification of the crude residue (*circa* pH 9) was performed with aqueous NaOH (1.0 M) and EtOAc was used for extraction (3 x 10mL). Purification by flash chromatography [SiO_2; 0-16% MeOH in CH_2Cl_2 with 1% NH_4OH] afforded thioether **161** as a colourless oil (260 mg, 72%). ^{1}H NMR (MeOD, 500 MHz) δ 2.17 (s, 3H, CH_3), 2.22 (s, 3H, CH_3), 2.32-2.35 (m, 2H, CH_2), 2.41-2.44 (m, 2H, CH_2), 7.02 (d, J = 8.0 Hz, 1H), 7.09 (dd, J = 2.0, 8.0 Hz, 1H), 7.16-7.21 (m, 3H), 7.24-7.27 (m, 4H), 7.38-7.41 (m, 4H). ^{13}C NMR (MeOD, 125 MHz) δ 19.30, 20.05, 36.08, 41.56, 67.55, 127.66, 128.21, 128.79, 130.00, 130.76, 131.94, 136.13, 136.97, 143.71, 146.56. HRMS (ESI+) calcd. for $C_{24}H_{28}NS$ $[M+H]^+$: 362.19370; found: 362.19257. Anal. calcd. for $C_{24}H_{27}NS \cdot ⅕CH_2Cl_2$: C, 76.79; H, 7.30; N, 3.70. Found: C, 77.05; H, 7.58; N, 2.93.

5.2.5.121. (2*R*)-2-Amino-3-(((5,6,7,8-tetrahydronaphthalen-2-yl)(diphenyl)methyl)sulfanyl)propanoic acid (**162**).

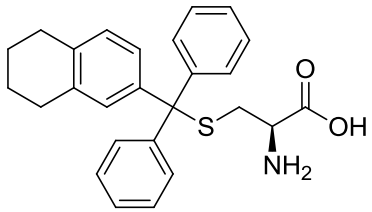

The title compound was prepared following general procedure (iii) with **46** (314 mg, 1.0 mmol) and L-cysteine (133 mg, 1.1 mmol) in trifluoroacetic acid (1 mL). Purification by flash chromatography [SiO_2; 0-25% MeOH in CH_2Cl_2] afforded the thioether **162** as a white solid (123 mg, 29%). Mpt. 145-148 °C. ^{1}H NMR (400 MHz, MeOD) δ = 1.75-1.80 (m, 4H), 2.64-2.75 (m, 5H), 2.82 (dd, 1H *J* = 4.1, 13.4 Hz), 3.02 (dd, 1H *J* = 4.1, 9.2 Hz), 6.98 (d, *J* = 8.2 Hz, 1H), 7.08-7.13 (m, 2H), 7.19-7.24 (m, 2H), 7.26-7.32 (m, 4H), 7.42-7.46 (m, 4H). ^{13}C NMR (100 MHz, MeOD) δ = 24.37, 29.93, 30.53, 34.32, 55.07, 67.94, 127.90, 128.00, 129.05, 129.76, 130.68, 130.72, 131.17, 136.99, 137.79, 142.67, 145.88, 145.93, 172.55. HRMS (ESI-) calcd. for $C_{26}H_{26}NO_2S$ $[M-H]^-$: 416.1690; found 416.1692. Anal. calcd. for $C_{26}H_{27}NO_2S \cdot ⅔H_2O$: C, 72.72; H, 6.65; N 3.26. Found: C, 72.46; H, 6.27; N, 3.15.

5.2.5.122. 2-((Diphenyl(5,6,7,8-tetrahydronaphthalen-2-yl)methyl)sulfanyl)ethanamine (**163**).

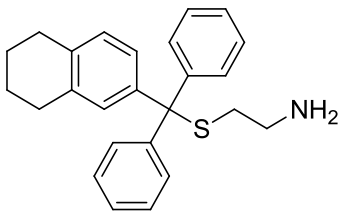

The title compound was prepared following general procedure (iii) with **46** (314 mg, 1.0 mmol) and cysteamine hydrochloride (125 mg, 1.1 mmol) in trifluoroacetic acid (1 mL) with the following modifications. Basification of the crude residue (*circa* pH 9) was performed with aqueous NaOH (1.0 M) and EtOAc was used for extraction (3 x 10mL). Purification by flash chromatography [SiO_2; 0-18% MeOH in CH_2Cl_2 with 1% NH_4OH] afforded thioether **163** as a colourless oil (262 mg, 70%). ^{1}H NMR (MeOD, 500 MHz) δ 1.76-1.79 (m, 4H, 2 x CH_2), 2.33-2.35 (m, 2H, CH_2), 2.42-2.45 (m, 2H, CH_2), 2.64-2.66 (m, 2H, CH_2), 2.71-2.73 (m, 2H, CH_2), 6.94-6.95 (m, 1H), 7.06-7.08 (m, 2H), 7.17-7.21 (m, 2H), 7.25-7.28 (m, 4H), 7.39-7.41 (m, 4H). ^{13}C NMR (MeOD, 125 MHz) δ 24.40, 29.92, 30.58, 36.02, 41.56, 67.61, 127.66, 128.07, 128.79, 129.51, 130.78, 131.23, 136.72,

137.49, 143.32, 146.57. HRMS (ESI+) calcd. for $C_{25}H_{28}NOS$ $[M+H]^+$: 374.19370; found: 374.19400. Anal. calcd. for $C_{25}H_{27}NS \cdot ¾CH_2Cl_2$: C, 70.73; H, 6.57; N, 3.20. Found: C, 71.00; H, 6.48; N, 3.35.

5.2.5.123. 4-(1,1-Diphenylbut-3-en-1-yl)-1,2-dimethylbenzene (**171**).

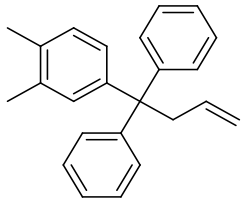

The title compound was prepared using an adaptation of the method reported by Kabalka *et al.*[192] *n*-Butyllithium (2.5 M in hexane, 6.12 mL, 15.3 mmol) was added cautiously by dropwise addition to a cooled (0 °C) solution of **37** (4.00 g, 13.9 mmol) in anhydrous CH_2Cl_2 (85 mL), the reaction mixture allowed to warm to room temperature and stirred for 30 min. Allyltrimethylsilane (6.02 mL, 36.9 mmol) and iron trichloride (5.19 g, 32.0 mmol) were then added and the reaction stirred at room temperature for 6 h. The reaction was quenched with H_2O (100mL) extracted with CH_2Cl_2 (3 x 100 mL). The combined organic layers were washed successively with saturated aqueous $NaHCO_3$ solution (150 mL) and brine (200 mL), dried (MgSO4) and concentrated *in vacuo.* Purification by flash chromatography [SiO_2; 0-10% EtOAc in hexane] afforded alkene **171** as a brown oil [3.119 g, 91% (based on 79% conversion)] and recovered starting material **37** (834 mg). ^{1}H NMR (400 MHz, $CDCl_3$) δ = 2.22 (s, 3H, CH_3), 2.26 (s, 3H, CH_3), 3.43-3.46 (m, 2H), 4.97 (ddd, *J* = 1.4, 3.4, 10.3 Hz, 1H), 5.06 (ddd, *J* = 1.5, 3.5, 17.0 Hz, 1H), 5.70 (ddd, *J* = 6.6, 10.4, 17.1 Hz, 1H), 6.94-6.98 (m, 1H), 7.03-7.08 (m, 2H), 7.19-7.34 (m, 10H). ^{13}C NMR (100 MHz, $CDCl_3$) δ = 19.40, 20.24, 45.67, 56.01, 117.18, 125.97, 126.97, 127.79, 129.14, 129.58, 130.62, 134.23, 135.87, 136.35, 144.92, 147.65. GC-MS (CI, methane) t_R = 16.44 min (*m/z* = 311.2, $[M-H]^+$). Anal. calcd. for $C_{24}H_{24}$: C, 92.26; H, 7.74. Found: C, 91.51; H, 7.28.

5.2.5.124. 4-(3,4-Dimethylphenyl)-4,4-diphenylbutan-1-ol (**172**).

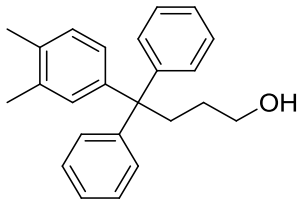

A solution of BH_3·THF (1.0 M in THF, 20.0 mL, 20.0 mmol) was added to a cooled (0 °C) solution of alkene **171** (3.11 g, 10.0 mmol) in THF (20 mL), and stirred at room temperature for 19 h. The reaction was cooled to 0 °C and quenched cautiously with H_2O (5 mL) and aqueous NaOH (3.0 M, 6.8 mL, 20.4 mmol), followed by slow dropwise addition of hydrogen peroxide (30% in H_2O, 5.1 mL, 50.0 mmol) over 5 min. The mixture was maintained at 0 °C for 30 min, and then allowed to warm to room temperature and stirred for a further 3.5 h, diluted with H_2O (50 mL) and extracted with Et_2O (3 x 50 mL). The combined organic extracts were washed successively with saturated aqueous $NaHCO_3$ solution (200 mL) and brine (200 mL), dried ($MgSO_4$) and concentrated *in vacuo*. Purification by flash chromatography [SiO_2; 0-22% EtOAc in hexane] afforded the primary alcohol **172** as a colourless oil (1.90 g, 58%). ^{1}H NMR (400 MHz, $CDCl_3$) δ = 1.31-1.40 (m, 2H, CH_2), 2.19 (s, 3H, CH_3), 2.21 (s, 3H, CH_3), 2.59-2.66 (m, 2H, CH_2), 3.62 (t, J = 6.4 Hz, 2H, CH_2), 6.97-7.03 (m, 2H), 7.04-7.09 (m, 1H), 7.14-7.19 (m, 2H), 7.22-7.31 (m, 8H). ^{13}C NMR (100 MHz, $CDCl_3$) δ = 19.36, 20.25, 29.36, 36.61, 56.06, 63.54, 125.85, 126.75, 127.89, 129.19, 129.36, 130.44, 134.11, 135.90, 144.94, 147.67. GC-MS (CI, methane) t_R = 17.91 min (m/z = 371.1, $[M+C_3H_5]^+$). Anal. calcd. for $C_{24}H_{26}O$·¼EtOAc: C, 85.19; H, 8.01. Found: C, 85.11; H, 7.81.

5.2.5.125. 4-(3,4-Dimethylphenyl)-4,4-diphenylbutanal (**173**).

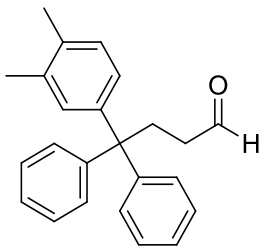

The title compound was prepared using an adaptation of the method developed by Dess *et al.* and the procedure reported by Wang *et al.*[138, 194] Dess-Martin periodinane (3.069 g, 7.24 mmol) was added to a solution of alcohol **172** (1.993 g, 6.03 mmol) in anhydrous CH_2Cl_2 (24 mL). The reaction was stirred at room temperature for 4 h, and then quenched cautiously with sodium thiosulfate solution (0.26 M in saturated aqueous $NaHCO_3$

solution, 100 mL) and extracted with CH_2Cl_2 (3 x 50 mL). The combined organic extracts were washed successively with saturated aqueous $NaHCO_3$ solution, H_2O, and brine (150 mL each), dried ($MgSO_4$) and concentrated *in vacuo*. Purification by flash chromatography [SiO_2; 0-16% EtOAc in hexane] afforded aldehyde **173** as a colourless oil (830 mg, 42%). ^{1}H (400 MHz, $CDCl_3$) δ = 2.20 (s, 3H, CH_3), 2.22 (s, 3H, CH_3), 2.29-2.35 (m, 2H, CH_2), 2.88-2.94 (m, 2H, CH_2), 6.97-7.06 (m, 3H), 7.15-7.22 (m, 2H), 7.24-7.30 (m, 8H). ^{13}C NMR (100 MHz, $CDCl_3$) δ = 19.36, 20.24, 31.99, 41.30, 55.63, 126.17, 126.60, 128.13, 129.18, 129.40, 130.26, 134.48, 136.21, 144.11, 146.96, 202.01. GC-MS (CI, methane) t_R = 17.57 min (*m/z* = 329.2 $[M+H]^+$).

5.2.5.126. 2-(Benzylamino)-5-(3,4-dimethylphenyl)-5,5-diphenylpentanenitrile (*rac*-**174**).

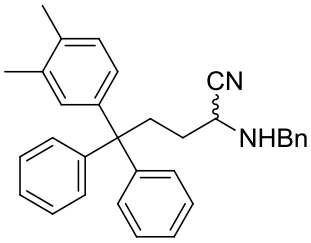

The title compound was prepared by an adaptation of the method reported by Yadav *et al.*[196] Mont. KSF clay (4.5 g) and 1-phenylmethanamine (549 µL, 5.02 mmol) was added to a solution of aldehyde **173** (300 mg, 1.0 mmol) in anhydrous CH_2Cl_2 (45 mL) at room temperature. Trimethylsilyl cyanide (686 µL, 5.48 mmol) was then added, and the reaction mixture was stirred at room temperature for 2.5 h, filtered and the clay rinsed with CH_2Cl_2. The filtrate was concentrated *in vacuo* and purification of the residue by flash chromatography [SiO_2; 0-16% EtOAc in hexane] afforded the α-aminonitrile *rac*-**174** as a pale yellow oil [931 mg, 68% (based on 79% conversion)] and unreacted 4-(3,4-dimethylphenyl)-4,4-diphenylbutanal **173** (485 mg). ^{1}H (500 MHz, $CDCl_3$) δ = 1.56-1.62 (m, 2H, CH_2), 2.20 (s, 3H, CH_3), 2.23 (s, 3H, CH_3), 2.71-2.81 (m, 2H, CH_2), 3.36-3.40 (m, 1H, CH), 3.78 (d, *J* = 12.8 Hz, 1H, $C\underline{H_a}H_bPh$), 4.02 (d, *J* = 12.8 Hz, 1H, $CH_a\underline{H_b}Ph$), 6.98-7.06 (m, 3H), 7.17-7.21 (m, 2H), 7.25-7.31 (m, 9H), 7.33-7.36 (m, 4H). ^{13}C NMR (100 MHz, $CDCl_3$) δ = 19.34, 20.22, 30.12, 36.31, 50.17, 51.78, 55.95, 120.33, 126.14, 126.64, 127.72, 128.10, 128.49, 128.74, 129.18, 129.39, 130.22, 134.43, 136.17, 138.42, 144.13, 147.03, 147.06. HRMS (ESI+) calcd. for $C_{32}H_{33}N_2$ $[M+H]^+$: 445.2638; found 445.2640.

5.2.5.127. 2-(Benzylamino)-5-(3,4-dimethylphenyl)-5,5-diphenylpentanoic acid (*rac*-**175**).

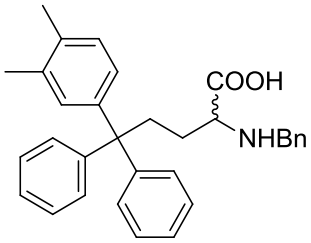

The title compound was prepared using an adaptation of the procedure reported by Wang *et al.*[138] Conc. HCl (12 M, 25 mL) was added to a solution of the nitrile *rac*-**174** (900 mg, 2.02 mmol) in dioxane (25 mL) and the mixture heated at reflux for 48 h. After cooling, the mixture was concentrated *in vacuo*. The crude residue was basified (*circa.* pH 9.5) with saturated aqueous sodium carbonate solution and extracted with CH_2Cl_2 (3 x 100 mL). The combined organic extracts were dried ($MgSO_4$) and concentrated *in vacuo*. Purification by flash chromatography [SiO_2; 0-20% MeOH in CH_2Cl_2 with 1% NH_4OH] afforded the protected amino acid *rac*-**175** as a white solid (538 mg, 57%). Mpt. 176-178 °C. ^{1}H (400 MHz, MeOD) δ = 1.51-1.70 (m, 2H, CH_2), 2.16 (s, 3H, CH_3), 2.19 (s, 3H, CH_3), 2.64-2.86 (m, 2H, CH_2), 2.64-2.85 (m, 2H, CH_2), 3.40-3.44 (m, 1H, CH), 3.92 (d, *J* = 12.8 Hz, 1H, $C\underline{H_a}H_bBn$), 4.02 (d, *J* = 12.8 Hz, 1H, $CH_a\underline{H_b}Bn$), 6.95-7.05 (m, 2H), 7.11-7.17 (m, 2H), 7.20-7.31 (m, 8H), 7.34-7.40 (m, 5H). ^{13}C NMR (100 MHz, MeOD) δ = 19.23, 20.09, 27.89, 36.66, 51.22, 57.06, 63.35, 126.93, 127.81, 128.87, 130.09, 130.30, 130.41, 131.08, 131.50, 132.78, 135.20, 136.91, 145.69, 148.55, 173.40. HRMS (ESI+) calcd. for $C_{32}H_{34}NO_2$ $[M+H]^+$: 464.2584; found 464.2585.

5.2.5.128. 2-Amino-5-(3,4-dimethylphenyl)-5,5-diphenylpentanoic acid (*rac*-**176**).

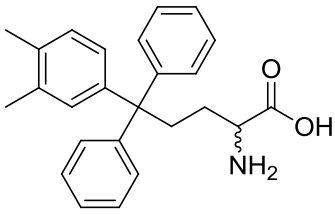

The title compound was prepared using an adaptation of the method reported by Ram *et al.*[197] A solution of benzyl amine *rac*-**175** (520 mg, 1.12 mmol), 10% Pd/C (250 mg) and ammonium formate (354 mg, 5.61 mmol) in anhydrous MeOH (7.5 mL) was heated at 60 °C for 2 h. After cooling to room temperature, the mixture was filtered through a thick pad of Celite®, the residue washed with MeOH (25 mL), and the filtrate concentrated *in vacuo*. Purification by flash chromatography [SiO_2; 0-25% MeOH in CH_2Cl_2] afforded the racemic amino acid *rac*-**176** as a white solid (346 mg, 83%). Mpt. 258-259 °C. ^{1}H (500

MHz, MeOD) δ = 1.57-1.65 (m, 2H, CH_2), 2.17 (s, 3H, CH_3), 2.20 (s, 3H, CH_3), 2.65-2.86 (m, 2H, CH_2), 3.53 (t, 1H, *J* = 6.0 Hz, CH), 6.97-7.05 (m, 2H), 7.13-7.17 (m, 2H), 7.22-7.31 (m, 8H). ^{13}C NMR (125 MHz, MeOD) δ = 19.22, 20.08, 28.93, 36.75, 56.33, 57.04, 126.92, 127.80, 128.85, 130.06, 130.33, 131.52, 135.18, 136.89, 145.72, 148.55, 148.59, 166.57. HRMS (ESI+) calcd. for $C_{25}H_{28}NO_2$ $[M+H]^+$: 374.2122; found: 374.2115. Anal. calcd. for $C_{25}H_{27}NO_2 \cdot H_2O$: C, 76.70; H, 7.47; N, 3.58. Found: C, 76.74; H, 7.27; N, 3.45.

5.2.5.129. 1-(1,1-Diphenylbut-3-en-1-yl)-4-methoxybenzene (**187**).

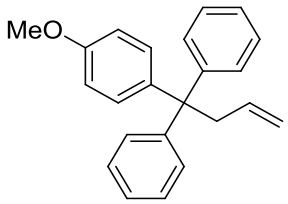

The title compound was prepared using an adaptation of the method reported by Kabalka *et al.*[192] *n*-Butyllithium (2.5 M in hexane, 20 mL, 50.0 mmol) was added by cautiously by slow dropwise addition over 15 min to a cooled (0 °C) solution of (4-methoxyphenyl)(diphenyl)methanol (10.00 g, 34.4 mmol) in anhydrous CH_2Cl_2 (40 mL), the reaction mixture allowed to warm to room temperature and stirred for 18 h. Allyltrimethylsilane (6.02 mL, 36.9 mmol) and iron trichloride (5.19 g, 32.0 mmol) were then added and the reaction stirred at room temperature for 24 h. The reaction was quenched with H_2O (25 mL), then aqueous HCl solution (0.25 M, 75 mL), and extracted with CH_2Cl_2 (3 x 75 mL). The combined organic layers were washed successively with aqueous HCl solution (0.25 M, 150 mL), H_2O (200 mL) and brine (200 mL), dried ($MgSO_4$) and concentrated *in vacuo*. Purification by flash chromatography [SiO_2; 0-6% EtOAc in hexane] afforded alkene **187** as a pale brown solid (6.44 g, 60%). Mpt. 71-72.5 °C. ^{1}H NMR (400 MHz, $CDCl_3$) δ = 3.42-3.45 (m, 2H, CH_2), 3.81 (s, 3H, CH_3), 4.95-4.98 (m, 1H), 5.03-5.08 (m, 1H), 5.65-5.73 (m, 1H), 6.81-6.84 (m, 2H), 7.13-7.17 (m, 2H), 7.19-7.26 (m, 6H), 7.26-7.30 (m, 4H). ^{13}C NMR (100 MHz, $CDCl_3$) δ = 45.84, 55.30, 55.77, 113.16, 117.30, 126.04, 127.86, 127.90, 129.48, 130.58, 136.25, 139.56, 147.76, 157.73. GC-MS (CI, methane) t_R = 17.12 min (*m/z* = 315.1, $[M+H]^+$). Anal. calcd. for $C_{23}H_{22}O$: C, 87.86; H, 7.05. Found: C, 86.38; H, 6.70.

5.2.5.130. 4-(4-Methoxyphenyl)-4,4-diphenylbutan-1-ol (**188**).

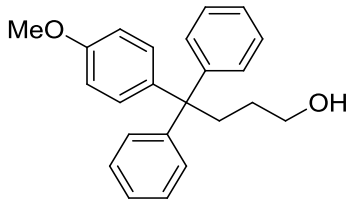

The title compound was prepared using an adaptation of the procedure reported by Starnes.[266] A solution of concentrated sulphuric acid (200 µL, 3.76 mmol) in anhydrous Et_2O (5.0 mL) was added slowly by dropwise addition to a solution of sodium borohydride (284 mg, 7.51 mmol) and alkene **187** (6.16 g, 19.6 mmol) in anhydrous diglyme (10 mL), and the reaction mixture stirred for 18 h at room temperature, then heated at 75 °C for a further 1 h. The reaction was cooled (0 °C) and treated successively with water (540 µL), aqueous NaOH (3.0 M, 2.49 mL) and hydrogen peroxide (30% in H_2O, 2.46 mL). The mixture was allowed to warm to room temperature and stirred for 5.5 h, then extracted with Et_2O (3 x 50 mL). The combined organics were washed with H_2O (75 mL), dried ($MgSO_4$) and concentrated *in vacuo*. Purification by flash chromatography [SiO_2; 0-35% EtOAc in hexane] afforded the primary alcohol **188** as a white solid (3.25 g, 50%). Mpt. 50-52 °C. ^{1}H NMR (500 MHz, $CDCl_3$) δ = 1.35-1.41 (m, 2H, CH_2), 2.61-2.66 (m, 2H, CH_2), 3.65 (t, 2H, J = 6.5 Hz, CH_2), 3.79 (s, 3H, CH_3), 6.79-6.83 (m, 2H), 7.16-7.22 (m, 4H), 7.24-7.30 (m, 8H). ^{13}C NMR (125 MHz, $CDCl_3$) δ = 29.34, 36.78, 55.31, 55.77, 63.50, 113.27, 125.92, 127.95, 129.20, 129.26, 130.36, 139.55, 147.77, 157.64. GC-MS (CI, methane) t_R = 18.34 min (m/z = 361.1, $[M+C_2H_5]^+$). Anal. calcd. for $C_{23}H_{24}O_2 \cdot H_2O$: C, 78.83; H, 7.48. Found: C, 79.16; H, 7.23.

5.2.5.131. 4-(4-Methoxyphenyl)-4,4-diphenylbutanal (**189**).

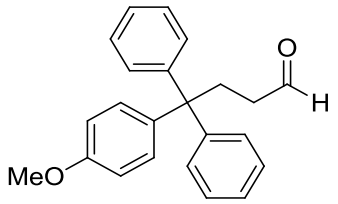

The title compound was prepared using an adaptation of the method developed by Dess *et al.* and the procedure reported by Wang *et al.*[138, 194] Dess-Martin periodinane (2.30 g, 5.42 mmol) was added to a solution of alcohol **188** (1.50 g, 4.51 mmol) in anhydrous CH_2Cl_2 (20 mL). The reaction was stirred at room temperature for 4.5 h, and then quenched cautiously with sodium thiosulfate solution (0.26 M in saturated aqueous $NaHCO_3$ solution, 100 mL) and extracted with CH_2Cl_2 (3 x 50 mL). The combined organic extracts were washed successively with saturated aqueous $NaHCO_3$ solution (100 mL), H_2O (150 mL) and brine (150 mL), dried ($MgSO_4$) and concentrated *in vacuo*. Purification by flash chromatography [SiO_2; 0-35% EtOAc in hexane] yielded aldehyde **189** as a white solid (1.238 g, 83%). Mpt. 112-113 °C. ^{1}H NMR (400 MHz, $CDCl_3$): 2.31-2.35 (m, 2H, CH_2), 2.89-2.93 (m, 2H, CH_2), 3.79 (s, 3H, CH_3), 6.80-6.84 (m, 2H), 7.16-7.21 (m, 4H), 7.26-7.29 (m, 8H), 9.63 (s, 1H, CHO). ^{13}C NMR (100 MHz, $CDCl_3$): 32.12, 41.27, 55.33, 113.49, 126.22, 128.18, 129.08, 130.21, 138.73, 147.01, 157.84, 201.91. HRMS (ESI+) calcd. for $C_{23}H_{23}O_2$ $[M+H]^+$: 331.1693; found: 331.1690. Anal. calcd. for $C_{23}H_{22}O_2$: C, 83.60; H, 6.71. Found: C, 83.22; H, 6.49.

5.2.5.132. 2-Fluoro-4-(4-methoxyphenyl)-4,4-diphenylbutan-1-ol (*rac*-**192**).

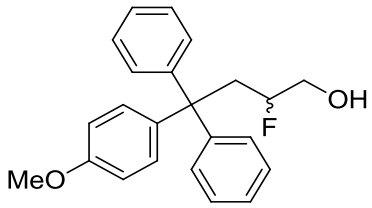

The title compound was prepared by adaptation of the method reported by Beeson *et al.*[202] THF (12.06 mL) and *i*-PrOH (1.34 mL) was added to a flask containing L-proline (62 mg, 0.54 mmol) and *N*-fluorobenzenesulfonimide (2.119 g, 6.72 mmol) and stirred until homogeneous. The mixture was cooled to -10 °C, aldehyde **189** (889 mg, 2.69 mmol) added and stirred for 2 h at ≤ -7.5 °C, before allowing the reaction to warm to room temperature and stirring for a further 21 h. The reaction mixture was cooled to -78 °C, diluted with Et_2O (15 mL) and filtered through a thin pad of silica, eluting with Et_2O.

Me_2S (2.5 mL, 34.00 mmol) was added to the filtrate, resulting in formation of a white precipitate. This suspension was washed successively with saturated aqueous $NaHCO_3$ solution (3 x 50 mL) and brine (50 mL), dried ($MgSO_4$), and concentrated *in vacuo*. The residual oil was dissolved in CH_2Cl_2 (15 mL) and EtOH (10 mL), cooled (0 °C), and sodium borohydride added (255 mg, 6.73 mmol). The reaction mixture was then allowed to warm to room temperature and stirred for 4 h. After cooling (0 °C), the reaction mixture was quenched cautiously with saturated aqueous NH_4Cl solution (100 mL), stirred for 10 min, then extracted with CH_2Cl_2 (3 x 50 mL). The organic extracts were washed successively with saturated aqueous $NaHCO_3$ solution (2 x 150 mL) and brine (150 mL), dried ($MgSO_4$) and concentrated *in vacuo*. Purification of the crude residue by flash chromatography [SiO_2; 0-35% EtOAc in hexane] afforded the β-fluorinated alcohol *rac*-**192** as a colourless oil (638 mg, 68%). The β,β-difluorinated alcohol **193** was also obtained as the minor product (165 mg, 17%; *vide infra*). ^{1}H NMR (400 MHz, $CDCl_3$) δ = 1.62-1.66 (m, 1H), 2.55-2.66 (m, 1H), 3.02-3.34 (m, 3H), 3.78 (s, 3H, CH_3), 4.39-4.57 (m, 1H), 6.78-6.83 (m, 2H), 7.16-7.32 (m, 12H). ^{19}F NMR (376.5 MHz, $CDCl_3$) δ = -180.84. ^{13}C NMR (100 MHz, $CDCl_3$) δ = 41.96 (d, J_{CF} = 21.4 Hz), 55.11 (d, J_{CF} = 3.5 Hz), 55.32, 65.54 (d, J_{CF} = 22.4 Hz), 93.06 (d, J_{CF} = 167.4 Hz), 113.48, 126.35, 128.20, 129.06 (d, J_{CF} = 2.2 Hz), 130.24, 138.59, 146.97, 157.90. GC-MS (CI, methane) t_R = 20.20 min (*m/z* = 379.1, $[M+C_2H_5]^+$). Anal. calcd. for $C_{23}H_{23}FO_2$: C, 78.83; H, 6.62. Found: C, 78.15; H, 6.18.

5.2.5.133. 2,2-Difluoro-4-(4-methoxyphenyl)-4,4-diphenylbutan-1-ol (**193**).

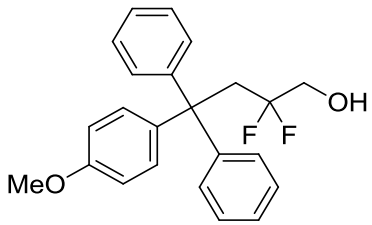

The title compound **193** was obtained as the minor product in the synthesis of *rac*-**192** as a colourless oil (165 mg, 17%). ^{1}H NMR (400 MHz, $CDCl_3$) δ = 1.76 (t, J = 7.0 Hz, 1H), 2.98-3.07 (m, 2H), 3.41 (t, J = 16.1 Hz, 2H, CH_2), 3.78 (s, 3H, CH_3), 6.78-6.83 (m, 2H), 7.16-7.21 (m, 2H), 7.24-7.30 (m, 6H), 7.35-7.39 (m, 4H). ^{19}F NMR (376.5 MHz, $CDCl_3$) δ = -98.71. ^{13}C NMR (100 MHz, $CDCl_3$) δ = 42.49 (t, J_{CF} = 22.9 Hz), 54.13, 55.30, 65.03 (t, J_{CF} = 32.0 Hz), 113.16, 122.90 (t, J_{CF} = 246.3 Hz), 126.26, 127.91, 129.16, 130.46, 138.48, 146.88, 157.85. GC-MS (CI, methane) t_R = 20.00 min (*m/z* = 397.1, $[M+C_2H_5]^+$). Anal. calcd. for $C_{23}H_{22}F_2O_2$: C, 74.98; H, 6.02. Found: C, 74.37; H, 6.65.

5.2.5.134. 2-Fluoro-4-(4-methoxyphenyl)-4,4-diphenylbutyl-4-methylbenzenesulfonate (*rac*-**194**).

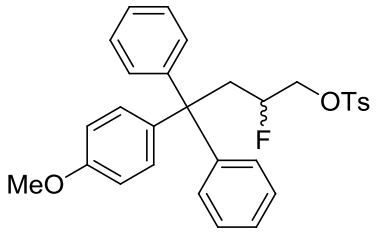

The title compound was prepared by an adaptation of the procedure reported by Moussa *et al.*[267] Tosyl chloride (220 mg, 1.73 mmol) and anhydrous pyridine (93 µL, 1.73 mmol) were added to a cooled (0 °C) solution of β-fluorinated *rac*-**192** in CH_2Cl_2 (4.6 mL) and stirred at room temperature for 3 h. The reaction was quenched with H_2O (5 mL) and saturated aqueous NH_4Cl solution (2.5 mL) and extracted with CH_2Cl_2 (3 x 20 mL). The combined organic extracts were dried ($MgSO_4$) and concentrated *in vacuo*. Purification of the crude residue by flash chromatography [SiO_2; 0-30% EtOAc in hexane] afforded the toyslate **194** as a colourless opaque oil [307 mg, 93% (based on 57% conversion)] and unreacted β-fluorinated alcohol *rac*-**192** (175 mg, 43%). ^{1}H NMR (400 MHz, $CDCl_3$) δ = 2.45 (s, 3H, CH_3), 2.49-2.61 (m, 1H), 3.22-3.36 (m, 1H), 3.42-3.59 (m, 2H), 3.78 (s, 3H, CH_3), 4.41-4.59 (m, 1H), 6.76-6.82 (m, 2H), 7.10-7.34 (m, 14H), 7.66-7.72 (m, 2H). ^{19}F NMR (376.5 MHz, $CDCl_3$) δ = -177.46. ^{13}C NMR (100 MHz, $CDCl_3$) δ = 21.80, 41.80 (d, J_{CF} = 21.7 Hz), 54.97 (d, J_{CF} = 3.7 Hz), 55.33, 71.14 (d, J_{CF} = 23.0 Hz), 88.92 (d, J_{CF} = 175.2 Hz), 113.61, 126.48, 128.08, 128.30, 128.88 (d, J_{CF} = 3.7 Hz), 129.94, 130.08, 132.76, 138.03, 145.04, 146.47, 158.00. GC-MS (CI, methane) t_R = 26.95 min (*m/z* = 503.8, $[M-H]^-$).

5.2.5.135. 1-(4-Azido-3-fluoro-1,1-diphenylbutyl)-4-methoxybenzene (*rac*-**195**).

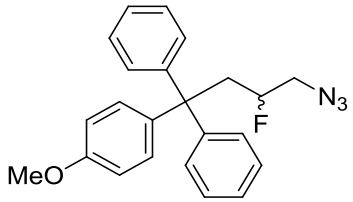

The title compound was prepared by an adaptation of the procedure reported by Jiang *et al.*[268] A solution of the tosylate *rac*-**194** (280 mg, 0.56 mmol) and sodium azide (91 mg, 1.40 mmol) in anhydrous DMSO (2.5 mL) was stirred at 40 °C for 18 h. The reaction mixture was diluted with brine (5 mL), extracted with Et_2O (3 x 10 mL), dried ($MgSO_4$) and concentrated *in vacuo*. Purification by flash chromatography [SiO_2; 0-15% EtOAc in

hexane] afforded the azide *rac*-**195** as a colourless oil, which was used directly in the next step (146 mg, 70%). ^{1}H NMR (400 MHz, $CDCl_3$) δ = 2.53-2.82 (m, 3H), 3.34-3.47 (m, 1H), 3.79 (s, 3H, CH_3), 4.46-4.64 (m, 1H), 6.80-6.85 (m, 2H), 7.16-7.24 (m, 4H), 7.25-7.33 (m, 8H). ^{19}F NMR (376.5 MHz, $CDCl_3$) δ = -174.12. ^{13}C NMR (100 MHz, $CDCl_3$) δ = 42.98 (d, J_{CF} = 21.7 Hz), 54.96 (d, J_{CF} = 21.7 Hz), 55.04, 55.35, 91.46 (d, J_{CF} = 172.2 Hz), 113.62, 126.51 (d, J_{CF} = 2.5 Hz), 128.34 (d, J_{CF} = 4.5 Hz), 128.95, 130.15, 138.23, 146.64, 158.01.

5.2.5.136. 2-Fluoro-4-(4-methoxyphenyl)-4,4-diphenylbutan-1-amine (*rac*-**182**).

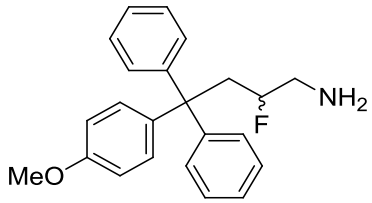

The title compound was prepared using an adaptation of the method reported by Ram *et al*.[197] A suspension of azide *rac*-**195** (130 mg, 0.35 mmol), 10% Pd/C (142 mg) and ammonium formate (110 mg, 1.74 mmol) in anhydrous MeOH (3.5 mL) was heated at 60 °C for 2 h. After cooling to room temperature, the mixture was filtered through a thick pad of Celite®, the residue washed with EtOAc (3 x 20 mL), and the filtrate concentrated *in vacuo*. Purification by flash chromatography [SiO_2; 0-20% MeOH in CH_2Cl_2] afforded the α-trifluoroamine *rac*-**182** as a colourless oil (79 mg, 65%). ^{1}H (400 MHz, $CDCl_3$) δ = 2.09-2.19 (m, 1H), 2.46-2.62 (m, 2H), 3.32-3.35 (m, 1H), 3.76 (s, 3H, CH_3), 4.27-4.42 (m, 1H), 6.80-6.84 (m, 2H), 7.14-7.33 (m, 12H). ^{19}F NMR (376.5 MHz, $CDCl_3$) δ = -180.78. ^{13}C NMR (125 MHz, $CDCl_3$) δ = 43.24 (d, J_{CF} = 21.7 Hz), 45.98 (d, J_{CF} = 22.2 Hz), 54.26, 55.00 (d, J_{CF} = 3.2 Hz), 92.99 (d, J_{CF} = 167.7 Hz), 112.88, 125.75, 127.57, 128.80, 130.00, 138.60, 147.07, 147.19, 157.98. HRMS (ESI+) calcd. for $C_{23}H_{25}NOF$ $[M+H]^+$: 350.1915; found 350.1914. LC-MS t_R = 12.92 min (*m/z* = 350.2, $[M+H]^+$; purity = 100%).

5.2.5.137. 1,1,1-Trifluoro-4-phenylbutan-2-ol (*rac*-**200**).

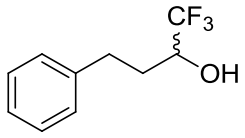

The title compound was prepared by an adaptation of the procedure reported by Crich *et al.*[269] TBAF (1.0 M in THF, 100 μL, 0.10 mmol) was added to a cooled (0 °C) solution of 3-phenylpropionaldehyde (263 μL, 2.00 mmol) and trimethyl(trifluoromethyl)silane solution (2.0 M in THF, 2.00 mL, 4.00 mmol) in THF (10 mL), and the reaction mixture stirred at room temperature for 21 h. TBAF (1.0 M in THF, 2.00 mL, 2.00 mmol) was then added, and the reaction stirred for a further 1.5 h at room temperature. The reaction was quenched with saturated aqueous NH_4Cl solution (10 mL) and extracted with EtOAc (3 x 10 mL). The combined organic extracts were then washed with brine (30 mL), dried ($MgSO_4$) and concentrated *in vacuo*. Purification by flash chromatography [SiO_2; 0-15% EtOAc in hexane] afforded the α-trifluoromethylalcohol *rac*-**200** as a yellow oil (249 mg, 61%). ^{1}H NMR (400 MHz, $CDCl_3$) δ = 1.89-2.08 (m, 2H), 2.19 (d, J = 6.0 Hz, 1H), 2.71-2.80 (m, 1H), 2.89-2.98 (m, 1H), 3.85-3.95 (m, 1H), 7.20-7.27 (m, 3H), 7.29-7.35 (m, 2H). ^{19}F NMR (376.5 MHz, $CDCl_3$) δ = -79.91. ^{13}C NMR (100 MHz, $CDCl_3$) δ = 30.95, 31.13, 69.71 (q, J_{CF} = 31.3 Hz), 123.93, 125.73 (q, J_{CF} = 280.0 Hz), 126.50, 128.61, 128.78, 140.53. GC-MS (EI, methane) t_R = 10.053 min (m/z = 205.1, $[M+H]^+$).

5.2.5.138. 1,1,1-Trifluoro-5-(4-methoxyphenyl)-5,5-diphenylpentan-2-ol (*rac*-**202**).

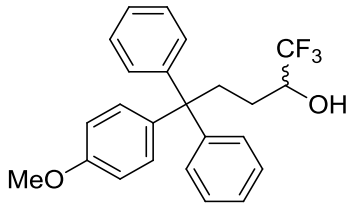

The title compound was prepared by an adaptation of the procedure reported by Crich *et al.*[269] TBAF (1.0 M in THF, 0.74 mL, 0.74 mmol) was added to a cooled (0 °C) solution of aldehyde **189** (2.46 g, 7.45 mmol) and trimethyl(trifluoromethyl)silane solution (2.0 M in THF, 7.40 mL, 14.80 mmol) in THF (30 mL), and the reaction mixture stirred at room temperature for 18 h. TBAF (1.0 M in THF, 2.00 mL, 2.00 mmol) was then added, and the reaction stirred for a further 4.5 h at room temperature. The reaction was quenched with saturated aqueous NH_4Cl solution (30 mL) and extracted with EtOAc (3 x 30 mL). The combined organic extracts were then washed with brine (80 mL), dried ($MgSO_4$) and concentrated *in vacuo*. Purification by flash chromatography [SiO_2; 0-15% EtOAc in

hexane] afforded *rac*-**202** as a colourless oil (2.29 g, 77%). ^{1}H NMR (400 MHz, $CDCl_3$) δ = 1.46-1.53 (m, 2H, CH_2), 2.19-2.24 (m, 1H), 2.50-2.59 (m, 1H), 2.97-3.05 (m, 1H), 3.77-3.85 (m, 4H), 6.80-6.84 (m, 2H), 7.16-7.22 (m, 4H), 7.25-7.31 (m, 8H). ^{19}F NMR (376.5 MHz, $CDCl_3$) δ = -79.75. ^{13}C NMR (100 MHz, $CDCl_3$) δ = 26.23, 35.76, 55.32, 55.72, 71.13 (q, J_{CF} = 30.8 Hz), 113.44, 125.15 (q, J_{CF} = 281.5 Hz), 126.14, 128.11, 129.14, 130.27, 138.97, 147.22, 147.26, 157.78. GC-MS (CI, methane) t_R = 17.62 min (*m/z* = 429.2, $[M+C_2H_5]^+$). Anal. calcd. for $C_{24}H_{23}F_3O_2$: C, 71.99; H, 5.79. Found: C, 72.39; H, 5.57.

5.2.5.139. 1,1,1-Trifluoro-5-(4-methoxyphenyl)-5,5-diphenylpentan-2-yl trifluoromethanesulfonate (*rac*-**203**).

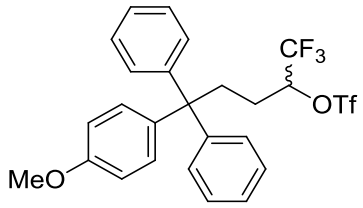

The title compound was prepared by an adaptation of the procedure reported by Jiang *et al.*[268] Trimethylsulphonic anhydride (1.0 M in CH_2Cl_2, 2.43 mL, 2.43 mmol) was added by slow dropwise addition over 15 min to a cooled (-50 °C) solution of alcohol *rac*-**202** (810 mg, 2.02 mmol) and anhydrous pyridine (327 µL, 4.05 mmol) in CH_2Cl_2. The reaction was stirred for 1 h at -50 °C and 1.5 h at ≤ -35 °C before allowing to warm to room temperature and quenching with with brine (15 mL). The aqueous layers were extracted with CH_2Cl_2 (2 x 10 mL), and the combined organic layers dried ($MgSO_4$) and concentrated *in vacuo*. Purification by flash chromatography [SiO_2; 0-20% EtOAc in hexane] afforded triflate *rac*-**203** as a colourless oil (834 mg, 78%). ^{1}H NMR (400 MHz, $CDCl_3$) δ = 1.70-1.89 (m, 2H, m, CH_2), 2.59-2.68 (m, 1H), 2.84-2.93 (m, 1H), 3.80 (s, 3H, CH_3), 4.88-4.97 (m, 1H, CH), 6.82-6.86 (m, 2H), 7.14-7.33 (m, 12H). ^{19}F NMR (376.5 MHz, $CDCl_3$) δ = -74.03 (q, *J* = 3.1 Hz), -76.20 (q, *J* = 3.1 Hz). ^{13}C NMR (100 MHz, $CDCl_3$) δ = 25.40, 34.59, 55.36, 55.50, 82.46 (q, J_{CF} = 34.3 Hz), 113.69, 118.49 (q, J_{CF} = 318.4 Hz), 122.07 (q, J_{CF} = 281.4 Hz), 126.48, 128.37, 128.44, 128.87, 130.03, 138.10, 146.40, 146.43, 158.02. GC-MS (CI, methane) t_R = 16.96 min (*m/z* = 561.2, $[M+C_2H_5]^+$). Anal. calcd. for $C_{25}H_{22}F_6O_4S$: C, 56.39; H, 4.16. Found: C, 56.30; H, 3.97.

5.2.5.140. 1,1,1-Trifluoro-5-(4-methoxyphenyl)-5,5-diphenylpentan-2-yl azide (*rac*-**204**).

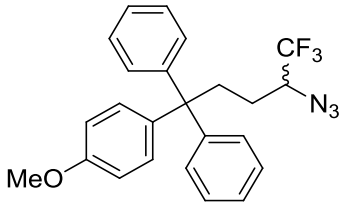

The title compound was prepared by an adaptation of the procedure reported by Jiang *et al.*[268] A solution of triflate *rac*-**203** (239 mg, 0.45 mmol) and sodium azide (80 mg, 1.23 mmol) in anhydrous DMSO (1.8 mL) was stirred at 40 °C for 18 h. The reaction mixture was diluted with brine (5 mL), extracted with Et_2O (3 x 10 mL), dried ($MgSO_4$) and concentrated *in vacuo*. Purification by flash chromatography [SiO_2; 0-20% EtOAc in hexane] afforded azide *rac*-**204** as a colourless oil (144 mg, 75%), which was used directly in the next step. ^{1}H NMR (400 MHz, $CDCl_3$) δ = 1.47-1.55 (m, 2H), 2.49-2.58 (m, 1H), 2.94-3.03 (m, 1H), 3.42-3.51 (m, 1H), 3.81 (s, 3H, CH_3), 6.82-6.87 (m, 2H), 7.17-7.24 (m, 4H), 7.27-7.32 (m, 8H). ^{19}F NMR (376.5 MHz, $CDCl_3$) δ = -74.96. ^{13}C NMR (100 MHz, $CDCl_3$) δ = 24.32, 36.19, 55.35, 55.74, 62.82 (q, J_{CF} = 29.8 Hz), 113.56, 124.94 (d, J_{CF} = 282.3 Hz), 126.31, 128.24, 129.05, 130.18, 138.60, 146.90, 146.95, 157.91.

5.2.5.141. 1,1,1-Trifluoro-5-(4-methoxyphenyl)-5,5-diphenylpentan-2-amine (*rac*-**184**).

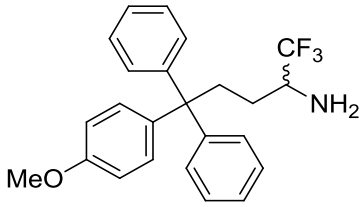

The title compound was prepared using an adaptation of the method reported by Ram *et al.*[197] A suspension of azide *rac*-**204** (142 mg, 0.33 mmol), 10% Pd/C (142 mg) and ammonium formate (105 mg, 1.67 mmol) in anhydrous MeOH (3.5 mL) was heated at 60 °C for 2 h. After cooling to room temperature, the mixture was filtered through a thick pad of Celite®, the residue washed with EtOAc (3 x 10 mL), and the filtrate concentrated *in vacuo*. Purification by flash chromatography [SiO_2; 0-40% EtOAc in hexane] afforded *rac*-**184** as a colourless oil (121 mg, 91%). ^{1}H NMR (500 MHz, $CDCl_3$) δ = 1.14-1.24 (m, 1H), 1.29-1.37 (br s, 2H, NH_2), 1.47-1.55 (m, 1H), 2.51-2.59 (m, 1H), 2.95-3.04 (m, 2H), 3.79 (s, 3H, CH_3), 6.79-6.83 (m, 2H), 7.16-7.21 (m, 4H), 7.24-7.30 (m, 8H). ^{19}F NMR (376.5 MHz, $CDCl_3$) δ = -78.87. ^{13}C NMR (125 MHz, $CDCl_3$) δ = 26.30, 36.81, 54.66 (d, J_{CF} = 29.3 Hz) 55.33, 55.85, 113.39, 126.09, 126.78 (q, J_{CF} = 282.3 Hz), 128.07, 129.17,

130.30, 139.11, 147.36, 147.39, 157.75. GC-MS (CI, methane) t_R = 17.55 min (*m/z* = 400.2, $[M+H]^+$). Anal. calcd. for $C_{24}H_{24}F_3NO$: C, 72.16; H, 6.06; N, 3.51. Found: C, 72.75; H, 6.28; N, 3.10.

5.2.5.142. 3-(Tritylsulfanyl)propanoic acid (**209**).

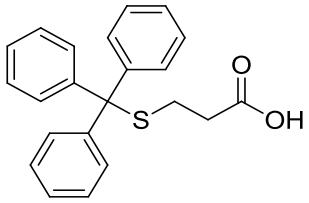

A solution of 3-mercaptopropionic acid (1.31 mL, 15.0 mmol) and triphenylmethanol (4.56 g, 17.5 mmol) in trifluoroacetic acid (15 mL) and CH_2Cl_2 (10 mL) was stirred for 2 h at room temperature. The volatiles were removed *in vacuo* and the crude suspended in H_2O (50 mL). The mixture was filtered, and the white precipitate washed successively with H_2O (100 mL), petroleum ether [(60/80), 50 mL], and Et_2O (50 mL). Purification by flash chromatography [SiO_2; 50-100% EtOAc in hexane] afforded acid **209** as a white solid (3.34 g, 55%). Mpt. 207-210 °C (lit.[270] 203-204 °C). ^{1}H NMR (125 MHz, DMSO-d_6) δ = 2.17 (t, *J* = 7.2 Hz, 2H, CH_2), 2.29 (t, *J* = 7.2 Hz, 2H, CH_2), 7.23-7.27 (m, 3H), 7.31-7.36 (m, 12H). ^{13}C NMR (125 MHz, DMSO-d_6) δ = 26.67, 32.88, 66.16, 126.72, 128.03, 129.08, 144.35, 172.67. HRMS (ESI-) calcd. for $C_{22}H_{19}O_2S$ $[M-H]^-$: 347.1111; found: 347.1120. Anal. calcd. for $C_{22}H_{20}O_2S$: C, 75.83; H, 5.79. Found: C, 75.55; H, 5.52.

5.2.5.143. 3-(Tritylsulfanyl)propanamide (**210**).

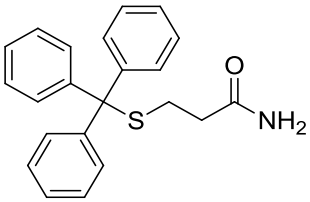

The title compound was prepared by an adaptation of the procedure reported by Dale *et al.*[271] Oxalyl chloride (100 μL, 1.17 mmol) and a catalytic amount of DMF (1 drop) was added to a solution of 3-(tritylsulfanyl)propanoic acid **209** (349 mg, 1.00 mmol) in anhydrous CH_2Cl_2 (3 ml) and stirred for 1.5 h at room temperature. Ammonia (0.5 M in dioxane, 7.4 mL, 3.70 mmol) was then added and the reaction stirred for 18 h at room temperature. The volatiles were removed *in vacuo*, and the residue partitioned between CH_2Cl_2 (10 mL) and saturated aqueous sodium carbonate solution (10 mL). The aqueous layer was extracted with CH_2Cl_2 (2 x 10 mL), and the combined organic layers washed

successively with H_2O (2 x 30 mL) and brine (30 mL), dried ($MgSO_4$) and concentrated *in vacuo*. Purification by flash chromatography [SiO_2; 0-15% MeOH in CH_2Cl_2 with 1% NH_4OH] afforded amide **210** as a white solid (195 mg, 56%). Mpt. 175-177 °C. ^{1}H NMR (400 MHz, DMSO-d_6) δ = 2.12 (t, J = 7.3 Hz, 2H, CH_2), 2.23 (t, J = 7.4 Hz, 2H, CH_2), 6.80 (s, 1H, NH_2), 7.23-7.27 (m, 3H), 7.29-7.37 (m, 13H). ^{13}C NMR (100 MHz, DMSO-d_6) δ = 27.32, 33.71, 65.95, 126.69, 128.00, 129.08, 144.47, 172.10. HRMS (ESI+) calcd. for $C_{21}H_{21}NOSNa$ $[M+Na]^+$: 370.1236; found: 370.1236. Anal. calcd. for $C_{22}H_{21}NOS$: C, 76.04; H, 6.09; N, 4.03. Found: C, 75.53; H, 5.31; N, 3.83.

5.2.5.144. (2*R*)-2-Amino-3-(tritylsulfanyl)-*N*-methylpropanamide (**216**).

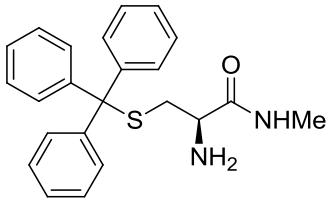

Methanamine hydrochloride (405 mg, 6.0 mmol), followed by triethylamine (2.51 mL, 18.0 mmol) and T3P® (50% in DMF, 1.52 mL, 2.60 mmol) were added to a cooled (0 °C) solution of *N*-(*tert*-butoxycarbonyl)-*S*-trityl-L-cysteine (927 mg, 2.0 mmol) in anhydrous THF (4 mL), and stirred at room temperature for 24 h. The reaction was quenched with H_2O (10 mL) and the volatiles were removed *in vacuo* and the crude residue extracted with CH_2Cl_2 (3 x 10 mL). The organic extracts were washed successively with aqueous HCl (0.125 M), H_2O, and brine (30 mL each), dried ($MgSO_4$), then concentrated *in vacuo*. Purification by flash chromatography [SiO_2; 0-10% MeOH in CH_2Cl_2] afforded (*R*)-*tert*-butyl (1-(methylamino)-1-oxo-3-(tritylthio)propan-2-yl)carbamate (**212**) as an off-white solid (669 mg, 70%), which was taken directly to the next step. A solution of **212** (669 mg, 1.40 mmol) was stirred in trifluoroacetic acid (2 mL) for 4 h at room temperature. The volatiles were removed *in vacuo*, and the crude basified (*circa.* pH 10) with saturated aqueous sodium carbonate solution and extracted with CH_2Cl_2 (3 x 10 mL). The combined organic extracts were dried ($MgSO_4$) and concentrated *in vacuo*. Purification by flash chromatography [SiO_2; 0-20% MeOH in CH_2Cl_2] afforded the crude product, which was dissolved in CH_2Cl_2 (20 mL) and washed with aqueous LiCl solution (5% *w/v*, 2 x 20 mL), brine (20 mL), dried ($MgSO_4$) and concentrated *in vacuo* to afford **216** as light brown oil (53 mg, 11%). ^{1}H NMR (500 MHz, MeOD) δ = 2.35-2.39 (m, 1H), 2.52-2.56 (m, 1H), 2.71 (s, 3H, CH_3), 3.09-3.12 (m, 1H), 7.20-7.24 (m, 3H), 7.27-7.32 (m, 6H), 7.36-7.43 (m, 6H). ^{13}C NMR (100 MHz, MeOD) δ = 26.22, 38.23, 55.33, 67.85, 127.89, 128.97, 130.75, 146.08, 176.08. HRMS (ESI+) calcd. for $C_{23}H_{25}N_2OS$ $[M+H]^+$: 377.1682; found:

307.1672. Anal. calcd. for $C_{23}H_{24}N_2OS \cdot ½H_2O$: C, 71.66; H, 6.54; N, 7.27. Found: C, 72.01; H, 6.27; N, 7.05.

5.2.5.145. (2*R*)-2-Amino-3-(tritylsulfanyl)-*N*,*N*-dimethylpropanamide (**217**).

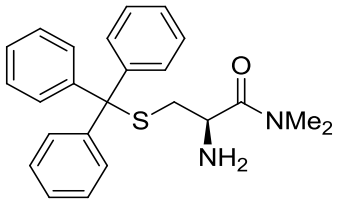

Dimethylamine hydrochloride (489 mg, 6.0 mmol), followed by triethylamine (2.51 mL, 18.0 mmol) and T3P® (50% in DMF, 1.52 mL, 2.60 mmol) were added to a cooled (0 °C) solution of *N*-(*tert*-butoxycarbonyl)-*S*-trityl-L-cysteine (927 mg, 2.0 mmol) in anhydrous THF (4 mL), and stirred at room temperature for 26 h. The reaction was quenched with H_2O (10 mL) and the volatiles were removed *in vacuo* and the crude residue extracted with CH_2Cl_2 (3 x 10 mL). The combined organic extracts were washed successively with aqueous HCl (0.125 M), H_2O, and brine (30 mL each), dried ($MgSO_4$), then concentrated *in vacuo*. Purification by flash chromatography [SiO_2; 0-10% MeOH in CH_2Cl_2] afforded the tertiary amide *(R)*-*tert*-butyl (1-(dimethylamino)-1-oxo-3-(tritylthio)propan-2-yl)carbamate (**213**) as an off-white solid (641 mg, 65%), which was taken directly to the next step. A solution of **213** (641 mg, 1.31 mmol) was stirred in trifluoroacetic acid (2 mL) for 2.5 h at room temperature. The volatiles were removed *in vacuo*, and the crude basified (*circa.* pH 10) with saturated aqueous sodium carbonate solution. The aqueous mixture was extracted with CH_2Cl_2 (3 x 10 mL) and the combined organic layers washed successively with H_2O (2 x 30 mL), brine (30 mL), dried ($MgSO_4$) and concentrated *in vacuo*. Purification by flash chromatography [SiO_2; 0-18% MeOH in CH_2Cl_2] afforded **217** as a pale brown oil (343 mg, 67%). ^{1}H NMR (400 MHz, MeOD) δ = 2.35-2.40 (m, 1H), 2.57-2.62 (m, 1H), 2.78 (s, 3H, CH_3), 2.87 (s, 3H, CH_3), 3.37-3.41 (m, 1H), 7.20-7.32 (m, 9H), 7.37-7.43 (m, 6H). ^{13}C NMR (100 MHz, MeOD) δ = 36.10, 37.59, 37.95, 51.21, 68.17, 127.95, 129.02, 130.80, 146.09, 174.94. HRMS (ESI+) calcd. for $C_{24}H_{27}N_2OS$ $[M+H]^+$: 391.1839; found: 391.1827. Anal. calcd. for $C_{24}H_{26}N_2OS \cdot ¼H_2O$: C, 72.97; H, 6.76; N, 7.09. Found: C, 72.39; H, 6.14; N, 6.76.

5.2.5.146. ((2*R*)-3-(Tritylsulfanyl)-1-(methoxy(methyl)amino)-1-oxopropan-2-yl)carbamate (**214**).

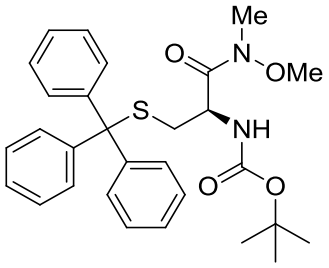

N,*O*-Dimethylhydroxylamine hydrochloride (878 mg, 9.0 mmol), followed by triethylamine (3.76 mL, 27.0 mmol) and T3P® (50% in DMF, 2.630 mL, 4.50 mmol) were added to a cooled (0 °C) solution of *N*-(*tert*-butoxycarbonyl)-*S*-trityl-L-cysteine (1.39 g, 3.0 mmol) in anhydrous THF (6 mL) and stirred at room temperature for 48 h. The reaction was quenched with saturated aqueous $NaHCO_3$ (15 mL), the volatiles removed *in vacuo*, and the mixture extracted with CH_2Cl_2 (3 x 15 mL). The organic extracts were washed successively with aqueous $CuSO_4$ solution (10% *w/v*, 50 mL), H_2O (2 x 50 mL) and brine (75 mL), dried ($MgSO_4$), then concentrated *in vacuo*. Purification by flash chromatography [SiO_2; 0-40% EtOAc in hexane] afforded **214** as a white solid (645 mg, 64%). Mpt. 98-100 °C. ^{1}H NMR (500 MHz, $CDCl_3$) δ = 1.43 (s, 9H, 3 x CH_3), 2.35-2.41 (m, 1H, CH_2), 2.53-2.57 (m, 1H, CH_2), 3.14 (s, 3H, CH_3), 3.64 (m, 3H, CH_3), 4.75 (br s, 1H, NH), 5.09-5.13 (m, 1H, CH), 7.18-7.23 (m, 3H), 7.25-7.30 (m, 6H), 7.38-7.42 (m, 6H). ^{13}C NMR (125 MHz, $CDCl_3$) δ = 28.49, 32.30, 34.29, 49.89, 61.69, 66.83, 126.87, 128.06, 129.73, 144.65, 155.32, 171.27. HRMS (ESI+) calcd. for $C_{29}H_{35}N_2O_4S$ $[M+H]^+$: 507.2312; found: 507.2299. Anal. calcd. for $C_{29}H_{34}N_2O_4S \cdot ¼H_2O$: C, 68.14; H, 6.80; N, 5.48. Found: C, 68.29; H, 6.69; N, 5.34.

5.2.5.147. (2*R*)-2-Amino-3-(tritylsulfanyl)-*N*-methoxy-*N*-methylpropanamide (**218**).

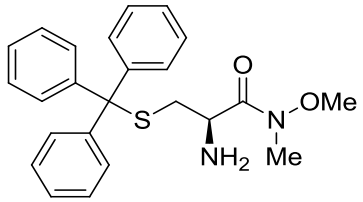

A solution of **214** (125 mg, 0.246 mmol) was stirred in trifluoroacetic acid (1 mL) for 1.5 h at room temperature. The volatiles were removed *in vacuo*, and the crude basified (*circa.* pH 10) with saturated aqueous sodium carbonate solution. The aqueous mixture was extracted with CH_2Cl_2 (3 x 10 mL) and the combined organics layers concentrated *in vacuo*. Purification by flash chromatography [SiO_2; 0-12% MeOH in CH_2Cl_2] afforded

218 as a colourless oil (44 mg, 43%). ^{1}H NMR (500 MHz, MeOD) δ = 2.30-2.36 (m, 1H, CH_2), 2.57-2.62 (m, 1H, CH_2), 3.14 (s, 3H, CH_3), 3.58-3.68 (m, 4H), 7.20-7.25 (m, 3H), 7.27-7.32 (m, 6H), 7.37-7.44 (m, 6H). ^{13}C NMR (125 MHz, MeOD) δ = 32.52, 37.34, 51.27, 62.24, 67.96, 127.90, 128.98, 130.77, 146.08, 173.27. HRMS (ESI+) calcd. for $C_{24}H_{27}N_2O_2S$ $[M+H]^+$: 407.1788; found: 407.1785. Anal. calcd. for $C_{24}H_{26}N_2O_2S \cdot \frac{1}{10}CH_2Cl_2$: C, 69.74; H, 6.36; N, 6.75. Found: C, 69.59; H, 5.62; N, 6.61

5.2.5.148. Methyl (2*R*)-2-amino-3-(tritylsulfanyl)propanoate hydrochloride (**219**).

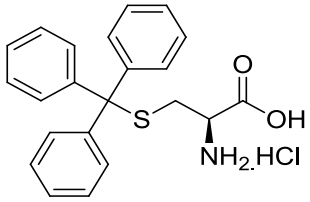

The title compound was prepared by an adaptation of the procedure reported by Rudolph *et al.*[272] Thionyl chloride (1.91 mL, 26.3 mmol) was added to a cooled (0 °C) suspension of *S*-trityl L-cysteine (1.27 g, 3.5 mmol) in anhydrous MeOH (25 mL). The reaction mixture was allowed to warm to room temperature, then refluxed for 6 h. After cooling to room temperature, the volatiles were removed *in vacuo*, to afford the crude methyl ester **219** as an off-white solid, which was used without further purification (1.43 g, 98%). Mpt. 79-81 °C (lit.[272] 78 °C). ^{1}H NMR (125 MHz, MeOD) δ = 2.75-2.85 (m, 2H, CH_2), 3.32-3.36 (m, 1H, CH), 3.76 (s, 3H, CH_3), 7.25-7.37 (m, 9H), 7.41-7.47 (m, 6H). ^{13}C NMR (125 MHz, MeOD) δ = 32.89, 53.07, 53.87, 68.77, 128.34, 129.31, 130.61, 145.16, 169.23. HRMS (ESI+) calcd. for $C_{23}H_{24}NO_2S$ $[M+H]^+$: 278.1522; found: 378.1523.

5.2.5.149. (2*R*)-2-Amino-*N*-hydroxy-3-(tritylsulfanyl)propanamide (**220**).

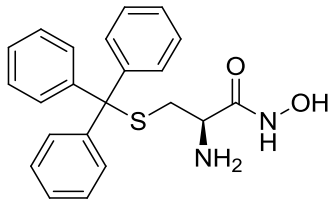

The title compound was prepared by an adaptation of the procedure reported by Tegoni *et al.*[212] Conc. aqueous NH_4OH (1 mL) was added to chloroform (4 mL) and stirred for 15 minutes at room temperature. The organic layer was separated, dried ($MgSO_4$) and the hydrochloride salt **219** (414 mg, 1.00 mmol) added. After the solution was stirred for 1 h at room temperature, the precipitate was filtered, and the filtrate concentrated *in vacuo* to give the methyl ester as a light brown oil. Separately, a solution of potassium hydroxide (336 mg, 5.98 mmol) in methanol (3.56 mL) was added to a solution of hydroxylamine hydrochloride (418 mg, 6.01 mmol) in methanol (3.05 mL) at 0 °C and stirred for 20 min. The precipitate was filtered and washed with methanol (1 mL), and approximately half of the methanolic hydroxylamine filtrate added to the crude methyl ester. The reaction mixture was stirred at room temperature for 24 h, then a further 24 h at 5 °C. The solution was filtered, washing with chloroform (5 mL). The filtrate was concentrated *in vacuo*, and the crude recrystallised from hot methanol and kept at 5 °C for 24 h, during which time a precipitate formed. After filtration, the pale orange precipitate was recrystallised from hot methanol and kept at 5 °C for 48 h. The solution was filtered again, and the precipitate collected, dissolved in CH_2Cl_2 and the solvent removed under reduced pressure to afford the hydroxamic acid **220** as a pale orange solid (90 mg, 24%). Mpt. 96-99 °C. ^{1}H NMR (400 MHz, DMSO-d_6) δ = 2.08-2.15 (m, 1H), 2.27-2.34 (m, 1H), 3.05-3.10 (m, 1H), 7.20-7.38 (m, 15H), 8.86 (br s, 1H), 10.79 (br s, 1H). ^{13}C NMR (100 MHz, DMSO-d_6) δ = 36.81, 51.92, 65.74, 126.99, 127.99, 129.07, 144.42, 169.38. HRMS (ESI-) calcd. for $C_{22}H_{21}N_2O_2S$ $[M-H]^-$: 377.1329; found: 377.1335. Anal. calcd. for $C_{22}H_{22}N_2O_2S \cdot ⅓CH_2Cl_2$: C, 65.98; H, 5.62; N, 6.89. Found: C, 66.49; H, 5.06; N, 7.13.

5.3. Molecular modeling

5.3.1. Calculation of ligand efficiencies

The equation for calculating ligand efficiencies is: LE = $-\Delta G/HAC \approx -RT.\ln(K_i^{app})/HAC$, where ΔG is the change in Gibbs free energy, T is the absolute temperature, R represents the gas constant and HAC is the heavy atom count for non-hydrogen atoms.[216] Ligand efficiencies were calculated in Pipeline Pilot 7.4 for Windows (Accelerys Software, San Diego, USA).

5.3.2. Calculation of physicochemical properties

Physicochemical properties were calculated in Pipeline Pilot 7.4 for Windows (Accelerys Software, San Diego, USA). The calculated ALog P and cLog $D_{7.4}$ values are based on the atom based method of Ghose and Cribben.[273] The cLog S values were calculated by the method of Tetko *et al.*[274]

Appendix

The calculated physicochemical properties for all tested inhibitor are provided in Table 24.

Table 24 – Calculated physicochemical properties for all tested inhibitors.

Cmpd	Molecular Formula	MWt.	ALog P	cLog $D_{7.4}$	cLog S	Polar Surface Area	H-bond acceptors	H-bond donors
6	$C_{22}H_{21}NO_2S$	363.473	1.739	1.739	-7.315	88.62	4	2
10	$C_{23}H_{23}NO_3S$	393.499	1.723	1.723	-7.411	97.85	5	2
16	$C_{21}H_{21}NS$	319.463	4.601	3.64	-7.566	51.32	2	1
101	$C_{22}H_{20}ClNO_2S$	397.918	2.404	2.404	-8.086	88.62	4	2
102	$C_{21}H_{20}FNS$	337.454	4.807	3.845	-7.579	51.32	2	1
103	$C_{22}H_{20}ClNO_2S$	397.918	2.404	2.404	-8.089	88.62	4	2
104	$C_{21}H_{20}ClNS$	353.908	5.266	4.304	-8.336	51.32	2	1
105	$C_{21}H_{20}BrNS$	398.359	5.35	4.388	-8.838	51.32	2	1
106	$C_{22}H_{23}NS$	333.49	5.087	4.126	-8.118	51.32	2	1
107	$C_{23}H_{25}NS$	347.516	5.544	4.582	-8.600	51.32	2	1
108	$C_{24}H_{27}NS$	361.543	5.795	4.834	-8.898	51.32	2	1
109	$C_{24}H_{27}NS$	361.543	6	5.038	-9.113	51.32	2	1
110	$C_{22}H_{20}F_3NS$	387.461	5.543	4.582	-8.464	51.32	2	1
111	$C_{22}H_{23}NOS$	349.489	4.585	3.623	-7.636	60.54	3	1
112	$C_{22}H_{23}NS_2$	365.555	5.143	4.182	-8.566	76.62	3	1
113	$C_{22}H_{20}F_3NOS$	403.461	6.721	5.76	-8.622	60.54	3	1
114	$C_{24}H_{23}NO_3S$	405.509	1.479	1.479	-7.674	105.68	5	2
115	$C_{23}H_{23}NOS$	361.5	4.341	3.38	-7.915	68.39	3	1
116	$C_{22}H_{23}NS$	333.49	5.087	4.582	-8.116	51.32	2	1
117	$C_{23}H_{25}NS$	347.516	5.544	5.038	-8.602	51.32	2	1
118	$C_{22}H_{23}NOS$	349.489	4.585	4.079	-7.672	60.54	3	1

Table 24 (continued) – Calculated physicochemical properties for all tested inhibitors.

Cmpd	Molecular Formula	MWt.	ALog P	cLog $D_{7.4}$	cLog S	Polar Surface Area	H-bond acceptors	H-bond donors
119	$C_{23}H_{25}NOS$	363.516	4.933	4.428	-8.041	60.54	3	1
120	$C_{22}H_{20}F_3NOS$	403.461	6.721	6.215	-8.776	60.54	3	1
121	$C_{24}H_{23}NO_3S$	405.509	1.479	1.479	-7.732	105.68	5	2
122	$C_{23}H_{23}NOS$	361.5	4.341	3.38	-7.915	68.39	3	1
123	$C_{22}H_{21}NO_3S$	379.472	1.497	1.497	-6.546	108.85	5	3
124	$C_{22}H_{21}NO_3S$	379.472	1.497	1.497	-6.671	108.85	5	3
125	$C_{21}H_{21}NOS$	335.463	4.359	3.329	-6.903	71.54	3	2
126	$C_{22}H_{20}N_2S$	344.473	4.48	3.519	-7.856	75.1	3	1
127	$C_{22}H_{24}N_2S$	348.504	3.707	1.774	-7.692	77.34	3	2
128	$C_{24}H_{26}N_2OS$	390.541	3.728	2.767	-8.202	80.42	3	2
129	$C_{22}H_{21}NO_2S$	363.473	1.752	1.791	-7.245	88.62	4	2
130	$C_{23}H_{22}N_2O_3S$	406.497	0.741	0.742	-7.191	131.71	5	3
131	$C_{22}H_{22}N_2OS$	362.488	3.603	2.642	-7.402	94.4	3	2
132	$C_{23}H_{24}N_2OS$	376.514	3.809	2.848	-7.711	80.42	3	2
133	$C_{24}H_{26}N_2OS$	390.541	4.015	3.054	-7.596	71.62	3	1
134	$C_{22}H_{23}NO_2S_2$	397.554	4.127	3.166	-7.619	93.84	4	1
135	$C_{22}H_{20}N_2S$	344.473	4.48	3.974	-7.908	75.1	3	1
136	$C_{22}H_{23}NOS$	349.489	3.997	3.491	-7.363	71.54	3	2
137	$C_{22}H_{24}N_2S$	348.504	3.707	2.202	-7.722	77.34	3	2
138	$C_{24}H_{26}N_2OS$	390.541	3.728	3.223	-8.249	80.42	3	2
139	$C_{22}H_{22}N_2OS$	362.488	3.603	3.098	-7.49	94.4	3	2
140	$C_{23}H_{24}N_2OS$	376.514	3.809	3.303	-7.784	80.42	3	2

Table 24 (continued) – Calculated physicochemical properties for all tested inhibitors.

Cmpd	Molecular Formula	MWt.	ALog P	cLog $D_{7.4}$	cLog S	Polar Surface Area	H-bond acceptors	H-bond donors
141	$C_{24}H_{26}N_2OS$	390.541	4.015	3.509	-7.668	71.62	3	1
142	$C_{22}H_{23}NO_2S_2$	397.554	4.127	3.621	-7.728	93.84	4	1
143	$C_{20}H_{20}N_2S$	320.451	3.451	2.847	-6.983	64.21	3	1
144	$C_{18}H_{18}N_2S_2$	326.479	3.463	2.46	-6.971	92.45	3	1
145	$C_{18}H_{18}N_2OS$	310.413	2.905	1.9	-6.136	77.35	3	1
146	$C_{23}H_{25}NS$	347.516	5.574	5.068	-8.667	51.32	2	1
rac-**147**	$C_{21}H_{20}ClNOS$	369.908	5.023	4.451	-7.664	71.54	3	2
rac-**148**	$C_{23}H_{25}NOS$	363.516	5.301	4.729	-7.902	71.54	3	2
rac-**149**	$C_{22}H_{23}NOS$	349.489	4.845	4.273	-7.439	71.54	3	2
rac-**150**	$C_{23}H_{22}N_2S$	358.499	4.966	4.46	-8.395	75.1	3	1
rac-**151**	$C_{23}H_{24}N_2OS$	376.514	4.09	3.584	-7.934	94.4	3	2
152	$C_{22}H_{22}FNS$	351.48	5.293	4.787	-7.896	51.32	2	1
153	$C_{22}H_{22}FNS$	351.48	5.293	4.787	-7.932	51.32	2	1
154	$C_{23}H_{22}FNO_3S$	411.489	1.928	1.929	-7.3	97.85	5	2
155	$C_{22}H_{22}FNOS$	367.48	4.79	4.284	-7.512	60.54	3	1
156	$C_{22}H_{22}FNOS$	367.48	4.79	4.284	-7.624	60.54	3	1
157	$C_{21}H_{19}Cl_2NS$	388.353	5.93	5.424	-9.1	51.32	2	1
158	$C_{24}H_{25}NO_2S$	391.526	2.712	2.712	-8.373	88.62	4	2
159	$C_{23}H_{25}NS$	347.516	5.574	5.068	-8.677	51.32	2	1
160	$C_{25}H_{27}NO_2S$	405.552	3.168	3.168	-8.824	88.62	4	2
161	$C_{24}H_{27}NS$	361.543	6.03	5.524	-9.163	51.32	2	1
162	$C_{26}H_{27}NO_2S$	417.563	3.252	3.253	-9.169	88.62	4	2

Table 24 (continued) – Calculated physicochemical properties for all tested inhibitors.

Cmpd	Molecular Formula	MWt.	ALog P	cLog $D_{7.4}$	cLog S	Polar Surface Area	H-bond acceptors	H-bond donors
163	$C_{25}H_{27}NS$	373.554	6.114	5.609	-9.563	51.32	2	1
rac-**176**	$C_{25}H_{27}NO_2$	373.487	2.802	2.895	-8.339	63.32	3	2
181	$C_{23}H_{25}NO$	331.451	4.675	3.855	-7.683	35.25	2	1
rac-**182**	$C_{23}H_{24}FNO$	349.441	4.648	4.639	-7.497	35.25	2	1
183	$C_{23}H_{23}F_2NO$	367.432	4.452	4.452	-7.289	35.25	2	1
rac-**184**	$C_{24}H_{24}F_3NO$	399.449	5.711	5.711	-8.739	35.25	2	1
210	$C_{21}H_{19}NOS$	333.447	4.284	4.284	-7.151	68.39	2	1
215	$C_{22}H_{22}N_2OS$	362.488	3.59	2.669	-7.412	94.4	3	2
216	$C_{23}H_{24}N_2OS$	376.514	3.796	3.65	-7.673	80.42	3	2
217	$C_{24}H_{26}N_2OS$	390.541	4.002	3.857	-7.558	71.62	3	1
218	$C_{24}H_{26}N_2O_2S$	406.54	3.848	3.607	-7.526	80.85	4	1
220	$C_{22}H_{22}N_2O_2S$	378.487	3.603	2.663	-7.265	100.65	4	3
rac-**221**	$C_{23}H_{23}NO_2$	345.434	1.83	1.923	-7.280	63.32	3	2
222	$C_{22}H_{23}N$	301.425	4.691	3.872	-7.581	26.01	1	1
223	$C_{22}H_{22}ClN$	335.87	5.356	4.536	-8.347	26.01	1	1
rac-**224**	$C_{24}H_{25}NO_2$	359.461	2.316	2.409	-7.803	63.32	3	2
225	$C_{23}H_{25}N$	315.451	5.178	4.358	-8.133	26.01	1	1
226	$C_{24}H_{27}N$	329.478	5.634	4.814	-8.615	26.01	1	1
227	$C_{25}H_{29}N$	343.504	5.886	5.066	-8.910	26.01	1	1
rac-**228**	$C_{24}H_{25}NO_2$	359.461	2.316	2.409	-7.807	63.32	3	2

Table 24 (continued) – Calculated physicochemical properties for all tested inhibitors.

Cmpd	Molecular Formula	MWt.	ALog P	cLog $D_{7.4}$	cLog S	Polar Surface Area	H-bond acceptors	H-bond donors
229	$C_{23}H_{25}N$	315.451	5.178	4.358	-8.131	26.01	1	1
230	$C_{24}H_{27}N$	329.478	5.634	4.814	-8.618	26.01	1	1
rac-**231**	$C_{24}H_{25}NO_3$	375.46	1.813	1.906	-7.372	72.55	4	2
232	$C_{23}H_{24}FNO$	349.441	4.881	4.061	-7.508	35.25	2	1
rac-**233**	$C_{23}H_{25}NO$	331.451	4.936	4.116	-7.446	46.25	2	2
rac-**234**	$C_{24}H_{27}NO_2$	361.477	4.164	3.805	-7.285	55.48	3	2
rac-**235**	$C_{24}H_{25}N_5O$	399.488	4.131	3.189	-7.403	89.71	5	2
Mean	n/a	363.742	4.048	3.533	-7.873	67.32	2.89	1.50

References

1. Newton, I. Volume 1, 1661-1675. In *The Correspondence of Isaac Newton*, Turnbull, H. W., Ed. Cambridge University Press: Cambridge, England, 1959; Vol. 1, p 416.
2. Nixon, R. M. "The National Cancer Act of 1971". *Public Law 92-218*, U.S. Senate, United States Statutes at Large, 1971; Senate Bill 1828.
3. Childhood Cancer - Great Britain & UK (November 2011). In *Cancer Stats report*, Cancer Research UK: 2011.
4. Mitry, E.; Rachet, B.; Quinn, M. J.; Cooper, N.; Coleman, M. P. Survival from cancer of the pancreas in England and Wales up to 2001. *British Journal of Cancer* **2008,** 99, S21-S23.
5. Hanahan, D.; Weinberg, R. A. The Hallmarks of Cancer. *Cell* **2000,** 100, 57-70.
6. Chabner, B. A.; Roberts, T. G. Chemotherapy and the war on cancer. *Nature Reviews Cancer* **2005,** 5, 65-72.
7. Hanahan, D.; Weinberg, Robert A. Hallmarks of Cancer: The Next Generation. *Cell* **2011,** 144, 646-674.
8. Sporn, M. B. The war on cancer. *The Lancet* **1996,** 347, 1377-1381.
9. Pollard, T. D.; Earnshaw, W. C. *Cell Biology*. 1st ed.; Saunders: Philadelphia, PA, 2002.
10. Kops, G. J. P. L.; Weaver, B. A. A.; Cleveland, D. W. On the road to cancer: aneuploidy and the mitotic checkpoint. *Nature Reviews Cancer* **2005,** 5, 773-785.
11. Scholey, J. M.; Brust-Mascher, I.; Mogilner, A. Cell division. *Nature* **2003,** 422, 746-752.
12. Jackson, J. R.; Patrick, D. R.; Dar, M. M.; Huang, P. S. Targeted anti-mitotic therapies: can we improve on tubulin agents? *Nature Reviews Cancer* **2007,** 7, 107-117.
13. Wittmann, T.; Hyman, A.; Desai, A. The spindle: a dynamic assembly of microtubules and motors. *Nature Cell Biology* **2001,** 3, E28-E34.
14. Jordan, M. A.; Wilson, L. Microtubules as a target for anticancer drugs. *Nature Reviews Cancer* **2004,** 4, 253-265.

15. Sharp, D. J.; Rogers, G. C.; Scholey, J. M. Microtubule motors in mitosis. *Nature* **2000,** 407, 41-47.

16. Wittmann, T.; Wilm, M.; Karsenti, E.; Vernos, I. Tpx2, a Novel Xenopus Map Involved in Spindle Pole Organization. *The Journal of Cell Biology* **2000,** 149, 1405-1418.

17. Perez, E. A. Microtubule inhibitors: Differentiating tubulin-inhibiting agents based on mechanisms of action, clinical activity, and resistance. *Molecular Cancer Therapeutics* **2009,** 8, 2086-2095.

18. Rieder, C. L.; Maiato, H. Stuck in Division or Passing through: What Happens When Cells Cannot Satisfy the Spindle Assembly Checkpoint. *Developmental Cell* **2004,** 7, 637-651.

19. Gascoigne, K. E.; Taylor, S. S. How do anti-mitotic drugs kill cancer cells? *Journal of Cell Science* **2009,** 122, 2579-2585.

20. Jordan, M. A.; Wendell, K.; Gardiner, S.; Brent Derry, W.; Copp, H.; Wilson, L. Mitotic Block Induced in HeLa Cells by Low Concentrations of Paclitaxel (Taxol) Results in Abnormal Mitotic Exit and Apoptotic Cell Death. *Cancer Research* **1996,** 56, 816-825.

21. Torres, K.; Horwitz, S. B. Mechanisms of Taxol-induced Cell Death Are Concentration Dependent. *Cancer Research* **1998,** 58, 3620-3626.

22. Woods, C. M.; Zhu, J.; McQueney, P. A.; Bollag, D.; Lazarides, E. Taxol-induced mitotic block triggers rapid onset of a p53-independent apoptotic pathway. *Molecular Medicine* **1995,** 1, 506-26.

23. Nettles, J. H.; Li, H.; Cornett, B.; Krahn, J. M.; Snyder, J. P.; Downing, K. H. The Binding Mode of Epothilone A on α,ß-Tubulin by Electron Crystallography. *Science* **2004,** 305, 866-869.

24. Gascoigne, K. E.; Taylor, S. S. Cancer Cells Display Profound Intra- and Interline Variation following Prolonged Exposure to Antimitotic Drugs. *Cancer Cell* **2008,** 14, 111-122.

25. Cancer in the UK: December 2011. In *Cancer Stats report*, Cancer Research UK: 2011.

26. Markman, M. Managing taxane toxicities. *Supportive Care in Cancer* **2003,** 11, 144-147.

27. Morris, R. L.; Hollenbeck, P. J. Axonal transport of mitochondria along microtubules and F-actin in living vertebrate neurons. *The Journal of Cell Biology* **1995,** 131, 1315-1326.

28. Quasthoff, S.; Hartung, H. P. Chemotherapy-induced peripheral neuropathy. *Journal of Neurology* **2002,** 249, 9-17.

29. Gidding, C. E. M.; Kellie, S. J.; Kamps, W. A.; de Graaf, S. S. N. Vincristine revisited. *Critical Reviews in Oncology/Hematology* **1999,** 29, 267-287.

30. Kavallaris, M. Microtubules and resistance to tubulin-binding agents. *Nature Reviews Cancer* **2010,** 10, 194-204.

31. Verrills, N. M.; Walsh, B. J.; Cobon, G. S.; Hains, P. G.; Kavallaris, M. Proteome Analysis of Vinca Alkaloid Response and Resistance in Acute Lymphoblastic Leukemia Reveals Novel Cytoskeletal Alterations. *Journal of Biological Chemistry* **2003,** 278, 45082-45093.

32. Gottesman, M. M.; Fojo, T.; Bates, S. E. Multidrug resistance in cancer: role of ATP-dependent transporters. *Nature Reviews Cancer* **2002,** 2, 48-58.

33. Wood, K. W.; Cornwell, W. D.; Jackson, J. R. Past and future of the mitotic spindle as an oncology target. *Current Opinion in Pharmacology* **2001,** 1, 370-377.

34. Gradishar, W. J. Albumin-bound paclitaxel: a next-generation taxane. *Expert Opinion on Pharmacotherapy* **2006,** 7, 1041-1053.

35. Johnson, I. S.; Armstrong, J. G.; Gorman, M.; Burnett, J. P. The Vinca Alkaloids: A New Class of Oncolytic Agents. *Cancer Research* **1963,** 23, 1390-1427.

36. Wani, M. C.; Taylor, H. L.; Wall, M. E.; Coggon, P.; McPhail, A. T. Plant antitumor agents. VI. Isolation and structure of taxol, a novel antileukemic and antitumor agent from Taxus brevifolia. *Journal of the American Chemical Society* **1971,** 93, 2325-2327.

37. Miglarese, M. R.; Carlson, R. O. Development of new cancer therapeutic agents targeting mitosis. *Expert Opinion on Investigational Drugs* **2006,** 15, 1411-1425.

38. Cohen, P. Protein kinases - the major drug targets of the twenty-first century? *Nature Reviews Drug Discovery* **2002,** 1, 309-315.

39. Zhang, J.; Yang, P. L.; Gray, N. S. Targeting cancer with small molecule kinase inhibitors. *Nature Reviews Cancer* **2009,** 9, 28-39.

40. Lapenna, S.; Giordano, A. Cell cycle kinases as therapeutic targets for cancer. *Nature Reviews Drug Discovery* **2009,** 8, 547-566.

41. Pollard, J. R.; Mortimore, M. Discovery and Development of Aurora Kinase Inhibitors as Anticancer Agents. *Journal of Medicinal Chemistry* **2009,** 52, 2629-2651.

42. Giet, R.; Uzbekov, R.; Cubizolles, F.; Le Guellec, K.; Prigent, C. The Xenopus laevis Aurora-related Protein Kinase pEg2 Associates with and Phosphorylates the Kinesin-related Protein XlEg5. *Journal of Biological Chemistry* **1999,** 274, 15005-15013.

43. Kollareddy, M.; Zheleva, D.; Dzubak, P.; Brahmkshatriya, P.; Lepsik, M.; Hajduch, M. Aurora kinase inhibitors: Progress towards the clinic. *Investigational New Drugs* **2012**, 1-22.

44. Komlodi-Pasztor, E.; Sackett, D. L.; Fojo, A. T. Inhibitors Targeting Mitosis: Tales of How Great Drugs against a Promising Target Were Brought Down by a Flawed Rationale. *Clinical Cancer Research* **2012,** 18, 51-63.

45. Strebhardt, K. Multifaceted polo-like kinases: drug targets and antitargets for cancer therapy. *Nature Reviews Drug Discovery* **2010,** 9, 643-660.

46. Takai, N.; Hamanaka, R.; Yoshimatsu, J.; Miyakawa, I. Polo-like kinases (Plks) and cancer. *Oncogene* **2005,** 24, 287-291.

47. Chopra, P.; Sethi, G.; Dastidar, S. G.; Ray, A. Polo-like kinase inhibitors: an emerging opportunity for cancer therapeutics. *Expert Opinion on Investigational Drugs* **2010,** 19, 27-43.

48. Sellers, J. R. Myosins: a diverse superfamily. *Biochimica et Biophysica Acta (BBA) - Molecular Cell Research* **2000,** 1496, 3-22.

49. Hirokawa, N.; Takemura, R. Kinesin Superfamily Proteins. In *Molecular Motors*, Schliwa, M., Ed. Wiley-VCH Verlag GmbH & Co. KGaA: Weinheim, Germany, 2004; pp 79-109.

50. Holzbaur, E. L. F.; Vallee, R. B. Dyneins: Molecular Structure and Cellular Function. *Annual Review of Cell Biology* **1994,** 10, 339-372.

51. Hirokawa, N.; Noda, Y.; Tanaka, Y.; Niwa, S. Kinesin superfamily motor proteins and intracellular transport. *Nature Reviews Molecular Cell Biology* **2009,** 10, 682-696.

52. Lawrence, C. J.; Dawe, R. K.; Christie, K. R.; Cleveland, D. W.; Dawson, S. C.; Endow, S. A.; Goldstein, L. S. B.; Goodson, H. V.; Hirokawa, N.; Howard, J.; Malmberg, R. L.; McIntosh, J. R.; Miki, H.; Mitchison, T. J.; Okada, Y.; Reddy, A. S. N.; Saxton, W. M.; Schliwa, M.; Scholey, J. M.; Vale, R. D.; Walczak, C. E.; Wordeman, L. A standardized kinesin nomenclature. *The Journal of Cell Biology* **2004,** 167, 19-22.

53. Hunter, A. W.; Caplow, M.; Coy, D. L.; Hancock, W. O.; Diez, S.; Wordeman, L.; Howard, J. The Kinesin-Related Protein MCAK Is a Microtubule Depolymerase that Forms an ATP-Hydrolyzing Complex at Microtubule Ends. *Molecular Cell* **2003,** 11, 445-457.

54. Vale, R. D.; Reese, T. S.; Sheetz, M. P. Identification of a novel force-generating protein, kinesin, involved in microtubule-based motility. *Cell* **1985,** 42, 39-50.

55. Brady, S. T. A novel brain ATPase with properties expected for the fast axonal transport motor. *Nature* **1985,** 317, 73-75.

56. Kozielski, F.; Sack, S.; Marx, A.; Thormählen, M.; Schönbrunn, E.; Biou, V.; Thompson, A.; Mandelkow, E. M.; Mandelkow, E. The Crystal Structure of Dimeric Kinesin and Implications for Microtubule-Dependent Motility. *Cell* **1997,** 91, 985-994.

57. Woehlke, G.; Schliwa, M. Walking on two heads: the many talents of kinesin. *Nature Reviews Molecular Cell Biology* **2000,** 1, 50-58.

58. Drummond, D. R. Regulation of microtubule dynamics by kinesins. *Seminars in Cell & Developmental Biology* **2011,** 22, 927-934.

59. Good, J. A. D.; Skoufias, D. A.; Kozielski, F. Elucidating the functionality of kinesins: An overview of small molecule inhibitors. *Seminars in Cell & Developmental Biology* **2011,** 22, 935-945.

60. Tanenbaum, M. E.; Medema, R. H. Mechanisms of Centrosome Separation and Bipolar Spindle Assembly. *Developmental Cell* **2010,** 19, 797-806.

61. Mazumdar, M.; Misteli, T. Chromokinesins: multitalented players in mitosis. *Trends in Cell Biology* **2005,** 15, 349-355.

62. Rieder, C. L.; Salmon, E. D. Motile kinetochores and polar ejection forces dictate chromosome position on the vertebrate mitotic spindle. *The Journal of Cell Biology* **1994,** 124, 223-33.

63. Zhu, C.; Zhao, J.; Bibikova, M.; Leverson, J. D.; Bossy-Wetzel, E.; Fan, J.-B.; Abraham, R. T.; Jiang, W. Functional Analysis of Human Microtubule-based Motor Proteins, the Kinesins and Dyneins, in Mitosis/Cytokinesis Using RNA Interference. *Molecular Biology of the Cell* **2005,** 16, 3187-3199.

64. Mayr, M. I.; Hümmer, S.; Bormann, J.; Grüner, T.; Adio, S.; Woehlke, G.; Mayer, T. U. The Human Kinesin Kif18A Is a Motile Microtubule Depolymerase Essential for Chromosome Congression. *Current Biology* **2007,** 17, 488-498.

65. Yen, T. J.; Li, G.; Schaar, B. T.; Szilak, I.; Cleveland, D. W. CENP-E is a putative kinetochore motor that accumulates just before mitosis. *Nature* **1992,** 359, 536-9.

66. Wood, K. W.; Chua, P.; Sutton, D.; Jackson, J. R. Centromere-Associated Protein E: A Motor That Puts the Brakes on the Mitotic Checkpoint. *Clinical Cancer Research* **2008,** 14, 7588-7592.

67. Du, Y.; English, C. A.; Ohi, R. The Kinesin-8 Kif18A Dampens Microtubule Plus-End Dynamics. *Current Biology* **2010,** 20, 374-380.

68. Ems-McClung, S. C.; Walczak, C. E. Kinesin-13s in mitosis: Key players in the spatial and temporal organization of spindle microtubules. *Seminars in Cell & Developmental Biology* **2010,** 21, 276-282.

69. Kline-Smith, S. L.; Khodjakov, A.; Hergert, P.; Walczak, C. E. Depletion of Centromeric MCAK Leads to Chromosome Congression and Segregation Defects Due to Improper Kinetochore Attachments. *Molecular Biology of the Cell* **2004,** 15, 1146-1159.

70. Bakhoum, S. F.; Thompson, S. L.; Manning, A. L.; Compton, D. A. Genome stability is ensured by temporal control of kinetochore-microtubule dynamics. *Nature Cell Biology* **2009,** 11, 27-35.

71. Gruneberg, U.; Neef, R.; Honda, R.; Nigg, E. A.; Barr, F. A. Relocation of Aurora B from centromeres to the central spindle at the metaphase to anaphase transition requires MKlp2. *The Journal of Cell Biology* **2004,** 166, 167-172.

72. Abaza, A.; Soleilhac, J.-M.; Westendorf, J.; Piel, M.; Crevel, I.; Roux, A.; Pirollet, F. M Phase Phosphoprotein 1 Is a Human Plus-end-directed Kinesin-related Protein Required for Cytokinesis. *Journal of Biological Chemistry* **2003,** 278, 27844-27852.

73. Mishima, M.; Pavicic, V.; Gruneberg, U.; Nigg, E. A.; Glotzer, M. Cell cycle regulation of central spindle assembly. *Nature* **2004,** 430, 908-913.

74. Zhu, C.; Jiang, W. Cell cycle-dependent translocation of PRC1 on the spindle by Kif4 is essential for midzone formation and cytokinesis. *Proceedings of the National Academy of Sciences of the United States of America* **2005,** 102, 343-348.

75. Mitchison, T. J. Towards a pharmacological genetics. *Chemistry & Biology* **1994,** 1, 3-6.

76. Bergnes, G.; Brejc, K.; Belmont, L. Mitotic Kinesins: Prospects for Antimitotic Drug Discovery. *Current Topics in Medicinal Chemistry* **2005,** 5, 127-145.

77. Sawin, K. E.; LeGuellec, K.; Philippe, M.; Mitchison, T. J. Mitotic spindle organization by a plus-end-directed microtubule motor. *Nature* **1992,** 359, 540-543.

78. Blangy, A.; Lane, H. A.; d'Hérin, P.; Harper, M.; Kress, M.; Nigg, E. A. Phosphorylation by p34cdc2 regulates spindle association of human Eg5, a kinesin-related motor essential for bipolar spindle formation *in vivo*. *Cell* **1995,** 83, 1159-1169.

79. Enos, A. P.; Morris, N. R. Mutation of a gene that encodes a kinesin-like protein blocks nuclear division in A. nidulans. *Cell* **1990,** 60, 1019-1027.

80. Cole, D. G.; Saxton, W. M.; Sheehan, K. B.; Scholey, J. M. A "slow" homotetrameric kinesin-related motor protein purified from Drosophila embryos. *Journal of Biological Chemistry* **1994,** 269, 22913-22916.

81. Kashina, A. S.; Baskin, R. J.; Cole, D. G.; Wedaman, K. P.; Saxton, W. M.; Scholey, J. M. A bipolar kinesin. *Nature* **1996,** 379, 270-272.

82. Valentine, M.; Fordyce, P.; Block, S. Eg5 steps it up! *Cell Division* **2006,** 1, 31.

83. Ma, N.; Titus, J.; Gable, A.; Ross, J. L.; Wadsworth, P. TPX2 regulates the localization and activity of Eg5 in the mammalian mitotic spindle. *The Journal of Cell Biology* **2011,** 195, 87-98.

84. Ferenz, N. P.; Gable, A.; Wadsworth, P. Mitotic functions of kinesin-5. *Seminars in Cell & Developmental Biology* **2010,** 21, 255-259.

85. Kapitein, L. C.; Peterman, E. J. G.; Kwok, B. H.; Kim, J. H.; Kapoor, T. M.; Schmidt, C. F. The bipolar mitotic kinesin Eg5 moves on both microtubules that it crosslinks. *Nature* **2005,** 435, 114-118.

86. Kapoor, T. M.; Mayer, T. U.; Coughlin, M. L.; Mitchison, T. J. Probing Spindle Assembly Mechanisms with Monastrol, a Small Molecule Inhibitor of the Mitotic Kinesin, Eg5. *The Journal of Cell Biology* **2000,** 150, 975-988.

87. Bartoli, K. M.; Jakovljevic, J.; Woolford, J. L.; Saunders, W. S. Kinesin molecular motor Eg5 functions during polypeptide synthesis. *Molecular Biology of the Cell* **2011,** 22, 3420-3430.

88. Ferhat, L.; Cook, C.; Chauviere, M.; Harper, M.; Kress, M.; Lyons, G. E.; Baas, P. W. Expression of the Mitotic Motor Protein Eg5 in Postmitotic Neurons: Implications for Neuronal Development. *The Journal of Neuroscience* **1998,** 18, 7822-7835.

89. Baas, P. W. Microtubules and Neuronal Polarity: Lessons from Mitosis. *Neuron* **1999,** 22, 23-31.

90. Haque, S. A.; Hasaka, T. P.; Brooks, A. D.; Lobanov, P. V.; Baas, P. W. Monastrol, a prototype anti-cancer drug that inhibits a mitotic kinesin, induces rapid bursts of axonal outgrowth from cultured postmitotic neurons. *Cell Motility and the Cytoskeleton* **2004,** 58, 10-16.

91. Yoon, S. Y.; Choi, J. E.; Huh, J.-W.; Hwang, O.; Lee, H. S.; Hong, H. N.; Kim, D. Monastrol, a selective inhibitor of the mitotic kinesin Eg5, induces a distinctive growth profile of dendrites and axons in primary cortical neuron cultures. *Cell Motility and the Cytoskeleton* **2005,** 60, 181-190.

92. Nadar, V. C.; Ketschek, A.; Myers, K. A.; Gallo, G.; Baas, P. W. Kinesin-5 Is Essential for Growth-Cone Turning. *Current Biology* **2008,** 18, 1972-1977.

93. Myers, K. A.; Baas, P. W. Kinesin-5 regulates the growth of the axon by acting as a brake on its microtubule array. *The Journal of Cell Biology* **2007,** 178, 1081-1091.

94. Falnikar, A.; Tole, S.; Baas, P. W. Kinesin-5, a mitotic microtubule-associated motor protein, modulates neuronal migration. *Molecular Biology of the Cell* **2011,** 22, 1561-1574.

95. Mayer, T. U.; Kapoor, T. M.; Haggarty, S. J.; King, R. W.; Schreiber, S. L.; Mitchison, T. J. Small Molecule Inhibitor of Mitotic Spindle Bipolarity Identified in a Phenotype-Based Screen. *Science* **1999,** 286, 971-974.

96. Maliga, Z.; Kapoor, T. M.; Mitchison, T. J. Evidence that monastrol is an allosteric inhibitor of the mitotic kinesin Eg5. *Chemistry & Biology* **2002,** 9, 989-996.

97. Yan, Y.; Sardana, V.; Xu, B.; Homnick, C.; Halczenko, W.; Buser, C. A.; Schaber, M.; Hartman, G. D.; Huber, H. E.; Kuo, L. C. Inhibition of a Mitotic Motor Protein: Where, How, and Conformational Consequences. *Journal of Molecular Biology* **2004,** 335, 547-554.

98. DeBonis, S.; Simorre, J.-P.; Crevel, I.; Lebeau, L.; Skoufias, D. A.; Blangy, A.; Ebel, C.; Gans, P.; Cross, R.; Hackney, D. D.; Wade, R. H.; Kozielski, F. Interaction of the Mitotic Inhibitor Monastrol with Human Kinesin Eg5. *Biochemistry* **2003,** 42, 338-349.

99. Maliga, Z.; Mitchison, T. Small-molecule and mutational analysis of allosteric Eg5 inhibition by monastrol. *BMC Chemical Biology* **2006,** 6, 2.

100. Turner, J.; Anderson, R.; Guo, J.; Beraud, C.; Fletterick, R.; Sakowicz, R. Crystal Structure of the Mitotic Spindle Kinesin Eg5 Reveals a Novel Conformation of the Neck-linker. *Journal of Biological Chemistry* **2001,** 276, 25496-25502.

101. Maliga, Z.; Xing, J.; Cheung, H.; Juszczak, L. J.; Friedman, J. M.; Rosenfeld, S. S. A Pathway of Structural Changes Produced by Monastrol Binding to Eg5. *Journal of Biological Chemistry* **2006,** 281, 7977-7982.

102. Hotha, S.; Yarrow, J. C.; Yang, J. G.; Garrett, S.; Renduchintala, K. V.; Mayer, T. U.; Kapoor, T. M. HR22C16: A Potent Small-Molecule Probe for the Dynamics of Cell Division. *Angewandte Chemie International Edition* **2003,** 42, 2379-2382.

103. Nakazawa, J.; Yajima, J.; Usui, T.; Ueki, M.; Takatsuki, A.; Imoto, M.; Toyoshima, Y. Y.; Osada, H. A Novel Action of Terpendole E on the Motor Activity of Mitotic Kinesin Eg5. *Chemistry & Biology* **2003,** 10, 131-137.

104. DeBonis, S.; Skoufias, D. A.; Lebeau, L.; Lopez, R.; Robin, G.; Margolis, R. L.; Wade, R. H.; Kozielski, F. *In vitro* screening for inhibitors of the human mitotic kinesin Eg5 with antimitotic and antitumor activities. *Molecular Cancer Therapeutics* **2004,** 3, 1079-1090.

105. Sakowicz, R.; Finer, J. T.; Beraud, C.; Crompton, A.; Lewis, E.; Fritsch, A.; Lee, Y.; Mak, J.; Moody, R.; Turincio, R.; Chabala, J. C.; Gonzales, P.; Roth, S.; Weitman, S.; Wood, K. W. Antitumor Activity of a Kinesin Inhibitor. *Cancer Research* **2004,** 64, 3276-3280.

106. Knight, S. D.; Parrish, C. A. Recent Progress in the Identification and Clinical Evaluation of Inhibitors of the Mitotic Kinesin KSP. *Current Topics in Medicinal Chemistry* **2008,** 8, 888-904.

107. Huszar, D.; Theoclitou, M.-E.; Skolnik, J.; Herbst, R. Kinesin motor proteins as targets for cancer therapy. *Cancer and Metastasis Reviews* **2009,** 28, 197-208.

108. Marcus, A. I.; Peters, U.; Thomas, S. L.; Garrett, S.; Zelnak, A.; Kapoor, T. M.; Giannakakou, P. Mitotic Kinesin Inhibitors Induce Mitotic Arrest and Cell Death in

Taxol-resistant and -sensitive Cancer Cells. *Journal of Biological Chemistry* **2005,** 280, 11569-11577.

109. Carol, H.; Lock, R.; Houghton, P. J.; Morton, C. L.; Kolb, E. A.; Gorlick, R.; Reynolds, C. P.; Maris, J. M.; Keir, S. T.; Billups, C. A.; Smith, M. A. Initial testing (stage 1) of the kinesin spindle protein inhibitor ispinesib by the pediatric preclinical testing program. *Pediatric Blood & Cancer* **2009,** 53, 1255-1263.

110. Hegde, P. S.; Cogswell, J.; Carrick, K.; Jackson, J.; Wood, K. W.; Eng, W. K.; Brawner, M.; Huang, P. S.; Bergsma, D. Differential gene expression analysis of kinesin spindle protein in human solid tumors. *Proceedings of the American Society of Clinical Oncology Annual Meeting* **2003,** 22, 2003 (abstr 535).

111. Nowicki, M. O.; Pawlowski, P.; Fischer, T.; Hess, G.; Pawlowski, T.; Skorski, T. Chronic myelogenous leukemia molecular signature. *Oncogene* **2003,** 22, 3952-3963.

112. Liu, M.; Wang, X.; Yang, Y.; Li, D.; Ren, H.; Zhu, Q.; Chen, Q.; Han, S.; Hao, J.; Zhou, J. Ectopic expression of the microtubule-dependent motor protein Eg5 promotes pancreatic tumourigenesis. *The Journal of Pathology* **2010,** 221, 221-228.

113. Castillo, A.; Morse, H. C.; Godfrey, V. L.; Naeem, R.; Justice, M. J. Overexpression of Eg5 Causes Genomic Instability and Tumor Formation in Mice. *Cancer Research* **2007,** 67, 10138-10147.

114. Vale, R. D.; Milligan, R. A. The Way Things Move: Looking Under the Hood of Molecular Motor Proteins. *Science* **2000,** 288, 88-95.

115. Rice, S.; Lin, A. W.; Safer, D.; Hart, C. L.; Naber, N.; Carragher, B. O.; Cain, S. M.; Pechatnikova, E.; Wilson-Kubalek, E. M.; Whittaker, M.; Pate, E.; Cooke, R.; Taylor, E. W.; Milligan, R. A.; Vale, R. D. A structural change in the kinesin motor protein that drives motility. *Nature* **1999,** 402, 778-784.

116. Cochran, J. C.; Gilbert, S. P. ATPase Mechanism of Eg5 in the Absence of Microtubules: Insight into Microtubule Activation and Allosteric Inhibition by Monastrol. *Biochemistry* **2005,** 44, 16633-16648.

117. Tao, W.; South, V. J.; Zhang, Y.; Davide, J. P.; Farrell, L.; Kohl, N. E.; Sepp-Lorenzino, L.; Lobell, R. B. Induction of apoptosis by an inhibitor of the mitotic kinesin KSP requires both activation of the spindle assembly checkpoint and mitotic slippage. *Cancer Cell* **2005,** 8, 49-59.

118. Tao, W.; South, V. J.; Diehl, R. E.; Davide, J. P.; Sepp-Lorenzino, L.; Fraley, M. E.; Arrington, K. L.; Lobell, R. B. An Inhibitor of the Kinesin Spindle Protein Activates the Intrinsic Apoptotic Pathway Independently of p53 and De Novo Protein Synthesis. *Molecular and Cellular Biology* **2007,** 27, 689-698.

119. Orth, J. D.; Tang, Y.; Shi, J.; Loy, C. T.; Amendt, C.; Wilm, C.; Zenke, F. T.; Mitchison, T. J. Quantitative live imaging of cancer and normal cells treated with Kinesin-5 inhibitors indicates significant differences in phenotypic responses and cell fate. *Molecular Cancer Therapeutics* **2008,** 7, 3480-3489.

120. Rello-Varona, S.; Vitale, I.; Kepp, O.; Senovilla, L.; Jemaá, M.; Métivier, D.; Castedo, M.; Kroemer, G. Preferential killing of tetraploid tumor cells by targeting the mitotic kinesin Eg5. *Cell Cycle* **2009,** 8, 1030-1035.

121. Shi, J.; Orth, J. D.; Mitchison, T. Cell Type Variation in Responses to Antimitotic Drugs that Target Microtubules and Kinesin-5. *Cancer Research* **2008,** 68, 3269-3276.

122. Saijo, T.; Ishii, G.; Ochiai, A.; Yoh, K.; Goto, K.; Nagai, K.; Kato, H.; Nishiwaki, Y.; Saijo, N. Eg5 expression is closely correlated with the response of advanced non-small cell lung cancer to antimitotic agents combined with platinum chemotherapy. *Lung Cancer* **2006,** 54, 217-225.

123. Weisberger, A. S.; Levine, B. Incorporation of Radioactive L-Cystine by Normal and Leukemic Leukocytes *in Vivo*. *Blood* **1954,** 9, 1082-1094.

124. Goodman, L.; Ross, L. O.; Baker, B. R. Potential Anticancer Agents. V. Some Sulfur-Substituted Derivatives of Cysteine. *The Journal of Organic Chemistry* **1958,** 23, 1251-1257.

125. Theodoropoulos, D. Synthesis of Certain *S*-Substituted L-Cysteines. *Acta Chemica Scandinavica* **1959,** 13, 383-384.

126. Zee-Cheng, K.-Y.; Cheng, C.-C. Experimental antileukemic agents. Preparation and structure-activity study of *S*-tritylcysteine and related compounds. *Journal of Medicinal Chemistry* **1970,** 13, 414-418.

127. Zee-Cheng, K. Y.; Cheng, C. C. Structural modification of *S*-trityl-L-cysteine. Preparation of some *S*-(substituted trityl)-L-cysteines and dipeptides of *S*-trityl-L-cysteine. *Journal of Medicinal Chemistry* **1972,** 15, 13-16.

128. Paull, K. D.; Lin, C. M.; Malspeis, L.; Hamel, E. Identification of Novel Antimitotic Agents Acting at the Tubulin Level by Computer-assisted Evaluation of Differential Cytotoxicity Data. *Cancer Research* **1992,** 52, 3892-3900.

129. Skoufias, D. A.; DeBonis, S.; Saoudi, Y.; Lebeau, L.; Crevel, I.; Cross, R.; Wade, R. H.; Hackney, D.; Kozielski, F. *S*-Trityl-L-cysteine Is a Reversible, Tight Binding Inhibitor of the Human Kinesin Eg5 That Specifically Blocks Mitotic Progression. *Journal of Biological Chemistry* **2006,** 281, 17559-17569.

130. DeBonis, S.; Skoufias, D. A.; Indorato, R.-L.; Liger, F.; Marquet, B.; Laggner, C.; Joseph, B.; Kozielski, F. Structure–Activity Relationship of *S*-Trityl-L-Cysteine Analogues as Inhibitors of the Human Mitotic Kinesin Eg5. *Journal of Medicinal Chemistry* **2008,** 51, 1115-1125.

131. Brier, S.; Lemaire, D.; DeBonis, S.; Forest, E.; Kozielski, F. Identification of the Protein Binding Region of *S*-Trityl-L-cysteine, a New Potent Inhibitor of the Mitotic Kinesin Eg5. *Biochemistry* **2004,** 43, 13072-13082.

132. Kaan, H. Y. K.; Ulaganathan, V.; Hackney, D. D.; Kozielski, F. An allosteric transition trapped in an intermediate state of a new kinesin–inhibitor complex. *Biochemical Journal* **2010,** 425, 55-60.

133. Wiltshire, C.; Singh, B. L.; Stockley, J.; Fleming, J.; Doyle, B.; Barnetson, R.; Robson, C. N.; Kozielski, F.; Leung, H. Y. Docetaxel-Resistant Prostate Cancer Cells Remain Sensitive to *S*-Trityl-L-Cysteine–Mediated Eg5 Inhibition. *Molecular Cancer Therapeutics* **2010,** 9, 1730-1739.

134. Kozielski, F.; Skoufias, D. A.; Indorato, R.-L.; Saoudi, Y.; Jungblut, P. R.; Hustoft, H. K.; Strozynski, M.; Thiede, B. Proteome analysis of apoptosis signaling by *S*-trityl-L-cysteine, a potent reversible inhibitor of human mitotic kinesin Eg5. *Proteomics* **2008,** 8, 289-300.

135. Nichols, D. B.; Fournet, G.; Gurukumar, K. R.; Basu, A.; Lee, J.-C.; Sakamoto, N.; Kozielski, F.; Musmuca, I.; Joseph, B.; Ragno, R.; Kaushik-Basu, N. Inhibition of Hepatitis C Virus NS5B Polymerase by *S*-Trityl-L-Cysteine Derivatives. *European Journal of Medicinal Chemistry* **2012,** 49, 191-199.

136. Kim, E. D.; Buckley, R.; Learman, S.; Richard, J.; Parke, C.; Worthylake, D. K.; Wojcik, E. J.; Walker, R. A.; Kim, S. Allosteric Drug Discrimination Is Coupled to Mechanochemical Changes in the Kinesin-5 Motor Core. *Journal of Biological Chemistry* **2010,** 285, 18650-18661.

137. Kaan, H. Y. K.; Weiss, J.; Menger, D.; Ulaganathan, V.; Tkocz, K.; Laggner, C.; Popowycz, F.; Joseph, B. t.; Kozielski, F. Structure−Activity Relationship and Multidrug Resistance Study of New *S*-trityl-L-Cysteine Derivatives As Inhibitors of Eg5. *Journal of Medicinal Chemistry* **2011,** 54, 1576-1586.

138. Wang, F.; Good, J. A. D.; Rath, O.; Kaan, H. Y. K.; Sutcliffe, O. B.; Mackay, S. P.; Kozielski, F. Triphenylbutanamines: Kinesin Spindle Protein Inhibitors with *in Vivo* Antitumor Activity. *Journal of Medicinal Chemistry* **2012,** 55, 1511-1525.

139. Abualhasan, M. N.; Good, J. A. D.; Wittayanarakul, K.; Anthony, N. G.; Berretta, G.; Rath, O.; Kozielski, F.; Sutcliffe, O. B.; Mackay, S. P. Doing the methylene shuffle – Further insights into the inhibition of mitotic kinesin Eg5 with *S*-trityl L-cysteine. *European Journal of Medicinal Chemistry* **2012,** 54, 483-498.

140. Cox, C. D.; Coleman, P. J.; Breslin, M. J.; Whitman, D. B.; Garbaccio, R. M.; Fraley, M. E.; Buser, C. A.; Walsh, E. S.; Hamilton, K.; Schaber, M. D.; Lobell, R. B.; Tao, W.; Davide, J. P.; Diehl, R. E.; Abrams, M. T.; South, V. J.; Huber, H. E.; Torrent, M.; Prueksaritanont, T.; Li, C.; Slaughter, D. E.; Mahan, E.; Fernandez-Metzler, C.; Yan, Y.; Kuo, L. C.; Kohl, N. E.; Hartman, G. D. Kinesin Spindle Protein (KSP) Inhibitors. 9. Discovery of (2*S*)-4-(2,5-Difluorophenyl)-*N*-[(3R,4S)-3-fluoro-1-methylpiperidin-4-yl]-2-(hydroxymethyl)-*N*-methyl-2-phenyl-2,5-dihydro-1*H*-pyrrole-1-carboxamide (MK-0731) for the Treatment of Taxane-Refractory Cancer. *Journal of Medicinal Chemistry* **2008,** 51, 4239-4252.

141. Ogo, N.; Oishi, S.; Matsuno, K.; Sawada, J.-i.; Fujii, N.; Asai, A. Synthesis and biological evaluation of L-cysteine derivatives as mitotic kinesin Eg5 inhibitors. *Bioorganic & Medicinal Chemistry Letters* **2007,** 17, 3921-3924.

142. Aller, S. G.; Yu, J.; Ward, A.; Weng, Y.; Chittaboina, S.; Zhuo, R.; Harrell, P. M.; Trinh, Y. T.; Zhang, Q.; Urbatsch, I. L.; Chang, G. Structure of P-Glycoprotein Reveals a Molecular Basis for Poly-Specific Drug Binding. *Science* **2009,** 323, 1718-1722.

143. Lin, J. H.; Yamazaki, M. Clinical Relevance of P-Glycoprotein in Drug Therapy. *Drug Metabolism Reviews* **2003,** 35, 417-454.

144. Raub, T. J. P-Glycoprotein Recognition of Substrates and Circumvention through Rational Drug Design. *Molecular Pharmaceutics* **2005,** 3, 3-25.

145. Szakacs, G.; Paterson, J. K.; Ludwig, J. A.; Booth-Genthe, C.; Gottesman, M. M. Targeting multidrug resistance in cancer. *Nature Reviews Drug Discovery* **2006,** 5, 219-234.

146. Miller, K.; Ng, C.; Ang, P.; Brufsky, A. M.; Lee, S. C.; Dees, E. C.; Piccart, M.; Verrill, M.; Wardley, A.; Loftiss, J.; Bal, J.; Yeoh, S.; Hodge, J.; Williams, D.; Dar, M.; Ho, P. T. C. Phase II, open label study of SB-715992 (Ispinesib) in subjects with advanced or metastatic breast cancer. *Breast Cancer Research and Treatment* **2005,** 94, S70-S70.

147. Tang, P. A.; Siu, L. L.; Chen, E. X.; Hotte, S. J.; Chia, S.; Schwarz, J. K.; Pond, G. R.; Johnson, C.; Colevas, A. D.; Synold, T. W.; Vasist, L. S.; Winquist, E. Phase II study of ispinesib in recurrent or metastatic squamous cell carcinoma of the head and neck. *Investigational New Drugs* **2008,** 26, 257-264.

148. Beer, T.; Goldman, B.; Synold, T.; Ryan, C.; Vasist, L.; Van Veldhuizen Jr, P.; Dakhil, S.; Lara Jr, P.; Drelichman, A.; Hussain, M.; Crawford, E. D. Southwest Oncology Group Phase II Study of Ispinesib in Androgen-Independent Prostate Cancer Previously Treated with Taxanes. *Clinical Genitourinary Cancer* **2008,** 6, 103-109.

149. Lee, C. W.; Belanger, K.; Rao, S. C.; Petrella, T. M.; Tozer, R. G.; Wood, L.; Savage, K. J.; Eisenhauer, E. A.; Synold, T. W.; Wainman, N.; Seymour, L. A phase II study of ispinesib (SB-715992) in patients with metastatic or recurrent malignant melanoma: a National Cancer Institute of Canada Clinical Trials Group trial. *Investigational New Drugs* **2008,** 26, 249-255.

150. Jones, S. F.; Plummer, E. R.; Burris, H. A.; Razak, A. R.; Meluch, A. A.; Bowen, C. J.; Williams, D. H.; Hodge, J. P.; Dar, M. M.; Calvert, A. H. Phase I study of ispinesib in combination with carboplatin in patients with advanced solid tumors. *Journal of Clinical Oncology* **2006,** 24, 85S-85S.

151. Blagden, S. P.; Molife, L. R.; Seebaran, A.; Payne, M.; Reid, A. H. M.; Protheroe, A. S.; Vasist, L. S.; Williams, D. D.; Bowen, C.; Kathman, S. J.; Hodge, J. P.; Dar, M. M.; de Bono, J. S.; Middleton, M. R. A phase I trial of ispinesib, a kinesin spindle protein inhibitor, with docetaxel in patients with advanced solid tumours. *British Journal of Cancer* **2008,** 98, 894-899.

152. Kivisto, K. T.; Kroemer, H. K.; Eichelbaum, M. The role of human cytochrome P450 enzymes in the metabolism of anticancer agents: Implications for drug interactions. *British Journal of Clinical Pharmacology* **1995,** 40, 523-530.

153. McDonald, A.; Bergnes, G.; Feng, B.; Morgans, D. J.; Knight, S. D.; Newlander, K. A.; Dhanak, D.; Brook, C. S.,inventors; Cytokinetics, Inc., USA, assignee "Compounds, compositions and methods."; World patent WO 03088903; Oct 30, 2003.

154. O'Connor, O. A.; Gerecitano, J.; Van Deventer, H.; Afanasyev, B.; Hainsworth, J.; Chen, M.; Saikali, K.; Seroogy, J.; Escandon, R.; Wolff, A.; Conlan, M. G. A Phase I/II Trial of the Kinesin Spindle Protein (KSP) Inhibitor SB-743921 Dosed Q14D without and with Prophylactic G-CSF in Non-Hodgkin (NHL) or Hodgkin Lymphoma (HL). *Blood* **2009,** 114, 667-667.

155. Holen, K.; Belani, C.; Wilding, G.; Ramalingam, S.; Volkman, J.; Ramanathan, R.; Vasist, L.; Bowen, C.; Hodge, J.; Dar, M.; Ho, P. A first in human study of SB-743921, a kinesin spindle protein inhibitor, to determine pharmacokinetics, biologic effects and establish a recommended phase II dose. *Cancer Chemotherapy and Pharmacology* **2011,** 67, 447-454.

156. Theoclitou, M.-E.; Aquila, B.; Block, M. H.; Brassil, P. J.; Castriotta, L.; Code, E.; Collins, M. P.; Davies, A. M.; Deegan, T.; Ezhuthachan, J.; Filla, S.; Freed, E.; Hu, H.; Huszar, D.; Jayaraman, M.; Lawson, D.; Lewis, P. M.; Nadella, M. V. P.; Oza, V.; Padmanilayam, M.; Pontz, T.; Ronco, L.; Russell, D.; Whitston, D.; Zheng, X. Discovery of (+)-*N*-(3-Aminopropyl)-*N*-[1-(5-benzyl-3-methyl-4-oxo-[1,2]thiazolo[5,4-*d*]pyrimidin-6-yl)-2-methylpropyl]-4-methylbenzamide (AZD4877), a Kinesin Spindle Protein Inhibitor and Potential Anticancer Agent. *Journal of Medicinal Chemistry* **2011,** 54, 6734-6750.

157. Infante, J.; Kurzrock, R.; Spratlin, J.; Burris, H.; Eckhardt, S.; Li, J.; Wu, K.; Skolnik, J.; Hylander-Gans, L.; Osmukhina, A.; Huszar, D.; Herbst, R. A Phase I study to assess the safety, tolerability, and pharmacokinetics of AZD4877, an intravenous Eg5 inhibitor in patients with advanced solid tumors. *Cancer Chemotherapy and Pharmacology* **2012,** 69, 165-172.

158. Kantarjian, H.; Padmanabhan, S.; Stock, W.; Tallman, M.; Curt, G.; Li, J.; Osmukhina, A.; Wu, K.; Huszar, D.; Borthukar, G.; Faderl, S.; Garcia-Manero, G.; Kadia, T.; Sankhala, K.; Odenike, O.; Altman, J.; Minden, M. Phase I/II multicenter study to assess the safety, tolerability, pharmacokinetics and pharmacodynamics of AZD4877 in patients with refractory acute myeloid leukemia. *Investigational New Drugs* **2011**, 1-9.

159. Liu, J.; Ali, S. M.; Ashwell, M. A.; Ye, P.; Guan, Y.; Ng, S.-C.; Palma, R.; Yohannes, D., inventors; Arqule Inc., USA, assignee; "Quinazolinone Compounds and Methods of Use Thereof."; US patent US2011217300; Sept 8th, 2011.

160. Chen, L. C.; Rosen, L. S.; Iyengar, T.; Goldman, J. W.; Savage, R.; Kazakin, J.; Chan, T. C. K.; Schwartz, B. E.; Abbadessa, G.; Hoff, D. D. V. First-in-human study with ARQ 621, a novel inhibitor of Eg5: Final results from the solid tumors cohort. *Journal of Clinical Oncology* **2011,** 29, 3076.

161. Burris, H.; Jones, S.; Williams, D.; Kathman, S.; Hodge, J.; Pandite, L.; Ho, P.; Boerner, S.; LoRusso, P. A phase I study of ispinesib, a kinesin spindle protein inhibitor, administered weekly for three consecutive weeks of a 28-day cycle in patients with solid tumors. *Investigational New Drugs* **2011,** 29, 467-472.

162. Schiemann, K.; Finsinger, D.; Zenke, F.; Amendt, C.; Knöchel, T.; Bruge, D.; Buchstaller, H.-P.; Emde, U.; Stähle, W.; Anzali, S. The discovery and optimization of hexahydro-2*H*-pyrano[3,2-*c*]quinolines (HHPQs) as potent and selective inhibitors of the mitotic kinesin-5. *Bioorganic & Medicinal Chemistry Letters* **2010,** 20, 1491-1495.

163. Bahleda, R.; Massard, C.; Deutsch, E.; Ribrag, V.; Loriot, Y.; Kroesser, S.; Gianella-Borradori, A.; Trandafir, L.; Soria, J.-C. In *A Phase I, dose-escalation study of the Eg5-inhibitor EMD534085 in subjects with advanced solid tumors and lymphoma*, 101st Annual Meeting of the American Association of Cancer Research, Washington, CA, April 17–21, 2010; Washington, CA, 2010.

164. Holen, K.; DiPaola, R.; Liu, G.; Tan, A.; Wilding, G.; Hsu, K.; Agrawal, N.; Chen, C.; Xue, L.; Rosenberg, E.; Stein, M. A phase I trial of MK-0731, a Kinesin Spindle Protein (KSP) inhibitor, in patients with solid tumors. *Investigational New Drugs* **2011**, 1-8.

165. Woessner, R.; Tunquist, B.; Lemieux, C.; Chlipala, E.; Jackinsky, S.; Dewolf, W.; Voegtli, W.; Cox, A.; Rana, S.; Lee, P.; Walker, D. ARRY-520, a Novel KSP Inhibitor with Potent Activity in Hematological and Taxane-resistant Tumor Models. *Anticancer Research* **2009,** 29, 4373-4380.

166. Khoury, H. J.; Garcia-Manero, G.; Borthakur, G.; Kadia, T.; Foudray, M. C.; Arellano, M.; Langston, A.; Bethelmie-Bryan, B.; Rush, S.; Litwiler, K.; Karan, S.; Simmons, H.; Marcus, A. I.; Ptaszynski, M.; Kantarjian, H. A phase 1 dose-escalation study of ARRY-520, a kinesin spindle protein inhibitor, in patients with advanced myeloid leukemias. *Cancer* **2012,** 118, 3556–3564.

167. Shah, J. J.; Zonder, J. A.; Cohen, A.; Weter, D.; Thomas, S.; Wang, M.; Kaufman, J. L.; Burt, S. M.; Walker, D.; Freeman, B.; Rush, S. A.; Ptaszynski, A.; Orlowski, R. Z.; Lonial, S. A Phase I/II Trial of the KSP Inhibitor ARRY-520 In Relapsed/Refractory Multiple Myeloma. *Blood* **2010,** 116, 817-817.

168. Lonial, S.; Cohen, A.; Zonder, J. A.; Benzinger, W. I.; Kaufman, J. L.; Orlowski, R. Z.; Harvey, R. D.; Alexanian, R.; Thomas, S. K.; Weber, D.; Walker, D.; Hilder, B.; Ptazynski, A.; Shah, J. J. The Novel KSP Inhibitor ARRY-520 Demonstrates Single-Agent Activity in Refractory Myeloma: Results From a Phase 2 Trial in Patients with Relapsed/Refractory Multiple Myeloma (MM). *Blood* **2011,** 118, 1266-1266.

169. Sanguinetti, M. C.; Tristani-Firouzi, M. hERG potassium channels and cardiac arrhythmia. *Nature* **2006,** 440, 463-469.

170. Murakata, C.; Kato, K.; Yamamto, J.; Nakai, R.; Okamoto, S.; Ino, Y.; Kitamura, Y.; Saitoh, T.; Katsuhira, T. Agent for treatment of solid tumour. 2006 Sept 28th, 2006.

171. Allison, M. Reinventing clinical trials. *Nature Biotechnology* **2012,** 30, 41-49.

172. Shih, K. C.; Infante, J. R.; Papadopoulos, K. P.; Bendell, J. C.; Tolcher, A. W.; Burris, H. A.; Beeram, M.; Jackson, L.; Arcos, R.; Westin, E. H.; Farrington, D.; McGlothlin, A.; Hynes, S.; Leohr, J.; Brandt, J. T.; Nasir, A.; Patnaik, A. A phase I dose-escalation study of LY2523355, an Eg5 inhibitor, administered either on days 1, 5, and 9; days 1 and 8; or days 1 and 5 with pegfilgrastim (peg) every 21 days (NCT01214642). *ASCO Meeting Abstracts* **2011,** 29, 2600.

173. 4SC. *Annual Report 2010*. 2010.

174. Venneman, M.; Baer, T.; Braugnger, J.; Zimmernman, A.; Gimmnich, P. Indolopyridines as Eg5 kinesin modulators. 2007 Aug 30, 2007.

175. Woessner, R.; Tunquist, B.; Cox, A.; Rana, S.; Walker, D.; Lee, P. A. Combination of the KSP Inhibitor ARRY-520 with Bortezomib or Revlimid Causes Sustained Tumor Regressions and Significantly Increased Time to Regrowth in Models of Multiple Myeloma. *Blood* **2009,** 114, 1115-1116.

176. Waring, M. J. Lipophilicity in drug discovery. *Expert Opinion on Drug Discovery* **2010,** 5, 235-248.

177. Ulrik, S. S.; Erik, F.; Tine, B. S.; Jerzy, W. J.; Ulf, M.; Povl, K.-L. Structural Determinants for AMPA Agonist Activity of Aryl or Heteroaryl Substituted AMPA Analogues. Synthesis and Pharmacology. *Archiv der Pharmazie* **2001,** 334, 62-68.

178. Fischer, E.; Speier, A. Darstellung der Ester. *Berichte der deutschen chemischen Gesellschaft* **1895,** 28, 3252-3258.

179. Hatano, M.; Suzuki, S.; Ishihara, K. Highly Efficient Alkylation to Ketones and Aldimines with Grignard Reagents Catalyzed by Zinc(II) Chloride. *Journal of the American Chemical Society* **2006,** 128, 9998-9999.

180. Luliński, S.; Zajac, K. Selective Generation of Lithiated Benzonitriles: the Importance of Reaction Conditions. *The Journal of Organic Chemistry* **2008,** 73, 7785-7788.

181. Neumann, W. P.; Penenory, A.; Stewen, U.; Lehnig, M. Sterically hindered free radicals. 18. Stabilization of free radicals by substituents as studied by using triphenylmethyls. *Journal of the American Chemical Society* **1989,** 111, 5845-5851.

182. Brown, D. J.; Ghosh, P. B. The spectra, ionization, and deuteriation of oxazoles and related compounds. *Journal of the Chemical Society B: Physical Organic* **1969**.

183. Hodges, J. C.; Patt, W. C.; Connolly, C. J. Reactions of lithiooxazole. *The Journal of Organic Chemistry* **1991,** 56, 449-452.

184. Schröder, R.; Schöllkopf, U.; Blume, E.; Hoppe, I. Synthesen mit α-metallierten Isocyaniden, XXVIII[1]) In 2-Stellung unsubstituierte Oxazole aus α-metallierten Isocyaniden und Acylierungsreagenzien. *Justus Liebigs Annalen der Chemie* **1975,** 1975, 533-546.

185. Wolff, L. Chemischen Institut der Universität Jena: Methode zum Ersatz des Sauerstoffatoms der Ketone und Aldehyde durch Wasserstoff. [Erste Abhandlung.]. *Justus Liebigs Annalen der Chemie* **1912,** 394, 86-108.

186. Huang-Minlon. A Simple Modification of the Wolff-Kishner Reduction. *Journal of the American Chemical Society* **1946,** 68, 2487-2488.

187. Nahm, S.; Weinreb, S. M. *N*-methoxy-*N*-methylamides as effective acylating agents. *Tetrahedron Letters* **1981,** 22, 3815-3818.

188. Qu, B.; Collum, D. B. Mechanism of Acylation of Lithium Phenylacetylide with a Weinreb Amide. *The Journal of Organic Chemistry* **2006,** 71, 7117-7119.

189. Wissmann, H.; Kleiner, H.-J. New Peptide Synthesis. *Angewandte Chemie International Edition in English* **1980,** 19, 133-134.

190. Maltese, M. Reductive Demercuration in Deprotection of Trityl Thioethers, Trityl Amines, and Trityl Ethers. *The Journal of Organic Chemistry* **2001,** 66, 7615-7625.

191. Lide, D. R. *CRC Handbook of Chemistry and Physics*. CRC Press, Taylor & Francis Group: London, 2006; Vol. 87th edn.

192. Kabalka, G. W.; Yao, M.-L.; Borella, S.; Goins, L. K. Iron Trichloride Mediated Allylation of Lithium Alkoxides through an Unusual Carbon−Oxygen Bond Cleavage. *Organometallics* **2007,** 26, 4112-4114.

193. Brown, H. C.; Rao, B. C. S. A New Technique for the Conversion of Olefins into Organoboranes and Related Alcohols. *Journal of the American Chemical Society* **1956,** 78, 5694-5695.

194. Dess, D. B.; Martin, J. C. Readily accessible 12-I-5 oxidant for the conversion of primary and secondary alcohols to aldehydes and ketones. *The Journal of Organic Chemistry* **1983,** 48, 4155-4156.

195. Strecker, A. Ueber die künstliche Bildung der Milchsäure und einen neuen, dem Glycocoll homologen Körper. *Justus Liebigs Annalen der Chemie* **1850,** 75, 27-45.

196. Yadav, J. S.; Reddy, B. V. S.; Eeshwaraiah, B.; Srinivas, M. Montmorillonite KSF clay catalyzed one-pot synthesis of α-aminonitriles. *Tetrahedron* **2004,** 60, 1767-1771.

197. Ram, S.; Spicer, L. D. Debenzylation of *N*-Benzylamino Derivatives by Catalytic Transfer Hydrogenation With Ammonium Formate. *Synthetic Communications: An International Journal for Rapid Communication of Synthetic Organic Chemistry* **1987,** 17, 415 - 418.

198. Coleman, P. J.; Schreier, J. D.; Cox, C. D.; Fraley, M. E.; Garbaccio, R. M.; Buser, C. A.; Walsh, E. S.; Hamilton, K.; Lobell, R. B.; Rickert, K.; Tao, W.; Diehl, R. E.; South, V. J.; Davide, J. P.; Kohl, N. E.; Yan, Y.; Kuo, L.; Prueksaritanont, T.; Li, C.; Mahan, E. A.; Fernandez-Metzler, C.; Salata, J. J.; Hartman, G. D. Kinesin spindle protein (KSP) inhibitors. Part 6: Design and synthesis of 3,5-diaryl-4,5-dihydropyrazole amides as potent inhibitors of the mitotic kinesin KSP. *Bioorganic & Medicinal Chemistry Letters* **2007,** 17, 5390-5395.

199. Davis, F. A.; Kasu, P. V. N.; Sundarababu, G.; Qi, H. Nonracemic α-Fluoro Aldehydes: Asymmetric Synthesis of 4-Deoxy-4-fluoro-d-arabinopyranose. *The Journal of Organic Chemistry* **1997,** 62, 7546-7547.

200. Enders, D.; Hüttl, M. R. M. Direct Organocatalytic α-Fluorination of Aldehydes and Ketones. *Synlett* **2005,** 2005, 0991,0993.

201. Marigo, M.; Fielenbach, D.; Braunton, A.; Kjærsgaard, A.; Jørgensen, K. A. Enantioselective Formation of Stereogenic Carbon–Fluorine Centers by a Simple Catalytic Method. *Angewandte Chemie International Edition* **2005,** 44, 3703-3706.

202. Beeson, T. D.; MacMillan, D. W. C. Enantioselective Organocatalytic α-Fluorination of Aldehydes. *Journal of the American Chemical Society* **2005,** 127, 8826-8828.

203. Steiner, D. D.; Mase, N.; Barbas, C. F. Direct Asymmetric α-Fluorination of Aldehydes. *Angewandte Chemie International Edition* **2005,** 44, 3706-3710.

204. Prakash, G. K. S.; Krishnamurti, R.; Olah, G. A. Synthetic methods and reactions. 141. Fluoride-induced trifluoromethylation of carbonyl compounds with trifluoromethyltrimethylsilane (TMS-CF_3). A trifluoromethide equivalent. *Journal of the American Chemical Society* **1989,** 111, 393-395.

205. Prakash, G. K. S.; Yudin, A. K. Perfluoroalkylation with Organosilicon Reagents. *Chemical Reviews* **1997,** 97, 757-786.

206. Differding, E.; Ofner, H. *N*-Fluorobenzenesulfonimide: A Practical Reagent For Electrophilic Fluorinations. *Synlett* **1991,** 1991, 187,189.

207. Umemoto, T.; Fukami, S.; Tomizawa, G.; Harasawa, K.; Kawada, K.; Tomita, K. Power- and structure-variable fluorinating agents. The *N*-fluoropyridinium salt system. *Journal of the American Chemical Society* **1990,** 112, 8563-8575.

208. Differding, E.; Rüegg, G. M. Nucleophilic substitution versus electron transfer: 1. On the mechanism of electrophilic fluorinations. *Tetrahedron Letters* **1991,** 32, 3815-3818.

209. Differring, E.; Wehrli, M. Nucleophilic substitution versus electron transfer: 2. S_N2 at flouride and electron transfer are competing and different pathways in electrophilic flourinations. *Tetrahedron Letters* **1991,** 32, 3819-3822.

210. Marigo, M.; Jorgensen, K. A. Organocatalytic direct asymmetric α-heteroatom functionalization of aldehydes and ketones. *Chemical Communications* **2006**, 2001-2011.

211. Wiedemann, J.; Heiner, T.; Mloston, G.; Prakash, G. K. S.; Olah, G. A. Direct Preparation of Trifluoromethyl Ketones from Carboxylic Esters: Trifluoromethylation with (Trifluoromethyl)trimethylsilane. *Angewandte Chemie International Edition* **1998,** 37, 820-821.

212. Tegoni, M.; Furlotti, M.; Tropiano, M.; Lim, C. S.; Pecoraro, V. L. Thermodynamics of Core Metal Replacement and Self-Assembly of $Ca2^{+}$ 15-Metallacrown-5. *Inorganic Chemistry* **2010,** 49, 5190-5201.

213. Gleeson, M. P.; Hersey, A.; Montanari, D.; Overington, J. Probing the links between in vitro potency, ADMET and physicochemical parameters. *Nature Reviews Drug Discovery* **2011,** 10, 197-208.

214. Gilbert, S. P.; Mackey, A. T. Kinetics: A Tool to Study Molecular Motors. *Methods* **2000,** 22, 337-354.

215. Copeland, R. A. Tight Binding Inhibition. In *Evaluation of Enzyme Inhibitors in Drug Discovery: A Guide for Medicinal Chemists and Pharmacologists*, 1st ed.; John Wiley & Sons: Hoboken, NJ, 2005; pp 178-213.

216. Hopkins, A. L.; Groom, C. R.; Alex, A. Ligand efficiency: a useful metric for lead selection. *Drug Discovery Today* **2004,** 9, 430-431.

217. Reynolds, C. H.; Tounge, B. A.; Bembenek, S. D. Ligand Binding Efficiency: Trends, Physical Basis, and Implications. *Journal of Medicinal Chemistry* **2008,** 51, 2432-2438.

218. Craig, P. N. Interdependence between physical parameters and selection of substituent groups for correlation studies. *Journal of Medicinal Chemistry* **1971,** 14, 680-684.

219. Jaffe, H. H. A Rexamination of the Hammett Equation. *Chemical Reviews* **1953,** 53, 191-261.

220. Fujita, T.; Iwasa, J.; Hansch, C. A New Substituent Constant, π, Derived from Partition Coefficients. *Journal of the American Chemical Society* **1964,** 86, 5175-5180.

221. Boonyapiwat, B.; Panaretou, B.; Forbes, B.; Mitchell, S. C.; Steventon, G. B. Human phenylalanine monooxygenase and thioether metabolism. *Journal of Pharmacy and Pharmacology* **2009,** 61, 63-67.

222. Good, J. A. D.; Wang, F.; Rath, O.; Kaan, H. Y. K.; Talapatra, S. S.; Podgórski, D.; Mackay, S. P.; Kozielski, F. "Optimized *S*-Trityl-L-Cysteine Based Inhibitors of Kinesin Spindle Protein with potent *in Vivo* Antitumor Activity in Lung Cancer Xenograft Models" (*manuscript in revision). Journal of Medicinal Chemistry* **2012**.

223. Lad, L.; Luo, L.; Carson, J. D.; Wood, K. W.; Hartman, J. J.; Copeland, R. A.; Sakowicz, R. Mechanism of inhibition of human KSP by Ispinesib. *Biochemistry* **2008,** 47, 3576-3585.

224. Cox, C. D.; Breslin, M. J.; Mariano, B. J.; Coleman, P. J.; Buser, C. A.; Walsh, E. S.; Hamilton, K.; Huber, H. E.; Kohl, N. E.; Torrent, M.; Yan, Y.; Kuo, L. C.; Hartman, G. D. Kinesin spindle protein (KSP) inhibitors. Part 1: The discovery of 3,5-diaryl-4,5-dihydropyrazoles as potent and selective inhibitors of the mitotic kinesin KSP. *Bioorganic & Medicinal Chemistry Letters* **2005,** 15, 2041-2045.

225. Bissantz, C.; Kuhn, B.; Stahl, M. A Medicinal Chemist's Guide to Molecular Interactions. *Journal of Medicinal Chemistry* **2010,** 53, 5061-5084.

226. Wilson, A. S.; Davis, C. D.; Williams, D. P.; Buckpitt, A. R.; Pirmohamed, M.; Park, B. K. Characterisation of the toxic metabolite(s) of naphthalene. *Toxicology* **1996,** 114, 233-242.

227. Hann, M. M. Molecular obesity, potency and other addictions in drug discovery. *MedChemComm* **2011,** 2.

228. Barsanti, P. A.; Wang, W.; Ni, Z.-J.; Duhl, D.; Brammeier, N.; Martin, E.; Bussiere, D.; Walter, A. O. The discovery of tetrahydro-β-carbolines as inhibitors of the kinesin Eg5. *Bioorganic & Medicinal Chemistry Letters* **2010,** 20, 157-160.

229. Houston, J. B. Utility of *in vitro* drug metabolism data in predicting *in vivo* metabolic clearance. *Biochemical Pharmacology* **1994,** 47, 1469-1479.

230. Kaan, H. Y. K.; Ulaganathan, V.; Rath, O.; Prokopcová, H.; Dallinger, D.; Kappe, C. O.; Kozielski, F. Structural Basis for Inhibition of Eg5 by Dihydropyrimidines: Stereoselectivity of Antimitotic Inhibitors Enastron, Dimethylenastron and Fluorastrol. *Journal of Medicinal Chemistry* **2010,** 53, 5676-5683.

231. Jamieson, C.; Moir, E. M.; Rankovic, Z.; Wishart, G. Medicinal Chemistry of hERG Optimizations: Highlights and Hang-Ups. *Journal of Medicinal Chemistry* **2006,** 49, 5029-5046.

232. Cox, C. D.; Breslin, M. J.; Whitman, D. B.; Coleman, P. J.; Garbaccio, R. M.; Fraley, M. E.; Zrada, M. M.; Buser, C. A.; Walsh, E. S.; Hamilton, K.; Lobell, R. B.; Tao, W.; Abrams, M. T.; South, V. J.; Huber, H. E.; Kohl, N. E.; Hartman, G. D. Kinesin spindle protein (KSP) inhibitors. Part 5: Discovery of 2-propylamino-2,4-diaryl-2,5-dihydropyrroles as potent, water-soluble KSP inhibitors, and modulation of their basicity by β-fluorination to overcome cellular efflux by P-glycoprotein. *Bioorganic & Medicinal Chemistry Letters* **2007,** 17, 2697-2702.

233. Meanwell, N. A. Synopsis of Some Recent Tactical Application of Bioisosteres in Drug Design. *Journal of Medicinal Chemistry* **2011,** 54, 2529-2591.

234. Rodriguez, D.; Ramesh, C.; Henson, L. H.; Wilmeth, L.; Bryant, B. K.; Kadavakollu, S.; Hirsch, R.; Montoya, J.; Howell, P. R.; George, J. M.; Alexander, D.; Johnson, D. L.; Arterburn, J. B.; Shuster, C. B. Synthesis and characterization of tritylthioethanamine derivatives with potent KSP inhibitory activity. *Bioorganic & Medicinal Chemistry* **2011,** 19, 5446-5453.

235. Kozielski, F.; DeBonis, S.; Skoufias, D. A. Screening for Inhibitors of Microtubule-Associated Motor Proteins. In *Microtubule Protocols*, Zhou, J., Ed. Humana Press: 2007; Vol. 137, pp 189-207.

236. Gleeson, M. P. Generation of a Set of Simple, Interpretable ADMET Rules of Thumb. *Journal of Medicinal Chemistry* **2008,** 51, 817-834.

237. Wienkers, L. C.; Heath, T. G. Predicting *in vivo* drug interactions from *in vitro* drug discovery data. *Nature Reviews Drug Discovery* **2005,** 4, 825-833.

238. Guengerich, F. P. Cytochrome P450 and Chemical Toxicology. *Chemical Research in Toxicology* **2007,** 21, 70-83.

239. Lin, J. H.; Lu, A. Y. H. Inhibition and Induction of Cytochrome P450 and the Clinical Implications. *Clinical Pharmacokinetics* **1998,** 35, 361-390.

240. Fiebig, H. H.; Dengler, W. A.; Roth, T. Human tumor xenografts. Predictivity, characterization and discovery of new new anticancer agents. In *Relevance of tumor models for anticancer drug development*, Fiebig, H. H.; Burger, A. M., Eds. Karger: Basel, 1999; Vol. 54, pp 29-50.

241. Humphries, M.; Woessner, R.; Bouhana, K.; Garrus, J.; Napier, C.; Lemieux, C.; Walker, D.; Winsk, S. In *Abstract 1782: Human tumor explants are better predictors of clinical trial outcome than cell line xenografts for the KSP inhibitor ARRY-520*, AACR 103rd Annual Meeting, Chicago, IL, April 15, 2012, 2012; Cancer Research: Chicago, IL, 2012.

242. Schöllkopf, U.; Groth, U.; Deng, C. Enantioselective Syntheses of *(R)*-Amino Acids Using L-Valine as Chiral Agent. *Angewandte Chemie International Edition in English* **1981,** 20, 798-799.

243. Giacomini, K. M.; Huang, S. M.; Tweedie, D. J.; Benet, L. Z.; Brouwer, K. L. R.; Chu, X. Y.; Dahlin, A.; Evers, R.; Fischer, V.; Hillgren, K. M.; Hoffmaster, K. A.; Ishikawa, T.; Keppler, D.; Kim, R. B.; Lee, C. A.; Niemi, M.; Polli, J. W.; Sugiyama, Y.; Swaan, P. W.; Ware, J. A.; Wright, S. H.; Yee, S. W.; Zamek-Gliszczynski, M. J.; Zhang, L. Membrane transporters in drug development. *Nature Reviews Drug Discovery* **2010,** 9, 215-236.

244. Kerns, E. H.; Di, L. Chapter 9 - Transporters. In *Drug-like Properties: Concepts, Structure Design and Methods*, Academic Press: San Diego, 2008; pp 228-241.

245. Morrison, J. F. Kinetics of the reversible inhibition of enzyme-catalysed reactions by tight-binding inhibitors. *Biochimica et Biophysica Acta (BBA) - Enzymology* **1969,** 185, 269-286.

246. Marvel, C. S.; Dietz, F. C.; Himel, C. M. The Dissociation Of Hexaarylethanes. XIII. Halogen Substituents. *The Journal of Organic Chemistry* **1942,** 07, 392-396.

247. Horn, M.; Mayr, H. Stabilities of Trityl-Protected Substrates: The Wide Mechanistic Spectrum of Trityl Ester Hydrolyses. *Chemistry – A European Journal* **2010,** 16, 7469-7477.

248. Gilman, H.; Gorsich, R. D. Some Reactions of *o*-Halobromobenzenes with *n*-Butyllithium. *Journal of the American Chemical Society* **1956,** 78, 2217-2222.

249. Kumar, S.; Ramachandran, U. Cinchona alkaloid phase-transfer catalysts revisited: influence of substituted aryl groups on the enantioselectivity of glycine ester enolate alkylation. *Tetrahedron* **2005,** 61, 7022-7028.

250. White, W. N.; Stout, C. A. A Determination of the HR Acidity Function for Sulfuric Acid—Aqueous Acetic Acid. *The Journal of Organic Chemistry* **1962,** 27, 2915-2917.

251. Talley, J. J.; Evans, I. A. Reaction of lithium *o*-lithiophenoxide with carbonyl compounds. *The Journal of Organic Chemistry* **1984,** 49, 5267-5269.

252. Bowden, S. T.; Beynon, K. I. 855. Free radicals and radical stability. Part XVII. (*m*-Hydroxyphenyl)diphenylmethanol and the corresponding free radical. *Journal of the Chemical Society (Resumed)* **1957**, 4253-4256.

253. Katritzky, A. R.; Lue, P. Directed metalation of benzenesulfinamides. A novel route to meta-substituted aromatic compounds. *The Journal of Organic Chemistry* **1990,** 55, 74-78.

254. Deshpande, P. P.; Ellsworth, B. A.; Buono, F. G.; Pullockaran, A.; Singh, J.; Kissick, T. P.; Huang, M.-H.; Lobinger, H.; Denzel, T.; Mueller, R. H. Remarkable *β*-Selectivity in the Synthesis of *β*-1-C-Arylglucosides: Stereoselective Reduction of Acetyl-Protected Methyl 1-C-Arylglucosides without Acetoxy-Group Participation. *The Journal of Organic Chemistry* **2007,** 72, 9746-9749.

255. Zhang, L.; Zhang, W.; Liu, J.; Hu, J. C−F Bond Cleavage by Intramolecular S_N2 Reaction of Alkyl Fluorides with O- and N-Nucleophiles. *The Journal of Organic Chemistry* **2009,** 74, 2850-2853.

256. Zarkadis, A. K.; Neumann, W. P.; Uzick, W. Über sterisch gehinderte freie Radikale, XIII. Über das Wittig-Radikal 4-Benzoyltriphenylmethyl und analoge mono-4-substituierte Tritylradikale. *Chemische Berichte* **1985,** 118, 1183-1192.

257. Parham, W. E.; Jones, L. D. Elaboration of bromoarylnitriles. *The Journal of Organic Chemistry* **1976,** 41, 1187-1191.

258. Fuson, R. C.; Miller, J. J. The Condensation of Grignard Reagents with 3-Pyridyl and 3-Quinolyl Ketones. *Journal of the American Chemical Society* **1957,** 79, 3477-3480.

259. Casadio, S.; Donetti, A.; Coppi, G. *N*-trisubstituted methylimidazoles as antifungal agents. *Journal of Pharmaceutical Sciences* **1973,** 62, 773-778.

260. Chackal-Catoen, S.; Miao, Y.; Wilson, W. D.; Wenzler, T.; Brun, R.; Boykin, D. W. Dicationic DNA-targeted antiprotozoal agents: Naphthalene replacement of benzimidazole. *Bioorganic & Medicinal Chemistry* **2006,** 14, 7434-7445.

261. Hirashima, S.; Suzuki, T.; Ishida, T.; Noji, S.; Yata, S.; Ando, I.; Komatsu, M.; Ikeda, S.; Hashimoto, H. Benzimidazole Derivatives Bearing Substituted Biphenyls as Hepatitis C Virus NS5B RNA-Dependent RNA Polymerase Inhibitors:

Structure−Activity Relationship Studies and Identification of a Potent and Highly Selective Inhibitor JTK-109. *Journal of Medicinal Chemistry* **2006,** 49, 4721-4736.

262. Iso, Y.; Grajkowska, E.; Wroblewski, J. T.; Davis, J.; Goeders, N. E.; Johnson, K. M.; Sanker, S.; Roth, B. L.; Tueckmantel, W.; Kozikowski, A. P. Synthesis and Structure−Activity Relationships of 3-[(2-Methyl-1,3-thiazol-4-yl)ethynyl]pyridine Analogues as Potent, Noncompetitive Metabotropic Glutamate Receptor Subtype 5 Antagonists; Search for Cocaine Medications. *Journal of Medicinal Chemistry* **2006,** 49, 1080-1100.

263. Creighton, A. M.; Jackman, L. M. 626. Hydrogen transfer. Part XIV. The quinone cyclodehydrogenation of acids and alcohols. *Journal of the Chemical Society (Resumed)* **1960**, 3138-3144.

264. Hwang, J. Y.; Arnold, L. A.; Zhu, F.; Kosinski, A.; Mangano, T. J.; Setola, V.; Roth, B. L.; Guy, R. K. Improvement of Pharmacological Properties of Irreversible Thyroid Receptor Coactivator Binding Inhibitors. *Journal of Medicinal Chemistry* **2009,** 52, 3892-3901.

265. Carroll, F. I.; Dickson, H. M.; Wall, M. E. Organic Sulfur Compounds. III. Synthesis of 2-(Substituted alkylamino)ethanethiols. *The Journal of Organic Chemistry* **1965,** 30, 33-38.

266. Starnes, W. H. Lead tetraacetate oxidation of 4,4,4-triphenyl-1-butanol, 3,3,3-triphenyl-1-propanol, and 4,4,4-triphenylbutyric acid. *The Journal of Organic Chemistry* **1968,** 33, 2767-2774.

267. Moussa, I. A.; Banister, S. D.; Beinat, C.; Giboureau, N.; Reynolds, A. J.; Kassiou, M. Design, Synthesis, and Structure−Affinity Relationships of Regioisomeric *N*-Benzyl Alkyl Ether Piperazine Derivatives as σ-1 Receptor Ligands. *Journal of Medicinal Chemistry* **2010,** 53, 6228-6239.

268. Jiang, Z.-X.; Qing, F.-L. Regioselective and Stereoselective Nucleophilic Ring Opening of Trifluoromethylated Cyclic Sulfates: Asymmetric Synthesis of Both Enantiomers of *syn*-(3-Trifluoromethyl)isoserine. *The Journal of Organic Chemistry* **2004,** 69, 5486-5489.

269. Crich, D.; Vinogradova, O. Synthesis and Glycosylation of a Series of 6-Mono-, Di-, and Trifluoro S-Phenyl 2,3,4-Tri-O-benzyl-thiorhamnopyranosides. Effect of the Fluorine Substituents on Glycosylation Stereoselectivity. *Journal of the American Chemical Society* **2007,** 129, 11756-11765.

270. Polidori, A.; Michel, N.; Fabiano, A. S.; Pucci, B. Exotic aqueous behavior of synthetic lipids: formation of vesicular nanotubes. *Chemistry and Physics of Lipids* **2005,** 136, 23-46.

271. Dale, T. J.; Rebek, J. Fluorescent Sensors for Organophosphorus Nerve Agent Mimics. *Journal of the American Chemical Society* **2006,** 128, 4500-4501.

272. Rudolph, J.; Theis, H.; Hanke, R.; Endermann, R.; Johannsen, L.; Geschke, F.-U. *seco*-Cyclothialidines: New Concise Synthesis, Inhibitory Activity toward Bacterial and Human DNA Topoisomerases, and Antibacterial Properties. *Journal of Medicinal Chemistry* **2001,** 44, 619-626.

273. Ghose, A. K.; Viswanadhan, V. N.; Wendoloski, J. J. Prediction of Hydrophobic (Lipophilic) Properties of Small Organic Molecules Using Fragmental Methods: An Analysis of ALOGP and CLOGP Methods. *The Journal of Physical Chemistry A* **1998,** 102, 3762-3772.

274. Tetko, I. V.; Tanchuk, V. Y.; Kasheva, T. N.; Villa, A. E. P. Estimation of Aqueous Solubility of Chemical Compounds Using E-State Indices. *Journal of Chemical Information and Computer Sciences* **2001,** 41, 1488-1493.